

A PHASE SHIFT METHOD

OF

MEASURING MICROWAVE ABSORPTION IN LIQUIDS

WITH EXPERIMENTAL RESULTS

A Thesis submitted to the University of London
for the Degree of Ph.D. in Physics

by

Adeline M. Southon

ProQuest Number: 10097990

All rights reserved

INFORMATION TO ALL USERS

The quality of this reproduction is dependent upon the quality of the copy submitted.

In the unlikely event that the author did not send a complete manuscript and there are missing pages, these will be noted. Also, if material had to be removed, a note will indicate the deletion.



ProQuest 10097990

Published by ProQuest LLC(2016). Copyright of the Dissertation is held by the Author.

All rights reserved.

This work is protected against unauthorized copying under Title 17, United States Code.
Microform Edition © ProQuest LLC.

ProQuest LLC
789 East Eisenhower Parkway
P.O. Box 1346
Ann Arbor, MI 48106-1346

A PHASE SHIFT METHOD
OF
MEASURING MICROWAVE ABSORPTION IN LIQUIDS
WITH EXPERIMENTAL RESULTS

ABSTRACT

The method evolved from an investigation of transmission line methods of measuring the absorption of electromagnetic radiations in liquids. An equation was derived relating the phase angle of the voltage reflection coefficient to the length of the liquid filled line beyond a short circuit.

$$\tan \phi = \frac{2\beta(\alpha \sinh 2\alpha l + \beta \sin 2\beta l)}{(\beta_0^2 - \alpha^2 - \beta^2) \cosh 2\alpha l - (\beta_0^2 + \alpha^2 + \beta^2) \cos 2\beta l}$$

The experimental results show that this equation describes exactly the behaviour of the phase angle as the depth of liquid filling the transmission line is varied. The equation has been shown to be true for a wide range of liquids:-

- (a) Non-absorbing liquids, i.e. Benzole.

- (b) Liquids with a low absorption, i.e. Chlorobenzene and Cyclohexanol.
- (c) Dilute solutions of polar substances in non-polar solvents, i.e. Chlorobenzene in Benzole.
- (d) Liquids with high absorptions, i.e. Water and Alcohol.
- (e) Electrolytic solutions, i.e. Sodium Chloride in water.

Values of the phase constants and attenuation coefficients for these liquids have been deduced from the graphs showing phase angle plotted against liquid depth, with an accuracy that compares favourably with other established methods.

The method has been applied to an investigation of the absorption of microwaves ($\lambda = 9.1$ cms) by ox blood and serum at room temperature and the inner body temperature of 37°C , and these results have been compared with those obtained for distilled water at these two temperatures.

The variation of the phase constant and attenuation coefficient of sodium chloride solutions with concentration has also been investigated, from 0.15N (physiological saline) up to 2N.

This method, which depends upon measurement of phase shift alone for the determination of α and β , requires a very much simpler form of apparatus than other methods.

The method is best suited to liquids with low values of α and high values of β , and a modification to the apparatus and experimental method has been suggested which should enable values to be obtained more rapidly. This modification has not so far been made, since the accuracy obtainable with this phase shift method is inferior to that of the null techniques recently introduced into dielectric measurements.

CONTENTS

<u>Introduction.</u>	<u>Page</u>
A general description of dielectric in the microwave region	1
<u>Chapter 1</u>	
<u>The theory of the phase angle method of absorption measurements</u>	11
1.1 Introduction	11
1.2 Derivation of the phase angle equation	11
1.3 An alternative method of deriving the phase angle equation	15
1.4 The relationship between the phase angle and the observed shift Δ of the standing wave pattern as the depth of the dielectric filling the line varies	17
1.5 Theoretical discussion of the variation of phase angle with liquid depth for different liquids	21
1.5.1 Non-absorbing liquids	21
1.5.2 Absorbing liquids	24
1.5.3 The effect of α and β on the variation of $\tan \phi$ with l	26

1.5.3.1	Liquids with low values of both α and β	26
1.5.3.2	Liquids with high values of both α and β	27
1.5.3.3	Liquids with a high value of α and a low value of β	28
1.5.4	The effect of β_0 on the variation of $\tan\phi$ with l	28
1.6	The variation of $ K ^2$ with l	29
1.7	An alternative method of deriving the $ K ^2$ equation	31

Chapter 2

	<u>Description of the apparatus and the experimental method</u>	34
2.1	Introduction	34
2.2	A general investigation of the tuning	35
2.2.1	The effect on the tuning of the intro- duction of liquid into the line	39
2.3	Description of the apparatus	41
2.4	Description of the experimental method	42
2.4.1	The measurement of the liquid depth	42
2.4.1.1	For liquids with low viscosity ...	42
2.4.1.2	For liquids with high viscosity ..	46

	<u>Page</u>
2.4.2	The measurement of the phase shift48
2.4.3	The entry of liquid into the line50
2.4.4	The recording of the galvanometer deflection51
2.5	The control of temperature52

Chapter 3

	<u>The calculation of α and β</u>55
3.1	Introduction55
3.2	The gradient of $\tan \phi$55
3.2.1	The gradient of the curve when $\tan \phi = 0$57
3.2.2	The gradient of the curve when $l = 0$...60
3.2.3	The turning points of the curve60
3.3	The gradient of the curve relating $ K ^2$ and l61
3.3.1	The turning points of the curve relating $ K ^2$ with l62
3.3.2	The condition for $ K ^2$ to be greater than one63
3.4	The condition for no standing wave along the line64
3.5	The calculation of β67
3.5.1	The calculation of β from the values of l when $\Delta = 0$ or $\pm \lambda/4$67

3.5.2	The calculation of β from the values of l when $ k $ has maximum and minimum values	67
3.6	Methods of determining the limits between which α must lie	68
3.6.1	The curve no longer going to infinity method	68
3.6.2	The change of sign of the gradient method	70
3.6.3	The curve no longer taking positive values method	71
3.6.4	The constant galvanometer signal method	72
3.7	The calculation of α	73
3.7.1	From the maximum and minimum values of Δ	73
3.7.2	From the gradient of the curve when $\tan \phi = 0$	73
3.7.3	Substitution of experimental values in the $\tan \phi$ equation	74
3.7.4	From the steady negative value of Δ	75
3.7.5	From the value of l when $\Delta = 0$	75

Chapter 4

	<u>Experimental results</u>	76
4.1	Introduction	76
4.2	Experimental results for a non-absorbing liquid	78
4.3	Experimental results for liquids with low absorptions	79
4.4	Experimental results for liquids with high values for both α and β	83
4.4.1	Results for distilled water	83
4.4.2	Results for ox blood and serum	89
4.4.3	Results for NaCl solutions of varying concentrations	94
4.5	Experimental results for liquids with a high value of α and a low value of β	101
4.5.1	Results for ethyl alcohol	101
4.6	Conclusions	103

Chapter 5

	<u>Criticism of the phase shift method</u>	106
5.1	Introduction	106
5.2	A suggested modification to the apparatus and the experimental method	107

5.3	Comparison with other methods	112
5.4	Conclusion	118
	<u>Appendix</u>	119
	<u>References</u>	134

ACKNOWLEDGMENTS

The author wishes to express her thanks to Professor H.T. Flint, under whose direction this work was carried out, and to the staff, both academic and technical, of Bedford College Physics Department for their generous help and encouragement.

The Physiology Department of Bedford College kindly provided the samples of ox blood and serum.

List of symbols

Symbols with the suffix \circ have been used to refer to quantities measured in air.

- α The attenuation coefficient measured in neper cms^{-1} .
- β The phase constant measured in radians cms^{-1} .
- P The propagation constant.
- Z_{\circ} The characteristic impedance of the air filled line.
- Z'_{\circ} The characteristic impedance of the dielectric filled portion of the line.
- k The voltage reflection coefficient of the termination.
- K The ratio of the amplitude of the reflected to that of the incident voltage.
- ϕ The phase change that occurs on reflection.
- R The resistance per unit length of the line.
- L The inductance per unit length of the line.
- G The conductance per unit length of the line.
- C The capacitance per unit length of the line.
- w The angular frequency.
- l The liquid depth.
- Δ The phase shift.

- L The length of the transmission line.
- λ The wavelength.
- $\bar{\epsilon}$ The complex dielectric constant.
- ϵ' The real part of the dielectric constant.
- ϵ'' The imaginary part of the dielectric constant.
- ϵ_s The static dielectric constant.
- ϵ_∞ The value ϵ' approaches at the highest frequencies.

INTRODUCTION

A general description of dielectric absorption in the microwave region.

When a dielectric material is subjected to an alternating field E , there is, in general a phase difference between the dielectric displacement vector D and the electric field vector E . This phase difference δ can be described by the introduction of a complex dielectric constant $\bar{\epsilon}$, where

$$\bar{\epsilon} = \epsilon' - j\epsilon'',$$

δ is known as the loss angle of the dielectric and

$$\tan \delta = \frac{\epsilon''}{\epsilon'}$$

where $\tan \delta$ is the dissipation factor. The energy dissipated in the dielectric is directly proportional to ϵ'' , so that ϵ'' is known as the loss factor.

The behaviour of a dielectric material depends upon the frequency of the alternating field, the chemical composition of the dielectric and its temperature. There are two distinct types of dielectric behaviour depending upon whether the phase

difference between D and E is a measurable quantity or not. If a phase difference exists between D and E there is a dissipation of energy in the dielectric and an absorption of electro-magnetic waves. If however, the phase difference is zero, $\epsilon'' = 0$, and the static relationship,

$$D = \epsilon E$$

is applicable to an alternating field, under these conditions no energy is absorbed from the electro-magnetic field.

The phase difference may be due to one or more of three causes.

- (a) Electrical conductivity.
- (b) Relaxation effects, due to the permanent dipoles in the dielectric being unable to follow the rapid changes in the direction of the field.
- (c) Resonance effects, due to the vibrations of atoms, ions or electrons.

Maxwell's electromagnetic equations brought out the close relationship between the static dielectric constant and the refractive index of the medium. The refractive index n at a certain frequency is defined by

$$v = \frac{c}{n}$$

where v is the phase velocity of the electromagnetic wave at that frequency and c the velocity in vacuum. If no moving charges are present, Maxwell showed that

$$v = \frac{c}{\sqrt{\epsilon\mu}}$$

where μ is the magnetic permeability of the medium, and does not differ appreciably from unity for the materials under consideration. Hence

$$\epsilon = n^2$$

This equation is also valid when the movements of the charges are slow compared with the velocity c , so that it applies when low frequency electromagnetic waves are propagated in the dielectric. This relationship is confirmed experimentally, for it is found that for wavelengths larger than a certain critical value, the dielectric constant is independent of frequency and equal to the static value of the dielectric constant ϵ_s , which is equal to the square of the refractive index. This critical wavelength depends upon the chemical composition of the dielectric and on its temperature. For example, for liquids possessing permanent dipoles such as water and alcohol it is about 15 and 40 cms. respectively at 20°C, whereas for non-polar dielectrics

it is generally in the infra-red when dielectric loss due to resonance effects begins.

In frequency regions where the complex dielectric constant differs from the static value, the refractive index is also found to be dependent on the frequency. This is expressed by the introduction of a complex refractive index \bar{n} where

$$\bar{n} = n' - jn''$$

which, since $n = n'$, is generally written in the form,

$$\bar{n} = n(I - jk)$$

where k is the absorption index.

ϵ' and ϵ'' are related to n and k by the equations:-

$$\epsilon' = n^2(I - k^2)$$

and
$$\epsilon'' = 2n^2k$$

The present work deals with measurements at a frequency of $3.3 \times 10^9 \text{ sec}^{-1}$, so that the effect of the phase difference in other regions of the electromagnetic spectrum is not discussed. This frequency lies in the microwave region which includes frequencies from 10^7 to 10^{11} sec^{-1} . In the microwave region the dielectric loss is mainly due to the relaxation effect

of the permanent dipoles, whereas at optical frequencies it is due to resonance effects. (The distinction between these two effects is rather arbitrary, but they are usually separated.)

The relaxation effect, when the permanent dipoles of the dielectric are unable to follow the very rapid alterations in the direction of the field E, can be described by the introduction of the dielectric relaxation time τ . The time which permanent dipoles require to reach an equilibrium distribution after the application of a static external field E is somewhere between 10^{-6} and 10^{-13} secs. The time depends upon the temperature and structure of the dielectric. It can be shown that the complex dielectric constant is related to τ by the relation,

$$\bar{\epsilon} = \epsilon_{\infty} + \frac{\epsilon_s - \epsilon_{\infty}}{1 + j\omega\tau}$$

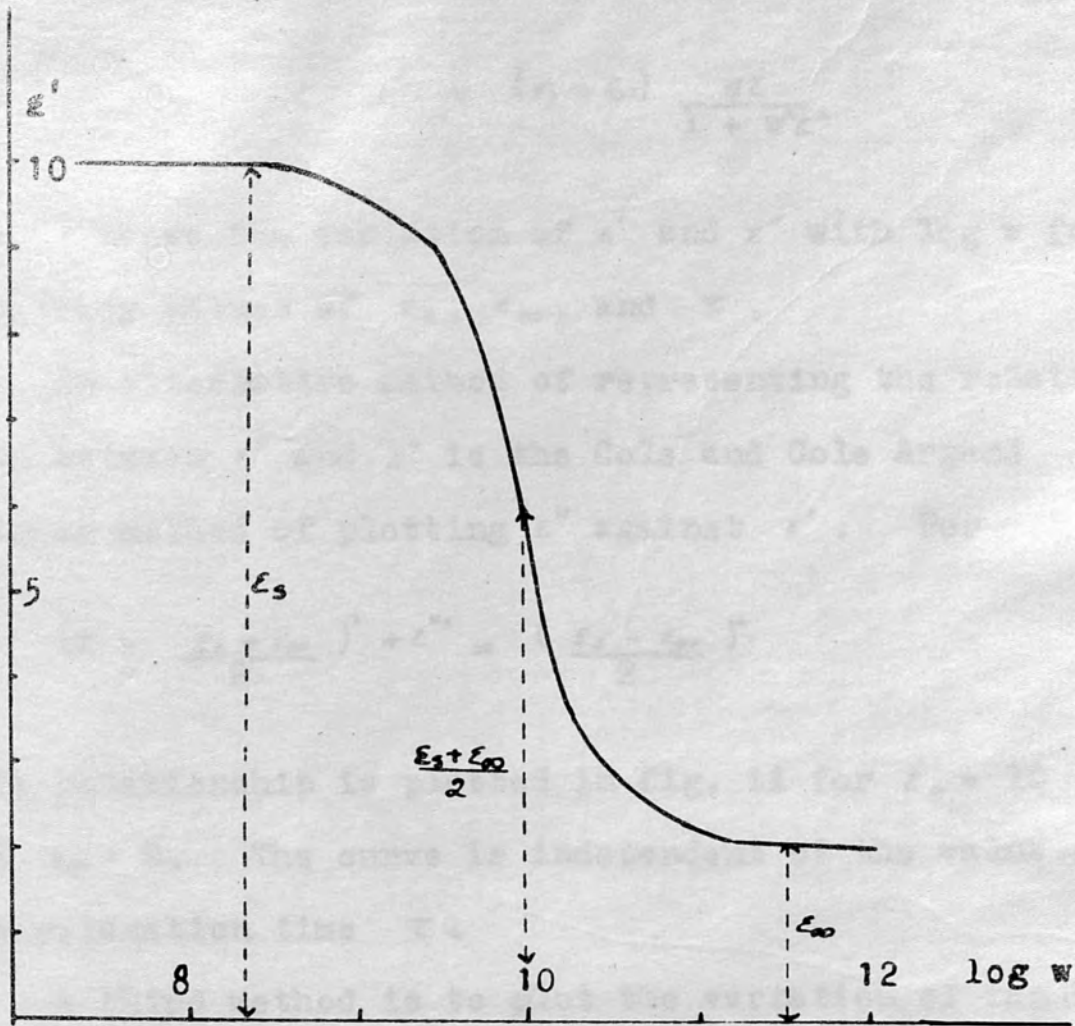
where ϵ_s is the static dielectric constant,

ϵ_{∞} is the value ϵ' approaches at the highest frequencies,

and $\bar{\epsilon}$ is the complex dielectric constant at the angular frequency ω .

Dividing $\bar{\epsilon}$ into its real and imaginary parts,

$$\epsilon' = \epsilon_{\infty} + \frac{\epsilon_s - \epsilon_{\infty}}{1 + \omega^2\tau^2}$$



$$\epsilon_s = 10, \quad \epsilon_\infty = 2, \quad \tau = 10^{-10} \text{ sec}$$

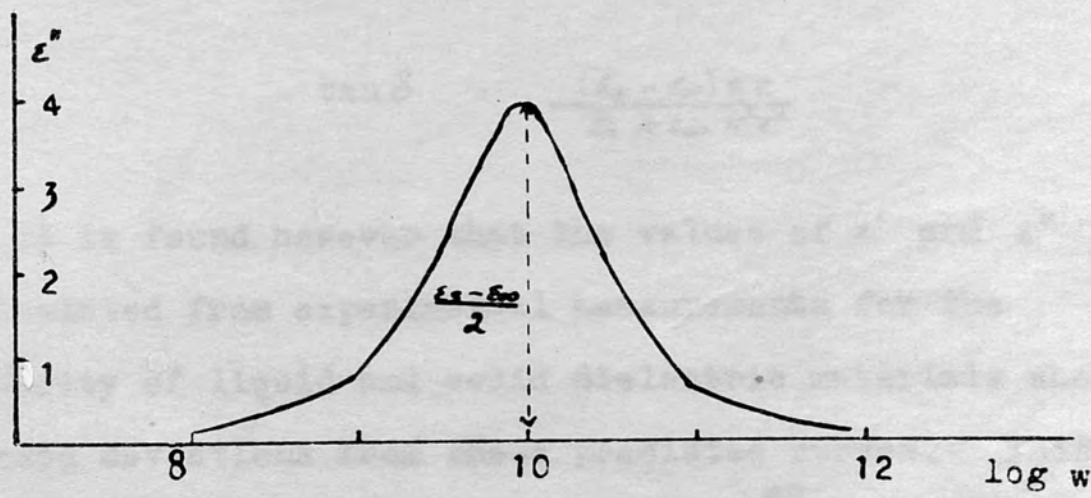


Fig. 1 The variation of ϵ' and ϵ'' with $\log_{10} w$.

and
$$\epsilon'' = (\epsilon_s - \epsilon_\infty) \frac{w\tau}{1 + w^2\tau^2}$$

Fig. i shows the variation of ϵ' and ϵ'' with $\log w$ for arbitrary values of ϵ_s , ϵ_∞ , and τ .

An alternative method of representing the relationship between ϵ' and ϵ'' is the Cole and Cole Argand diagram method of plotting ϵ'' against ϵ' . For

$$\left(\epsilon' - \frac{\epsilon_s + \epsilon_\infty}{2}\right)^2 + \epsilon''^2 = \left(\frac{\epsilon_s - \epsilon_\infty}{2}\right)^2$$

This relationship is plotted in fig. ii for $\epsilon_s = 10$ and $\epsilon_\infty = 2$. The curve is independent of the value of the relaxation time τ .

A third method is to plot the variation of $\tan \delta$ against $\log w$ as is shown in fig. iii for the same arbitrary values of ϵ_s , ϵ_∞ and τ .

$$\tan \delta = \frac{(\epsilon_s - \epsilon_\infty) w\tau}{\epsilon_s + \epsilon_\infty + w^2\tau^2}$$

It is found however that the values of ϵ' and ϵ'' calculated from experimental measurements for the majority of liquid and solid dielectric materials show marked deviations from these predicted curves. This indicates that the model used by Debye^{*2} in deriving these equations is too simple for general validity.

* Debye uses a relaxation time τ^* related to the τ used above by $\tau = \tau^*(\epsilon_s + 2)/(\epsilon_\infty + 2)$

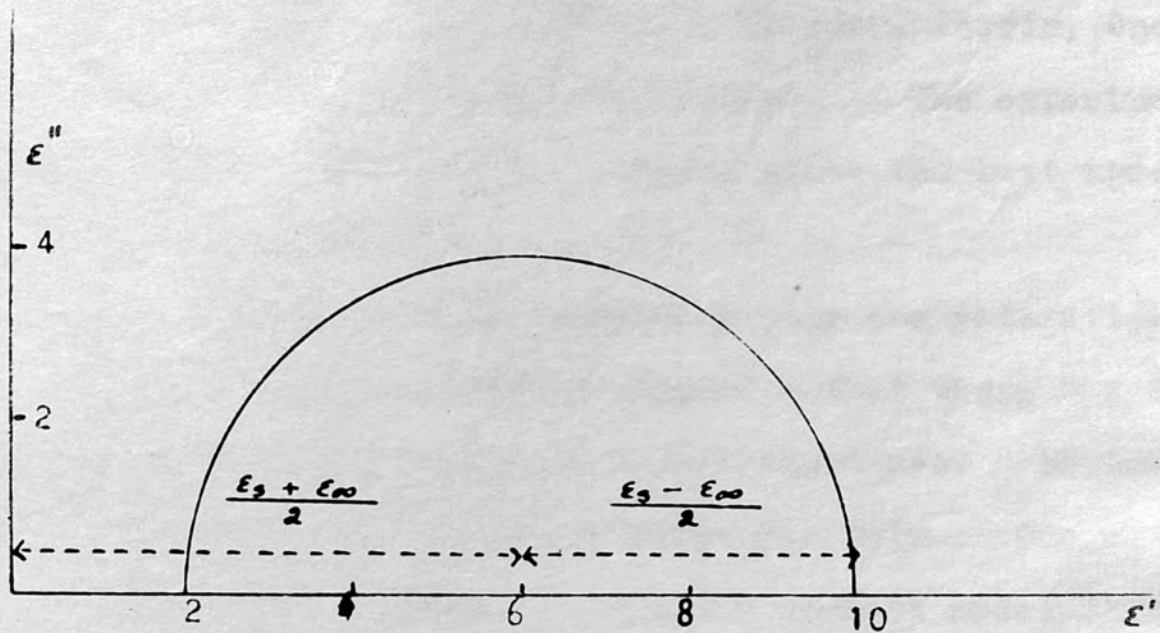


Fig. ii Cole and Cole diagram.

$$\epsilon_s = 10, \quad \epsilon_\infty = 2, \quad \tau = 10^{-10} \text{ sec}$$

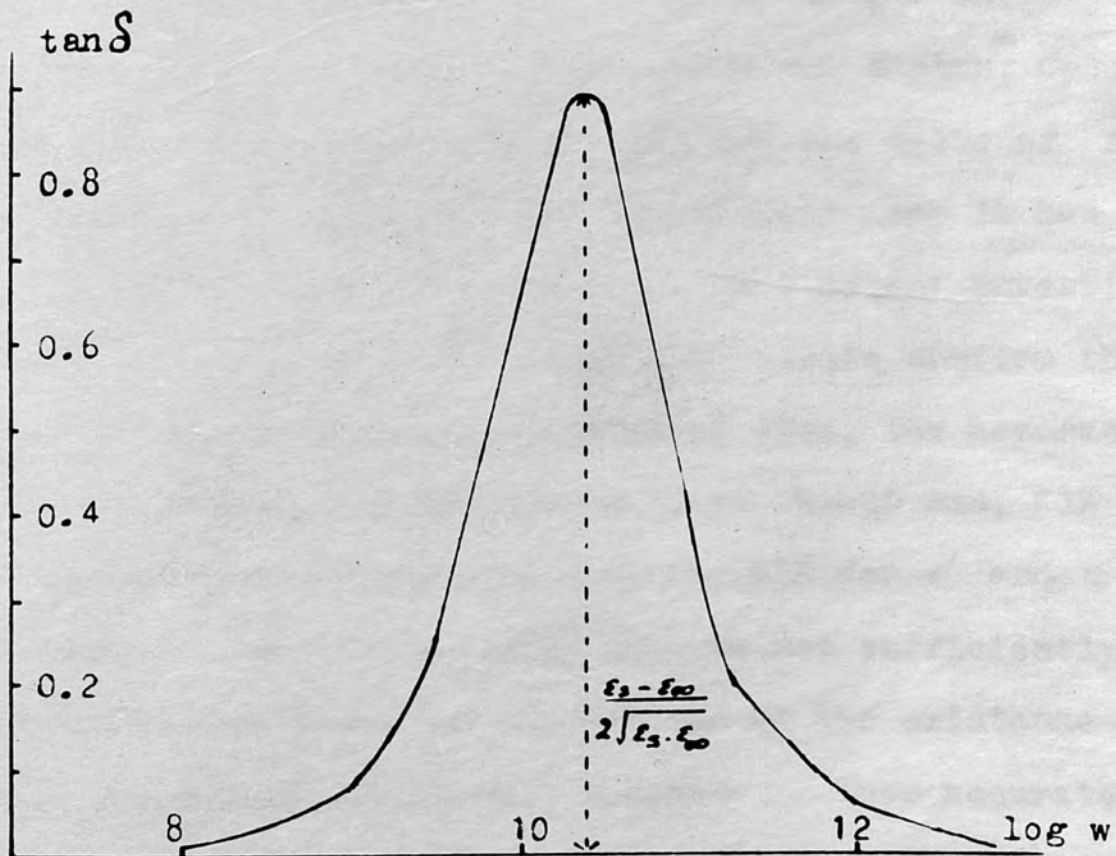


Fig. iii The variation of $\tan \delta$ with $\log_{10} w$.

Various alternative models and extensions to the general theory have been put forward by Onsager,³ Perrin,⁴ Oncley,⁵ Cole and Cole,¹ Kirkwood⁶ and others.^{7,8} The experimental data is used to see which theory gives the best agreement with experiment.

The simple theory considers only one relaxation time. Experiment however suggests that there may in fact be a distribution of relaxation times. Böttcher,⁹ page 363, discusses the evidence for this. One of the difficulties in deciding upon the correct model is that reliable values of ϵ' and ϵ'' in this frequency range are difficult to obtain. For instance, water, which has been investigated by many authors using a variety of methods, is claimed by some (Lane and Saxton,¹⁰ Collie, Ritson and Hasted)¹¹ to possess but one value of τ , while others (Younker and von Hippel)¹² say it has a wide variety of relaxation times. In a recent investigation¹³ of water by Cook, although his results confirm the existence of a single relaxation time, the accuracy of his results ($\pm 2\%$ for ϵ' and ϵ'' at $\lambda_0 = 10$ cms, $\pm 1\%$ for ϵ' , $\pm 2.5\%$ for ϵ'' at $\lambda_0 = 6.48$ cms, and $\pm 1\%$ for ϵ' and ϵ'' at $\lambda_0 = 3.195$ cms and $\lambda_0 = 1.262$ cms) is not sufficiently high to rule out the possibility of the existence of a narrow relaxation time spectrum. Thus accurate measurement of quantities from which ϵ' and ϵ'' can be

calculated is of great importance in giving information as to the structure of dielectric materials.

In the microwave region, ϵ' and ϵ'' can be found indirectly by transmission line or optical methods. In the transmission line methods $\bar{\epsilon}$ is derived from the impedance Z or the propagation constant P of the dielectric medium, while in the optical methods it is calculated from measurements of n and k . Standing or travelling waves may be used for measuring any of these quantities. Travelling waves are used for the general optical method. The intensities of the reflected and transmitted beam are measured and n and k calculated from Fresnel's equation. Baz¹⁴ and Kebbel¹⁵ used this method, but in the microwave region boundary problems arise owing to the wavelength being comparable to the dimensions of the sample and standing waves are set up between the transmitter and the receiver causing intensity fluctuations. So it is seen that the optical method is not satisfactory when carried into the microwave region.

The longer wavelength of the microwave region as opposed to optical wavelengths is an advantage if standing waves are used. Drude¹⁶ was the first to use this technique using Lecher lines and his two methods have since been adapted in many variations. Knerr¹⁷ measured n and k for water using both an optical free wave

method and a standing wave method with Lecher lines, covering a range of wavelengths from 20.44 to 6.48 cms. He found the Lecher line method slightly superior to the optical one. It was not however until the electromagnetic field was enclosed in a hollow pipe or coaxial line, so eliminating the effects of stray fields and boundary effects, that the transmission line method superceded the optical one.

Oscillators capable of producing undamped oscillations at these wavelengths were only available by about 1936, and the previous dielectric measurements, with damped electric waves from spark sources, are unreliable. The development of radar during the 1939-45 war brought great advances not only in the design of microwave oscillators, such as the magnetron and the klystron, but in all circuit elements and the techniques required at these frequencies.

The Roberts and von Hippel¹⁸ method of measuring ϵ' and $\tan \delta$ from measurements on the standing wave pattern set up in a short circuited transmission line or waveguide was developed during the war; and the use¹⁹ of resonant cavities was introduced by Willis Jackson and others for measurements on materials with small loss angles. Redheffer²⁰ reviews the large number of methods used for dielectric measurements at microwave frequencies

and shows how they are all developed from the same basic equations.

Advances in the design of piston attenuators and phase changers at microwave frequencies have made possible null methods of measurement within the medium. (Buchanan²¹ and Branin and Smyth.²²)

In addition to providing evidence as to the structure of dielectric materials, measurements of the absorption of electromagnetic waves by body fluids and tissues are of great importance medically so that the effects on the human body of irradiation by these wavelengths can be known. Recent work on this problem has been carried out by England and Sharples^{23,24} and Cook.¹³

Chapter 1

THE THEORY OF THE PHASE ANGLE METHOD
OF ABSORPTION MEASUREMENTS

1.1 Introduction.

This method is based on an equation relating the phase angle ϕ , due to the presence of a thickness l of dielectric above a short circuit in a transmission line, to l . The variation of ϕ with l is described and the effect of different liquids on this variation discussed.

1.2 Derivation of the phase angle equation.

Consider a transmission line filled to a distance l with a dielectric with an appreciable value of α .

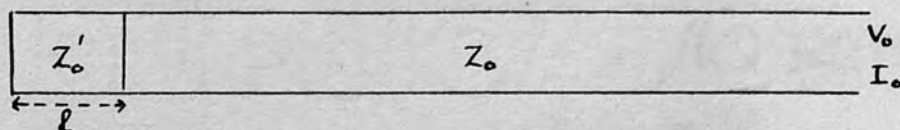


Fig. 1.1

From standard transmission line theory, the equations describing the voltage and current wave configurations in the filled part of the line are,

$$V' = V'_o (e^{Pl} + Ke^{j\phi - Pl})$$

and
$$I' = \frac{V_o'}{Z_o'} (e^{Pl} - Ke^{j\phi - Pl})$$

where P is the propagation constant and $k = Ke^{j\phi}$ is the voltage reflection coefficient of the dielectric. Thus the terminating impedance of the unfilled line, Z_T , or the input impedance of the filled line, Z' input, is given by the expression

$$Z_T = Z' \text{ input} = Z_o' \frac{(e^{Pl} + Ke^{j\phi - Pl})}{(e^{-Pl} - Ke^{-Pl})}$$

If the filled line is terminated in a short circuit, $K = 1$ and $\phi = \pi$, and

$$\begin{aligned} Z' \text{ input} &= Z_o' \frac{(e^{Pl} - e^{-Pl})}{(e^{-Pl} + e^{Pl})} \\ &= Z_o' \tanh Pl \dots\dots\dots(1.1) \end{aligned}$$

For the airfilled portion of the line:-

The propagation constant $P_o = j\beta_o$

$$= \sqrt{(R_o + j\omega L_o)(G_o + j\omega C_o)}$$

 and at V.H.F. $P_o = j\omega \sqrt{L_o C_o} \dots\dots\dots(1.2)$

The characteristic impedance $Z_o = \sqrt{\frac{R_o + j\omega L_o}{G_o + j\omega C_o}}$
 and at V.H.F. $Z_o = \sqrt{\frac{L_o}{C_o}} \dots\dots\dots(1.3)$

While for the dielectric filled portion:-

The propagation constant $P = \alpha + j\beta \dots\dots\dots(1.4)$

$$= \sqrt{(R + j\omega L)(G + j\omega C)}$$

and at V.H.F. $P = \sqrt{j\omega L(G + j\omega C)} \dots(1.5)$

The characteristic impedance $Z'_o = \sqrt{\frac{R + j\omega L}{G + j\omega C}}$

and at V.H.F. $Z'_o = \sqrt{\frac{j\omega L}{G + j\omega C}} \dots\dots\dots(1.6)$

Thus from equations (1.2) and (1.5)

$$\frac{P_o}{P} = \frac{j\omega \sqrt{L_o C_o}}{[j\omega L(G + j\omega C)]^{1/2}} \dots(1.7)$$

$$= \sqrt{\frac{j\omega L_o C_o}{L(G + j\omega C)}} \dots\dots(1.7)$$

and from equations (1.3) and (1.6)

$$\frac{Z'_o}{Z_o} = \sqrt{\frac{j\omega L}{(G + j\omega C)} \frac{C_o}{L_o}} \dots(1.8)$$

$$= \frac{L}{L_o} \sqrt{\frac{j\omega C_o}{(G + j\omega C)} \frac{L_o}{L}} \dots(1.8)$$

and from equation (1.7)

$$\frac{Z'_o}{Z_o} = \frac{L P_o}{L_o P} \dots\dots\dots(1.8)$$

Hence if $L_o = L$,

$$\frac{Z'_o}{Z_o} = \frac{P_o}{P} = \frac{j\beta_o}{\alpha + j\beta} \dots\dots\dots(1.9)$$

Thus equation (1.1) may be written, using equation (1.9),

$$\frac{Z_r}{Z_o} = \frac{j\beta_o}{\alpha + j\beta} \tanh(\alpha + j\beta)l \dots\dots\dots(1.10)$$

The voltage reflection coefficient

$$k = K e^{j\phi}$$

is related to the terminating impedance of the line, Z_T , by the expression

$$\frac{Z_T}{Z_0} = \frac{1 + k}{1 - k} \dots\dots\dots(1.11)$$

or $k = \frac{Z_T/Z_0 - 1}{Z_T/Z_0 + 1} \dots\dots\dots(1.11)$

Substituting for Z_T/Z_0 in equation (1.11) from (1.10)

$$k = \frac{j\beta_0 \sinh(\alpha + j\beta)l - (\alpha + j\beta) \cosh(\alpha + j\beta)l}{j\beta_0 \sinh(\alpha + j\beta)l + (\alpha + j\beta) \cosh(\alpha + j\beta)l} \dots(1.12)$$

Rationalising equation (1.12), putting

$$M = \alpha + j\beta$$

and $N = \alpha - j\beta$

$$k = \frac{\beta_0^2 \text{sh}Ml \text{sh}Nl - (\alpha^2 + \beta^2) \text{ch}Ml \text{ch}Nl + j\beta_0 M \text{ch}Ml \text{sh}Nl + j\beta_0 N \text{sh}Ml \text{ch}Nl}{\beta_0^2 \text{sh}Ml \text{sh}Nl + (\alpha^2 + \beta^2) \text{ch}Ml \text{ch}Nl - j\beta_0 M \text{ch}Ml \text{sh}Nl + j\beta_0 N \text{sh}Ml \text{ch}Nl} \dots\dots\dots(1.12)$$

$$= \frac{\beta_0^2 (\text{ch}2\alpha l - \text{ch}j2\beta l)^{\frac{1}{2}} - (\alpha^2 + \beta^2) (\text{ch}2\alpha l + \text{ch}j2\beta l)^{\frac{1}{2}}}{D} + \frac{j\{\beta_0 M (\text{sh}2\alpha l - \text{sh}j2\beta l)^{\frac{1}{2}} + \beta_0 N (\text{sh}2\alpha l + \text{sh}j2\beta l)^{\frac{1}{2}}\}}{D} \dots(1.12)$$

where D is

$$\beta_0^2 (\text{ch}2\alpha l - \text{ch}j2\beta l)^{\frac{1}{2}} + (\alpha^2 + \beta^2) (\text{ch}2\alpha l + \text{ch}j2\beta l)^{\frac{1}{2}} + j\beta_0 \{M (\text{sh}2\alpha l - \text{sh}j2\beta l)^{\frac{1}{2}} - N (\text{sh}2\alpha l + \text{sh}j2\beta l)^{\frac{1}{2}}\}$$

Whence writing

$$a = \beta_0^2 - \alpha^2 - \beta^2 \quad \text{and} \quad b = \beta_0^2 + \alpha^2 + \beta^2$$

$$k = \frac{a \operatorname{ch} 2\alpha l - b \cos 2\beta l + j 2\beta (\alpha \operatorname{sh} 2\alpha l + \beta \sin 2\beta l)}{b \operatorname{ch} 2\alpha l - a \cos 2\beta l + 2\beta_0 \beta \operatorname{sh} 2\alpha l - 2\beta \alpha \sin 2\beta l}$$

Therefore

$$\tan \phi = \frac{2\beta (\alpha \operatorname{sh} 2\alpha l + \beta \sin 2\beta l)}{(\beta_0^2 - \alpha^2 - \beta^2) \operatorname{ch} 2\alpha l - (\beta_0^2 + \alpha^2 + \beta^2) \cos 2\beta l} \dots\dots\dots(1.13)$$

1.3 An alternative method of deriving the phase angle equation.

An alternative method of deriving equation (1.13) is as follows.

Let $\frac{Z_r}{Z_0} = u + jv \dots\dots\dots(1.14)$

Then using equation (1.11) the reflection coefficient may be expressed,

$$k = \frac{u + jv - 1}{u + jv + 1} \dots\dots\dots(1.15)$$

which when rationalised becomes,

$$k = \frac{u^2 + v^2 + 2jv - 1}{u^2 + v^2 + 1 + 2u} \dots\dots\dots(1.15)$$

and since

$$k = K e^{j\phi}$$

$$\tan \phi = \frac{2v}{u^2 + v^2 - 1} \dots\dots\dots(1.16)$$

From equation (1.10)

$$\frac{Z_r}{Z_0} = \frac{j\beta_0 \tanh(\alpha + j\beta)l}{\alpha + j\beta} = u + jv$$

Thus

$$\begin{aligned}
 u + jv &= \frac{j\beta(\alpha - j\beta)}{\alpha^2 + \beta^2} \cdot \frac{\sinh(\alpha + j\beta) \text{lcosh}(\alpha - j\beta)}{\cosh(\alpha + j\beta) \text{lcosh}(\alpha - j\beta)} \\
 &= \frac{(\beta\beta - j\beta\alpha)}{\alpha^2 + \beta^2} \left\{ \frac{\sinh 2\alpha 1 + j\sin 2\beta 1}{\cosh 2\alpha 1 + \cos 2\beta 1} \right\}
 \end{aligned}$$

Therefore equating real and imaginary parts:-

$$u = \frac{\beta\beta \sinh 2\alpha 1 - \beta\alpha \sin 2\beta 1}{(\alpha^2 + \beta^2)(\cosh 2\alpha 1 + \cos 2\beta 1)}$$

$$\text{and } v = \frac{\beta\alpha \sinh 2\alpha 1 + \beta\beta \sin 2\beta 1}{(\alpha^2 + \beta^2)(\cosh 2\alpha 1 + \cos 2\beta 1)}$$

Substituting these values for u and v in equation (1.16)

$\tan \phi$

$$\begin{aligned}
 &= \frac{2\beta(\alpha \text{sh} 2\alpha 1 + \beta \sin 2\beta 1)(\alpha^2 + \beta^2)(\text{ch} 2\alpha 1 + \cos 2\beta 1)}{\beta^2(\beta^2 \text{sh} 2\alpha 1 + \alpha^2 \sin 2\beta 1 + \alpha^2 \text{sh} 2\alpha 1 + \beta^2 \sin 2\beta 1) - (\alpha^2 + \beta^2)^2 (\text{ch} 2\alpha 1 + \cos 2\beta 1)^2} \\
 &= \frac{2\beta(\alpha \text{sh} 2\alpha 1 + \beta \sin 2\beta 1)(\alpha^2 + \beta^2)(\text{ch} 2\alpha 1 + \cos 2\beta 1)}{(\alpha^2 + \beta^2) \{ \beta^2 (\text{ch} 2\alpha 1 - 1 + 1 - \cos 2\beta 1) - (\alpha^2 + \beta^2) (\text{ch} 2\alpha 1 + \cos 2\beta 1) \}} \\
 &= \frac{2\beta(\alpha \text{sh} 2\alpha 1 + \beta \sin 2\beta 1)(\text{ch} 2\alpha 1 + \cos 2\beta 1)}{\{ \beta^2 (\text{ch} 2\alpha 1 - \cos 2\beta 1) - (\alpha^2 + \beta^2) (\text{ch} 2\alpha 1 + \cos 2\beta 1) \} \times (\text{ch} 2\alpha 1 + \cos 2\beta 1)} \\
 &= \frac{2\beta(\alpha \sinh 2\alpha 1 + \beta \sin 2\beta 1)}{(\beta^2 - \alpha^2 - \beta^2) \cosh 2\alpha 1 - (\beta^2 + \alpha^2 + \beta^2) \cos 2\beta 1}
 \end{aligned}$$

as obtained in equation (1.13).

1.4 The relationship between the phase angle ϕ and the observed shift Δ of the standing wave pattern as the depth of the dielectric filling the line varies.

In testing the validity of equation (1.13) experimentally, the shift Δ of the standing wave pattern as the depth of dielectric filling the transmission line was observed instead of the phase angle ϕ .

Fig. (1.2) represents a length L of transmission line terminated in an impedance Z_T .

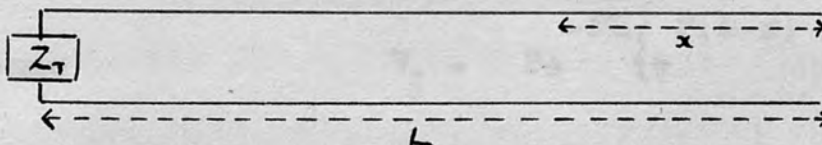


Fig. 1.2

The expressions for the voltage and current at any point x are given by

$$V_x = Ae^{Px} + Be^{-Px}$$

and
$$I_x = \frac{Be^{-Px} - Ae^{Px}}{Z_0}$$

When $x = L$,

$$V_L = Ae^{PL} + Be^{-PL}$$

and
$$I_L = \frac{Be^{-PL} - Ae^{PL}}{Z_0}$$

But
$$Z_T = \frac{V_L}{I_L} = Z_0 \frac{(Ae^{PL} + Be^{-PL})}{Be^{-PL} - Ae^{PL}}$$

or $Ae^{PL} (Z_r + Z_0) = Be^{-PL} (Z_r - Z_0)$

From equation (1.11)

$$k = \frac{Z_r - Z_0}{Z_r + Z_0}$$

Therefore $A = kBe^{-2PL}$

Thus the voltage at any point x may be written,

$$V_x = B(ke^{-2PL - Px} + e^{-Px})$$

k is complex, $k = Ke^{j\phi}$

Hence $V_x = Be^{-PL} \left\{ e^{P(L-x)} + Ke^{j\phi} e^{-P(L-x)} \right\}$

For a transmission line in air, $\alpha_0 = 0$, and so $P = j\beta_0$.

With a crystal detector, which obeys a square law, the observed signal is proportional to $|V_x|^2$. Hence multiplying by the complex conjugate,

$$|V_x|^2 = B^2 e^{-2PL} \left\{ 1 + K^2 + K(e^{j2\beta_0(L-x) - j\phi} + e^{-j2\beta_0(L-x) + j\phi}) \right\} \dots\dots\dots(1.17)$$

$$= B^2 e^{-2PL} \left\{ 1 + K^2 + K2\cosh j[2\beta_0(L-x) - \phi] \right\} \dots(1.17)$$

$$= B^2 e^{-2PL} \left\{ 1 + K^2 + 2K\cos 2 \left[\beta_0(L-x) - \frac{\phi}{2} \right] \right\} \dots(1.17)$$

The maximum and minimum values of $|V_x|^2$ occur when the cosine term of equation (1.17) is 1 or -1 respectively.

Hence, writing $y = L-x$, the conditions for maximum and minimum signals are:-

$$2(\beta_0 y - \frac{\phi}{2}) = 2n\pi$$

and $2(\beta_0 y - \frac{\phi}{2}) = (2n+1)\pi$ respectively,

where $n = 0, 1, 2, 3, \dots$

Thus maximum signals occur when

$$\beta_0 y = n\pi + \frac{\phi}{2}$$

so that the phase angle ϕ of the voltage on reflection from the termination Z_T is determined when the positions of the maxima have been found.

If the terminal impedance is a short circuit, i.e. $Z_T = 0$, $k = -1$ and $\phi = \pi$, the position of the maxima y_0 is given by,

$$y_0 = \frac{\pi(n + \frac{1}{2})}{\beta_0}$$

When the terminating impedance is a short circuited length of line containing liquid, the phase angle becomes $\pi + \phi$, and the new position of the maxima y' is given by,

$$y' = \frac{1}{\beta_0} (n\pi + \frac{\pi}{2} + \frac{\phi}{2})$$

So that the shift of the maxima as liquid enters above the short circuit is $y' - y_0$, i.e.,

$$y' - y_0 = \frac{\phi}{2\beta_0} = \frac{\phi\lambda_0}{4\pi} = \Delta \dots\dots\dots(1.18)$$

This shift Δ of the maxima (or minima) can be found experimentally, and so the phase angle of equation (1.13) due to the introduction of a depth l of liquid dielectric in a short circuited transmission line, can be calculated by multiplying the observed shift Δ by $\frac{4\pi}{\lambda_0}$, for from equation (1.18)

$$\phi = \frac{4\pi}{\lambda_0} \Delta \dots\dots\dots(1.19)$$

Since a shift Δ of $\lambda_0/4$ may equally well be interpreted as a shift of minus $\lambda_0/4$, the phase angle ϕ may be considered to lie always in the range plus $2\beta_0\lambda_0/4$ to minus $2\beta_0\lambda_0/4$, that is from plus π to minus π .

Equation (1.13) may be expressed in terms of the phase shift using equation (1.19):-

$$\Delta = \frac{\lambda_0}{4\pi} \tan^{-1} \left\{ \frac{2\beta_0(\alpha \operatorname{sh} 2\alpha l + \beta \sin 2\beta l)}{(\beta_0^2 - \alpha^2 - \beta^2) \operatorname{ch} 2\alpha l - (\beta_0^2 + \alpha^2 + \beta^2) \cos 2\beta l} \right\} \dots\dots\dots(1.20)$$

This equation was verified experimentally by observing the shift Δ caused by the introduction of

different depths l of liquids into a short circuited line coaxial transmission). The form of the graph of Δ against l depends upon the attenuation coefficient and phase constant of the liquid used, and it has been found possible to deduce values for α and β from these graphs. The effect of the liquid dielectric is discussed in the next paragraph.

1.5 Theoretical discussion of the variation of phase angle with liquid depth for different liquids.

Equation (1.13) may be written:-

$$\tan \phi = - \frac{2\beta_0\beta}{(\beta^2 + \alpha^2 + \beta_0^2)} \left\{ \frac{\sin 2\beta l + \frac{\alpha \sinh 2\alpha l}{\beta}}{\cos 2\beta l + \frac{\beta^2 + \alpha^2 - \beta_0^2}{\beta^2 + \alpha^2 + \beta_0^2} \cosh 2\alpha l} \right\} \dots\dots\dots(1.21)$$

1.5.1 Non-absorbing liquids.

For non-absorbing liquids $\alpha = 0$, and equation (1.21) becomes:-

$$\tan \phi = - \frac{2\beta_0\beta}{\beta^2 + \beta_0^2} \left\{ \frac{\sin 2\beta l}{\cos 2\beta l + \frac{\beta^2 - \beta_0^2}{\beta^2 + \beta_0^2}} \right\}$$

Thus, neglecting the constant term

$$\frac{2\beta_0\beta}{\beta^2 + \beta_0^2} ,$$

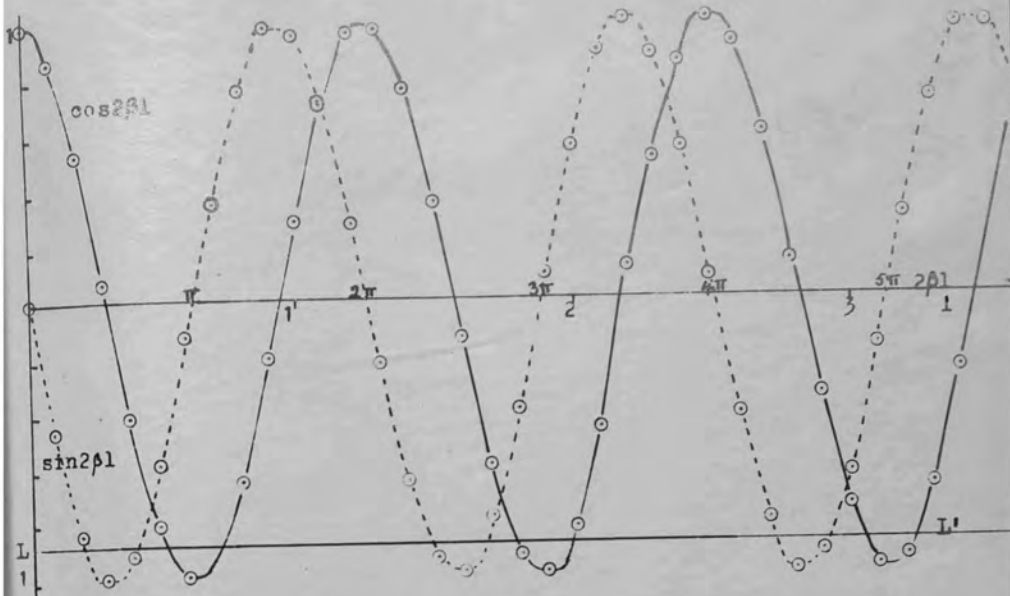


Fig. 1.3 $\beta_0 = 0.6, \alpha = 0, \beta = 2.5$

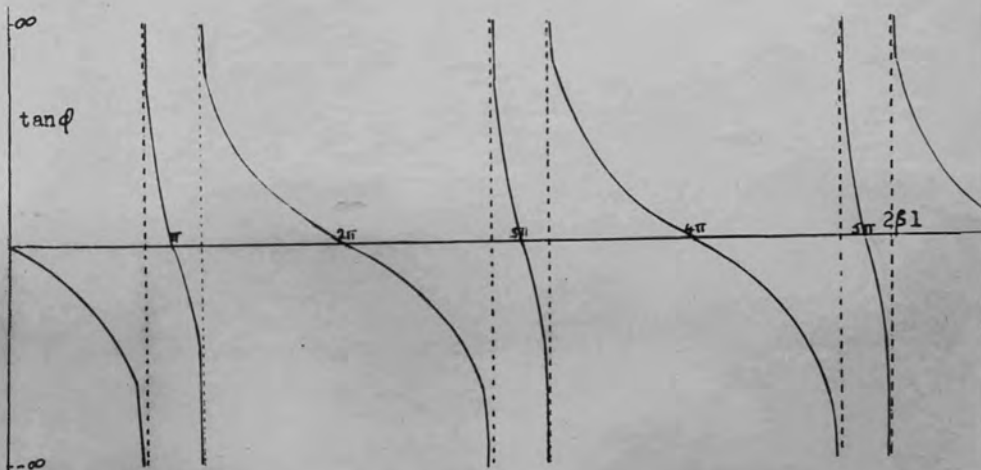


Fig. 1.4 The variation of $\tan \phi$ with l .

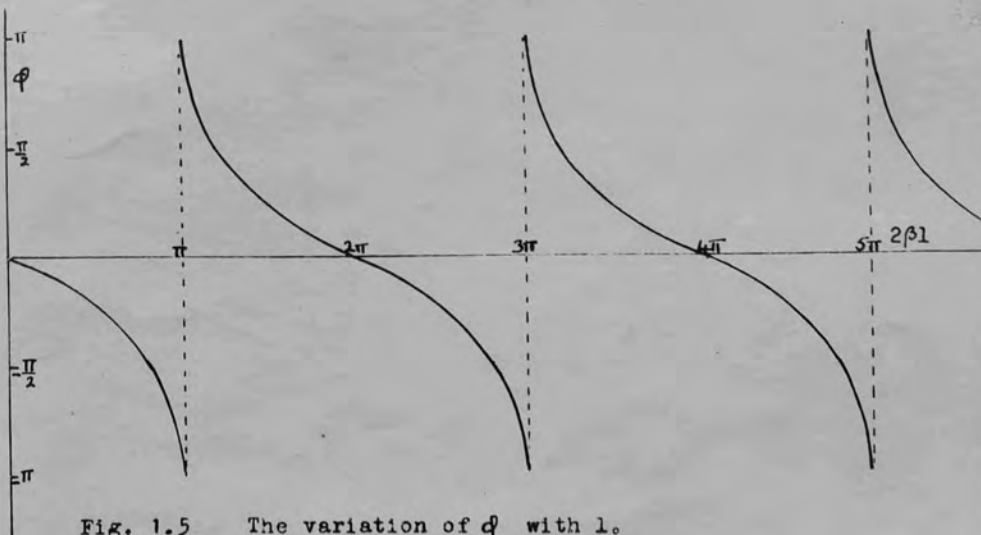


Fig. 1.5 The variation of ϕ with l .

the numerator of $\tan \phi$ is given by $\sin 2\beta l$, and the denominator by the height of the $\cos 2\beta l$ curve above the line

$$y = \frac{\beta^2 - \beta_0^2}{\beta^2 + \beta_0^2}$$

(LL' in fig. 1.3). Thus $\tan \phi$ is zero when $\sin 2\beta l$ is zero, and approaches infinity when $\cos 2\beta l$ and the line LL' intersect, (denominator zero). The curves for $\tan \phi$ and ϕ (ϕ being considered to lie always between plus and minus π) against $2\beta l$ are shown in figs. (1.4) and (1.5). For figs. (1.3), (1.4) and (1.5) the arbitrary values chosen for β_0 and β were 0.6 and 2.5 respectively, giving for LL' Values

$$y = 0.89$$

and corresponding to a liquid with a dielectric constant of 17.

If $\beta = \beta_0$, i.e. an air filled line, LL' coincides with the $2\beta l$ axis and $\tan \phi$ becomes infinite at $\pi/2$.

(See fig. 1.6)

As the ratio of β/β_0 increases, LL' moves downwards and its points of intersection with $\cos 2\beta l$ close up in pairs so that the gradients of $\tan \phi$ and ϕ become relatively less steep in the range

$$\phi = +\frac{\pi}{2} \text{ to } -\frac{\pi}{2}$$

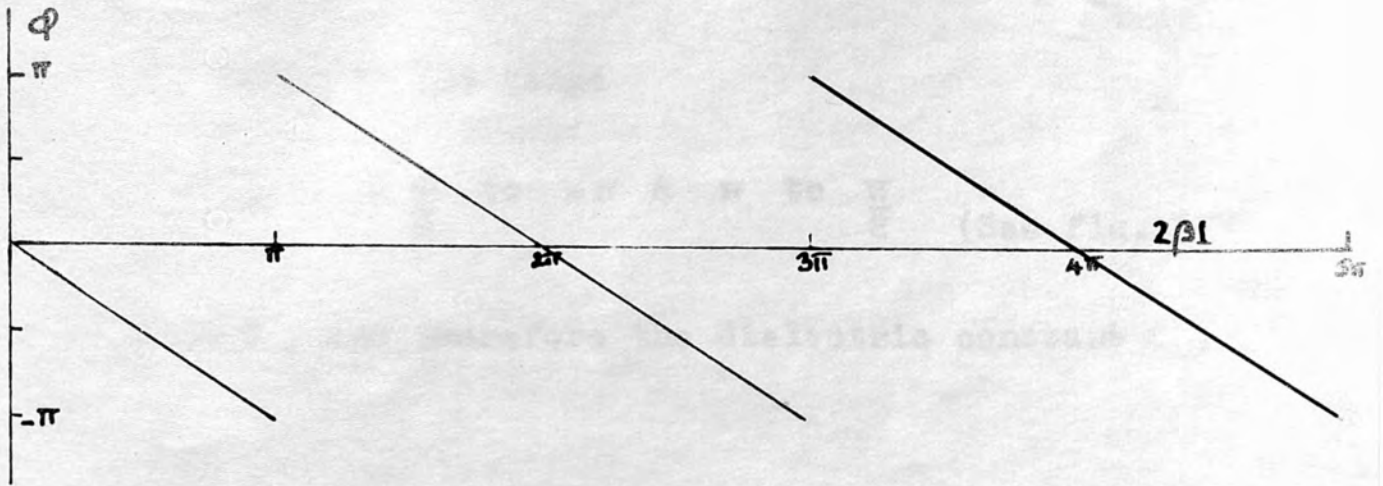


Fig. 1.6 $\beta_0 = \beta$

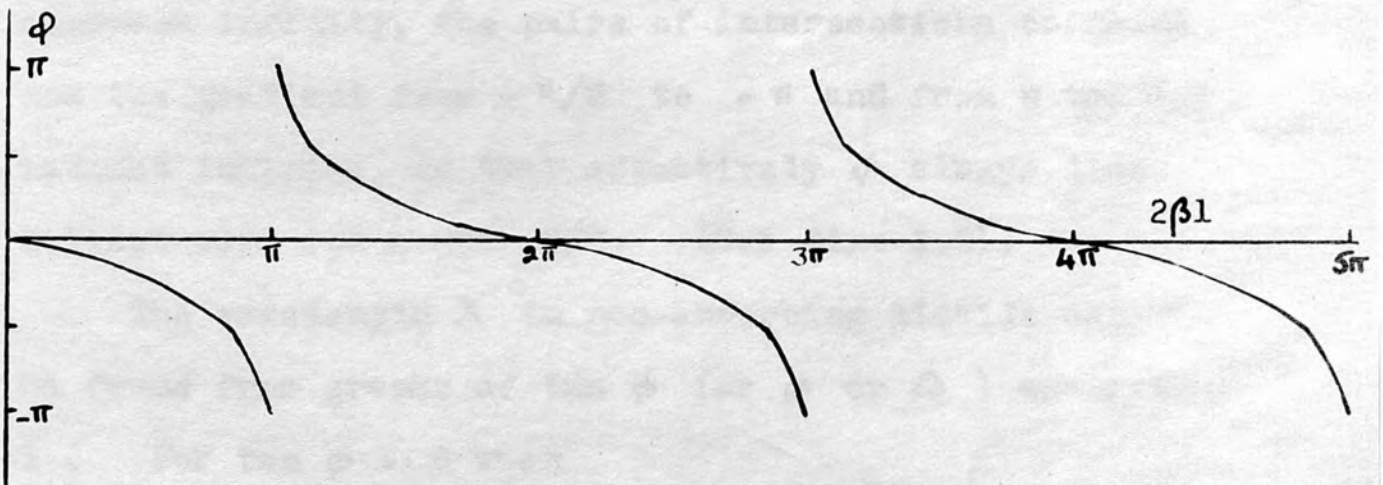


Fig. 1.7

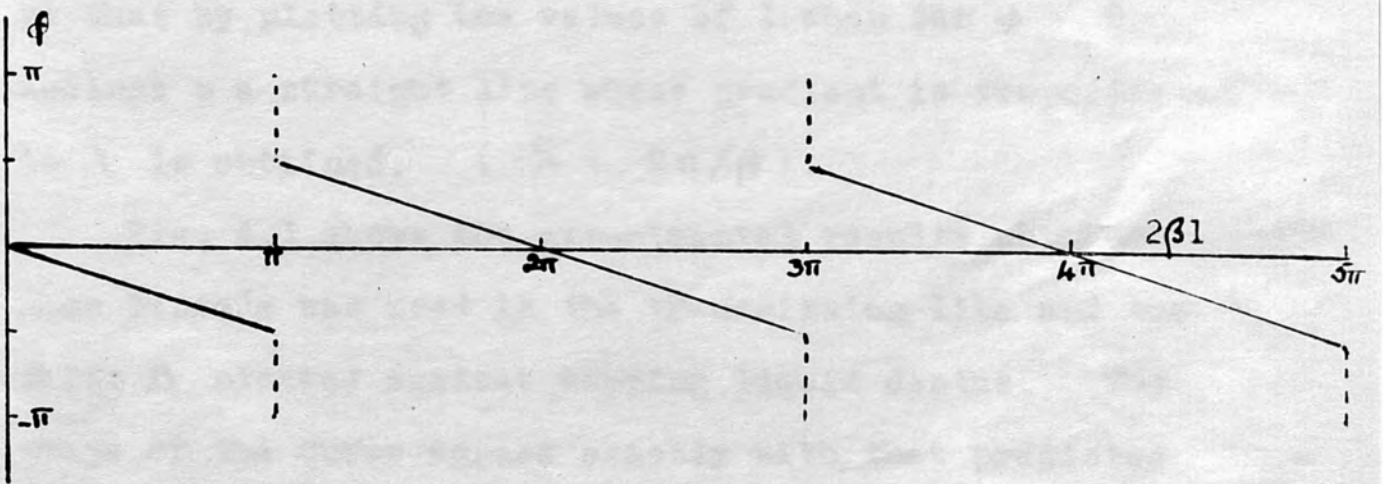


Fig. 1.8 $\beta \rightarrow \infty$

and more steep in the range

$$\phi = -\frac{\pi}{2} \text{ to } -\pi \text{ \& \ } \pi \text{ to } \frac{\pi}{2} \quad (\text{See fig. 1.7})$$

When β , and therefore the dielectric constant ϵ ,
for

$$\epsilon = \left(\frac{\lambda_0}{\lambda}\right)^2 = \left(\frac{\beta}{\beta_0}\right)^2$$

approach infinity, the pairs of intersections coincide
and the gradient from $-\pi/2$ to $-\pi$ and from π to $\pi/2$
becomes infinite, so that effectively ϕ always lies
between plus and minus $\pi/2$. (See fig. 1.8).

The wavelength λ in non-absorbing liquids can
be found from graphs of $\tan \phi$ (or ϕ or Δ) against
 l . For $\tan \phi = 0$ when

$$2\beta l = n\pi$$

so that by plotting the values of l when $\tan \phi = 0$
against n a straight line whose gradient is proportional
to λ is obtained. ($\lambda = 2\pi/\beta$).

Fig. 4.1 shows the experimental results obtained
when benzole was used in the transmission line and the
shift Δ plotted against varying liquid depths. The
shape of the curve agrees exactly with that predicted
by the above theory.

1.5.2 Absorbing liquids.

For absorbing liquids $\alpha > 0$, and equation (1.21) applies.

$$\tan \phi = - \frac{2\beta_0\beta}{(\beta^2 + \alpha^2 + \beta_0^2)} \left\{ \frac{\sin 2\beta l + \frac{\alpha \sinh 2\alpha l}{\beta}}{\cos 2\beta l + \left(\frac{\beta^2 + \alpha^2 - \beta_0^2}{\beta^2 + \alpha^2 + \beta_0^2} \right) \cosh 2\alpha l} \right\} \dots (1.21)$$

Thus neglecting the constant term,

$$\frac{2\beta_0\beta}{\beta^2 + \alpha^2 + \beta_0^2}$$

the numerator of $\tan \phi$ is given by the height of the curve

$$y = -\sin 2\beta l \quad \text{above} \quad y = \frac{\alpha \sinh 2\alpha l}{\beta}$$

and the denominator by the height of

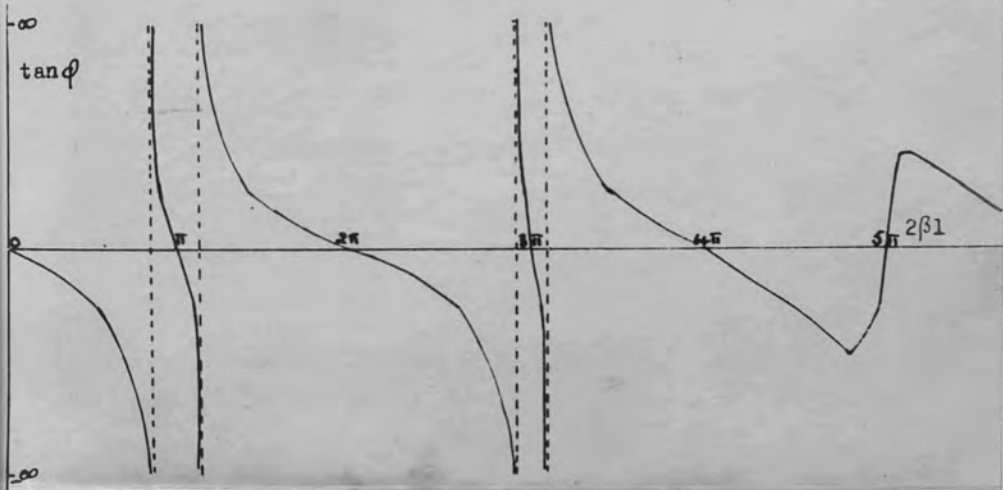
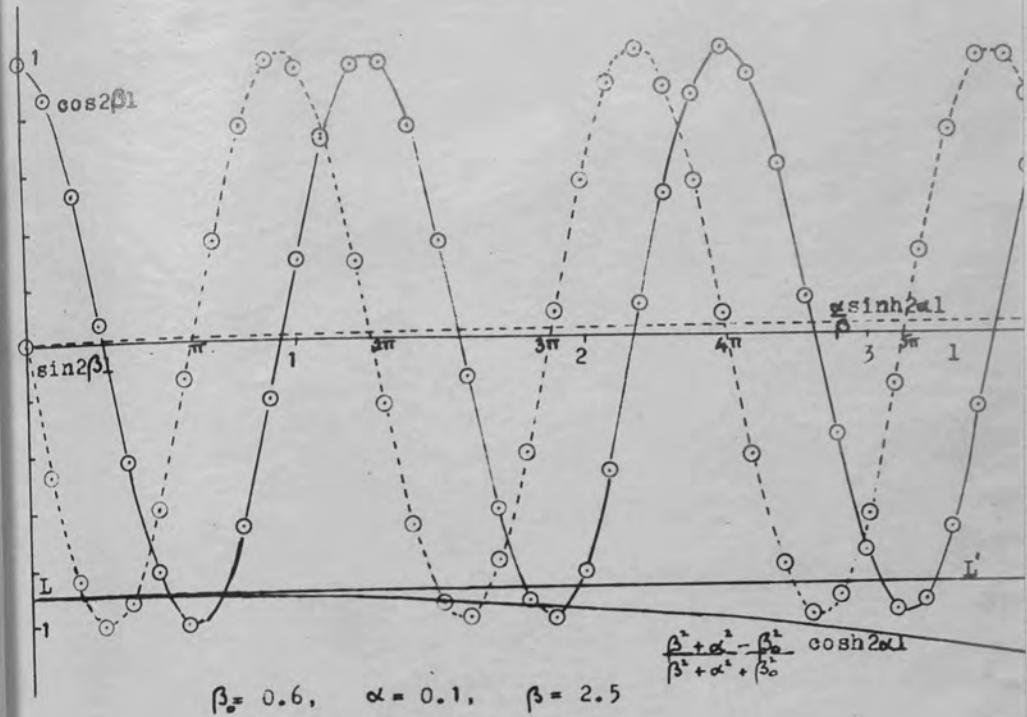
$$y = \cos 2\beta l \quad \text{above} \quad y = \frac{\beta^2 + \alpha^2 - \beta_0^2}{\beta^2 + \alpha^2 + \beta_0^2} \cosh 2\alpha l$$

This is illustrated in fig. 1.9 with the arbitrary values,

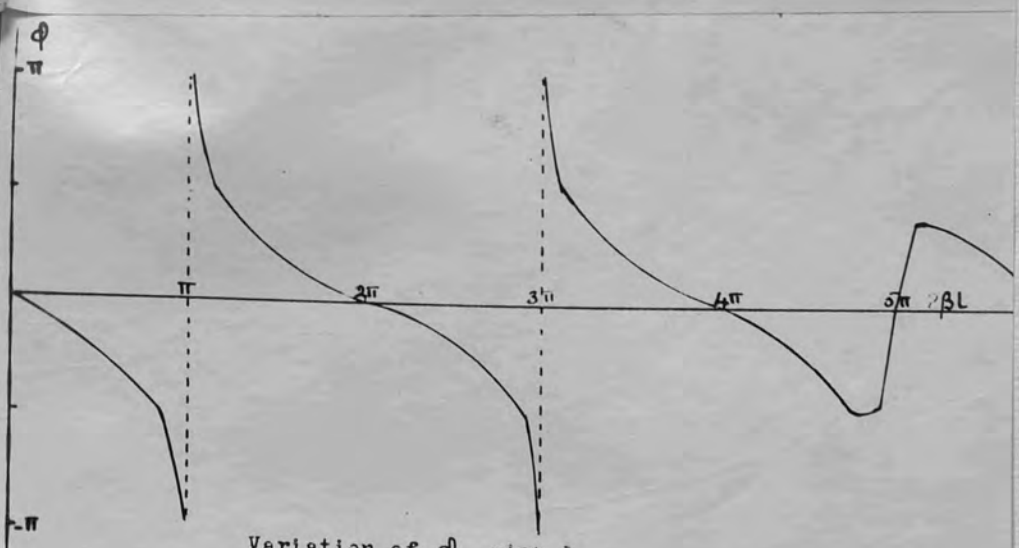
$$\beta_0 = 0.6 \quad \beta = 2.5 \quad \alpha = 0.1$$

The effect of the term containing α in the numerator is to shift the zeros of $\tan \phi$ (and of ϕ) slightly, alternate zeros being shifted in opposite directions.

The effect of the term containing α in the denominator is to replace the line LL' by an inverted



The variation of $\tan \phi$ with l .



Variation of ϕ with l .

Fig. 1.9

cosh curve, so that the points of intersection of the cosine and cosh curves, which give the positions at which $\tan \phi$ approaches infinity, are closer the greater the depth of the liquid. Eventually the two curves do not intersect, and $\tan \phi$ no longer reaches infinity. ϕ then has minima and maxima which are respectively greater than $-\pi/2$ and less than $\pi/2$.

As l approaches infinity,

$$\cosh 2\alpha l \rightarrow \sinh 2\alpha l$$

and both functions approach infinity. Equation (1.13) may be written,

$$\tan \phi = - \frac{2\beta_0 \left\{ \frac{\beta \sin 2\beta l}{\cosh 2\alpha l} + \alpha \tanh 2\alpha l \right\}}{(\beta^2 + \alpha^2 + \beta_0^2) \frac{\cos 2\beta l}{\cosh 2\alpha l} + (\beta^2 + \alpha^2 - \beta_0^2)} \dots\dots(1.22)$$

$\tanh 2\alpha l$ differs from 1 by less than 1% if $2\alpha l$ is greater than 2.65, and $\sinh 2\alpha l$ and $\cosh 2\alpha l$ approach infinity for $2\alpha l$ greater than about 5. So that under these conditions,

$$\tan \phi \rightarrow - \frac{2\beta_0 \alpha}{\beta^2 + \alpha^2 - \beta_0^2} \dots\dots\dots(1.23)$$

Since $\beta \gg \beta_0$, this expression must be negative and therefore $\tan \phi$ (and ϕ and Δ) will eventually settle down to a steady negative value.

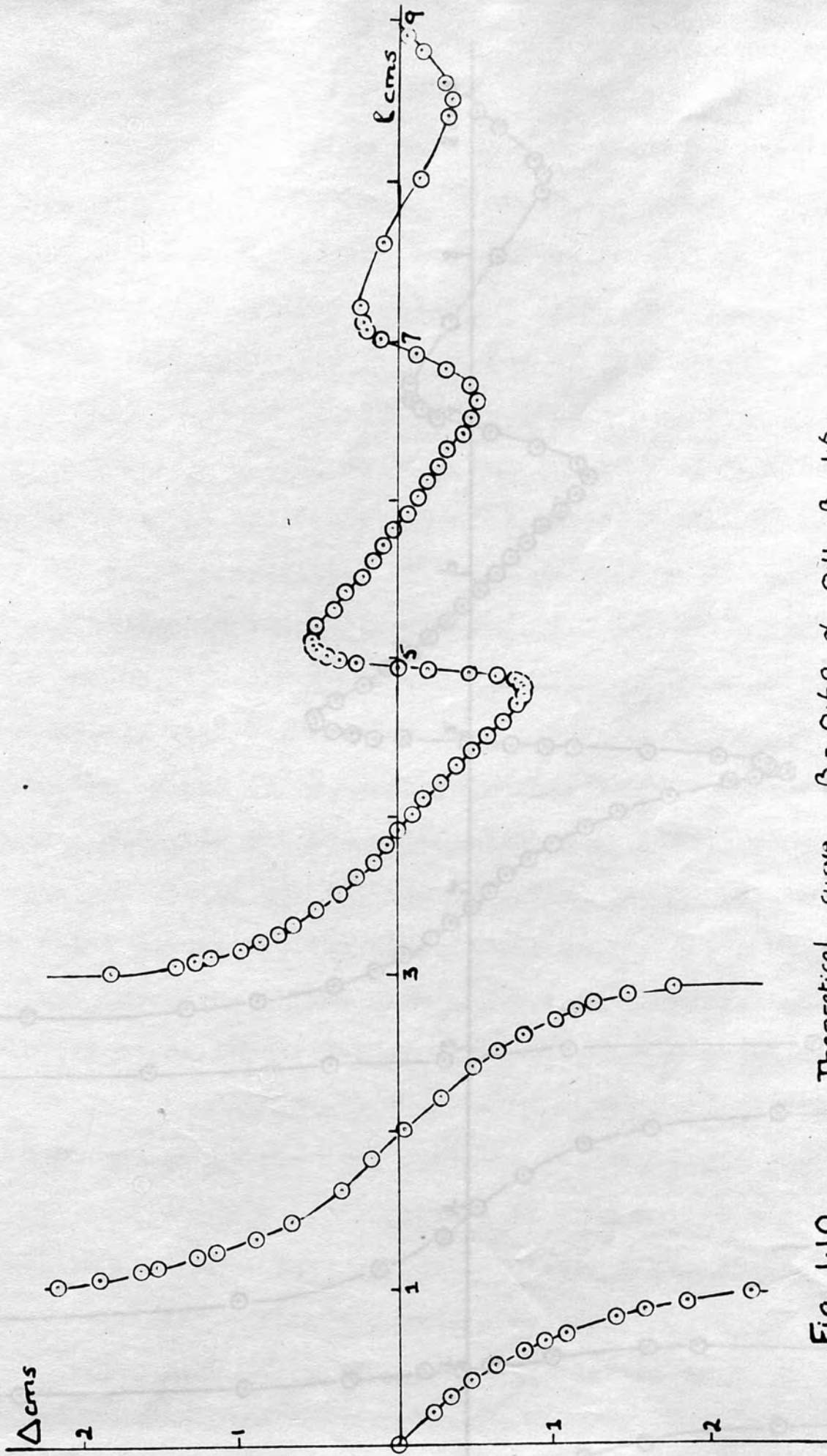
1.5.3 The effect of α and β on the variation of $\tan \phi$ with l .

At a wavelength of 10 cms, liquids at room temperature show a variation in α from 0 to about 0.8 nepers cms⁻¹, and in β from slightly greater than 1 to about 6 radians cms⁻¹.

1.5.3.1 Liquids with low values of both α and β .

The effect of a liquid with a value of β only slightly greater than one, which corresponds to a wavelength λ in the liquid of the order of 6 cms, is to expand the sine and cosine curves of fig. 1.9 laterally. With a small value for α , of the order of 0.01, the term in $\sinh 2\alpha l$ is going to have very little effect, while the inverted cosh term will start at about - 0.5 and will increase only slowly in value intersecting the cosine curve several times before reaching a value greater than 1. The $\tan \phi$ curve then no longer goes off to infinity but has turning points, the value of $\tan \phi$ at these turning points gradually decreasing as l increases until the liquid depth is about 200 cms when $\tan \phi$ will have a constant negative value.

Figs. 1.10 and 1.11 show graphs of the variation of Δ and $\tan \phi$ with l calculated from equations (1.13) and (1.19) for $\beta_0 = 0.69$, $\alpha = 0.11$, & $\beta = 1.6$.



Theoretical curve $\beta_0 = 0.6q$, $\alpha = 0.11$, $\beta = 1.6$

Fig. 1.10

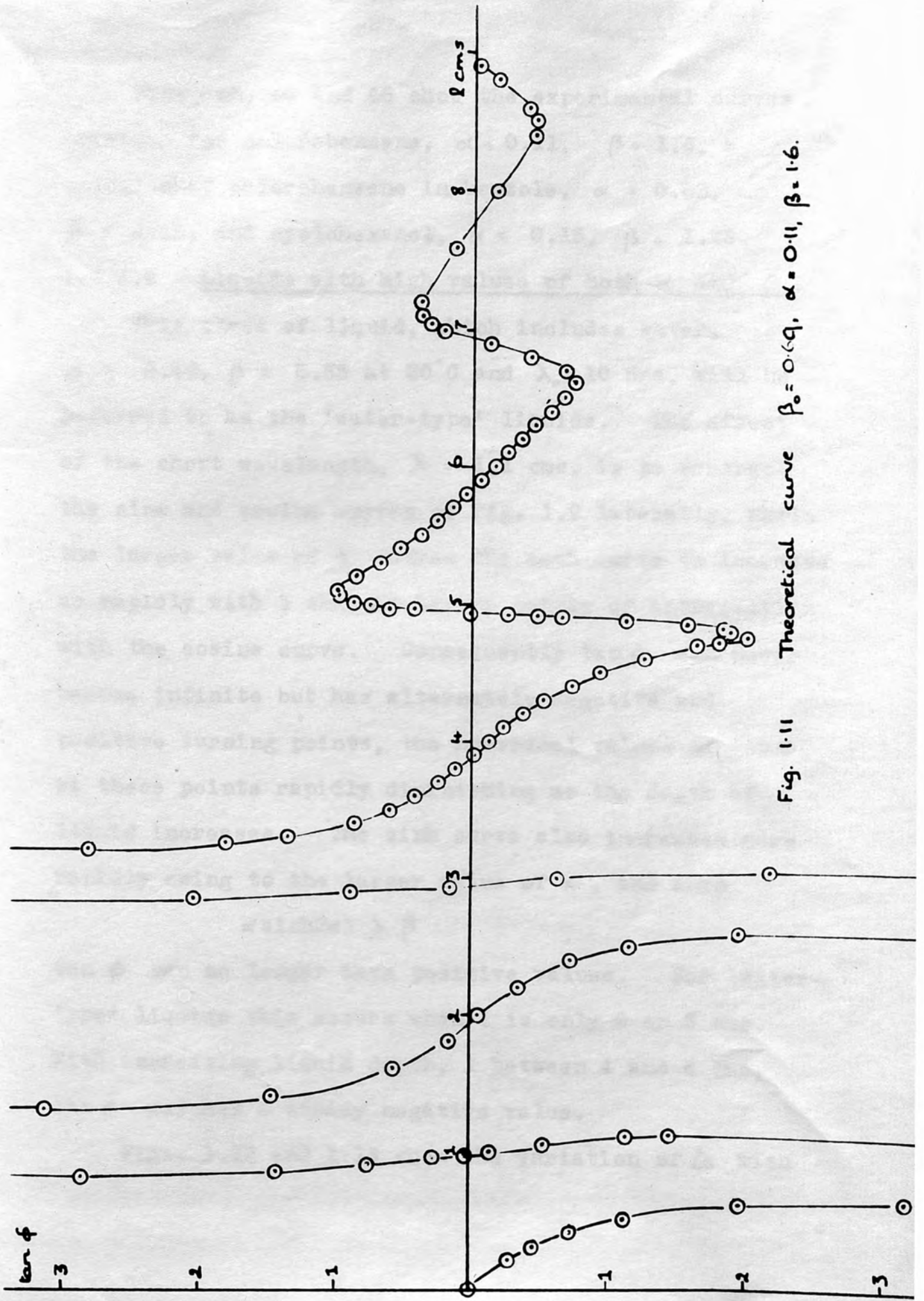


Fig. 1-11 Theoretical curve $\beta_0 = 0.69$, $\alpha = 0.11$, $\beta = 1.6$.

Figs. 43, 44 and 45 show the experimental curves obtained for chlorobenzene, $\alpha = 0.11$, $\beta = 1.6$, a solution of chlorobenzene in benzole, $\alpha = 0.08$, $\beta = 1.45$; and cyclohexanol, $\alpha = 0.15$, $\beta = 1.23$.

1.5.3.2 Liquids with high values of both α and β .

This class of liquid, which includes water, $\alpha = 0.46$, $\beta = 5.55$ at 20°C and $\lambda_0 = 10$ cms, will be referred to as the 'water-type' liquids. The effect of the short wavelength, $\lambda = 1.1$ cms, is to contract the sine and cosine curves of fig. 1.9 laterally, while the larger value of α causes the cosh curve to increase so rapidly with l that it has no points of intersection with the cosine curve. Consequently $\tan \phi$ can never become infinite but has alternately negative and positive turning points, the numerical values of $\tan \phi$ at these points rapidly diminishing as the depth of liquid increases. The sinh curve also increases more rapidly owing to the larger value of α , and when

$$\alpha \sinh 2\alpha l > \beta$$

$\tan \phi$ can no longer have positive values. For 'water-type' liquids this occurs when l is only 2 or 3 cms. With increasing liquid depth, l between 4 and 6 cms, $\tan \phi$ assumes a steady negative value.

Figs. 1.12 and 1.13 show the variation of Δ with

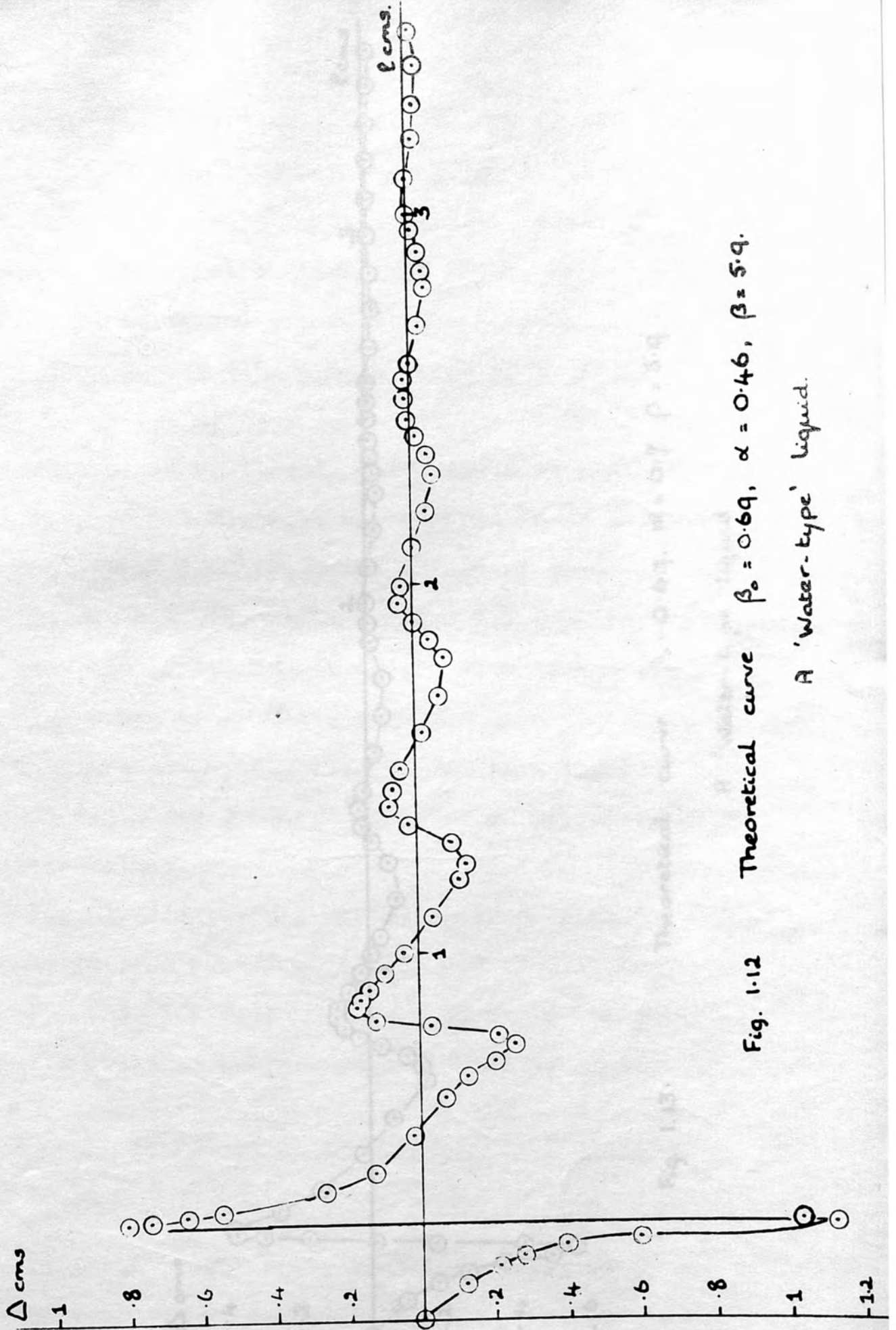
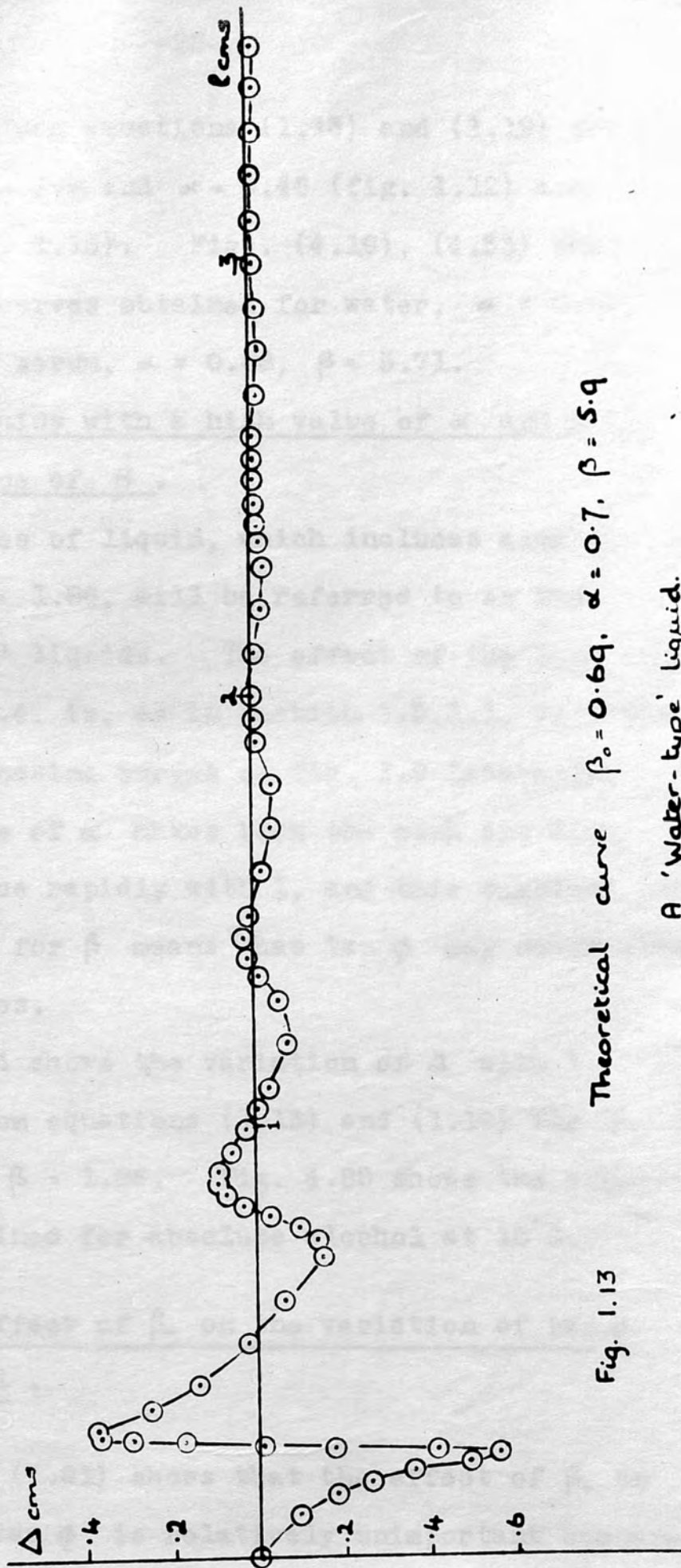


Fig. 1.12 Theoretical curve $\beta_0 = 0.69$, $\alpha = 0.46$, $\beta = 5.9$.
A 'water-type' liquid.



Theoretical curve $\beta_0 = 0.69$, $\alpha = 0.7$, $\beta = 5.9$

A 'Water-type' liquid.

Fig. 1.13

l calculated from equations (1.13) and (1.19) for $\beta_0 = 0.69$, $\beta = 5.9$ and $\alpha = 0.46$ (fig. 1.12) and $\alpha = 0.7$ (fig. 1.13). Figs. (4.19), (4.33) show the experimental curves obtained for water, $\alpha = 0.57$, $\beta = 5.99$, ox serum, $\alpha = 0.68$, $\beta = 5.71$.

1.5.3.3 Liquids with a high value of α and a low value of β .

This class of liquid, which includes alcohol, $\alpha = 0.7$, $\beta = 1.86$, will be referred to as the 'alcohol-type' liquids. The effect of the long wavelength, $\lambda = 3.4$, is, as in section 1.5.3.1, to expand the sine and cosine curves of fig. 1.9 laterally. The high value of α makes both the cosh and sinh curves increase rapidly with l, and this combined with a small value for β means that $\tan \phi$ may never attain positive values.

Fig. 1.14 shows the variation of Δ with l calculated from equations (1.13) and (1.19) for $\beta_0 = 0.69$, $\alpha = 0.7$ and $\beta = 1.86$. Fig. 4.80 shows the experimental curve obtained for absolute alcohol at 18°C.

1.5.4 The effect of β_0 on the variation of $\tan \phi$ with l.

Equation (1.21) shows that the effect of β_0 on the value of $\tan \phi$ is relatively unimportant compared

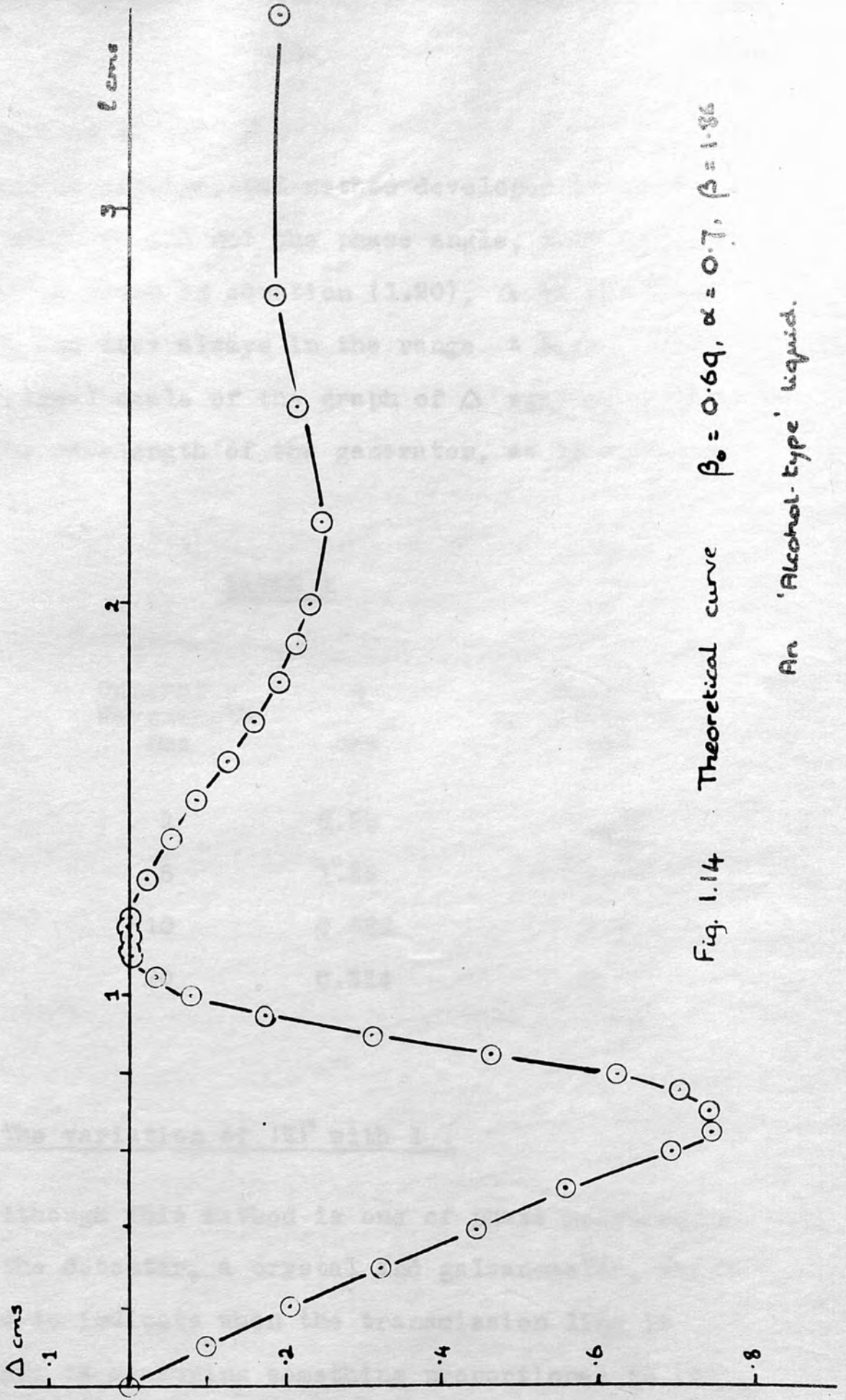


Fig. 1.14 Theoretical curve $\beta_0 = 0.69, \alpha = 0.7, \beta = 1.86$

An 'Alcohol-type' liquid.

with that of α and β .

In the experimental method developed it is the phase shift Δ and not the phase angle, that is measured, and, as is shown in equation (1.20), Δ varies directly with λ_0 and lies always in the range $\pm \lambda_0/4$. Hence the vertical scale of the graph of Δ against l depends upon the wavelength of the generator, as is shown in Table 1.

TABLE 1

Generator Wavelength cms	β_0 cms ⁻¹	Maximum variation of Δ cms
1	6.28	0.25
5	1.25	1.25
10	0.628	2.5
20	0.314	5

1.6 The variation of $|K|^2$ with l .

Although this method is one of phase measurement only, the detector, a crystal and galvanometer, which is used to indicate when the transmission line is resonant, is measuring something proportional to $|K|^2$,

where K, the ratio of the amplitude of the reflected to the incident voltage, is given by

$$k = K e^{j\phi}$$

Hence it is of interest to investigate the variation of $|K|^2$ with l .

From equation (1.12)

$$k = \frac{j\beta_0 \sinh(\alpha + j\beta)l - (\alpha + j\beta) \cosh(\alpha + j\beta)l}{j\beta_0 \sinh(\alpha + j\beta)l + (\alpha + j\beta) \cosh(\alpha + j\beta)l} \dots (1.12)$$

Multiplying by the complex conjugate, and putting

$$M = \alpha + j\beta$$

and $N = \alpha - j\beta$

$$\begin{aligned} |K|^2 &= \frac{\beta_0^2 \text{sh}Ml \text{sh}Nl + MN \text{ch}Ml \text{ch}Nl + j(\beta_0 M \text{ch}Ml \text{sh}Nl - \beta_0 N \text{sh}Ml \text{ch}Nl)}{\beta_0^2 \text{sh}Ml \text{sh}Nl + MN \text{ch}Ml \text{ch}Nl - j(\beta_0 M \text{ch}Ml \text{sh}Nl - \beta_0 N \text{sh}Ml \text{ch}Nl)} \\ &= \frac{\frac{1}{2}\beta_0^2 (\text{ch}2\alpha l - \text{ch}j2\beta l) + \frac{1}{2}(\alpha^2 + \beta^2) (\text{ch}2\alpha l + \text{ch}j2\beta l)}{D} \\ &\quad + \frac{-j\left\{\frac{1}{2}\beta_0 M (\text{sh}2\alpha l - \text{sh}j2\beta l) - \frac{1}{2}\beta_0 N (\text{sh}2\alpha l + \text{sh}j2\beta l)\right\}}{D} \dots (1.24) \end{aligned}$$

where D is

$$\begin{aligned} &\frac{1}{2}\beta_0^2 (\text{ch}2\alpha l - \cos 2\beta l) + \frac{1}{2}(\alpha^2 + \beta^2) (\text{ch}2\alpha l + \cos 2\beta l) \\ &- j\left\{\frac{1}{2}\beta_0 M (\text{sh}2\alpha l - j \sin 2\beta l) - \frac{1}{2}\beta_0 N (\text{sh}2\alpha l + j \sin 2\beta l)\right\} \end{aligned}$$

Whence writing

$$a = \beta_0^2 - \alpha^2 - \beta^2 \quad \text{and} \quad b = \beta_0^2 + \alpha^2 + \beta^2$$

$$|K|^2 = \frac{b \cosh 2\alpha l - a \cos 2\beta l - 2\beta(\beta \sinh 2\alpha l - \alpha \sin 2\beta l)}{b \cosh 2\alpha l - a \cos 2\beta l + 2\beta(\beta \sinh 2\alpha l - \alpha \sin 2\beta l)} \dots\dots(1.24)$$

1.7 An alternative method of deriving the $|K|^2$ equation.

Following the treatment of section 1.3, where

$$\frac{Z_T}{Z_0} = u + jv \dots\dots(1.14)$$

the reflection coefficient may be expressed,

$$k = \frac{u + jv - 1}{u + jv + 1}$$

Multiplying by the complex conjugate,

$$|K|^2 = \frac{u^2 - 2u + v^2 + 1}{u^2 + 2u + v^2 + 1} \dots\dots\dots(1.25)$$

From section 1.3

$$u = \frac{\beta \beta \sinh 2\alpha l - \beta \alpha \sin 2\beta l}{(\alpha^2 + \beta^2)(\cosh 2\alpha l + \cos 2\beta l)}$$

$$\text{and } v = \frac{\beta \alpha \sinh 2\alpha l + \beta \beta \sin 2\beta l}{(\alpha^2 + \beta^2)(\cosh 2\alpha l + \cos 2\beta l)}$$

$$\text{Let } |K|^2 = \frac{N}{D} = \frac{u^2 - 2u + v^2 + 1}{u^2 + 2u + v^2 + 1} \dots\dots\dots(1.25)$$

$$\text{and } u = \frac{X}{Z}, \quad v = \frac{Y}{Z}$$

$$\text{Hence } |K|^2 = \frac{X^2 + Y^2 + Z(Z-2X)}{X^2 + Y^2 + Z(Z+2X)} = \frac{N}{D}$$

and substituting the values of u and v given above

$$\begin{aligned}
 N &= \beta_0^2(\alpha^2 + \beta^2) \text{sh}^2 2\alpha l + \beta_0^2(\alpha^2 + \beta^2) \text{sin}^2 2\beta l + (\alpha^2 + \beta^2)^2 (\text{ch} 2\alpha l + \cos 2\beta l)^2 \\
 &\quad - 2\beta_0(\beta \text{sh} 2\alpha l - \alpha \text{sin} 2\beta l) (\alpha^2 + \beta^2) (\text{ch} 2\alpha l + \cos 2\beta l) \\
 &= (\alpha^2 + \beta^2) \left\{ \beta_0^2 (\text{ch}^2 2\alpha l - \cos^2 2\beta l) + (\alpha^2 + \beta^2) (\text{ch} 2\alpha l + \cos 2\beta l)^2 \right. \\
 &\quad \left. - 2\beta_0(\beta \text{sh} 2\alpha l - \alpha \text{sin} 2\beta l) (\text{ch} 2\alpha l + \cos 2\beta l) \right\} \\
 &= (\alpha^2 + \beta^2) (\text{ch} 2\alpha l + \cos 2\beta l) \left\{ (\beta_0^2 + \alpha^2 + \beta^2) \text{ch} 2\alpha l \right. \\
 &\quad \left. + (\alpha^2 + \beta^2 - \beta_0^2) \cos 2\beta l - 2\beta_0(\beta \text{sh} 2\alpha l - \alpha \text{sin} 2\beta l) \right\}
 \end{aligned}$$

Similarly,

$$\begin{aligned}
 D &= (\alpha^2 + \beta^2) (\text{ch} 2\alpha l + \cos 2\beta l) \left\{ (\beta_0^2 + \alpha^2 + \beta^2) \text{ch} 2\alpha l \right. \\
 &\quad \left. + (\alpha^2 + \beta^2 - \beta_0^2) \cos 2\beta l + 2\beta_0(\beta \text{sh} 2\alpha l - \alpha \text{sin} 2\beta l) \right\}
 \end{aligned}$$

Therefore,

$$\frac{N}{D} = \frac{(\beta_0^2 + \alpha^2 + \beta^2) \text{ch} 2\alpha l + (\alpha^2 + \beta^2 - \beta_0^2) \cos 2\beta l - 2\beta_0(\beta \text{sh} 2\alpha l - \alpha \text{sin} 2\beta l)}{(\beta_0^2 + \alpha^2 + \beta^2) \text{ch} 2\alpha l + (\alpha^2 + \beta^2 - \beta_0^2) \cos 2\beta l + 2\beta_0(\beta \text{sh} 2\alpha l - \alpha \text{sin} 2\beta l)}$$

or putting $a = \beta_0^2 - \alpha^2 - \beta^2$ and $b = \beta_0^2 + \alpha^2 + \beta^2$

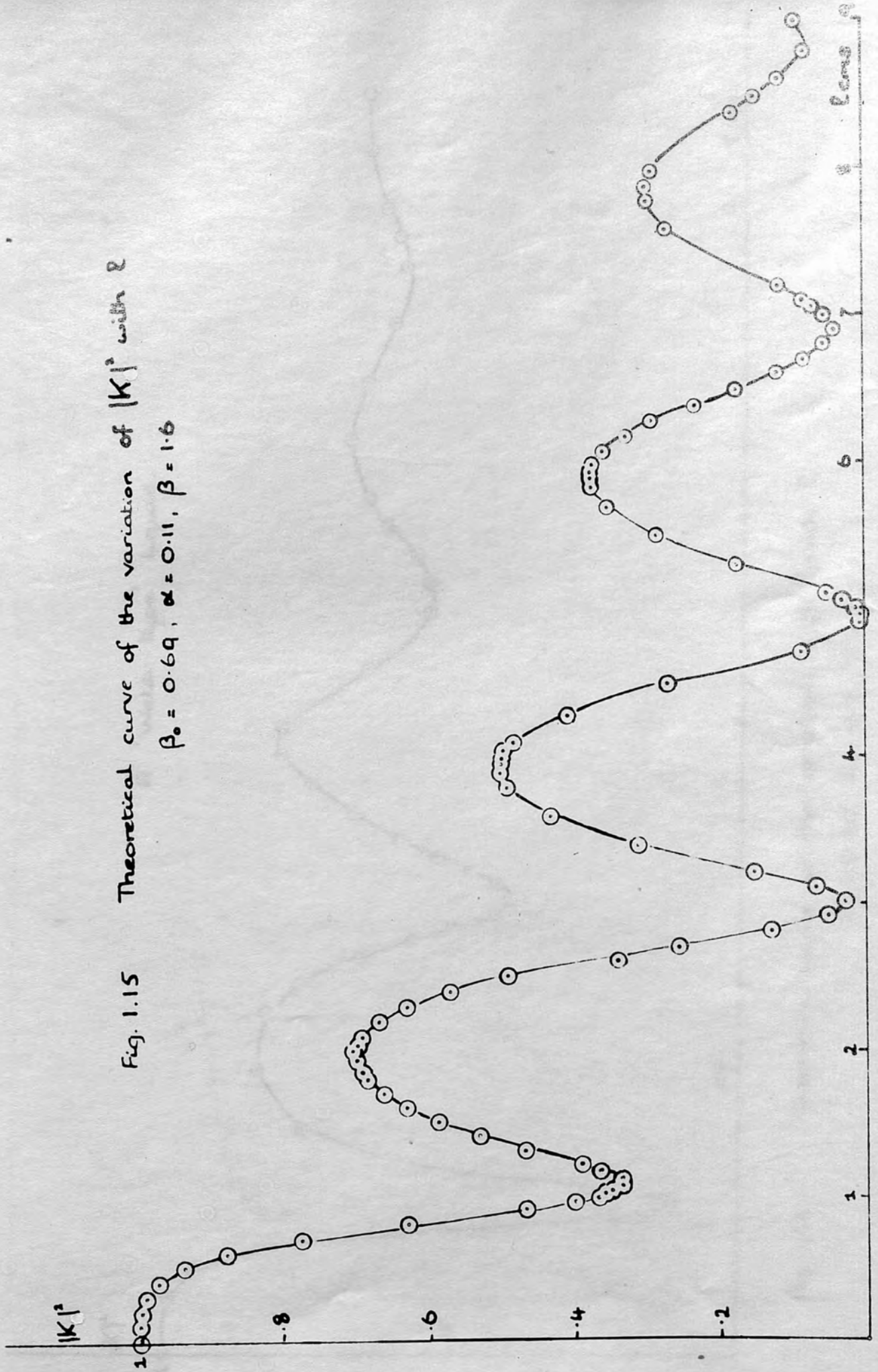
$$|K|^2 = \frac{b \text{ch} 2\alpha l - a \cos 2\beta l - 2\beta_0(\beta \text{sh} 2\alpha l - \alpha \text{sin} 2\beta l)}{b \text{ch} 2\alpha l - a \cos 2\beta l + 2\beta_0(\beta \text{sh} 2\alpha l - \alpha \text{sin} 2\beta l)}$$

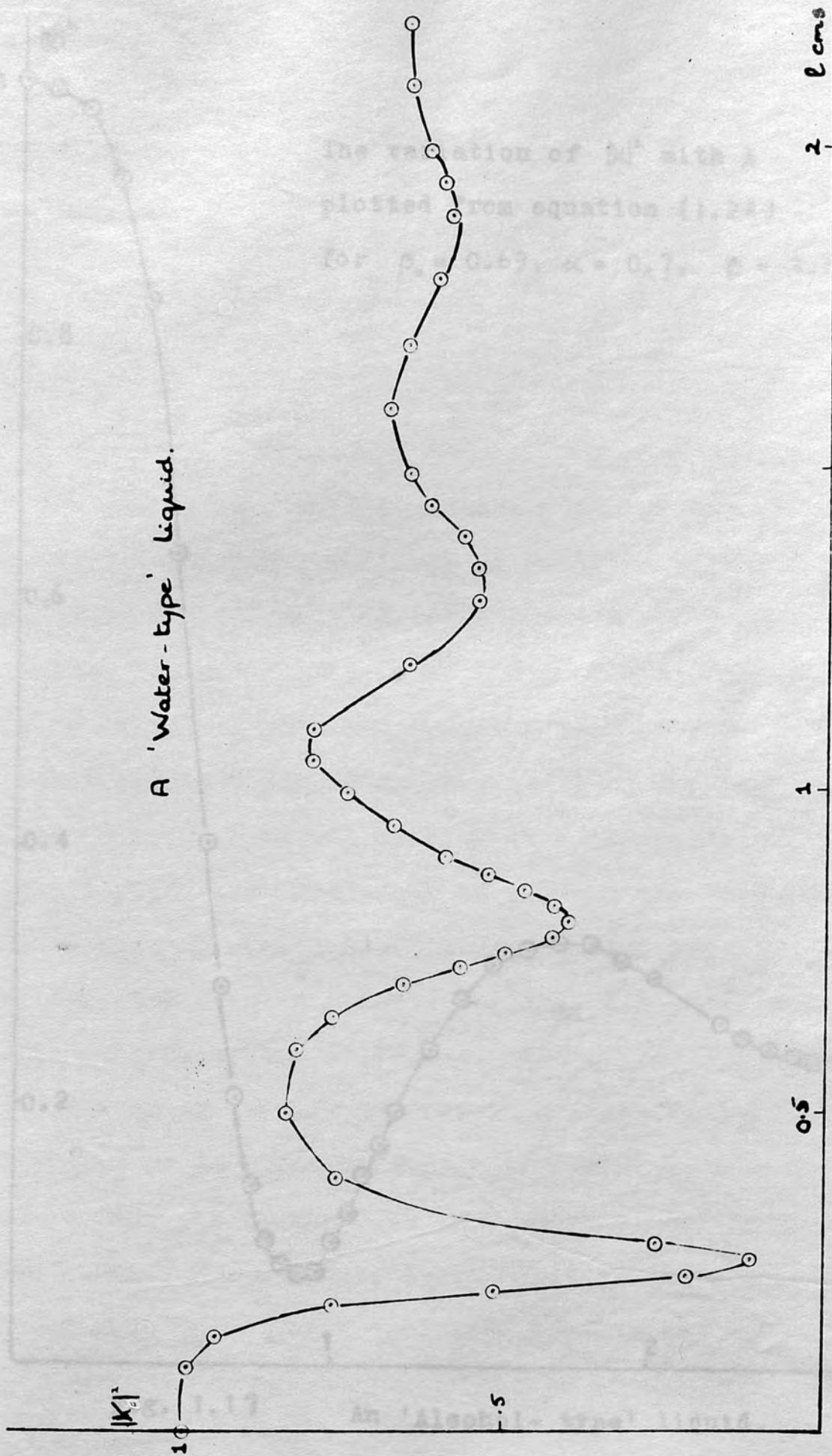
as in equation (1.24) of section 1.6.

Fig. 1.15 shows the variation of $|K|^2$ with l calculated from equation (1.24) for $\beta_0 = 0.69$, $\alpha = 0.11$, and $\beta = 1.6$ representing the behaviour for a liquid with low absorption, and fig. 1.16 shows the behaviour

for a 'water-type' liquid calculated for $\alpha = 0.7$ and $\beta = 5.9$, and fig. 1.17 for an 'alcohol-type' liquid calculated for $\alpha = 0.7$ and $\beta = 1.86$.

Fig. 1.15 Theoretical curve of the variation of $|K|^2$ with ξ
 $\beta_0 = 0.69, \alpha = 0.11, \beta = 1.6$





A 'Water-type' liquid.

Fig. 1.16 Theoretical curve of the variation of $|K|^2$ with l .
 $\beta_0 = 0.69, \alpha = 0.7, \beta = 5.9$

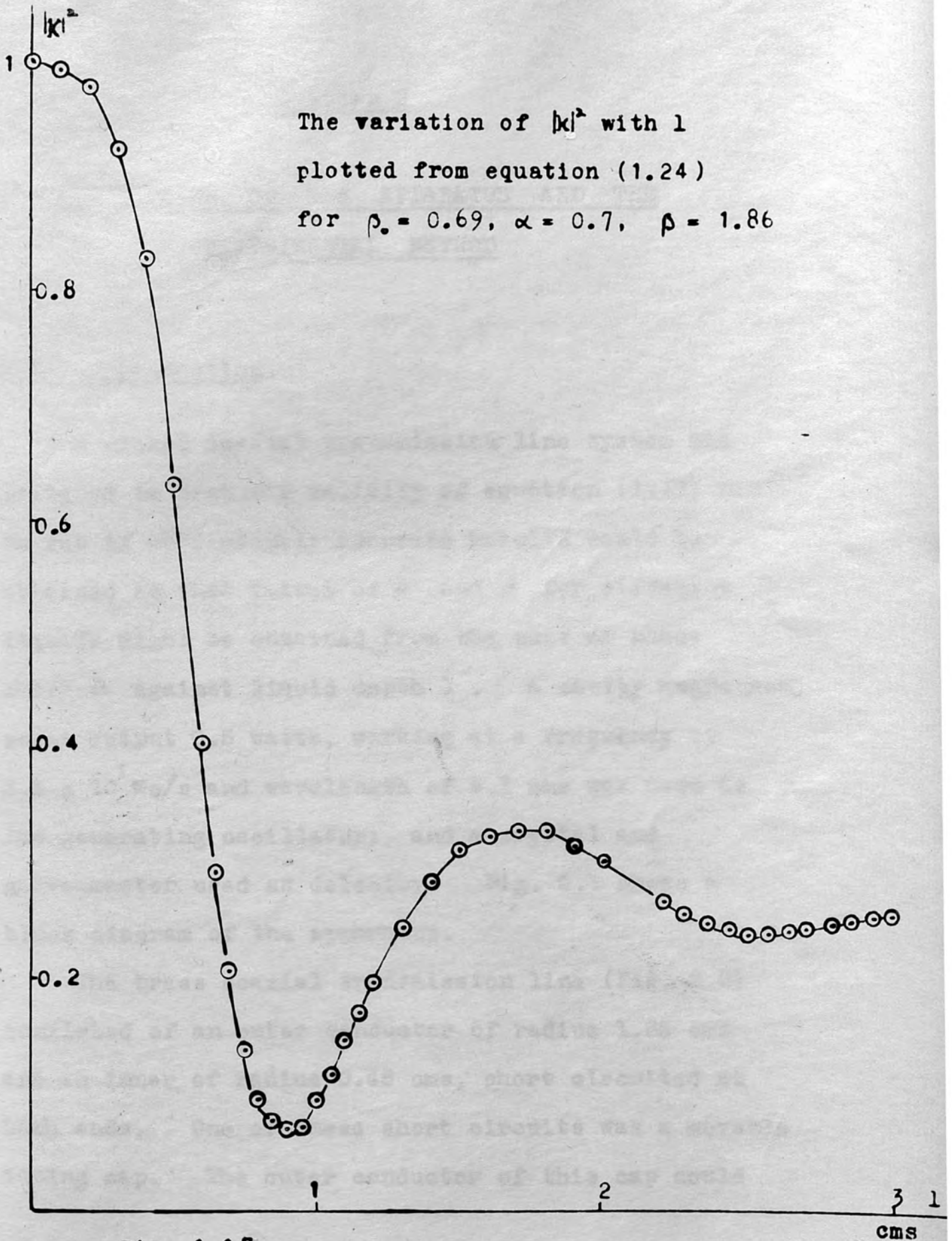


Fig. 1.17

An 'Alcohol-type' liquid.

cms

Chapter 2

DESCRIPTION OF THE APPARATUS AND THE EXPERIMENTAL METHOD

2.1 Introduction.

A closed coaxial transmission line system was designed to test the validity of equation (1.13) and to see if sufficiently accurate results could be obtained so that values of α and β for different liquids might be obtained from the plot of phase shift Δ against liquid depth l . A cavity magnetron, power output 0.5 watts, working at a frequency of 3.3×10^3 Mc/s and wavelength of 9.1 cms was used as the generating oscillator; and a crystal and galvanometer used as detector. Fig. 2.1 shows a block diagram of the apparatus.

The brass coaxial transmission line (Fig. 2.2) consisted of an outer conductor of radius 1.85 cms and an inner of radius 0.45 cms, short circuited at both ends. One of these short circuits was a movable tuning cap. The outer conductor of this cap could

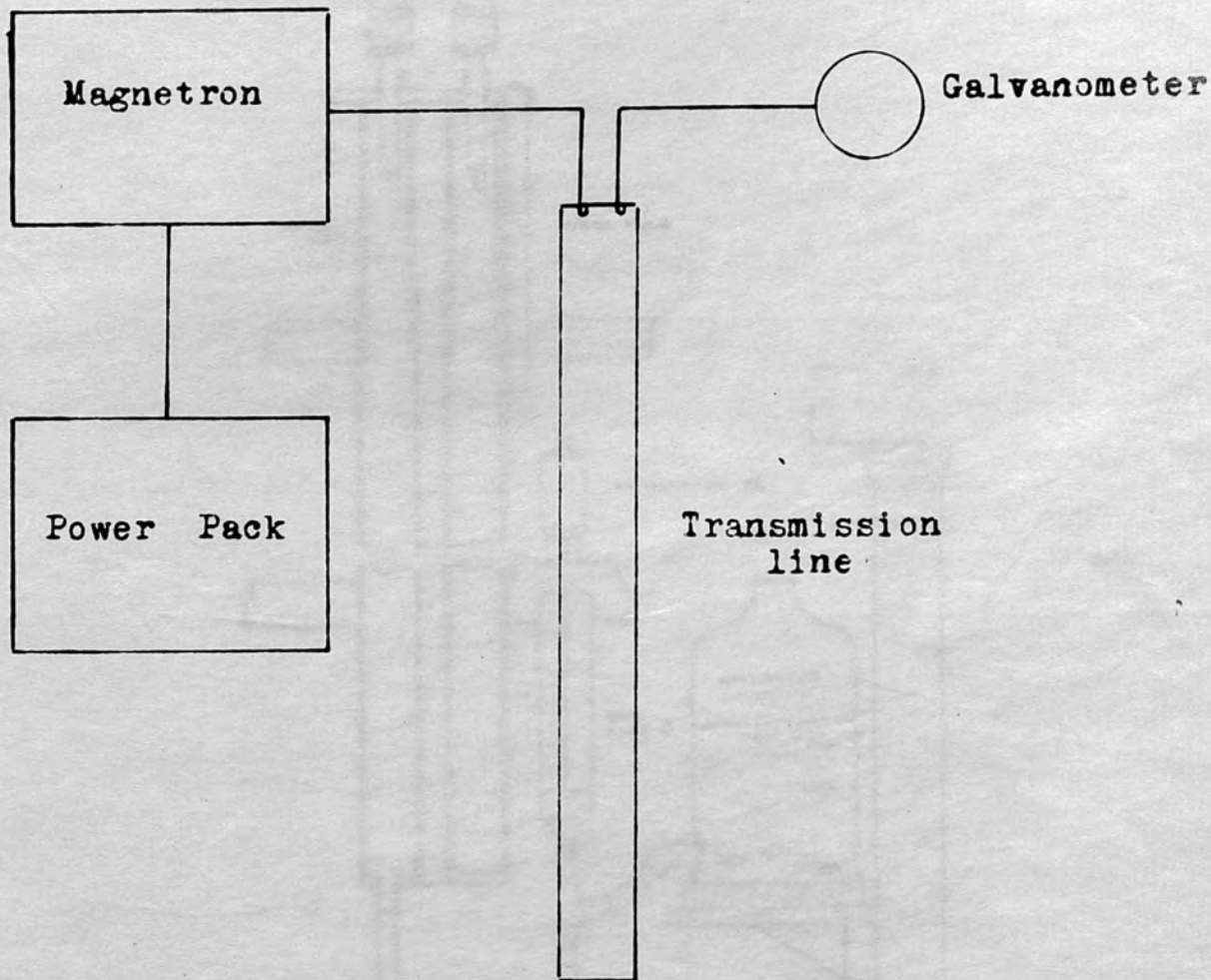


Fig.2.1 Block diagram of the apparatus.

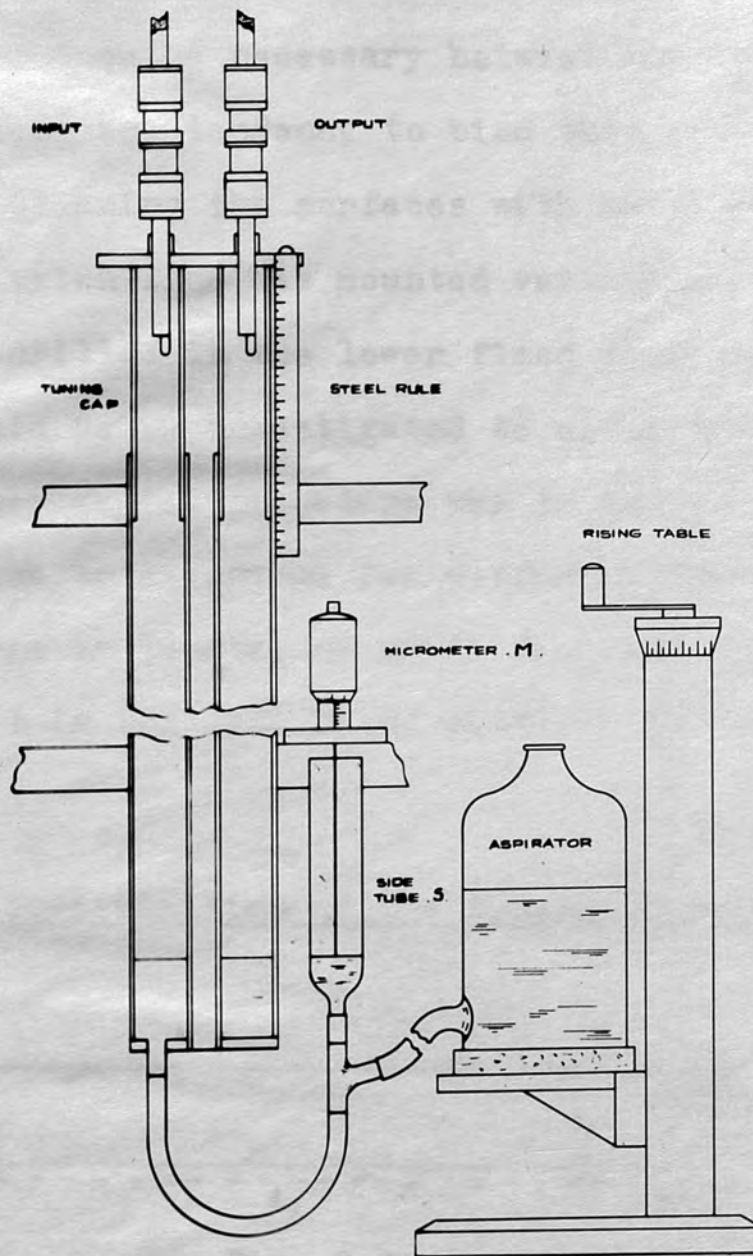


Fig. 2.2 Diagram of apparatus.

slide freely inside the outer conductor of the main line, while its inner conductor could slide freely over the inner of the main transmission line. No lubricant was found to be necessary between the two metal surfaces, but any tendency to bind that occurred was remedied by cleaning the surfaces with metal polish.

The transmission line was mounted vertically and a circular hole drilled in the lower fixed short circuit enabled the liquid being investigated to enter the line. The required experimental procedure was to adjust the length of the line to resonance for different liquid levels, the change in length, or shift Δ , and the depth of liquid l in the line being measured as accurately as possible.

2.2 A general investigation of the tuning of such a system.

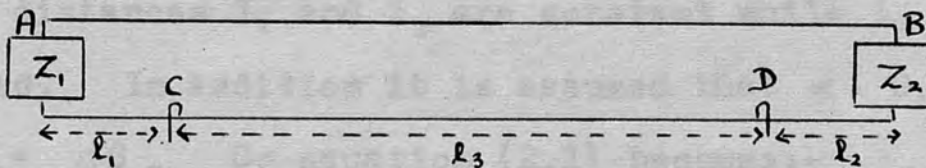


Fig. 2.3

Fig. 2.3 shows a length l of transmission line, characteristic impedance Z_0 , attenuation coefficient α and phase constant β , terminated at its two ends by impedances Z_1 and Z_2 . A voltage injecting loop C is

located at a distance l_1 from Z_1 and a current detecting loop D at a point distant l_2 from Z_2 . Willis Jackson²⁵ derives an expression for the current I in the detector D of this system in equation (5.13) in his monograph on 'High Frequency Transmission Lines', page 108.

$$I = \frac{E}{Z_0} \frac{\cosh(P l_1 + \psi_1) \cosh(P l_2 + \psi_2)}{\sinh(P l_1 + \psi_1 + \psi_2)} \dots\dots\dots(2.1)$$

where E is the E.M.F. injected in series with the line at C,

$$\frac{Z_1}{Z_0} = \tanh \psi_1 = \tanh(u_1 + jv_1)$$

and $\frac{Z_2}{Z_0} = \tanh \psi_2 = \tanh(u_2 + jv_2)$

In the system described in section 2.1, Z_1 of fig. 2.3 represents the movable short circuited tuning cap and Z_2 the fixed short circuit.

Hence $Z_1 = Z_2 = 0$ and $\psi_1 = \psi_2 = 0$

and the distances l_2 and l_3 are constant while l_1 can be varied. In addition it is assumed that $\alpha = 0$, so that $P = j\beta$. So equation (2.1) becomes:-

$$I = \frac{E}{Z_0} \frac{\cos\beta l_1 \cos\beta l_2}{j \sin\beta(l_1 + l_2 + l_3)} \dots\dots\dots(2.2)$$

Movement of the tuning cap, the alteration of l_1 , affects terms in both the numerator and denominator of equation (2.2). The term $\cos\beta l_1$ affects only the scale

of the standing wave pattern, while the effect of l_3 in the denominator is to alter the positions of the maxima.

Multiplying equation (2.2) by its complex conjugate,

$$|I|^2 = \frac{E^2}{Z_0^2} \frac{\cos^2 \beta l_1 \cos^2 \beta l_2}{\sin^2 \beta l} \dots\dots\dots(2.3)$$

where $l = l_1 + l_2 + l_3$

Differentiating equation (2.3) with respect to the variable l_1 ,

$$\begin{aligned} \frac{d|I|^2}{dl_1} &= - \frac{E^2}{Z_0^2} \frac{2\beta \cos^2 \beta l_2 (\sin^2 \beta l \cos \beta l_1 \sin \beta l_1 + \cos^2 \beta l_1 \sin \beta l \cos \beta l)}{\sin^4 \beta l} \\ &= - \frac{E^2}{Z_0^2} \frac{2\beta \cos \beta l_1 \sin \beta l \cos^2 \beta l_2 (\sin \beta l \sin \beta l_1 + \cos \beta l \cos \beta l_1)}{\sin^4 \beta l} \\ &= - \frac{E^2}{Z_0^2} \frac{2\beta \cos^2 \beta l_2 \cos \beta l \cos \beta (l-l_1)}{\sin^3 \beta l} \\ &= - \frac{E^2}{Z_0^2} \frac{2\beta \cos^2 \beta l_2 \cos \beta (l_2 + l_3) \cos \beta l_1}{\sin^3 \beta l} \\ &= \text{Constant} \frac{\cos \beta l_1}{\sin^3 \beta l} \dots\dots\dots(2.4) \end{aligned}$$

Hence $\frac{d|I|^2}{dl_1} = 0$ when $\cos \beta l_1 = 0$. This condition

only gives the minimum value of $|I|^2$

From equation (2.3) it is clear that $|I|^2$ will be a maximum when $\sin^2 \beta l$ is zero, and the tuning will be sharpest if, in addition, $\cos^2 \beta l_1$ is 1. That is if,

$$\beta (l_1 + l_2 + l_3) = \beta l_1 + n\pi$$

i.e. $\beta (l_2 + l_3) = n\pi$

or $l_2 + l_3 = n\lambda/2$

The most unfavourable condition for sharp tuning occurs when,

$$\beta(l_1 + l_2 + l_3) = \beta l_1 + (2n+1)\pi/2$$

i.e. $\beta(l_2 + l_3) = (2n+1)\pi/2$

or $l_2 + l_3 = (2n+1)\lambda/4$

Then $\cos^2 \beta l_1 = \sin^2 \beta l$

and $|I|^2$, equation (2.3), is independent of the variation of l_1 .

To consider a general case, let $\beta(l_2 + l_3) = \theta$

Equation (2.3) becomes,

$$|I|^2 = \frac{E^2 \cos^2 \beta l_1 \cos^2 (\beta l - \theta)}{Z_0^2 \sin^2 \beta l} \dots\dots\dots(2.5)$$

$$= \frac{E^2 \cos^2 \beta l_1 (\cos \beta l \cos \theta + \sin \beta l \sin \theta)^2}{Z_0^2 \sin^2 \beta l} \dots\dots(2.5)$$

$$= \frac{E^2 \cos^2 \beta l_1 (\cot \beta l \cos \theta + \sin \theta)^2}{Z_0^2} \dots\dots\dots(2.5)$$

The maximum signal should be infinite whatever the value of $\cos \theta$. The tuning however will be sharper the more closely $\cos \theta$ approaches one. The affect of the added term $\sin \theta$ is negligible as $\cot \beta l$ approaches infinity but it will make the maximum asymmetrical.

If, however, the apparatus can be designed so that

$$l_1 = l_3 = 0$$

that is with input and output loops C and D located in the short circuiting tuning cap, or probes at a distance of $\lambda/4$ from it, then $\theta = \beta l_1$, and equation (2.5) becomes:-

$$|I|^2 = \frac{E^2}{Z_0^2} \cot^2 \beta l_1 \dots\dots\dots(2.6)$$

and the sharpness of the tuning is no longer affected by the length of the line. (Fig. 2.4).

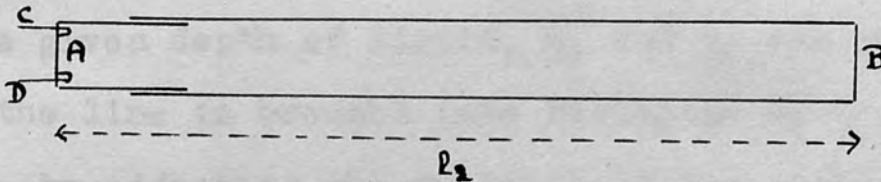


Fig. 2.4

2.2.1 The effect on the tuning of the introduction of liquid into the line.

Let Z_2 be the impedance at B caused by the introduction of a depth l of liquid.

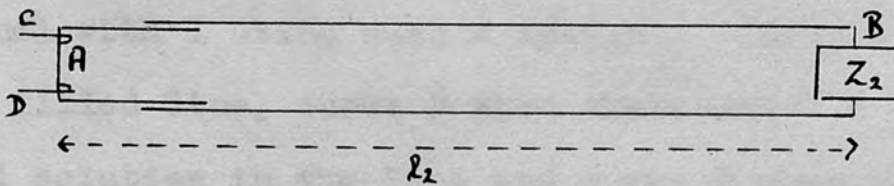


Fig. 2.5

Then $\frac{Z_2}{Z_0} = \tanh \psi_2 = \tanh(u_2 + jv_2)$

and equation (2.1) becomes:-

$$I = \frac{E \cosh(\beta l_2 + \psi_2)}{Z_0 \sinh(\beta l_2 + \psi_2)} \dots\dots\dots(2.7)$$

$$= \frac{E \cosh(\beta l_2 + u_2 + jv_2)}{Z_0 \sinh(\beta l_2 + u_2 + jv_2)} \dots\dots\dots(2.7)$$

Multiplying equation (2.7) by its complex conjugate,

$$|I|^2 = \frac{E^2}{Z_0^2} \left\{ \frac{\text{ch}^2(\beta l_2 + u_2) \cos^2 v_2 + \text{sh}^2(\beta l_2 + u_2) \sin^2 v_2}{\text{sh}^2(\beta l_2 + u_2) \cos^2 v_2 + \text{ch}^2(\beta l_2 + u_2) \sin^2 v_2} \right\} \dots\dots(2.8)$$

$$= \frac{E^2}{Z_0^2} \left\{ \frac{\text{sh}^2(\beta l_2 + u_2) + \cos^2 v_2}{\text{sh}^2(\beta l_2 + u_2) + \sin^2 v_2} \right\} \dots\dots\dots(2.8)$$

For a given depth of liquid, u_2 and v_2 are constant, and the line is brought into resonance by the variation of l_2 by adjusting the position of the tuning cap until a maximum signal is obtained on the galvanometer. The sharpness of tuning will thus vary as Z_2 is altered, i.e. as the liquid depth is varied, but by placing the input and output loops in the tuning cap the most favourable conditions may be obtained.

Fig. 2.6 shows the variation of the galvanometer signal with l using such a system. Curve A is for an air filled line, curve B when there are 1.2 cms of a 2N NaCl solution in the line and curve C when there are 0.21 cms of a 0.66N NaCl solution in the line. Curve B represents the tuning sharpness usually observed while curve C represents poor tuning conditions. The coupling of the input and output loops to the line was not the

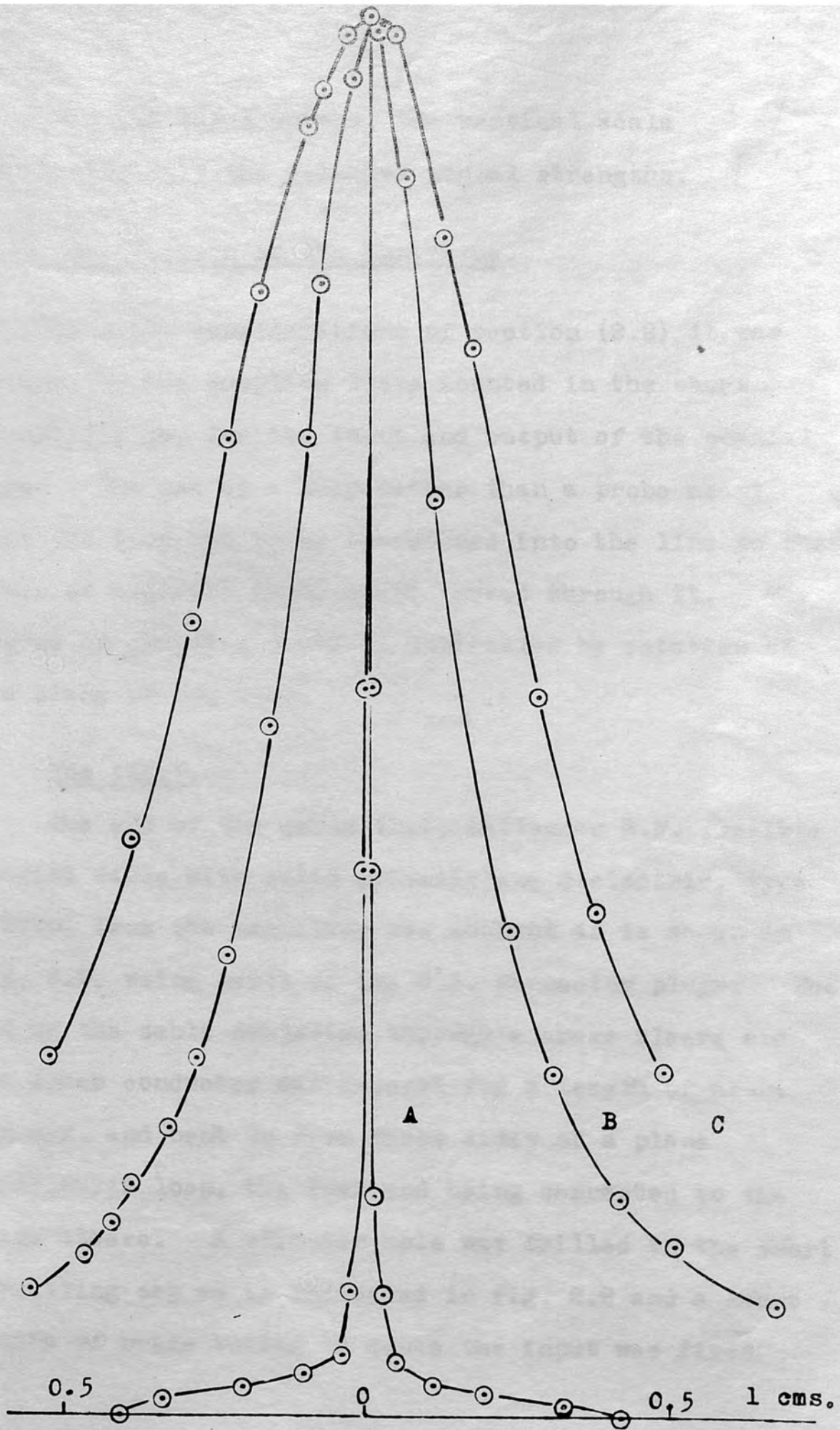


Fig. 2.6 The variation of the Q of the line.

same for the three curves, the vertical scale indicating only the relative signal strengths.

2.3 Description of the apparatus.

From the considerations of section (2.2) it was decided to use coupling loops mounted in the short circuiting cap for the input and output of the coaxial line. The use of a loop rather than a probe meant that the loop had to be introduced into the line so that lines of magnetic force could thread through it. The degree of coupling could be controlled by rotation of the plane of the loop.

The input.

The end of the cable (B.I. Callender R.F. flexible coaxial cable with solid polyethylene dielectric, type T 3020) from the magnetron was mounted as is shown in fig. 2.2, using parts of the W.S. connector plugs. The end of the cable projected through a brass sleeve and the inner conductor was exposed for a length of about two cms. and bent to form three sides of a plane rectangular loop, the free end being connected to the brass sleeve. A circular hole was drilled in the short circuiting cap as is indicated in fig. 2.2 and a short length of brass tubing to house the input was fixed

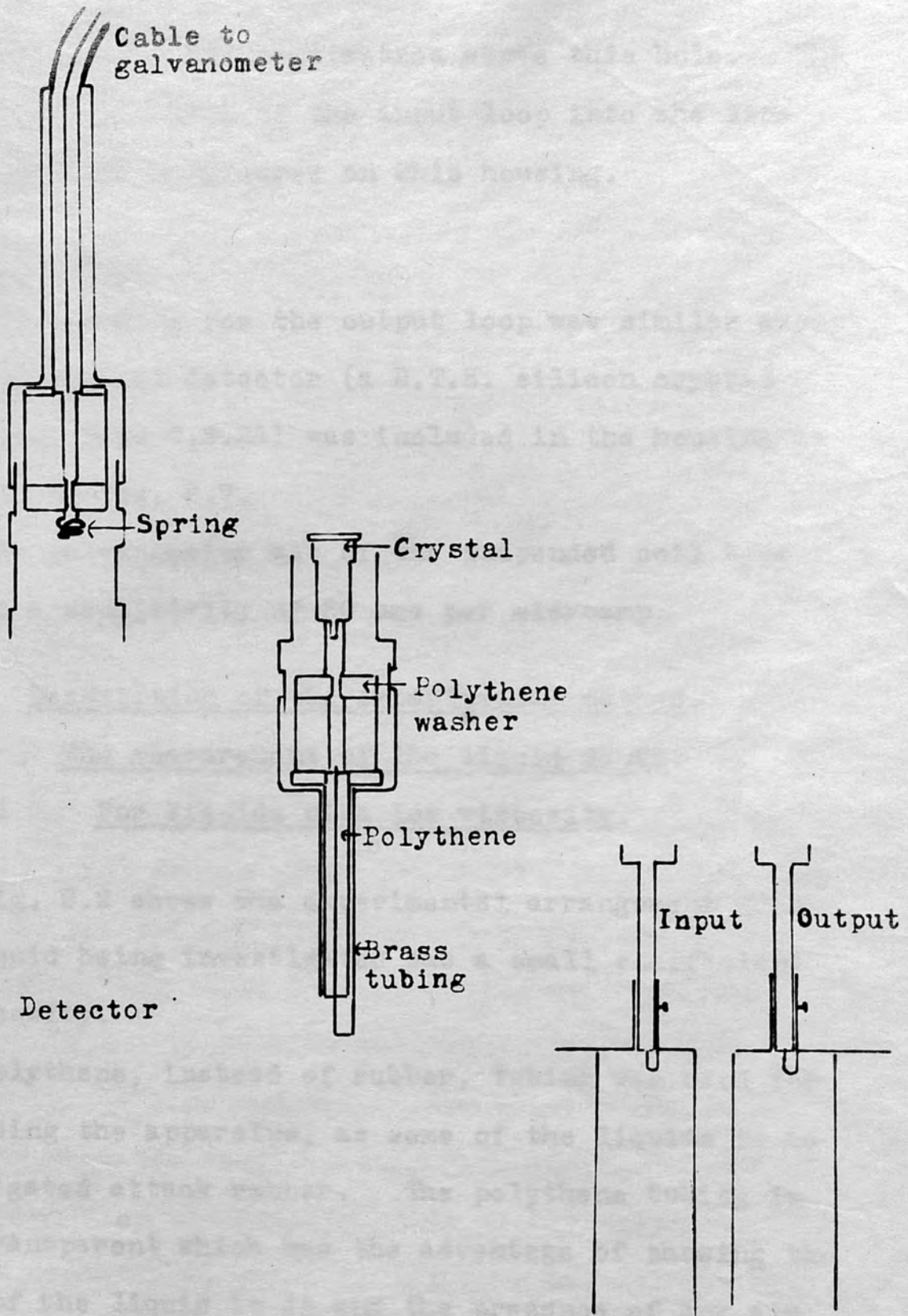


Fig. 2.7

Part of tuning cap,
showing mounting of coupling
loops.

projecting about two centimetres above this hole. The depth of penetration of the input loop into the line was controlled by a screw on this housing.

The output.

The mounting for the output loop was similar except that the crystal detector (a B.T.H. silicon crystal rectifier, type C.S.2A) was included in the housing as is shown in fig. 2.7.

The galvanometer was of the suspended coil type and had a sensitivity of 20 cms per microamp.

2.4 Description of the experimental method.

2.4.1 The measurement of the liquid depth.

2.4.1.1 For liquids with low viscosity.

Fig. 2.2 shows the experimental arrangement when the liquid being investigated has a small coefficient of viscosity.

Polythene, instead of rubber, tubing was used for connecting the apparatus, as some of the liquids to be investigated attack rubber. The polythene tubing is semi-transparent which has the advantage of showing the level of the liquid in it and the presence of any air bubbles. Its lack of flexibility compared with rubber made it awkward to handle, but it was found that

satisfactory polythene-glass and polythene-brass joints could be made by warming the ends to be joined by blowing hot air through them.

The liquid being investigated was poured into the 250 cc aspirator on the rising table. One revolution of the screw on the rising table caused an alteration of height of 5 mm., and the head was divided into five equal divisions, each corresponding to 1 mm. The setting of the screw could be judged to the nearest tenth of a millimeter.

The liquid in the transmission line so far described was not at atmospheric pressure, so that the level of the liquid in the side tube S gave no indication of the level in the line. This difficulty was overcome by drilling two small holes in the outer conductor of the transmission line. To prevent any radiation from the line it was essential to keep these holes as small as possible, and so the minimum size of hole that would give atmospheric pressure in the line was determined experimentally by observing when the liquid levels were equal. Two holes of diameter 0.15 cms were found to be satisfactory.

The depth of liquid l in the line was determined by the change of liquid level in the glass tube S. The long metal pointed tipped rod was attached at its other

end to the micrometer head M. This rod was adjusted so that its tip just broke the surface of the liquid in S when the liquid was on the point of entering the transmission line. (This was determined either by observing when the galvanometer deflection fell from its maximum reading of air resonance, or by the removal of the tuning cap and direct observation. The latter method was found the more satisfactory.) A certain amount of liquid was allowed to enter the line by raising the reservoir on the rising table. The stick was withdrawn to just above the liquid level in S by means of the micrometer screw M and then slowly turned till it broke the liquid surface again. The surface was well illuminated while this adjustment was being made. The difference between the two readings of the micrometer screw gave l . More consistent results were obtained by lowering the stick into the liquid surface and then reading the vernier, rather than by taking the reading when the pin broke away from the surface. The surface tension of the liquid being investigated effected these readings, but with care the relative change of liquid depth in the line could be determined. The scale on the micrometer head M was divided into five divisions covering a distance of 1.270 cms. The vernier enabled each division to be read to the nearest

one hundredth, and since each division corresponded to 0.254 cms, the depth could be read to 0.002 of a cm. A screw at the top of the micrometer enabled the stick to be reset when l was greater than 1.27 cms.

At first the micrometer head had been fixed to the movable short circuiting cap and a very long stick was required. It had been hoped with this arrangement to determine both l and Δ from the readings of the micrometer, the adjustment of the tuning cap being made by a screw on a rack and pinion arrangement. The rack and pinion was not satisfactory and it was found that it was better to adjust the tuning cap manually. As the tuning cap had to be capable of fairly easy movement, it was found that the slight pressure required in moving the micrometer might alter the position of the tuning cap, so that the advantage of having the micrometer attached to the tuning cap was lost. In addition the long stick required with this arrangement was unsatisfactory due to whip in the stick and the consequent circular motion of its tip in the liquid surface at S. It was found that the shorter the length of this stick the greater was the accuracy which could be obtained. The micrometer head was therefore removed from the tuning cap and attached to a lower horizontal bar

on the framework supporting the apparatus. The length of stick required for a set of observations depended on the length of liquid it was desired to investigate. For liquids with high values of α this length is not likely to exceed 5 or 6 cms, while for liquids with a low value of α it may be as much as 20 or 30 cms. So before beginning a series of readings with a particular liquid the likely maximum value of l required was estimated and the position of the apparatus on the rigid supporting framework adjusted so that the total length of the stick could be kept to this minimum length.

The reading of the screw of the rising table was recorded during a set of observations in addition to that of the micrometer head as a check.

2.4.1.2 For liquids with high viscosity.

Fig. 2.8 shows the experimental arrangement when the liquid being investigated had a large coefficient of viscosity.

A vessel, with a lip, such as a beaker, of a suitable depth (the depth depending upon the depth of liquid to which it was wished to continue the readings) and a diameter somewhat greater than that of the transmission line, was filled to the brim with the liquid.

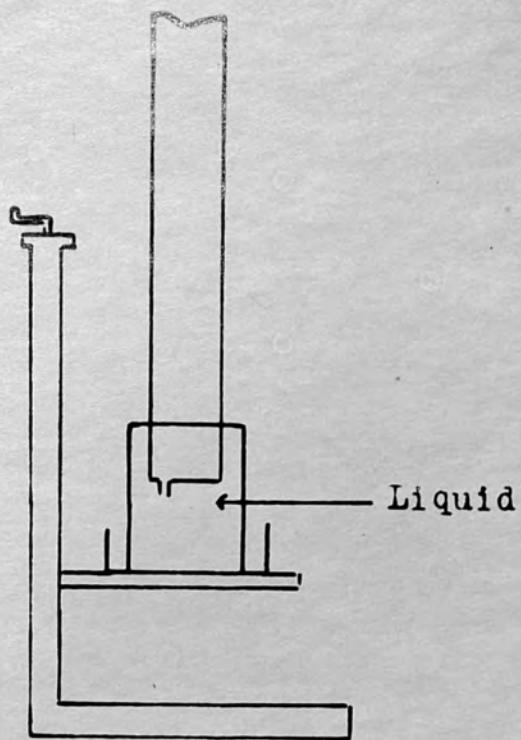


Fig. 2.8 Apparatus used for liquids with a high viscosity.

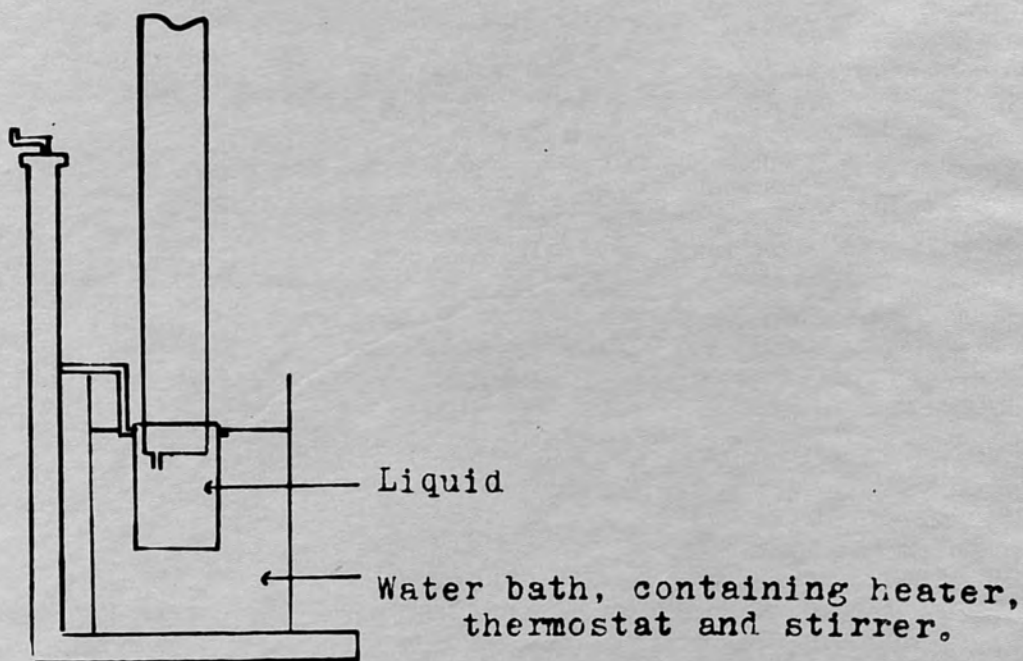
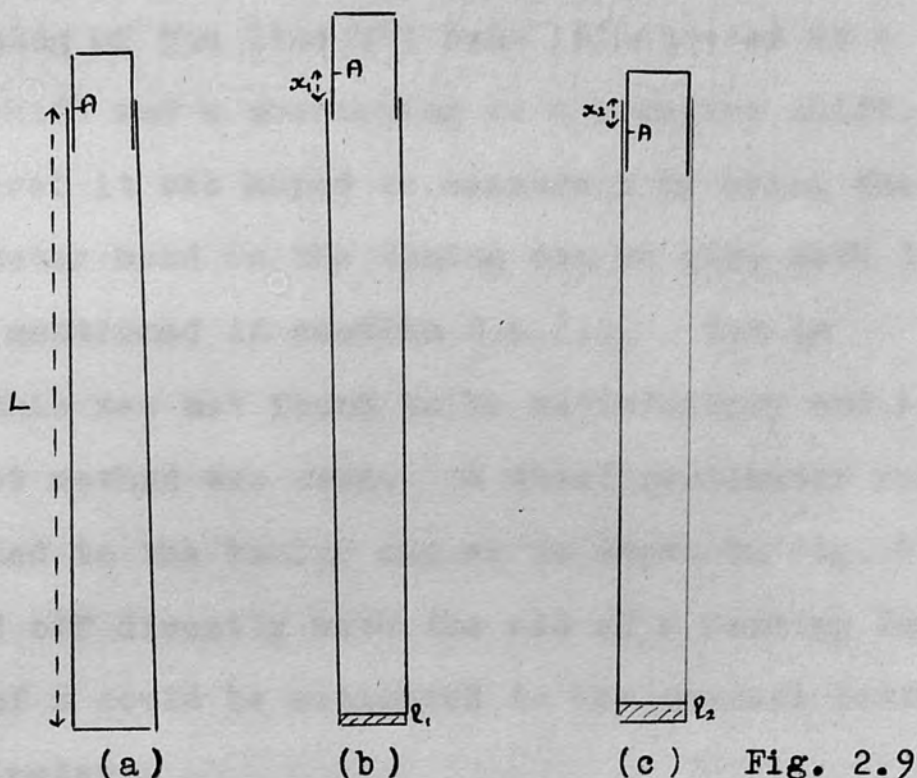


Fig. 2.10 Apparatus used for controlling the temperature of the liquid.

This vessel was placed on the platform of the rising table immediately below the short circuited end of the transmission line. The lip of the vessel allowed the liquid displaced by the transmission line as l was increased to over flow into the trough below and so no correction for liquid displacement was necessary. With this arrangement the depth of liquid filling the line was determined by the distance travelled by the screw of the rising table, which could be read to the nearest tenth of a millimetre.

When the experimental arrangement of section 2.4.1.1 was used for a viscous liquid such as cyclohexanol ($\eta = 0.2$ poise at 39°C) the time taken for the liquid levels to equalise was so long that the time taken between each observation made the method impracticable. With the simpler arrangement of this section however, the liquid quickly assumed its new level. This was indicated by the rapid and definite movement of the galvanometer mirror after a change in l .

2.4.2 The measurement of the phase shift.



In Fig. 2.9, let L be the length of the line from the terminating fixed short circuit to its free upper rim. When resonance is obtained with an air filled line, fig. 2.9a, let A be a point on the tuning cap coinciding with the upper rim of the line. Suppose that on the introduction of a depth l_1 of liquid the line length has to be increased by x_1 to obtain resonance again. (Fig.2.9b). Then

$$L + \Delta_1 = L + x_1 - l_1 \dots\dots\dots(2.9)$$

If, fig. 2.9c, the introduction of a depth l_2 causes a reduction x_2 in the length of line necessary for

resonance, then

$$L + \Delta_x = L - (x_1 + l_1) \dots\dots\dots(2.10)$$

A lengthening of the line has been interpreted as a positive shift and a shortening as a negative shift.

At first it was hoped to measure x by using the one micrometer head on the tuning cap to give both l and x , as mentioned in section 2.4.1.1. But in practice this was not found to be satisfactory and a more direct method was used. A steel centimeter rule was attached to the tuning cap as is shown in fig. 2.2, and x read off directly with the aid of a reading lens. Readings of x could be estimated to the nearest tenth of a millimeter.

The position of a point on the rim of the fixed portion of the transmission line against the scale when air resonance was obtained was recorded. This was the arbitrary origin A . The new position of the point on the rim when a certain depth l of liquid was in the line under resonant conditions was recorded. The difference in these two readings gave x . The liquid depth l was either subtracted or added, depending on whether the length of the line had been lengthened or shortened and hence, by equations (2.9) and (2.10), the phase shift for a given depth of liquid obtained.

2.4.3 The entry of liquid into the line.

The entry of a liquid into the line was observed by removing the tuning cap after the air resonance position had been recorded. The short circuited end of the transmission line was illuminated and the reservoir raised through small intervals. If the liquid was viscous, a short interval of time was allowed to elapse between each incremental rise of the reservoir. The liquid rose up through the small circular hole in the short circuiting plate, and as it became level with the short circuiting plate the light reflected from its surface changed - in a manner similar to that of the light reflected from the liquid at the end of a capillary tube when its surface tension is being measured by Ferguson's method. The moment it was plane could be determined accurately. If the base plate was dry, the liquid continued to rise in the tube and bulged up a little way before spreading over the surface. It then started to spread over the plate in an irregular manner. The entry and exit of the liquid into the line was observed several times. The effects of surface tension were greater with a dry tube than with a wet one. When the reservoir level was lowered below the level of the short circuiting plate a little liquid remained in the

line unless the reservoir was lowered very slowly. The use of a slightly curved plate to enable the liquid to drain away completely was not however found to be satisfactory.

It is shown in section 3.2.2 that the gradient of the $\tan \phi$ curve at $l = 0$ depends only on β_0 .

$$\frac{d\phi}{dl} = -2\beta_0 = -\frac{4\pi}{\lambda_0}$$

Differentiating equation (1.19) with respect to l gives

$$\frac{d\Delta}{dl} = \frac{\lambda_0}{4\pi} \frac{d\phi}{dl}$$

so that the gradient of the experimental curve of phase shift against liquid depth should be -1 at the origin. This gave a rough check on whether the position of the origin had been correctly chosen.

2.4.4 The recording of the galvanometer deflection.

In addition to measuring l and x , the galvanometer deflection at resonance was also recorded. As is shown in section 1.6, the galvanometer deflection is proportional to $|k|^2$, where k is the ratio of the amplitude of the reflected to the incident voltage.

Before the liquid entered the line, the coupling of the input and output loops was reduced to a minimum in order to reduce the signal obtained at air resonance

so that the spot of light reflected from the galvanometer mirror remained on the scale. As the liquid entered the line this deflection fell and very shortly the coupling would have to be increased to obtain a reasonable signal at resonance. As l increased however the deflection at resonance became larger and sometimes it was necessary to decrease the coupling between the loops in order to keep the spot of light on the scale. It would then be necessary to increase the degree of coupling again as l was increased further, and so on as the liquid level increased. This alteration in the degree of coupling between the loops is indicated on the graphs showing the variation of galvanometer signal with l by a sudden discontinuity in the curve.

These readings, unlike the measurements of the phase shift, are not independent of any fluctuations that may occur in the input voltage. The regularity of the experimental curves shows that the fluctuations must have been slight.

2.5 The control of temperature.

The majority of the liquids were investigated at room temperature and at first no special precautions were made to keep the temperature constant. A

thermometer was placed in the reservoir containing the liquid being investigated and its readings were recorded at intervals throughout the experiment. A series of readings might take five or six hours to complete and variations of one or two degrees in the temperature might be observed during the day. The apparatus was set up in a semi-basement room against an inside wall which accounted for this small fluctuation of temperature.

When it was decided to apply this method to an investigation of the microwave absorption in blood it was realised that the results at body temperature would be of greater value than those at room temperature and so a thermostatic control system was designed. The experimental arrangement of section 2.4.1.2 had to be used. The beaker containing the liquid to be investigated was held in a clamp attached to a rod on the rising table. (Fig. 2.10). The beaker was supported so that its neck was just above the level of the water in a glass tank. The tank also contained a heating element, stirrer and the controlling thermometer so that the water in the tank could be maintained at any desired temperature. As the level of the liquid in the transmission line increased the beaker was raised out of the tank, so that before starting a series of

readings the maximum liquid depth to be investigated was decided and the level of the water in the tank adjusted so that it was possible to add water to the tank during the readings so that all the liquid in the beaker remained in the water tank.

Chapter 3

THE CALCULATION OF α AND β

3.1 Introduction.

From the graph of the experimentally observed variation of phase shift Δ with liquid depth the attenuation coefficient α and the phase constant β of a liquid may be deduced. The methods available depend upon the type of liquid. Before outlining these methods expressions for the gradient of the $\tan \phi$ curve, the turning points of the $|k|^2$ curve and the condition for no standing wave on the line will be derived.

3.2 The gradient of $\tan \phi$.

From equation (1.13)

$$\tan \phi = \frac{2\beta(\alpha \sinh 2\alpha l + \beta \sin 2\beta l)}{(\beta^2 - \alpha^2 - \beta^2) \cosh 2\alpha l - (\beta^2 + \alpha^2 + \beta^2) \cos 2\beta l}$$

Differentiating with respect to l , and putting

$$a = \beta^2 - \alpha^2 - \beta^2 \quad \text{and} \quad b = \beta^2 + \alpha^2 + \beta^2$$

$$\frac{d(\tan \phi)}{dl} = (a \operatorname{ch} 2\alpha l - b \cos 2\beta l) 4\beta (\alpha^2 \operatorname{ch} 2\alpha l + \beta^2 \cos 2\beta l) - 4\beta (\alpha \operatorname{sh} 2\alpha l + \beta \sin 2\beta l) (a\alpha \operatorname{sh} 2\alpha l + b\beta \sin 2\beta l) / D^2$$

where

$$D^2 = a^2 \operatorname{ch}^2 \alpha l - 2ab \operatorname{ch} 2\alpha l \cos 2\beta l + b^2 \cos^2 2\beta l$$

Therefore

$$\frac{d(\tan \phi)}{dl} = \frac{4\beta}{D^2} \left\{ a\alpha^2 - b\beta^2 + (a\beta^2 - b\alpha^2) \operatorname{ch} 2\alpha l \cos 2\beta l - (a+b)\alpha\beta \operatorname{sh} 2\alpha l \sin 2\beta l \right\} \dots\dots\dots (3.1)$$

But

$$\frac{d(\tan \phi)}{dl} = \sec^2 \phi \frac{d\phi}{dl}$$

Therefore

$$\frac{d\phi}{dl} = \frac{1}{(1 + \tan^2 \phi)} \frac{d(\tan \phi)}{dl} \dots\dots\dots (3.2)$$

Hence substituting from equations (1.13) and (3.1)

$$\frac{d\phi}{dl} = \frac{D^2}{D^2 + 4\beta^2 (\alpha \operatorname{sh} 2\alpha l + \beta \sin 2\beta l)^2} \times \frac{4\beta}{D^2} \left\{ a\alpha^2 - b\beta^2 + (a\beta^2 - b\alpha^2) \operatorname{ch} 2\alpha l \cos 2\beta l - (a+b)\alpha\beta \operatorname{sh} 2\alpha l \sin 2\beta l \right\} \dots\dots\dots (3.2)$$

$$\frac{d\phi}{dl} = \frac{4\beta \{ a\alpha^2 - b\beta^2 + (a\beta^2 - b\alpha^2) \operatorname{ch} 2\alpha l \cos 2\beta l - (a+b)\alpha\beta \operatorname{sh} 2\alpha l \sin 2\beta l \}}{D}$$

where

$$D = a^2 \operatorname{ch}^2 \alpha l - 2ab \operatorname{ch} 2\alpha l \cos 2\beta l + b^2 \cos^2 2\beta l + 4\beta^2 \alpha^2 \operatorname{sh}^2 \alpha l + 8\beta^2 \alpha\beta \operatorname{sh} 2\alpha l \sin 2\beta l + 4\beta^2 \beta^2 \sin^2 2\beta l \dots\dots\dots (3.2)$$

It was shown in section 1.4 that

$$\Delta = \frac{\lambda}{4\pi} \phi \dots\dots\dots (1.19)$$

so that the gradient of the experimental curve $d\Delta/dl$ is related to $d\phi/dl$ by the expression,

$$\frac{d\Delta}{dl} = \frac{\lambda}{4\pi} \frac{d\phi}{dl} \dots\dots\dots(3.3)$$

3.2.1 The gradient of the curve when $\tan \phi = 0$.

When $\tan \phi = 0$, equation (3.2) becomes,

$$\frac{d\phi}{dl} = \frac{d(\tan \phi)}{dl}$$

and equation (1.13) shows that $\tan \phi = 0$ when

$$\sin 2\beta l = \frac{\alpha}{\beta} \sinh 2\alpha l \dots\dots\dots(3.4)$$

but for small liquid depths and low values of α ,

$$\frac{\alpha \sinh 2\alpha l}{\beta} \rightarrow 0$$

i.e. $\sin 2\beta l = 0 \dots\dots\dots(3.5)$

or $2\beta l = n\pi$ where n is $0, 1, 2, 3, \dots\dots$

and $\cos 2\beta l = \pm 1$

depending on whether n is even or odd.

Substituting these conditions in equation (3.2),

$$\frac{d\phi}{dl} = \frac{4\beta \{a\alpha^2 - b\beta^2 \pm (a\beta^2 - b\alpha^2) \operatorname{ch} 2\alpha l\}}{(a \operatorname{ch} 2\alpha l \mp b)^2} \dots\dots\dots(3.6)$$

$$= \frac{4\beta \{ \beta^2(\alpha^2 - \beta^2) - (\alpha^2 + \beta^2)^2 \pm [\beta^2(\beta^2 - \alpha^2) - (\alpha^2 + \beta^2)^2] \operatorname{ch} 2\alpha l \}}{[(\beta^2 - \alpha^2 - \beta^2) \operatorname{ch} 2\alpha l \mp (\beta^2 + \alpha^2 + \beta^2)]^2}$$

Thus the gradient of the curve when $\tan \phi = 0$ and n is even is,

$$\frac{d\phi}{dl} = \frac{4\beta \{ \beta^2(\alpha^2 - \beta^2) - (\alpha^2 + \beta^2)^2 + [\beta^2(\beta^2 - \alpha^2) - (\alpha^2 + \beta^2)^2] \operatorname{ch} 2\alpha l \}}{[(\beta^2 - \alpha^2 - \beta^2) \operatorname{ch} 2\alpha l - (\beta^2 + \alpha^2 + \beta^2)]^2} \dots\dots\dots(3.7)$$

and when n is odd,

$$\frac{d\phi}{dl} = \frac{4\beta_0 \{ \beta_0^2 (\alpha^2 - \beta^2) - (\alpha^2 + \beta^2)^2 - [\beta_0^2 (\beta^2 - \alpha^2) - (\alpha^2 + \beta^2)^2] \text{ch} 2\alpha l \}}{[(\beta_0^2 - \alpha^2 - \beta^2) \text{ch} 2\alpha l + (\beta_0^2 + \alpha^2 + \beta^2)]^2} \dots\dots\dots(3.8)$$

Since for equation (3.5) to hold α must be small, the effect of α^2 in (3.6) is negligible. Hence equations (3.7) and (3.8) become, when n is even,

$$-\frac{d\phi}{dl} = \frac{4\beta_0 \{ \beta_0^2 \beta^2 + \beta^4 + (\beta^4 - \beta_0^2 \beta^2) \text{ch} 2\alpha l \}}{[(\beta^2 - \beta_0^2) \text{ch} 2\alpha l + \beta_0^2 + \beta^2]^2} \dots\dots\dots(3.7a)$$

and when n is odd,

$$-\frac{d\phi}{dl} = \frac{4\beta_0 \{ \beta_0^2 \beta^2 + \beta^4 - (\beta^4 - \beta_0^2 \beta^2) \text{ch} 2\alpha l \}}{[(\beta^2 - \beta_0^2) \text{ch} 2\alpha l - (\beta_0^2 + \beta^2)]^2} \dots\dots\dots(3.8a)$$

Thus, for a given liquid, the gradient when $\tan \phi = 0$ and n is even, is always negative; and as l increases the numerical value of the gradient decreases until the steady negative value of $\tan \phi$ is reached. When, however, n is odd, the gradient at $\tan \phi = 0$ has at first (assuming the value of α is sufficiently low for $\tan \phi$ to go to infinity for small liquid depths) a fairly high negative value which increases with l until a critical depth is reached where the slope of the curve suddenly changes sign, (this corresponds to $\tan \phi$ no longer reaching infinity) and from this point

onwards the curve has positive gradients of decreasing magnitude at points where n is odd, until the steady negative value of $\tan \phi$ is reached. This is illustrated in figs. 1.10 and 1.11. For 'water-type' liquids, (figs. 1.12 and 1.13), the gradients at $\tan \phi = 0$ are alternately negative and positive, as n is even or odd, and of decreasing numerical value as l increases.

Equations (3.7a) and (3.8a) may be simplified further. It has been assumed that α is small and that $\alpha^2 \ll \beta^2$.

When n is even,

$$-\frac{d\phi}{dl} = \frac{4\beta_0\beta^2(\beta^2 - \beta_0^2) \cosh 2\alpha l + \beta_0^2 + \beta^2}{[(\beta^2 - \beta_0^2) \cosh 2\alpha l + \beta_0^2 + \beta^2]^2} \dots\dots\dots(3.7a)$$

$$= \frac{4\beta_0\beta^2}{(\beta^2 - \beta_0^2) \cosh 2\alpha l + \beta_0^2 + \beta^2}$$

But $\cosh 2\alpha l$ may be expanded as:-

$$\cosh 2\alpha l = 1 + \frac{(2\alpha l)^2}{2!} + \frac{(2\alpha l)^4}{4!} + \dots$$

hence with the condition that α is small,

$$\cosh 2\alpha l \rightarrow 1 \quad \text{and}$$

$$-\frac{d\phi}{dl} \rightarrow \frac{4\beta_0\beta^2}{2\beta^2} \rightarrow 2\beta \quad \dots\dots\dots(3.7b)$$

Similarly, when n is odd,

$$-\frac{d\phi}{dl} = \frac{4\beta_0\beta^2}{(\beta_0^2 + \beta^2) - (\beta^2 - \beta_0^2) \cosh 2\alpha l} \dots\dots\dots(3.8a)$$

and as $\cosh 2\alpha l \rightarrow 1$,

$$- \frac{d\phi}{dl} \rightarrow \frac{2\beta^2}{\beta_0} \dots\dots(3.8b)$$

3.2.2 The gradient of the curve when $l = 0$.

When $n = 0$ and $l = 0$, $\cosh 2\alpha l = 1$, so that equation (3.7) becomes,

$$\begin{aligned} \frac{d\phi}{dl} &= \frac{4\beta_0 \{ \beta_0^2(\alpha^2 - \beta^2) - (\alpha^2 + \beta^2)^2 + \beta_0^2(\beta^2 - \alpha^2) - (\alpha^2 + \beta^2)^2 \}}{[(\beta_0^2 - \alpha^2 - \beta^2) - (\beta_0^2 + \alpha^2 + \beta^2)]^2} \\ &= - 2\beta_0 \end{aligned}$$

Thus the gradient at $l = 0$ is independent of the liquid used and depends only on β_0 , i.e. on the wavelength λ_0 of the oscillator. Hence the longer λ_0 , the less steep is the gradient at $l = 0$, and the shorter λ_0 , the steeper is the gradient. Thus for a given λ_0 , the gradient at $l = 0$ on the graph of Δ against l must be the same for all liquids.

This fact, as was shown in section 2.4.3, may be used to indicate when the liquid enters the line.

3.2.3 The turning points of the curve.

The turning points of the $\tan \phi$ curve occur when $d\phi/dl = 0$. From equation (3.2) this is when:-

$$\begin{aligned} 4\beta_0 \{ a\alpha^2 - b\beta^2 + (a\beta^2 - b\alpha^2) \operatorname{ch} 2\alpha l \cos 2\beta l - (a+b)\alpha\beta \operatorname{sh} 2\alpha l \sin 2\beta l \\ = 0 \dots\dots\dots(3.9) \end{aligned}$$

Substituting for a and b,

$$\alpha^2 \beta_0^2 - \alpha^4 - 2\alpha^2 \beta^2 - \beta_0^2 \beta^2 - \beta^4 + (\beta_0^2 \beta^2 - 2\alpha^2 \beta^2 - \beta^4 - \alpha^2 \beta_0^2 - \alpha^4) \text{ch}2\alpha l \cos 2\beta l$$

$$= 2\beta_0^2 \alpha \beta \text{sh}2\alpha l \sin 2\beta l \quad \dots\dots\dots(3.9)$$

If, as is generally the case, $\alpha^2 \ll \beta^2$, then equation (3.9) becomes:-

$$-\beta_0^2 \beta^2 - \beta^4 - 2\alpha^2 \beta^2 + (\beta_0^2 \beta^2 - 2\alpha^2 \beta^2 - \beta^4) \text{ch}2\alpha l \cos 2\beta l$$

$$= 2\beta_0^2 \alpha \beta \text{sh}2\alpha l \sin 2\beta l \quad \dots\dots\dots(3.9a)$$

or neglecting α^2 ,

$$-\beta_0^2 \beta^2 - \beta^4 + (\beta_0^2 \beta^2 - \beta^4) \text{ch}2\alpha l \cos 2\beta l$$

$$= 2\beta_0^2 \alpha \beta \text{sh}2\alpha l \sin 2\beta l \quad \dots\dots\dots(3.9b)$$

3.3 The gradient of the curve relating $|k|^2$ with l.

From equation (1.24)

$$|k|^2 = \frac{b \text{ch}2\alpha l - a \cos 2\beta l - 2\beta_0 (\beta \text{sh}2\alpha l - \alpha \sin 2\beta l)}{b \text{ch}2\alpha l - a \cos 2\beta l + 2\beta_0 (\beta \text{sh}2\alpha l - \alpha \sin 2\beta l)}$$

Differentiating with respect to l, and writing D for the denominator of equation (1.24),

$$D^2 \frac{d|k|^2}{dl} = (b \text{ch}2\alpha l - a \cos 2\beta l + 2\beta_0 \beta \text{sh}2\alpha l - 2\beta_0 \alpha \sin 2\beta l)$$

$$\times (2\alpha b \text{sh}2\alpha l + 2\beta a \sin 2\beta l - 4\beta_0 \alpha \beta \text{ch}2\alpha l + 4\beta_0 \alpha \beta \cos 2\beta l)$$

$$- (b \text{ch}2\alpha l - a \cos 2\beta l - 2\beta_0 \beta \text{sh}2\alpha l + 2\beta_0 \alpha \sin 2\beta l)$$

$$\times (2\alpha b \text{sh}2\alpha l + 2\beta a \sin 2\beta l + 4\beta_0 \alpha \beta \text{ch}2\alpha l - 4\beta_0 \alpha \beta \cos 2\beta l)$$

$$\dots\dots\dots(3.10)$$

which, on simplification, reduces to

$$D \frac{d|k|^2}{dl} = 8\beta_0 \{ (\beta_0^2 \beta^2 - \beta_0^2 \alpha^2 - \beta^4 - \alpha^4 - 2\alpha^2 \beta^2) \text{sh}2\alpha l \sin 2\beta l + 2\beta_0^2 \alpha \beta \text{ch}2\alpha l \cos 2\beta l - 2\beta_0^2 \alpha \beta \} \dots\dots\dots(3.10)$$

3.3.1 The turning points of the curve relating $|k|^2$ with l .

The turning points of the curve occur when $d|k|^2/dl = 0$. From equation (3.10) this is when:-

$$(\beta_0^2 \beta^2 - \beta_0^2 \alpha^2 - \beta^4 - \alpha^4 - 2\alpha^2 \beta^2) \text{sh}2\alpha l \sin 2\beta l + 2\beta_0^2 \alpha \beta \text{ch}2\alpha l \cos 2\beta l = 2\beta_0^2 \alpha \beta \dots\dots\dots(3.11)$$

If α is sufficiently small for α^2 to be neglected equation (3.11) may be simplified. Dividing by $2\beta_0^2 \alpha \beta$, and omitting terms in α^2 and α^4 ,

$$\frac{\beta^2(\beta_0^2 - \beta^2)}{2\beta_0^2 \alpha \beta} \text{sh}2\alpha l \sin 2\beta l + \text{ch}2\alpha l \cos 2\beta l - 1 = 0 \dots\dots(3.12)$$

Since $\text{sh}2\alpha l = 2\alpha l + \frac{(2\alpha l)^3}{3!} + \text{higher terms}$

and $\text{ch}2\alpha l = 1 + \frac{(2\alpha l)^2}{2!} + \text{higher terms}$

equation (3.12) may be written, neglecting α^2 and higher powers of α ,

$$\frac{\beta(\beta_0^2 - \beta^2)}{\beta_0^2} l \sin 2\beta l + \cos 2\beta l - 1 = 0 \dots\dots\dots(3.12)$$

$$\frac{\beta(\beta_0^2 - \beta^2) 2l \sin \beta l \cos \beta l - 2 \sin^2 \beta l}{\beta_0^2} = 0 \dots\dots\dots(3.12)$$

Therefore, $\frac{\beta(\beta_0^2 - \beta^2)l}{\beta_0^2} = \tan\beta l$

provided $\sin\beta l \neq 0$

Hence the turning points of the curve occur where

$$\begin{aligned} \beta l &= n\pi + \tan^{-1} \left[\frac{\beta(\beta_0^2 - \beta^2)l}{\beta_0^2} \right] \\ &= n\pi + \tan^{-1} [\beta l(1 - \epsilon)] \quad \dots\dots\dots(3.13) \end{aligned}$$

provided α is small and $\sin\beta l \neq 0$.

3.3.2 The condition for $|K|^2$ to be greater than one.

From equation (1.24)

$$|K|^2 = \frac{bch2\alpha l - a\cos2\beta l - 2\beta_0(\beta \operatorname{sh}2\alpha l - \alpha \sin2\beta l)}{bch2\alpha l - a\cos2\beta l + 2\beta_0(\beta \operatorname{sh}2\alpha l - \alpha \sin2\beta l)}$$

if $\alpha \sin2\beta l > \beta \operatorname{sh}2\alpha l$

then $|K|^2 > 1$

This occurs for very small values of l , and is more noticeable in liquids with large values of α or β , i.e. with the 'water' or 'alcohol-type' liquids.

Fig. 4.55 shows the observed increase in the galvanometer signal, which is proportional to $|K|^2$, for a depth of 0.01 cms of physiological saline.

When $|K|^2 = 1$, and $l \neq 0$, a galvanometer signal equal to that obtained with an air filled line is observed, then, for this depth of liquid,

$$\alpha \sin2\beta l = \beta \operatorname{sh}2\alpha l$$

This equation is not however suitable for calculating

α or β if one of these quantities is known. For the value of l at which this effect occurs is so very small ($l = 0.016$ cms for a 0.15N NaCl solution) that

$$\sin 2\beta l \rightarrow 2\beta l \quad \text{and} \quad \sinh 2\alpha l \rightarrow 2\alpha l$$

so that both sides of the equation approach $2\alpha\beta l$.

3.4 The condition for no standing wave along the line.

If the denominator and numerator of $\tan \phi$, equation (1.13), should both become zero for a certain liquid depth, then $d(\tan \phi)/dl$, equation (3.1), is infinite so that the positions of the turning points are indeterminate. This means that there is no standing wave system along the line, i.e. $Z_T = Z_o$, and the line is correctly terminated. Under these conditions equation (1.10) becomes:-

$$\frac{Z_T}{Z_o} = \frac{j\beta_o}{\alpha + j\beta} \tanh(\alpha + j\beta)l = 1$$

Rationalising:-

$$\frac{Z_T}{Z_o} = \frac{j\beta_o(\alpha - j\beta)}{(\alpha^2 + \beta^2)} \left\{ \frac{\text{sh}2\alpha l + j\sin 2\beta l}{\text{ch}2\alpha l + \cos 2\beta l} \right\} = 1$$

Thus, equating real and imaginary parts, the condition

for Z_T to equal Z_0 is that:-

$$\frac{\beta_0 \beta \operatorname{sh} 2\alpha l - \beta_0 \alpha \sin 2\beta l}{(\alpha^2 + \beta^2)(\operatorname{ch} 2\alpha l + \cos 2\beta l)} = 1 \dots\dots\dots(3.14a)$$

and

$$\beta_0 \alpha \operatorname{sh} 2\alpha l + \beta_0 \beta \sin 2\beta l = 0 \dots\dots\dots(3.14b)$$

From equation (1.13) the conditions for the denominator and numerator of $\tan \phi$ to be zero are respectively:-

$$(\beta_0^2 - \alpha^2 - \beta^2) \operatorname{ch} 2\alpha l - (\beta_0^2 + \alpha^2 + \beta^2) \cos 2\beta l = 0 \dots\dots(3.15a)$$

and

$$\alpha \operatorname{sh} 2\alpha l + \beta \sin 2\beta l = 0 \dots\dots(3.15b)$$

Equations (3.14b) and (3.15b) are identical. If equation (3.15a), with the use of equation (3.15b), can be shown to be identical with equation (3.14a), then there is no standing wave pattern when both the numerator and denominator of $\tan \phi$ are zero. Equation (3.15a) may be written:-

$$(\beta_0^2 - \alpha^2 - \beta^2) \operatorname{ch} 2\alpha l = (\beta_0^2 + \alpha^2 + \beta^2) \cos 2\beta l$$

Multiplying both sides by $(\alpha^2 + \beta^2)(\operatorname{ch} 2\alpha l + \cos 2\beta l)$,

$$\begin{aligned} &(\alpha^2 + \beta^2) \{ (\beta_0^2 - \alpha^2 - \beta^2) \operatorname{ch}^2 2\alpha l + (\beta_0^2 - \alpha^2 - \beta^2) \operatorname{ch} 2\alpha l \cos 2\beta l \} \\ &= (\alpha^2 + \beta^2) \{ (\beta_0^2 + \alpha^2 + \beta^2) \operatorname{ch} 2\alpha l \cos 2\beta l + (\beta_0^2 + \alpha^2 + \beta^2) \cos^2 2\beta l \} \end{aligned}$$

$$\begin{aligned} \text{or} \quad &(\alpha^2 + \beta^2) (\beta_0^2 \operatorname{ch}^2 2\alpha l - \beta_0^2 \cos^2 2\beta l) \\ &= (\alpha^2 + \beta^2)^2 (\operatorname{ch}^2 2\alpha l + 2 \operatorname{ch} 2\alpha l \cos 2\beta l + \cos^2 2\beta l) \end{aligned}$$

$$\begin{aligned}
 & (\alpha^2 + \beta^2) \beta_0^2 (1 + \text{sh}^2 \alpha l - 1 + \text{sin}^2 \beta l) \\
 = & (\alpha^2 + \beta^2)^2 (\text{ch}^2 \alpha l + \cos^2 \beta l)^2 \dots\dots\dots(3.15a) \\
 & \beta_0^2 (\alpha^2 \text{sh}^2 \alpha l + \beta^2 \text{sh}^2 \alpha l + \alpha^2 \text{sin}^2 \beta l + \beta^2 \text{sin}^2 \beta l) \\
 = & (\alpha^2 + \beta^2)^2 (\text{ch}^2 \alpha l + \cos^2 \beta l)^2 \dots\dots\dots(3.15a)
 \end{aligned}$$

Squaring equation (3.15b),

$$\alpha^2 \text{sh}^2 \alpha l + \beta^2 \text{sin}^2 \beta l - 2\alpha\beta \text{sh}^2 \alpha l \text{sin}^2 \beta l$$

and substituting in equation (3.15a)

$$\begin{aligned}
 & \beta_0^2 (\beta^2 \text{sh}^2 \alpha l + \alpha^2 \text{sin}^2 \beta l - 2\alpha\beta \text{sh}^2 \alpha l \text{sin}^2 \beta l) \\
 = & (\alpha^2 + \beta^2)^2 (\text{ch}^2 \alpha l + \cos^2 \beta l)^2 \dots\dots\dots(3.15a)
 \end{aligned}$$

$$\text{or } \beta_0^2 (\beta \text{sh}^2 \alpha l - \alpha \text{sin}^2 \beta l)^2 = (\alpha^2 + \beta^2)^2 (\text{ch}^2 \alpha l + \cos^2 \beta l)^2 \dots\dots\dots(3.15a)$$

which, on taking the square root, is identical with equation (3.14a),

$$\frac{\beta (\beta \text{sh}^2 \alpha l - \alpha \text{sin}^2 \beta l)}{(\alpha^2 + \beta^2) (\text{ch}^2 \alpha l + \cos^2 \beta l)} = 1 \dots\dots\dots(3.15a)$$

Thus the conditions which make $Z_T = Z_0$ are also the conditions which make the numerator and denominator of $\tan \phi$ zero together.

This condition of no standing wave pattern was observed experimentally with a depth of 0.28 cms of distilled water at a temperature of 36.5°C, indicating $\alpha = 0.36$ assuming $\beta = 5.95$.

3.5 The calculation of β , the phase constant.

After the observed values of Δ and l have been plotted, an approximate value of β is found using one of the two methods given below.

3.5.1 The calculation of β from the values of l when $\Delta = 0$ or $\pm\lambda_0/4$.

From equation (1.13)

$$\tan \phi = \frac{2\beta(\alpha \operatorname{sh} 2\alpha l + \beta \sin 2\beta l)}{(\beta_0^2 - \alpha^2 - \beta^2) \operatorname{ch} 2\alpha l - (\beta_0^2 + \alpha^2 + \beta^2) \cos 2\beta l}$$

If $\alpha = 0$, $\tan \phi = 0$ when $2\beta l = n\pi$.

This condition holds approximately if α is small or if n is small. Thus an approximate value of β can be obtained from the gradient of the graph of the values of l at $\Delta = 0$ and $\pm\lambda_0/4$ plotted against n . The smaller the value of α the better is this approximation for β .

This method fails for the 'alcohol-type' liquids for then positive values of Δ are not obtained.

3.5.2 The calculation of β from the values of l when $|k|^2$ has maximum and minimum values.

At the turning points of the $|k|^2$ curve, (section 3.3.1) $\sin \beta l \neq 0$, but $\sin 2\beta l \rightarrow 0$. Hence for liquids that do not give positive values of Δ , the

'alcohol-type' or electrolytic solutions, an approximate value of β may be found from the gradient of the graph of the values of l when the galvanometer readings at resonance, (proportional to $|K|^2$), have maximum and minimum values, against n .

3.6 Methods of determining the limits between which α must lie.

An approximate value for β having been found, it is used to determine the limits between which α must lie, using one or more of the methods described in this section.

3.6.1 The curve no longer going to infinity method.

For liquids with low values of α , it is seen from the experimental ^{graphs} of Δ against l that for small liquid depths the curve goes to minus $\lambda_0/8$ and plus $\lambda_0/8$, ($\Delta = 1.1375$ cms) alternately, corresponding to $\tan \phi = \mp \infty$. After a certain liquid depth is reached, which varies with the liquid used, a phase shift as great as $\lambda_0/8$ is no longer obtained, the curve turning and crossing the axis again. This change in behaviour of the curve depends upon the absorption of the liquid and the limits between which α must lie for a particular liquid may be quickly

determined as follows.

Tan $\phi = \infty$ when the denominator of equation (1.13) is zero, i.e. when

$$(\beta_0^2 - \alpha^2 - \beta^2) \text{ch}2\alpha l = (\beta_0^2 + \alpha^2 + \beta^2) \cos2\beta l \dots\dots(3.16)$$

Cosh $2\alpha l$ must always be greater than 1, whereas $\cos2\beta l$ cannot be greater than 1. Hence $\tan\phi$ can go to infinity when

$$\text{ch}2\alpha l < \frac{\beta_0^2 + \alpha^2 + \beta^2}{\beta_0^2 - \alpha^2 - \beta^2}$$

but can no longer go to infinity when

$$\text{ch}2\alpha l > \frac{\beta_0^2 + \alpha^2 + \beta^2}{\beta_0^2 - \alpha^2 - \beta^2}$$

$$\text{Let } k' = \frac{\beta_0^2 + \alpha^2 + \beta^2}{\beta_0^2 - \alpha^2 - \beta^2}$$

Since α must be small for a phase shift of $\lambda_0/8$ to be obtained at all, α^2 may be neglected. Therefore

$$k' = \frac{\beta_0^2 + \beta^2}{\beta_0^2 - \beta^2} \dots\dots\dots(3.17)$$

For the magnetron oscillator used, $\lambda_0 = 9.1$ cms giving $\beta_0 = 0.69$ so that for a given liquid k' can be calculated using the value of β obtained from the method of section 3.5.1. The greatest value of l for which $\Delta = 1.1375$ cms,

$\tan \phi = \infty$, is read off from the graph of Δ against l . Let it be l_1 . Then α is the only unknown in the equation

$$\text{ch}2\alpha l_1 < k' \dots\dots\dots(3.18)$$

and so is readily calculated.

The value of l , l_2 say, when the curve instead of reaching $\Delta = 1.1375$ cms turns round, is used to fix a lower limit for α .

$$\text{ch}2\alpha l_2 > k' \dots\dots\dots(3.18)$$

For liquids with higher values of α , the 'water-type' liquids, $\tan \phi$ may never reach infinity and then this method can give only a lower limit for α .

3.6.2 The change of sign of the gradient method.

The change of sign of the gradient at $\tan \phi = 0$ when n is odd for a critical liquid depth was described in section 3.2.1. It gives a quick method of fixing limits between which α must lie for liquids with low values of α .

From equation (3.8a), the gradient when $\tan \phi = 0$ and n is odd, will be negative if:-

$$\beta_0^2 \beta^2 + \beta^4 > (\beta^4 - \beta_0^2 \beta^2) \text{ch}2\alpha l \dots\dots\dots(3.19)$$

and positive if:-

$$\beta_0^2 \beta^2 + \beta^4 < (\beta^4 - \beta_0^2 \beta^2) \text{ch}2\alpha l \dots\dots\dots(3.20)$$

In these equations β_0 is known and for low absorbing liquids β is obtained with some accuracy by the method of section 3.5.1. The value of l at the highest odd value of n giving a negative gradient when $\tan \phi = 0$, or $\Delta = \pm \lambda_0/4$, is read off from the experimental curve of the shift Δ against l and substituted in equation (3.19). Similarly, the value l at the next higher odd value of n position where the gradient has become positive is substituted in equation (3.20), and thus the limits between which α must lie can be determined.

3.6.3 The curve no longer taking positive values method.

From equation (1.13)

$$\tan \phi = \frac{2\beta_0(\alpha \operatorname{sh} 2\alpha l + \beta \sin 2\beta l)}{(\beta_0^2 - \alpha^2 - \beta^2) \operatorname{ch} 2\alpha l - (\beta_0^2 + \alpha^2 + \beta^2) \cos 2\beta l}$$

Since β is always greater than β_0 , the cosh term in the denominator of equation (1.13) is always negative, its value increasing with l . The cosine term in the denominator is alternately positive and negative, its maximum value being $(\beta_0^2 + \alpha^2 + \beta^2)$. Thus for sufficiently large values of l the denominator becomes negative and remains negative as l is increased still further.

When the liquid depth is such that the denominator is

always negative as l increases, positive values of $\tan \phi$ or Δ will occur when the numerator is also negative. The first term of the numerator, $\alpha \sinh 2\alpha l$, is always positive, while the second term, $\beta \sin 2\beta l$, is alternately positive and negative. The maximum value of this second term is $\pm \beta$. Thus when

$$\alpha \sinh 2\alpha l > \beta \dots\dots\dots(3.21)$$

Δ can no longer take positive values.

The value of l when Δ no longer assumes positive values, l_3 , is read off from the experimental graph and substituted in equation (3.21)

$$\alpha \sinh 2\alpha l_3 > \beta \dots\dots\dots(3.21)$$

α is then the only unknown in this equation which can be solved graphically.

This method is applicable to all types of liquids, but it is likely to be more accurate for liquids with higher absorptions. This is because with high values of α the depth of liquid required for the curve to assume only negative values is small, of the order of 3 or 4 cms, and with the method of measurement used at present any inaccuracies in the measurements increase with l .

3.6.4 The constant galvanometer signal method.

$|k|^2$ approaches a constant value as $\sinh 2\alpha l$ and

$\cosh 2\alpha l$ approach infinity. This occurs when $2\alpha l > 5$. Thus if the value of l when the galvanometer signal remains constant for increasing liquid depths is substituted in this condition, a lower limit is obtained for α .

3.7 Methods of finding α .

After the limits for α have been found from one or more of the methods in section 3.6, one or more of the following methods is used to find α exactly. Any of these methods may equally well be used to determine β exactly, assuming a value for α .

3.7.1 From the maximum and minimum values of Δ .

The value of l at a clearly defined turning point of the experimental graph is substituted in equation (3.9a) or (3.9b) of section 3.2.3. Neglecting α^2 ,

$$\begin{aligned}
 -\beta_0^2 \beta^2 - \beta^4 + (\beta_0^2 \beta^2 - \beta^4) \operatorname{ch} 2\alpha l \cos 2\beta l \\
 = 2\beta_0^2 \alpha \beta \operatorname{sh} 2\alpha l \sin 2\beta l \quad \dots\dots\dots (3.9b)
 \end{aligned}$$

Assuming β is known this equation can then be solved graphically for α .

3.7.2 From the gradient of the curve when $\tan \phi = 0$.

Equations (3.7a) and (3.7a) of section 3.2.1 give expression for the gradients of the curve at $\tan \phi = 0$

when α' is neglected.

When n is even,

$$- \frac{d\phi}{dl} = \frac{4\beta_o \{ \beta_o^2 \beta^2 + \beta^4 + (\beta^4 - \beta_o^2 \beta^2) \cosh 2\alpha l \}}{[(\beta^2 - \beta_o^2) \cosh 2\alpha l + (\beta_o^2 + \beta^2)]^2} \dots\dots(3.7a)$$

and when n is odd,

$$- \frac{d\phi}{dl} = \frac{4\beta_o \{ \beta_o^2 \beta^2 + \beta^4 - (\beta^4 - \beta_o^2 \beta^2) \cosh 2\alpha l \}}{[(\beta^2 - \beta_o^2) \cosh 2\alpha l - (\beta_o^2 + \beta^2)]^2} \dots\dots(3.8a)$$

The gradient at $\tan \phi = 0$, $\Delta = 0$ or $\pm \lambda_o/4$, for some value of n of the phase shift against l graph, $d\Delta/dl$ is measured, and the value of l noted. It was found necessary to draw the portion of the curve near $\tan \phi = 0$ on a large scale to obtain an accurate value of $d\Delta/dl$. From equation (3.3)

$$\frac{d\phi}{dl} = \frac{4\pi}{\lambda_o} \frac{d\Delta}{dl}$$

On substitution of these values in either (3.7a or ^{3.8a}b), according to whether n is even or odd, a quadratic in $\cosh 2\alpha l$ is obtained, which on solution gives α .

3.7.3 Substitution of experimental values in the $\tan \phi$ equation.

α can be found by substitution of β and any pair of experimental values of Δ and l in equation (1.13)

$$\tan \phi = \frac{2\beta_0(\alpha \operatorname{sh}2\alpha l + \beta \sin2\beta l)}{(\beta_0^2 - \alpha^2 - \beta^2) \operatorname{ch}2\alpha l - (\beta_0^2 + \alpha^2 + \beta^2) \cos2\beta l}$$

and

$$\phi = \frac{4\pi}{\lambda_0} \Delta \dots\dots\dots(1.19)$$

The resulting equation can then be solved graphically for α .

3.7.4 From the steady negative value of Δ .

In section 1.6.2 it was shown that for sufficiently large values of l

$$\tan \phi \rightarrow - \frac{2\beta_0\alpha}{\beta^2 + \alpha^2 - \beta_0^2} \dots\dots\dots(1.23)$$

The steady negative value of Δ is read off from the graph, $\tan \phi$ calculated and substituted in equation (1.23) with β_0 and β , so giving a value for α .

3.7.5 From the value of l when $\Delta = 0$.

The method of section 3.6.3 may sometimes be used to give a definite value for α . If the value of Δ approaches zero very closely but does not become positive for a particular value of l , (see the results for alcohol, fig. 4.80) then this value of l may be substituted with β in the equation

$$\alpha \operatorname{sh}2\alpha l + \beta \sin2\beta l = 0$$

and the resulting equation solved for α .

Chapter 4

EXPERIMENTAL RESULTS

4.1 Introduction.

In the experimental method used so far a very large number of readings of Δ are taken corresponding to different values of l . The accuracy with which Δ may be measured depends upon the sharpness of the tuning, which, as was shown in section 2.2, varies for different values of l . In general the tuning is sharp except at the first turning point of the $\tan \phi$ curve. Uncertainty in the exact value of Δ is indicated on the experimental graphs by a vertical line extending over the range of values of Δ giving maximum signal. Tables 2, 10 and 14 in the Appendix give the readings recorded for representative liquids of the three main types.

The methods available for the calculation of α and β have been outlined in chapter 3. The methods used depend upon the type of liquid, the deduction of α and β amounting to a method of successive approximations.

The experimental disadvantages of the present method are:-

- (i) Measurements of l and Δ are not independent, so that any inaccuracy in l affects Δ and increases with increasing depth.
- (ii) The uncertainty of knowing when the liquid covers the short circuiting base.
- (iii) The time necessary to make the required number of observations.

A modified form of the apparatus is described in chapter 5 which would give independent measurements of Δ and l , and would permit the use of a very much quicker experimental method for determining the critical points of the $\tan \phi$ curve. This method, however, involves the use of a movable short circuiting piston and has not yet been used owing to the difficulties of designing a movable piston which would act as a true short circuit. This problem is discussed more fully in chapter 5.

The accuracy to which values for α and β may be calculated from the experimental curves depends upon the method used, and the estimated error is indicated in the tables of results. The final values of α and β obtained by this phase shift method are compared with those obtained by other workers using different

methods. To facilitate comparison the real and imaginary parts of the dielectric constant ϵ' and ϵ'' have been calculated from these values of α and β . The relationships³⁶ between ϵ' , ϵ'' and the propagation constants for materials in coaxial lines or waveguides and carrying travelling or standing waves are:-

$$\epsilon' = \left[\beta^2 - \alpha^2 + \left(\frac{2\pi}{\lambda_c} \right)^2 \right] \left(\frac{\lambda_0}{2\pi} \right)^2 \dots\dots\dots(4.1)$$

$$\epsilon'' = 2\alpha\beta \left(\frac{\lambda_0}{2\pi} \right)^2 \dots\dots\dots(4.2)$$

where λ_c is the cut-off wavelength. For coaxial lines $\lambda_c = \infty$ for the principal wave so that equation (4.1) becomes:-

$$\epsilon' = (\beta^2 - \alpha^2) \left(\frac{\lambda_0}{2\pi} \right)^2 \dots\dots\dots(4.3)$$

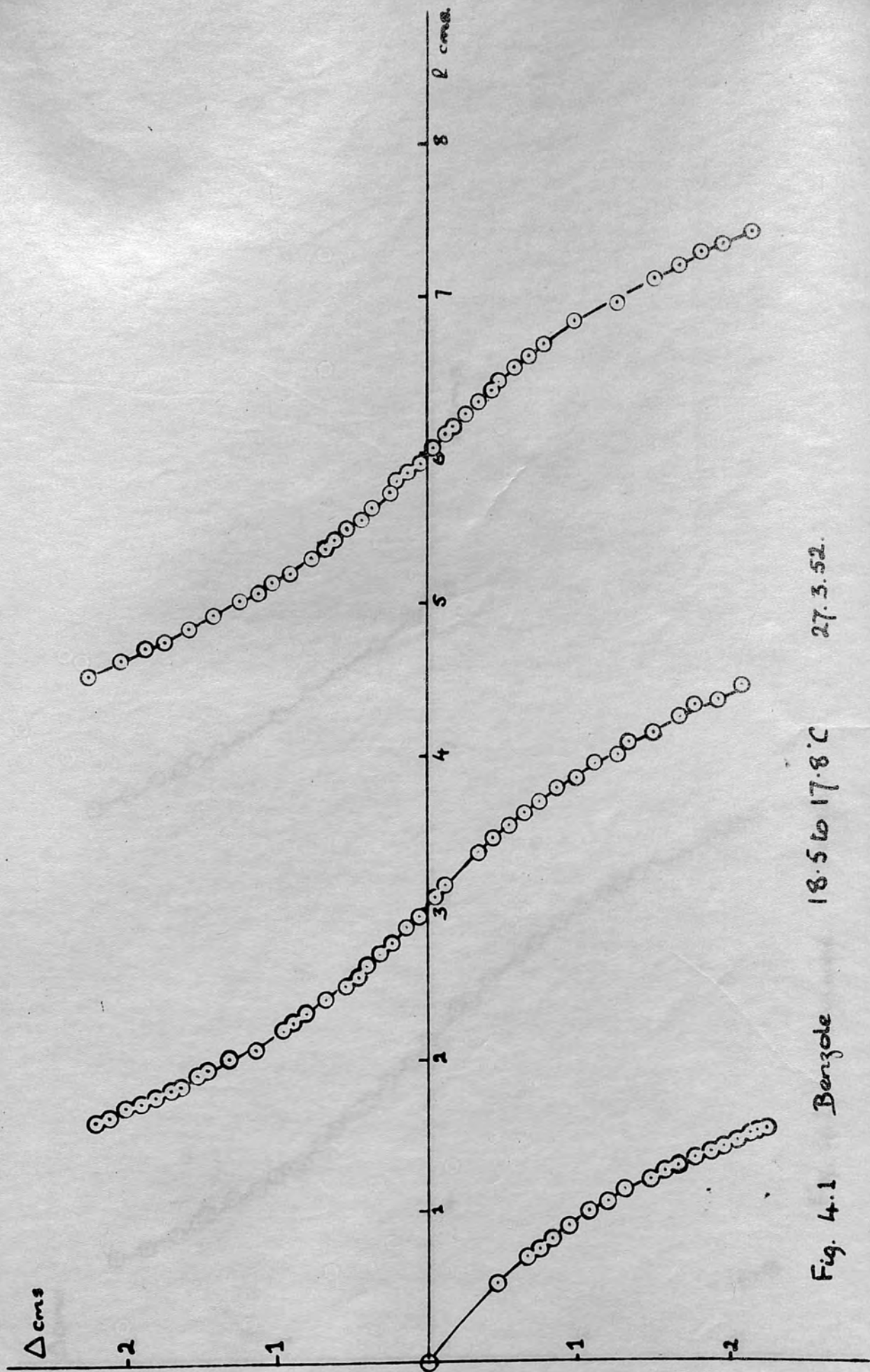
Solving these equations for α and β gives:

$$\alpha = \frac{2\pi}{\lambda_0} \left\{ \frac{\epsilon'}{2} \left[\pm \sqrt{1 + \left(\frac{\epsilon''}{\epsilon'} \right)^2} - 1 \right] \right\}^{1/2}$$

and
$$\beta = \frac{2\pi}{\lambda_0} \left\{ \frac{\epsilon'}{2} \left[1 \pm \sqrt{1 + \left(\frac{\epsilon''}{\epsilon'} \right)^2} \right] \right\}^{1/2}$$

4.2 Experimental results for a non-absorbing liquid.

The non-absorbing liquid benzole was used; the variation of phase shift with liquid depth is shown in



27.3.52.

18.5 to 17.8°C

Fig. 4.1 Benzole

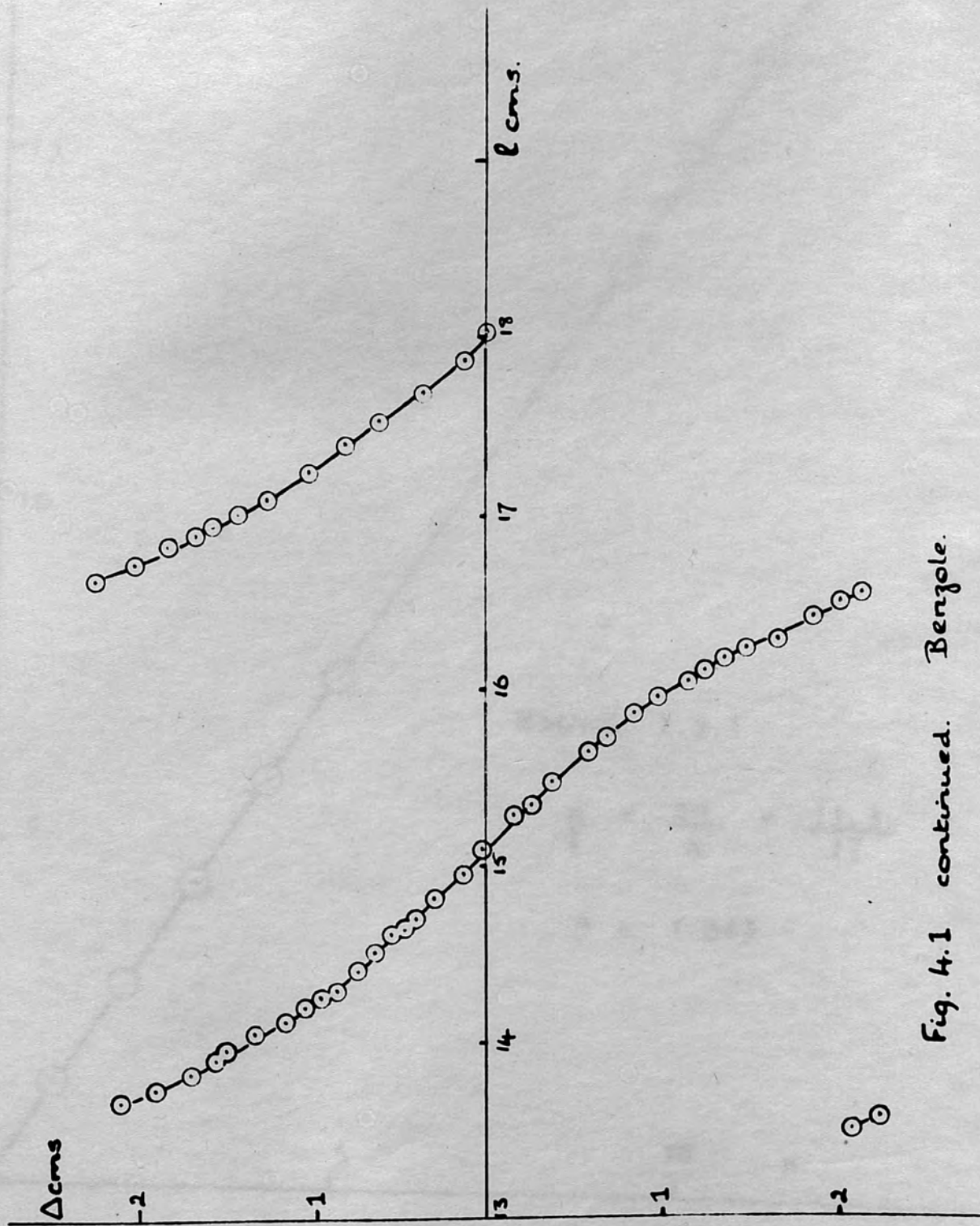


Fig. 4.1 continued. Benzole.

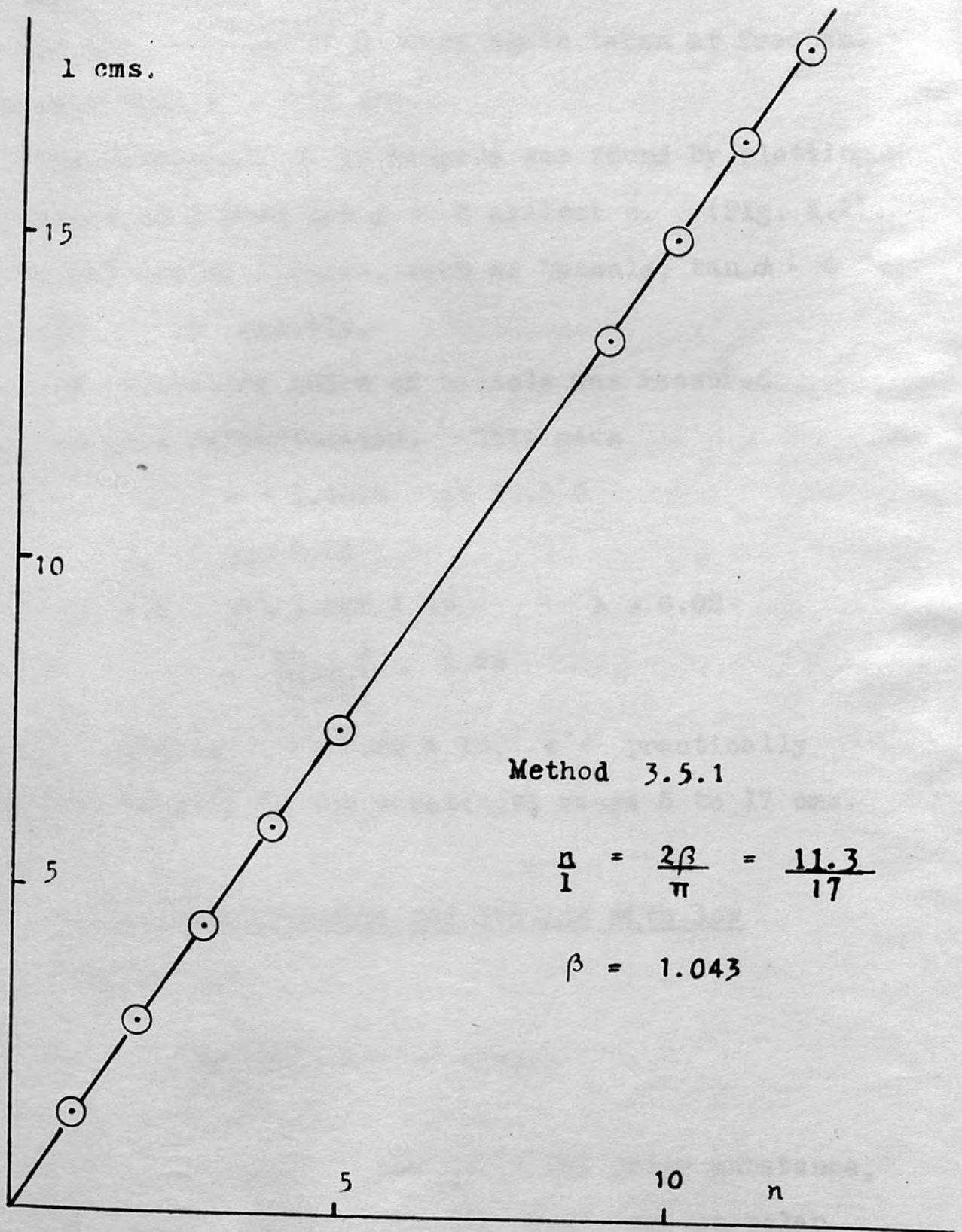


Fig. 4.2 Benzole.

fig. 4.1. Measurements of Δ were taken at frequent intervals as the liquid depth was increased from 0 to 7.5 cms. The liquid depth was then increased to 13.4 cms and the readings of Δ were again taken at frequent intervals till $l = 18$ cms.

The wavelength λ in benzole was found by plotting the values of l when $\tan \phi = 0$ against n . (Fig. 4.2). For non-absorbing liquids, such as benzole, $\tan \phi = 0$ when $2\beta l = n\pi$ exactly.

The refractive index of benzole was measured using an Abbé refractometer. This gave

$$\mu = 1.4999 \quad \text{at } 19.5^\circ \text{C}$$

or $\epsilon_3 = 2.25$

From fig. 4.2 $\beta = 1.043 \pm 1\%$ $\lambda = 6.02$

giving $\epsilon' = \left[\frac{9.1}{6.02} \right]^2 = 2.28$

²⁶ Abadie obtains $\epsilon' = 2.29 \pm 1\%$, $\epsilon'' =$ practically zero, for benzene in the wavelength range 3 to 17 cms.

4.3 Experimental results for liquids with low absorptions.

The liquids investigated were:-

- (i) Chlorobenzene.
- (ii) A solution of 200 cc of the polar substance, chlorobenzene, in 100 cc of the non-polar

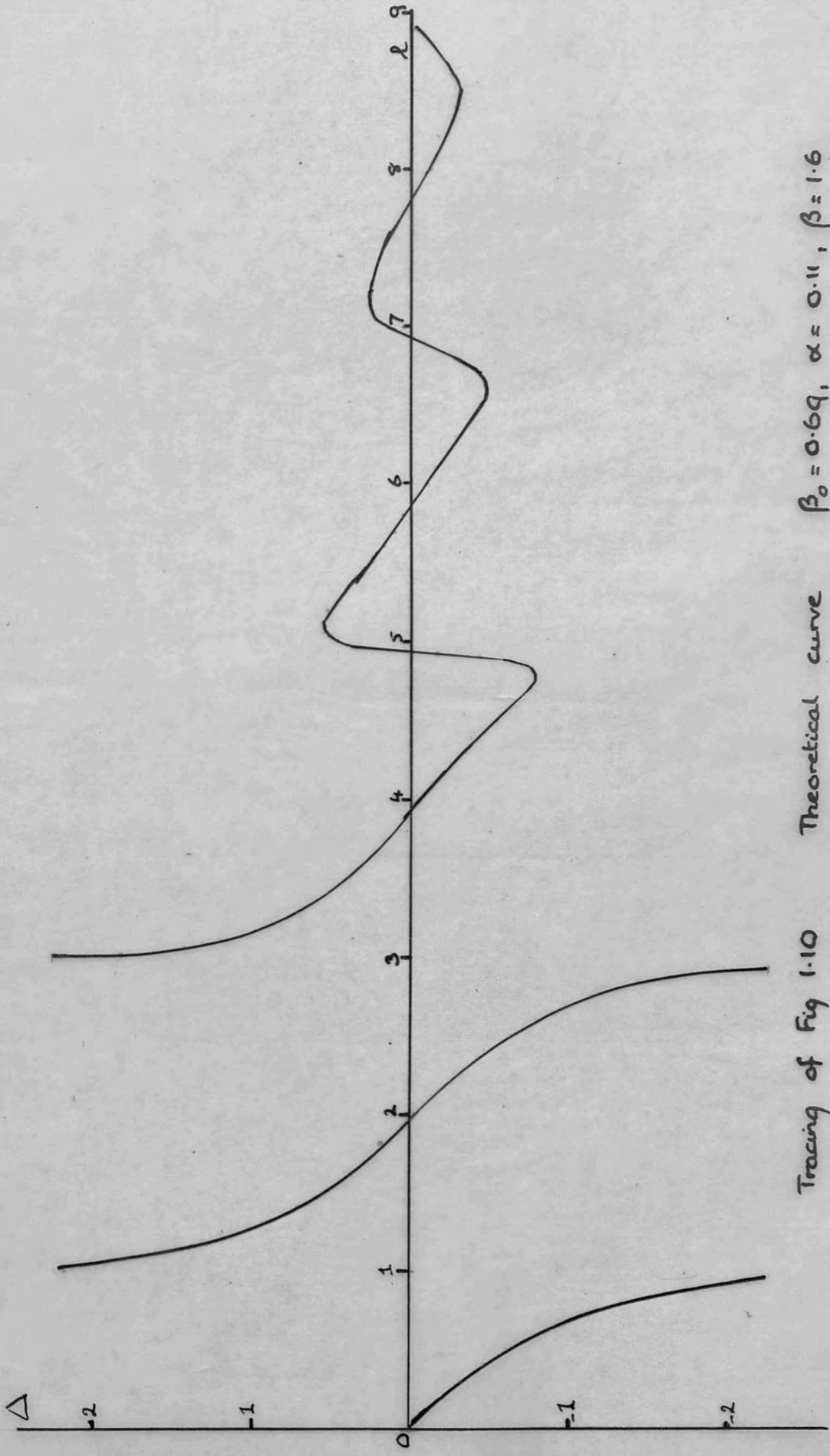
solvent, benzole. (63.3 mole % of chlorobenzene.

(iii) Cyclohexanol,
at room temperature.

Cyclohexanol is a highly viscous liquid ($\eta = 0.2$ poise at 39°C) so that the experimental arrangement described in section 2.4.1.2 was used for this liquid.

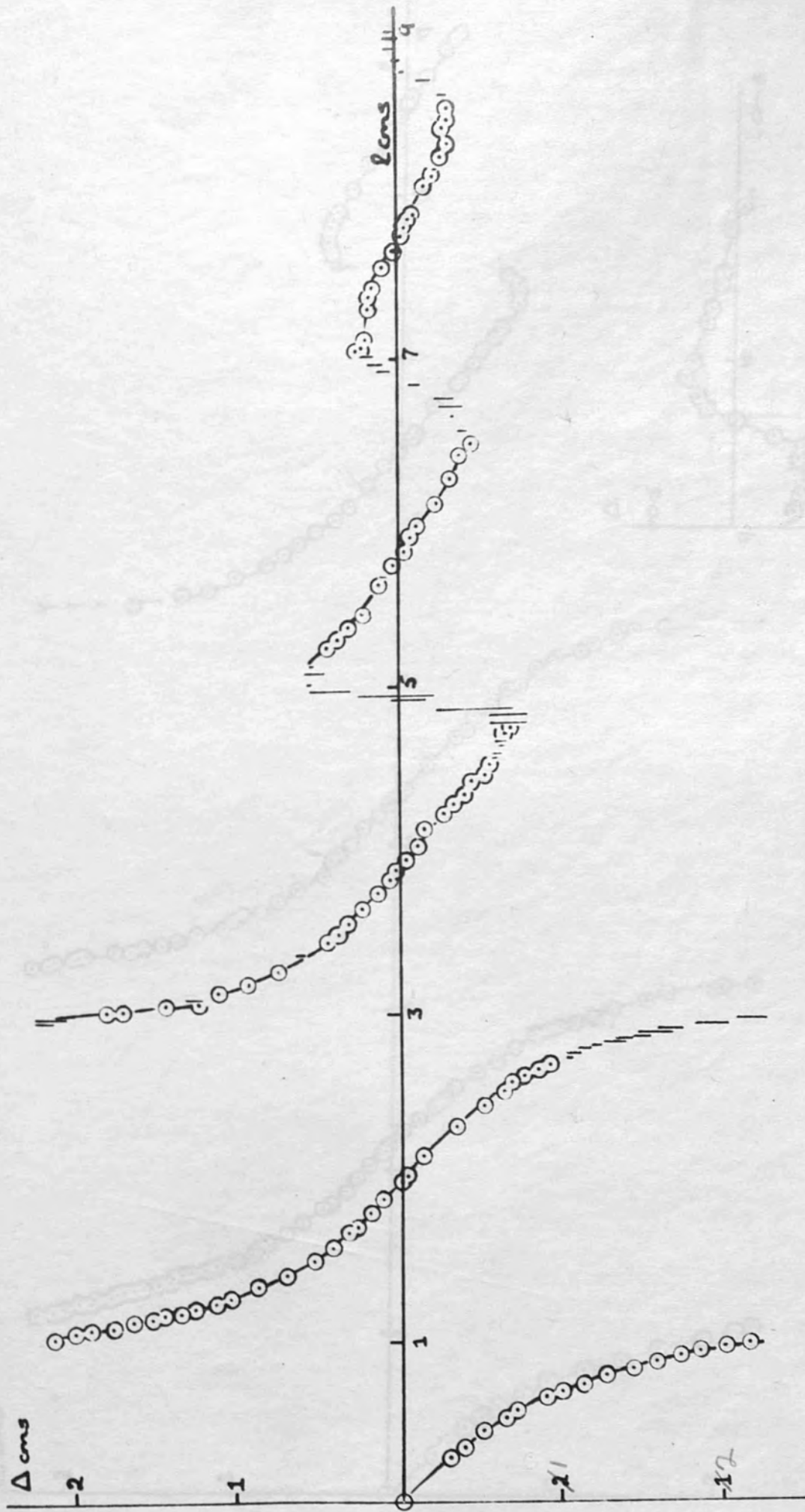
Table 2 in the Appendix gives the experimental readings recorded when chlorobenzene was used.

Figs. 4.3, 4.4 and 4.5 show the experimentally observed variations in phase shift with liquid depth for the three liquids. The variation in galvanometer signal with increasing liquid depth is also plotted for cyclohexanol in fig. 4.6. Table 3, 4 and 5 summarise the values of β , the limits of α and values of α obtained by the application of some of the methods outlined in chapter 3.



Theoretical curve $\beta_0 = 0.69, \alpha = 0.11, \beta = 1.6$

Tracing of Fig 1.10

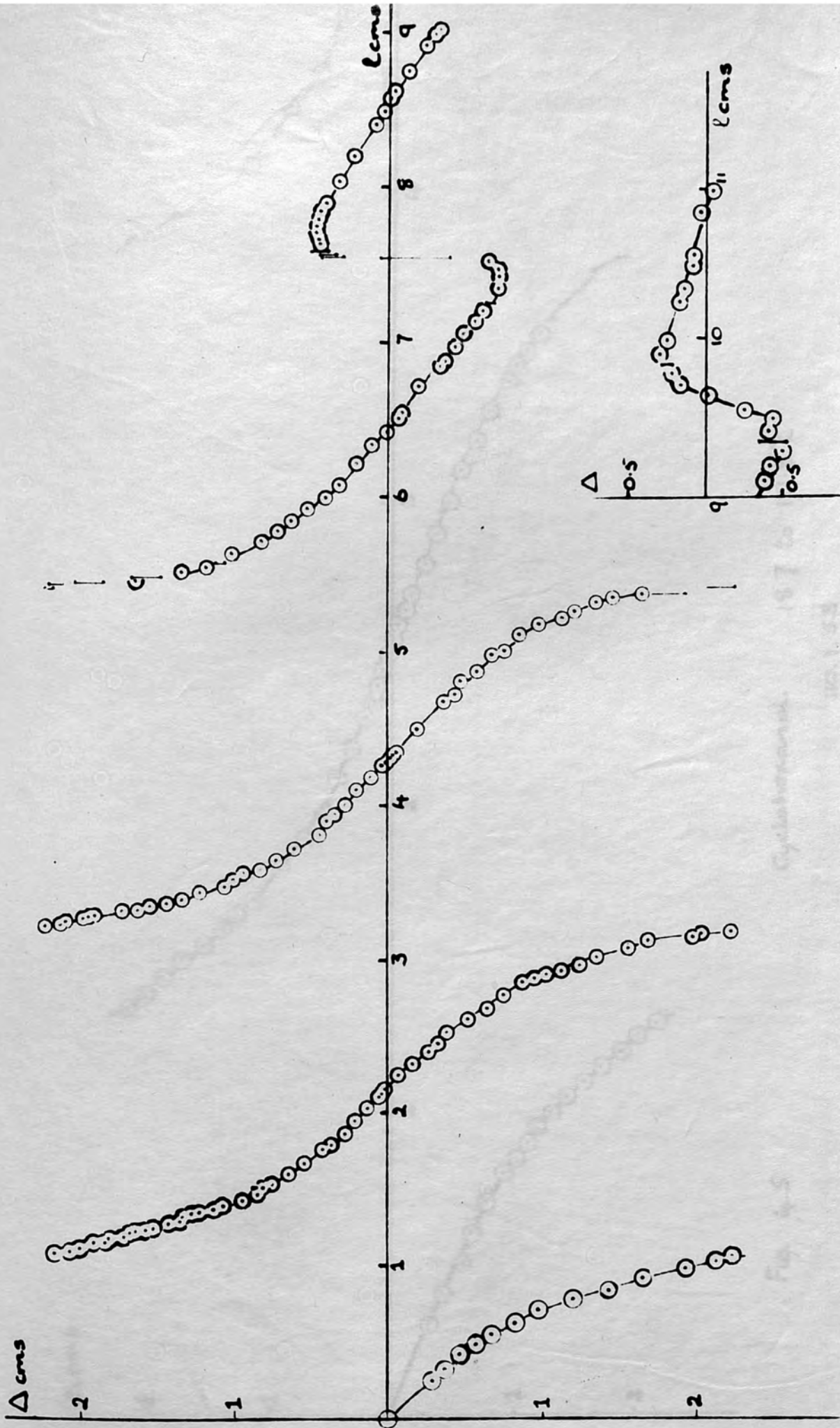


4.3.52.

19°C

Chlorobenzene

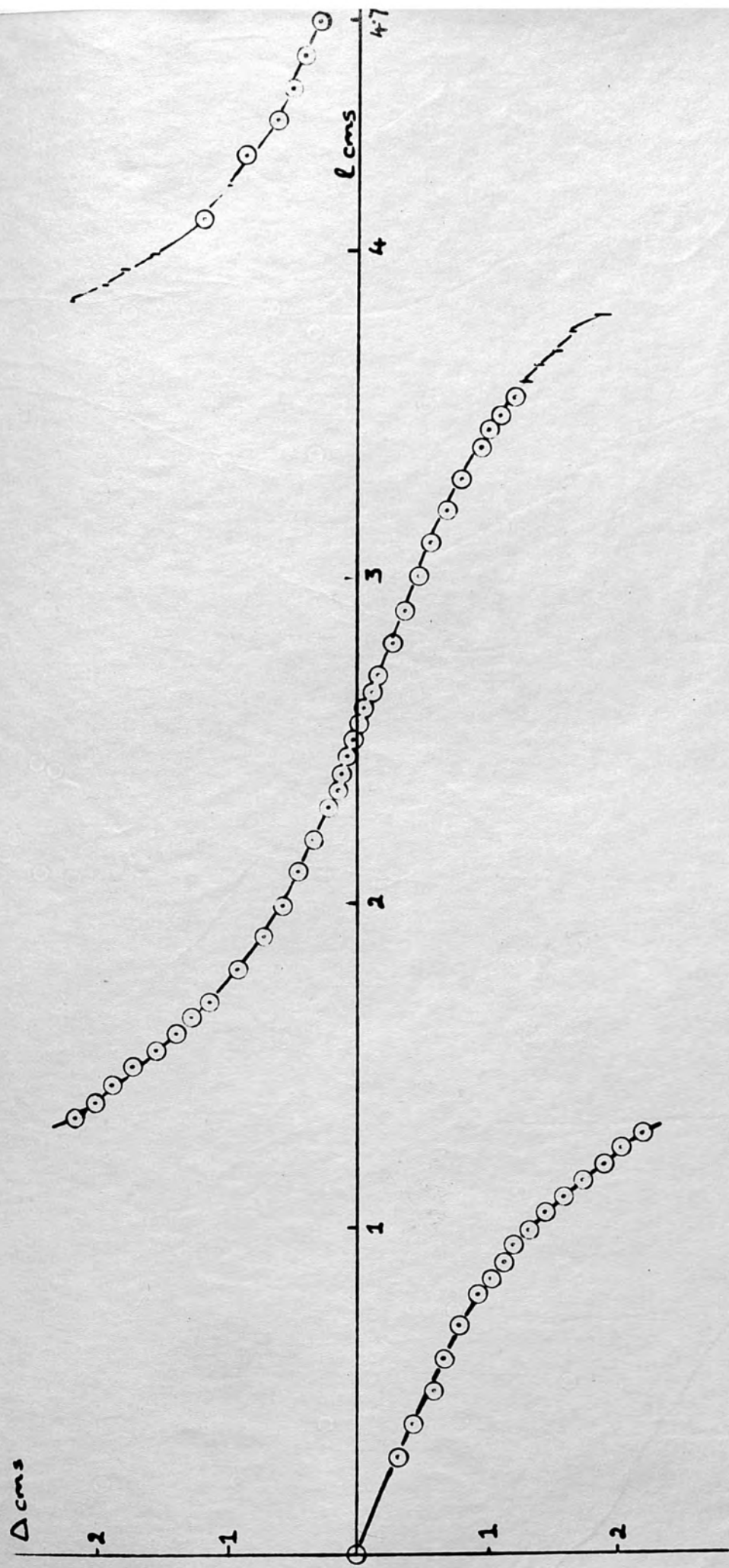
Fig. 4.3



24.3.52.

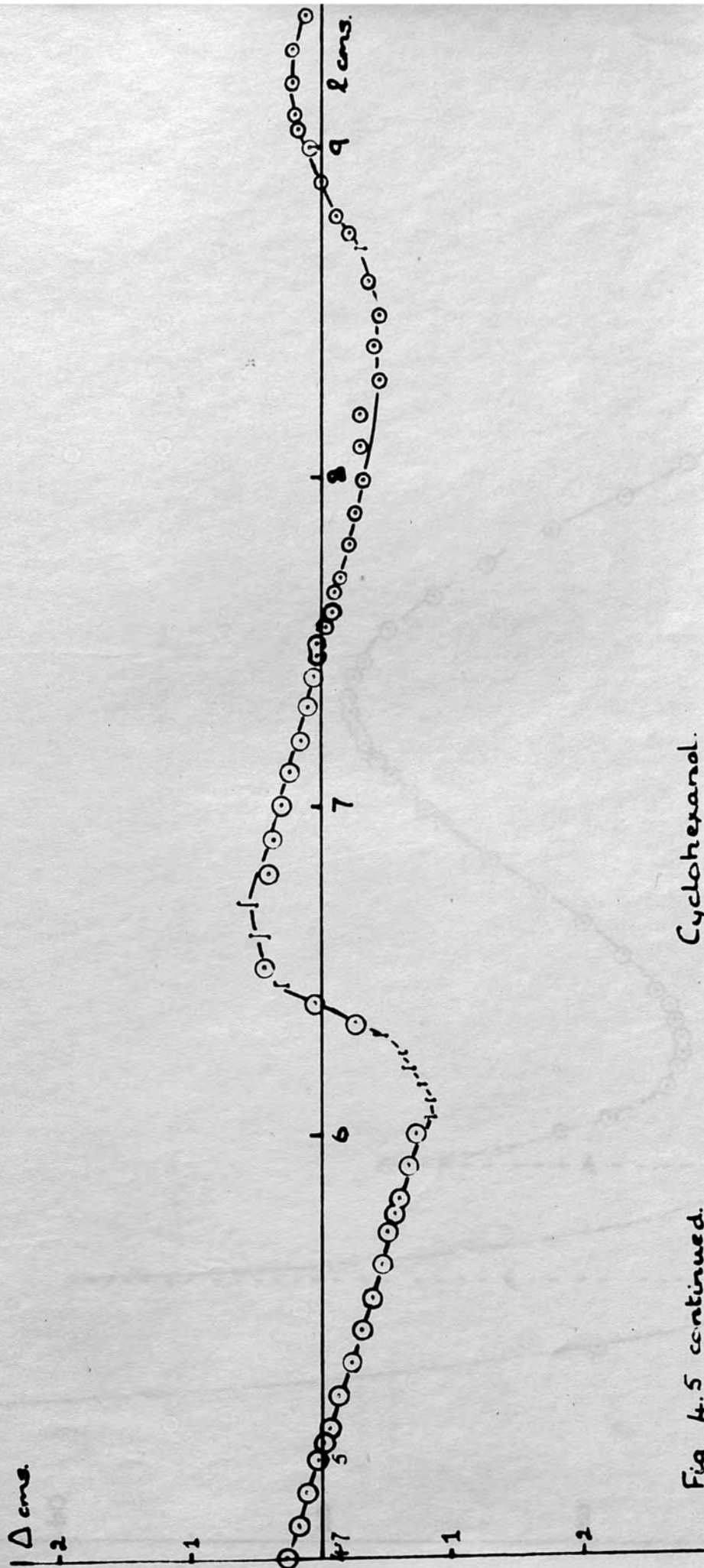
18°C

Fig. 4.4 Mixture of Chlorobenzene and Benzole.



Cyclohexanol. 18.7 to 19.8°C
20.1.53.

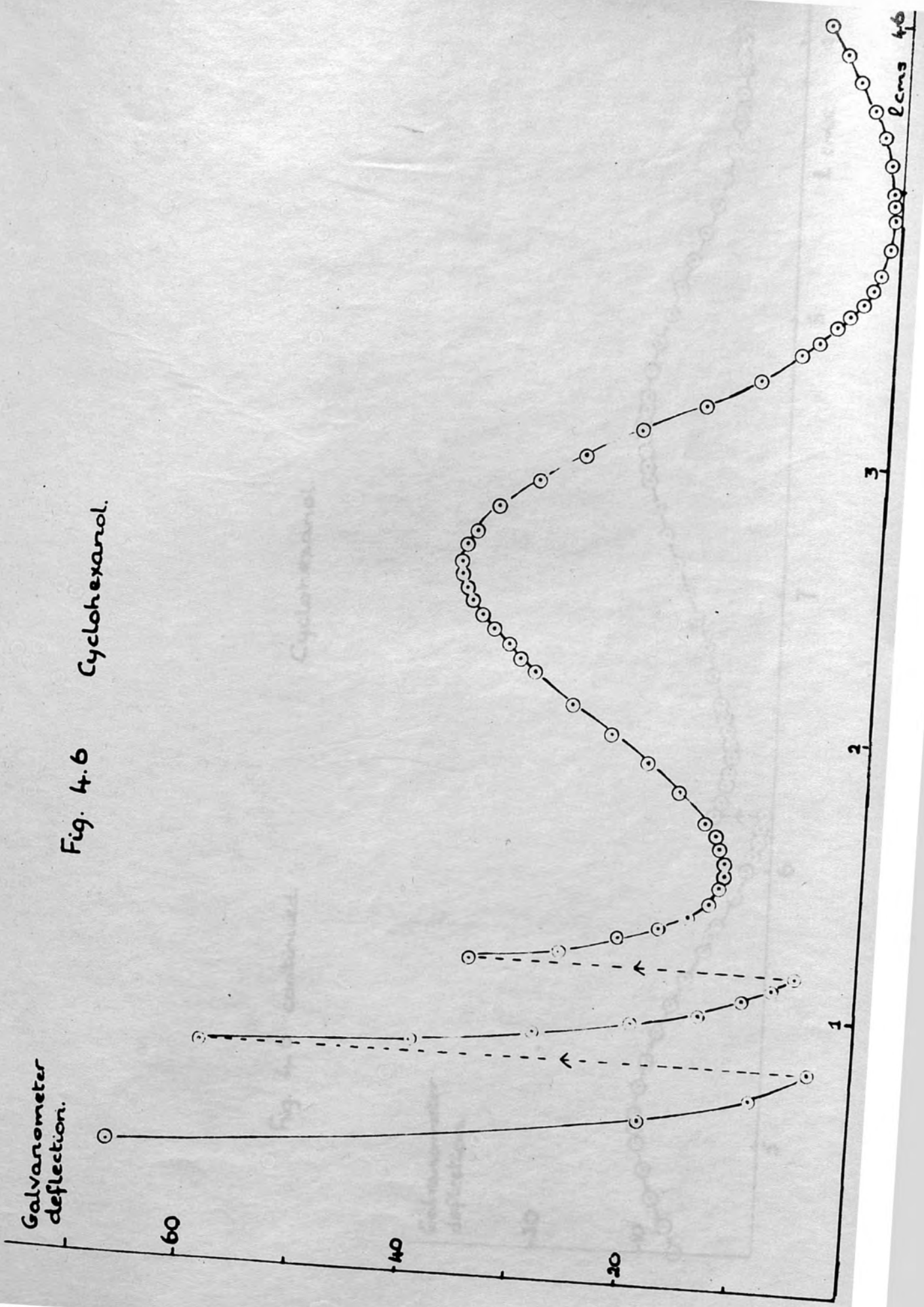
Fig. 4.5



Cyclohexanol.

Fig. 4.5 continued.

Fig. 4.6 Cyclohexanol.



Cyclohexanol.

Fig. 4.6 continued.

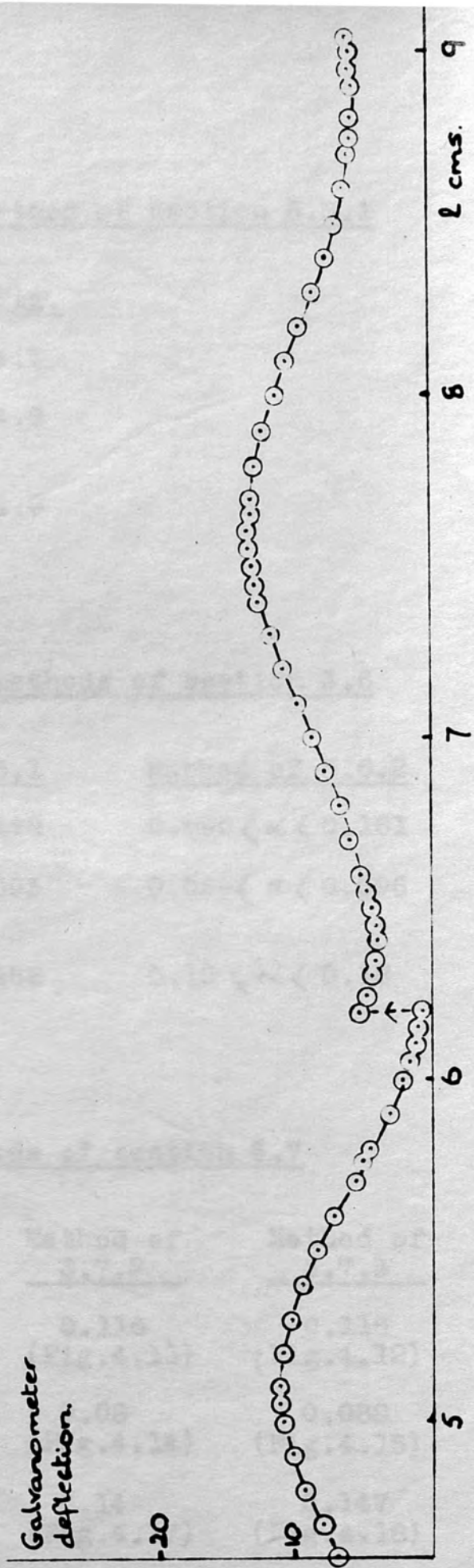


Table 3

β calculated by the method of section 3.5.1

<u>Liquid</u>	<u>β</u>	<u>Fig.</u>
Chlorobenzene	1.60	4.7
63.3 mole % chlorobenzene	1.45	4.8
Cyclohexanol	1.23	4.9

Table 4

The limits of α by the methods of section 3.6

<u>Liquid</u>	<u>Method of 3.6.1</u>	<u>Method of 3.6.2</u>
Chlorobenzene	0.093 $< \alpha <$ 0.148	0.096 $< \alpha <$ 0.161
63.3 mole % chlorobenzene	0.063 $< \alpha <$ 0.093	0.069 $< \alpha <$ 0.096
Cyclohexanol	0.105 $< \alpha <$ 0.156	0.10 $< \alpha <$ 0.18

Table 5

α calculated by the methods of section 3.7

<u>Liquid</u>	<u>Method of 3.7.1</u>	<u>Method of 3.7.2</u>	<u>Method of 3.7.3</u>
Chlorobenzene	0.113 (Fig.4.10)	0.116 (Fig.4.11)	0.116 (Fig.4.12)
63.3 mole % chlorobenzene	0.071 (Fig.4.13)	0.08 (Fig.4.14)	0.088 (Fig.4.15)
Cyclohexanol	0.149 (Fig.4.16)	0.14 (Fig.4.17)	0.147 (Fig.4.18)

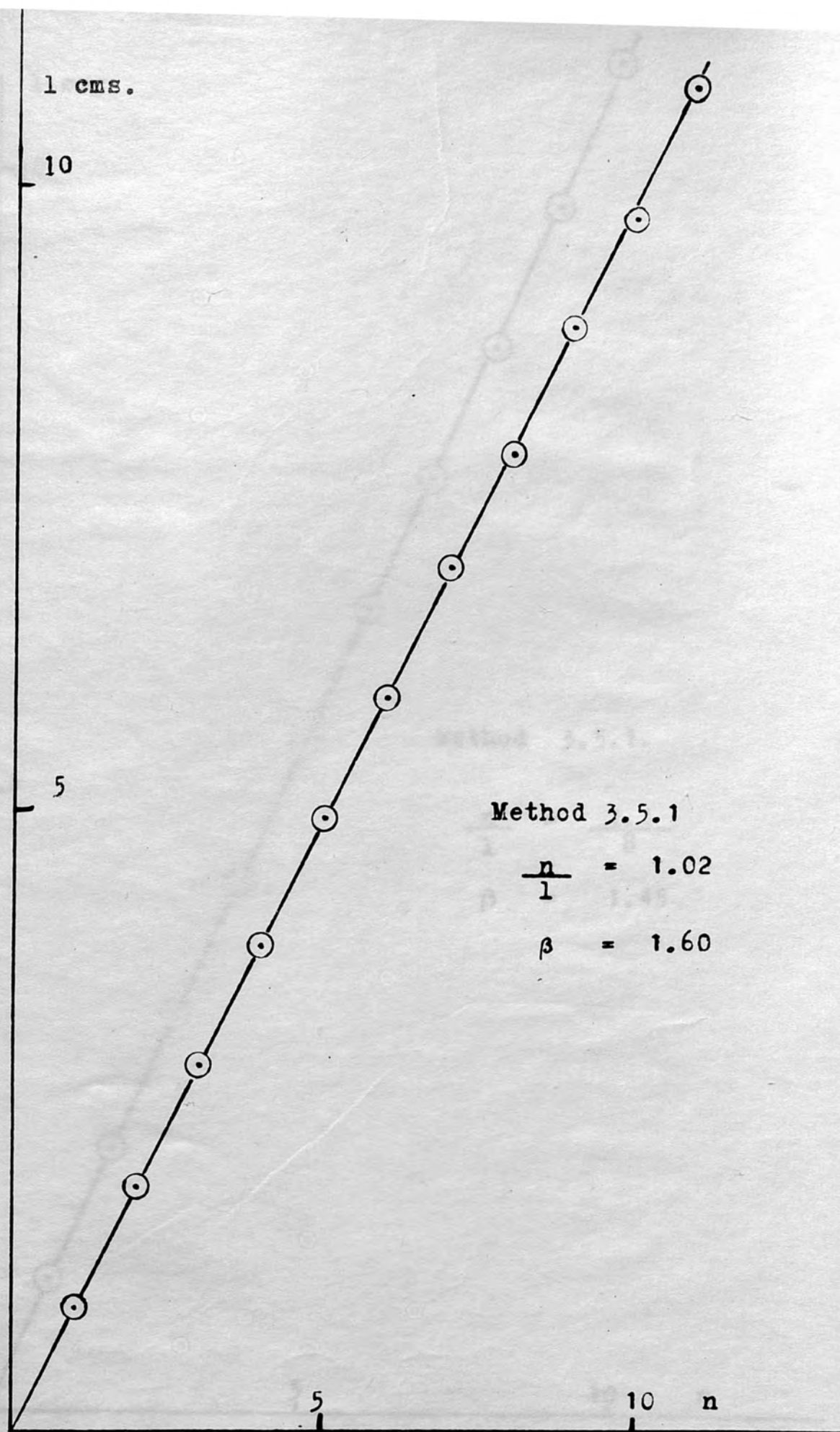


Fig. 4.7 Chlorobenzene.

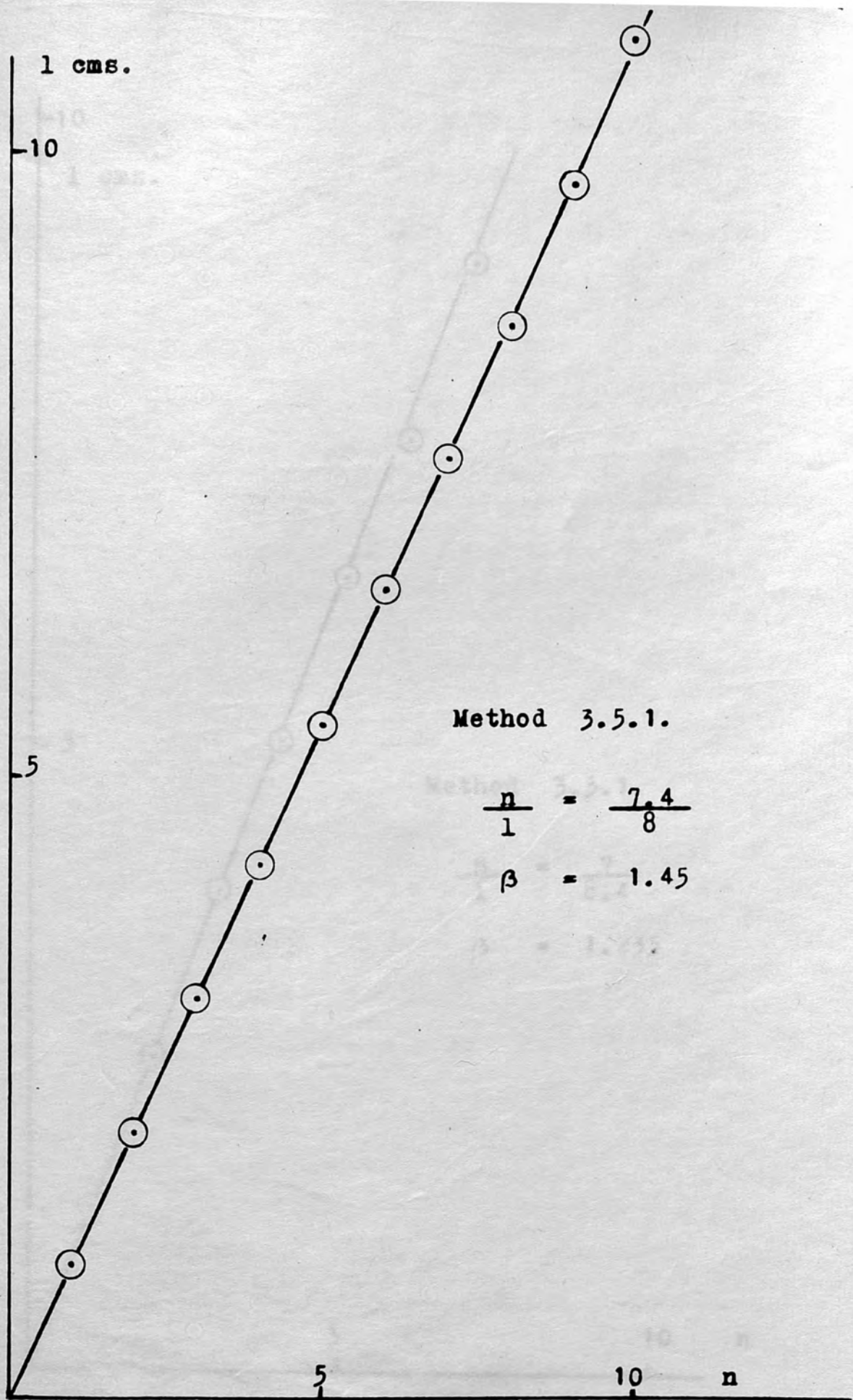


Fig. 4.8 Chlorobenzene - benzole mixture.

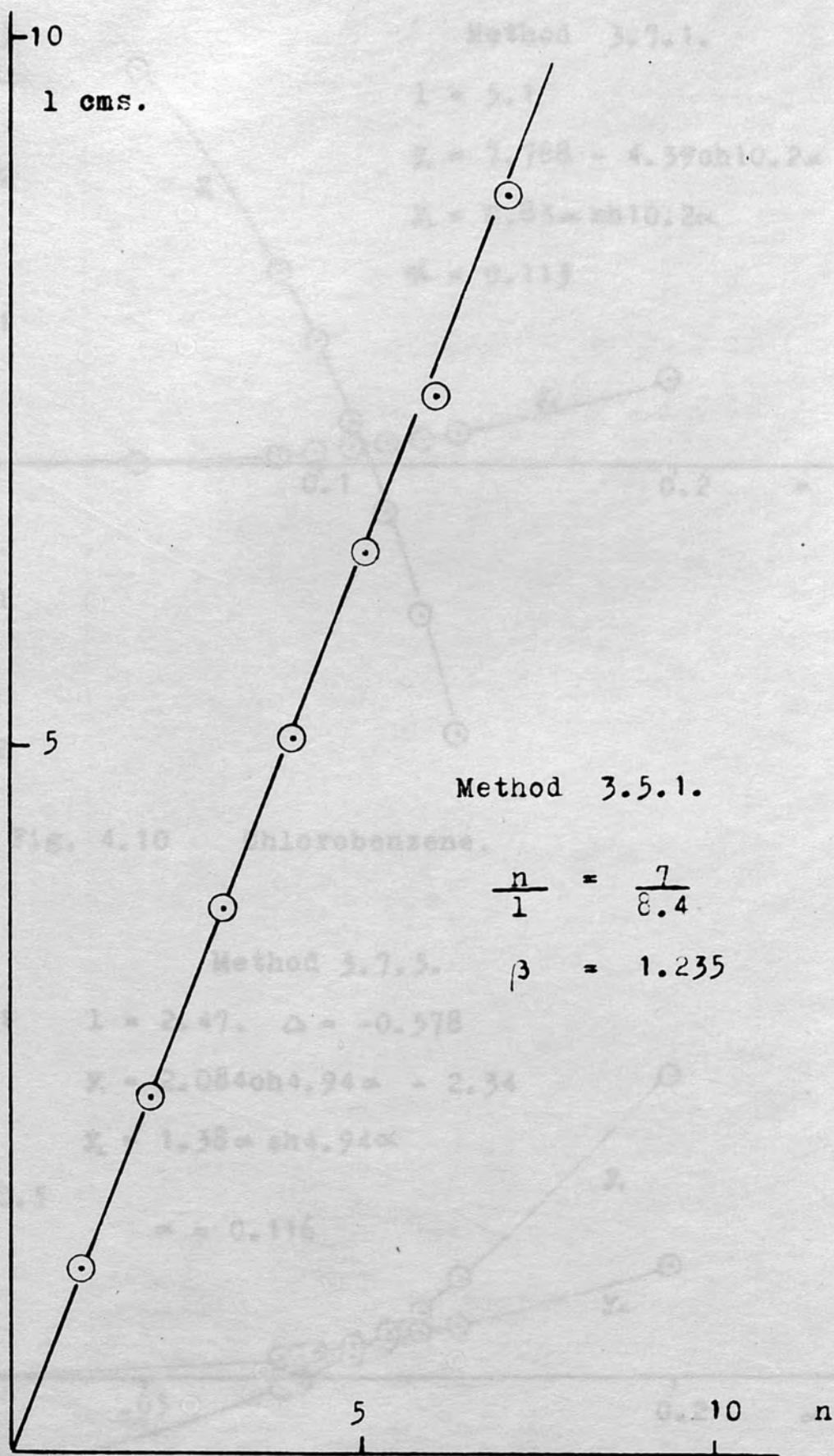


Fig. 4.9 Cyclohexanol.

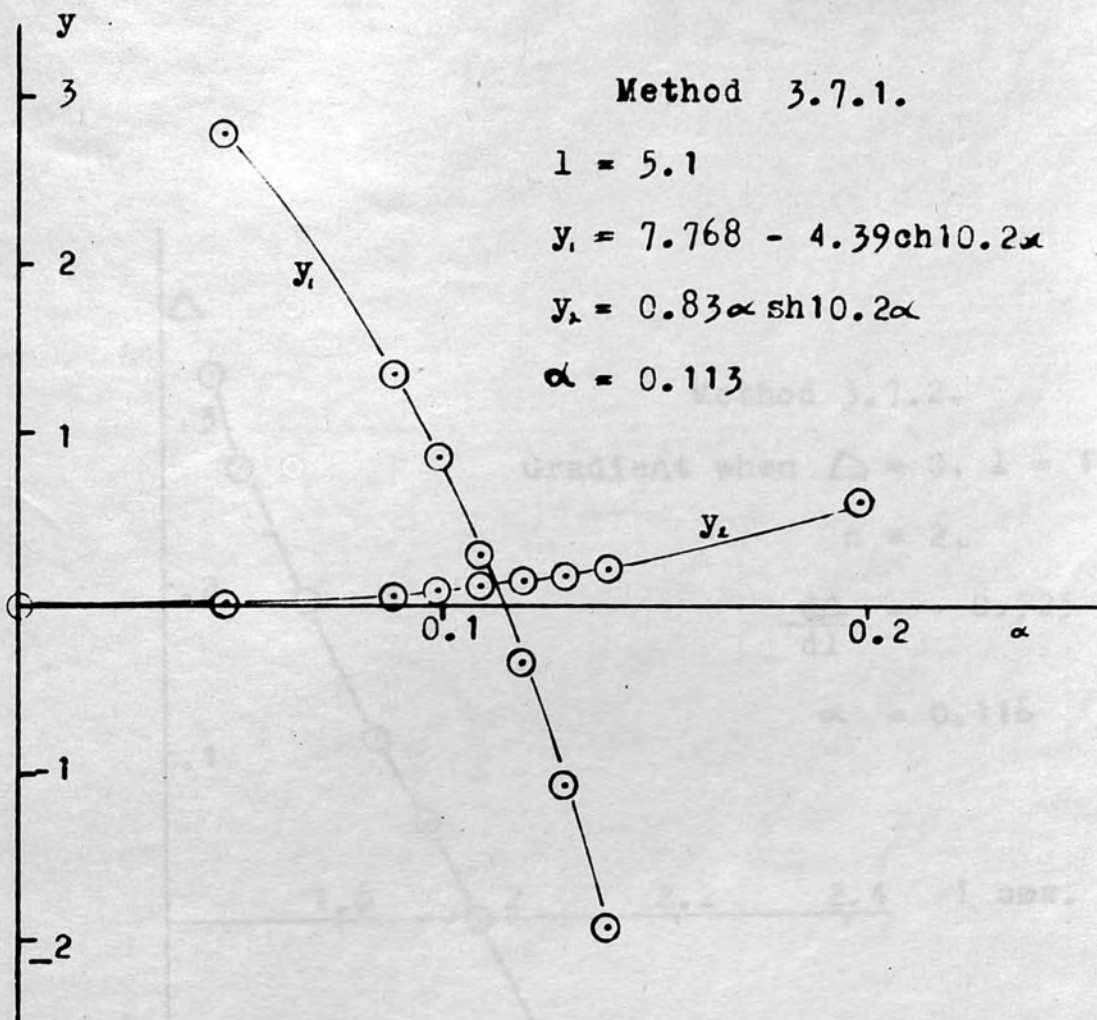


Fig. 4.10 Chlorobenzene.

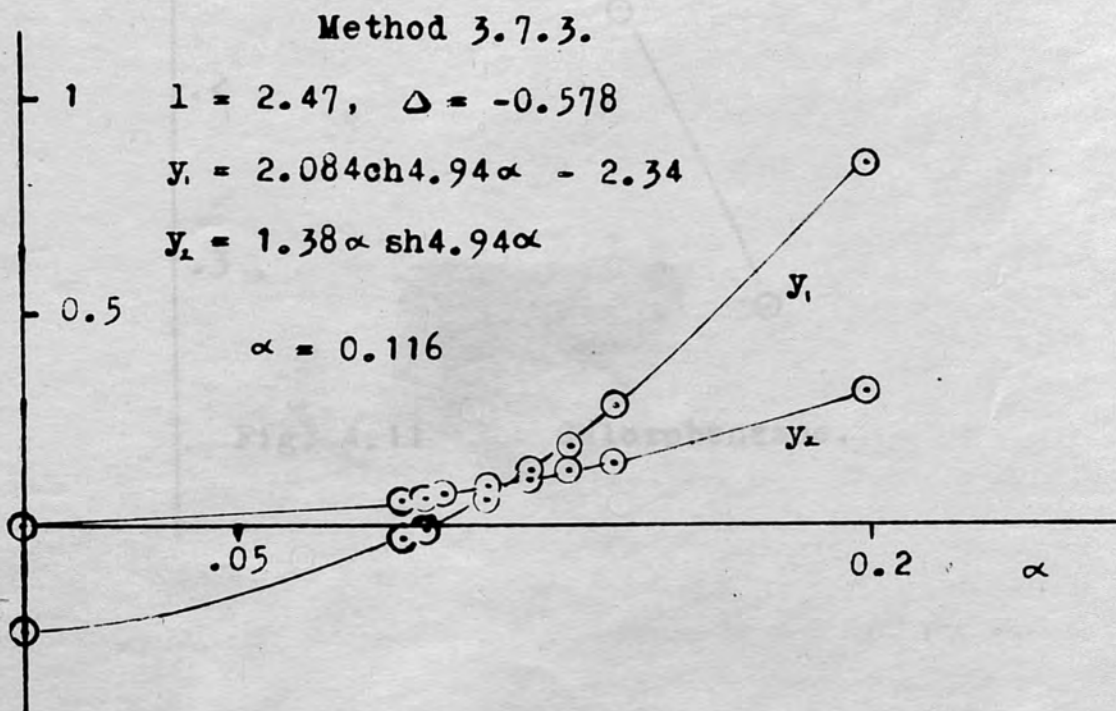


Fig. 4.12 Chlorobenzene.

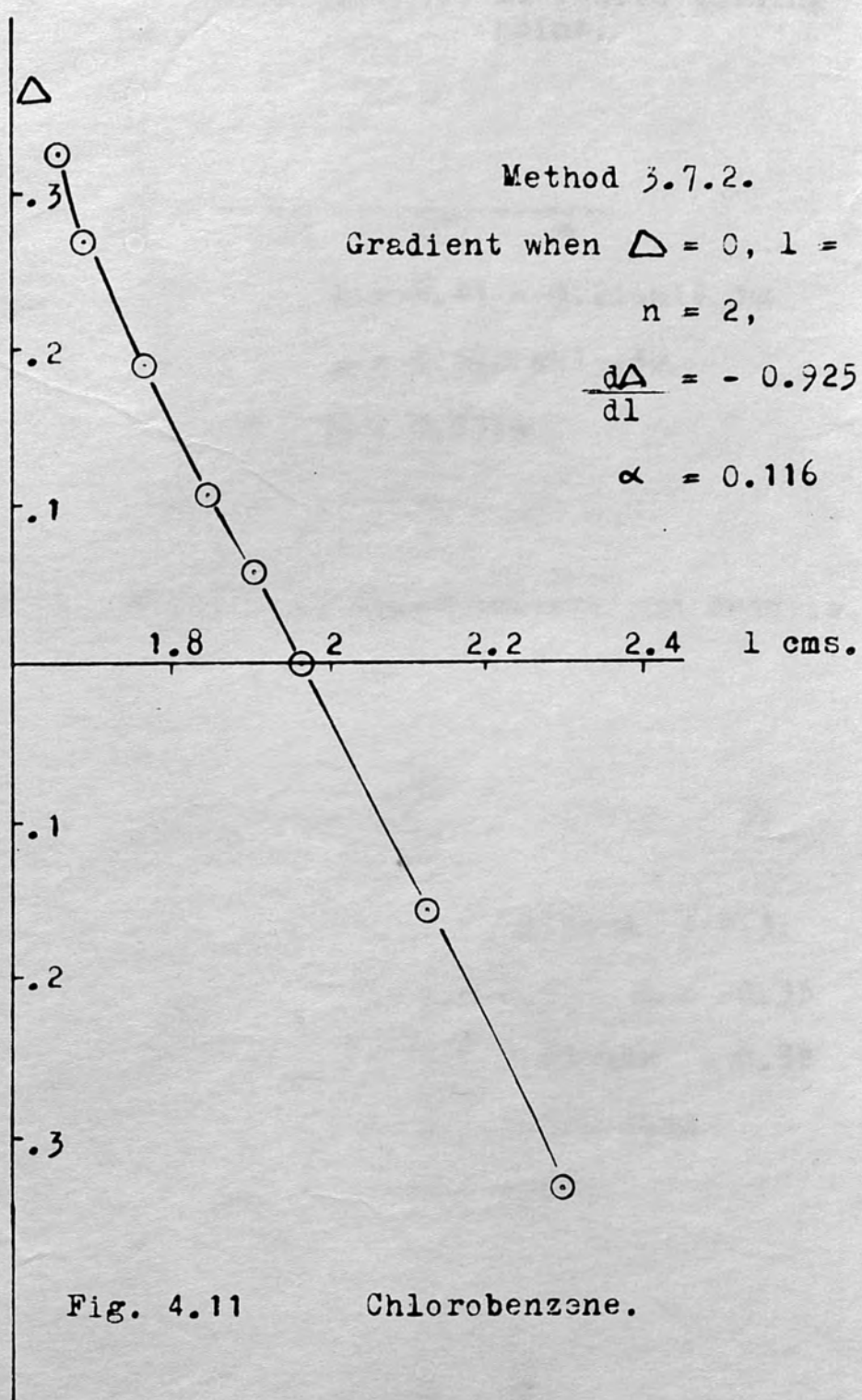


Fig. 4.11

Chlorobenzene.

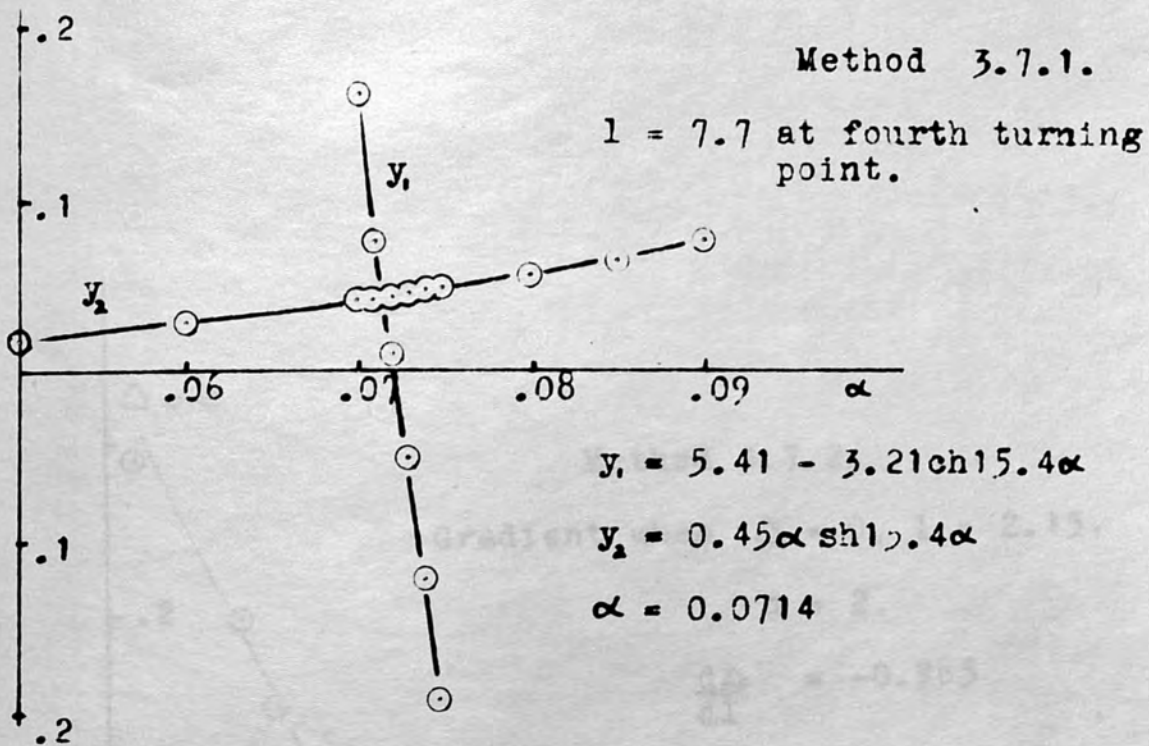


Fig. 4.13 Mixture of Chlorobenzene and Benzole.

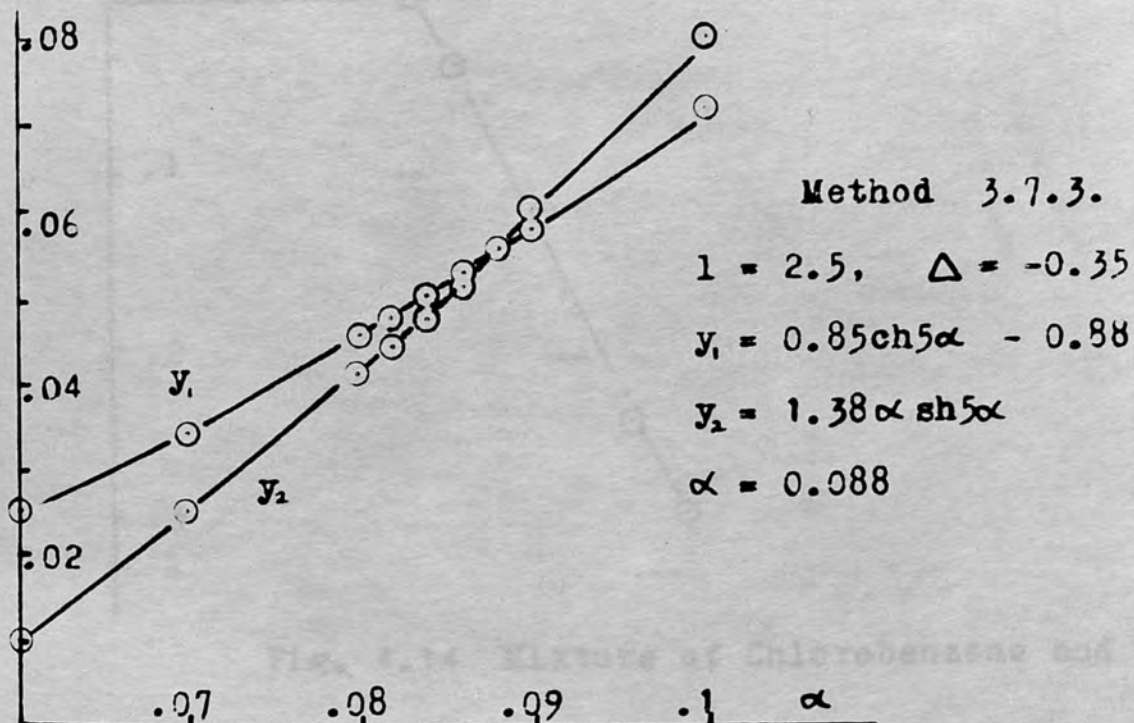


Fig. 4.15 Mixture of Chlorobenzene and Benzole.

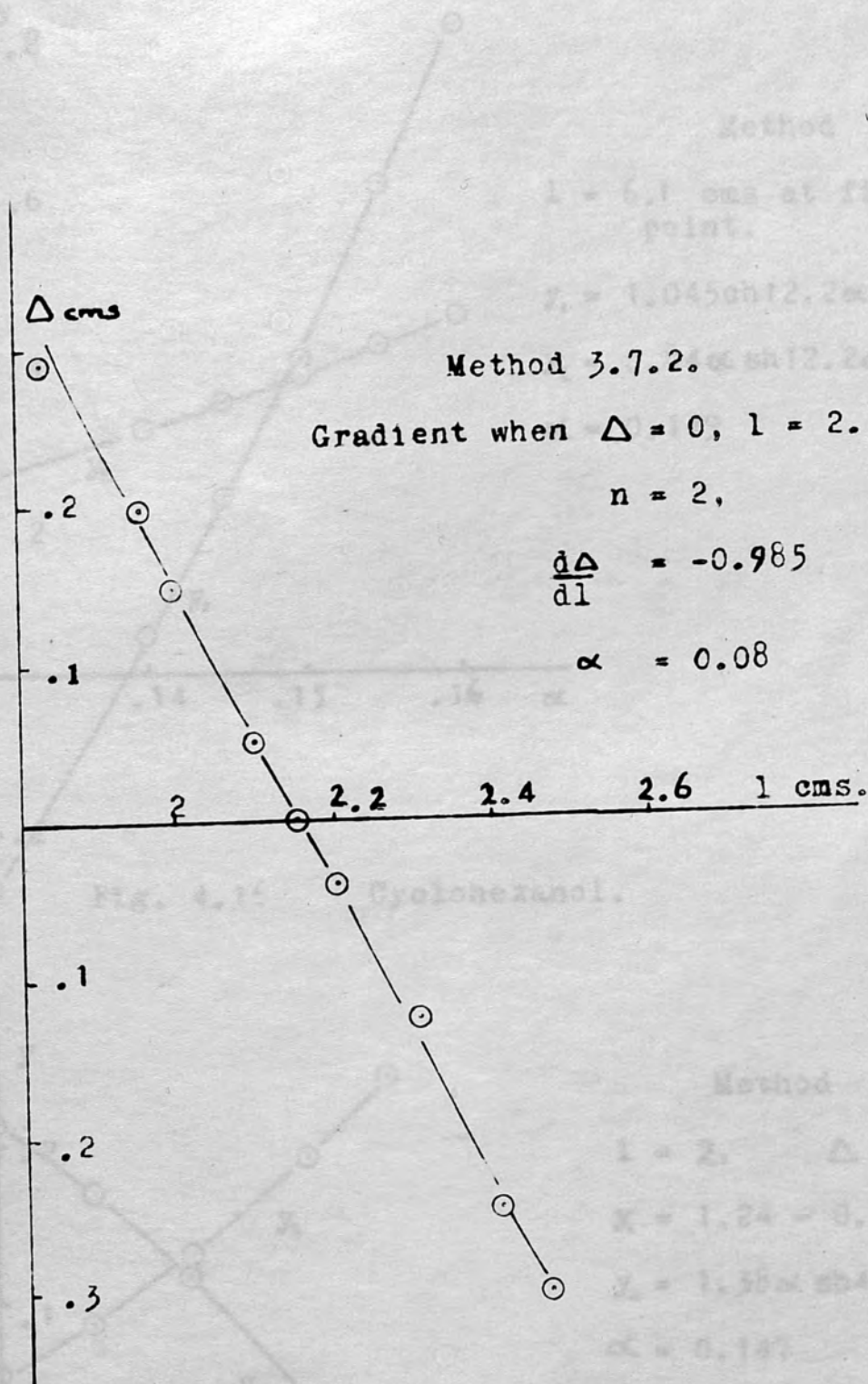


Fig. 4.14 Mixture of Chlorobenzene and Benzole.

Fig. 4.18 Cyclohexanol.

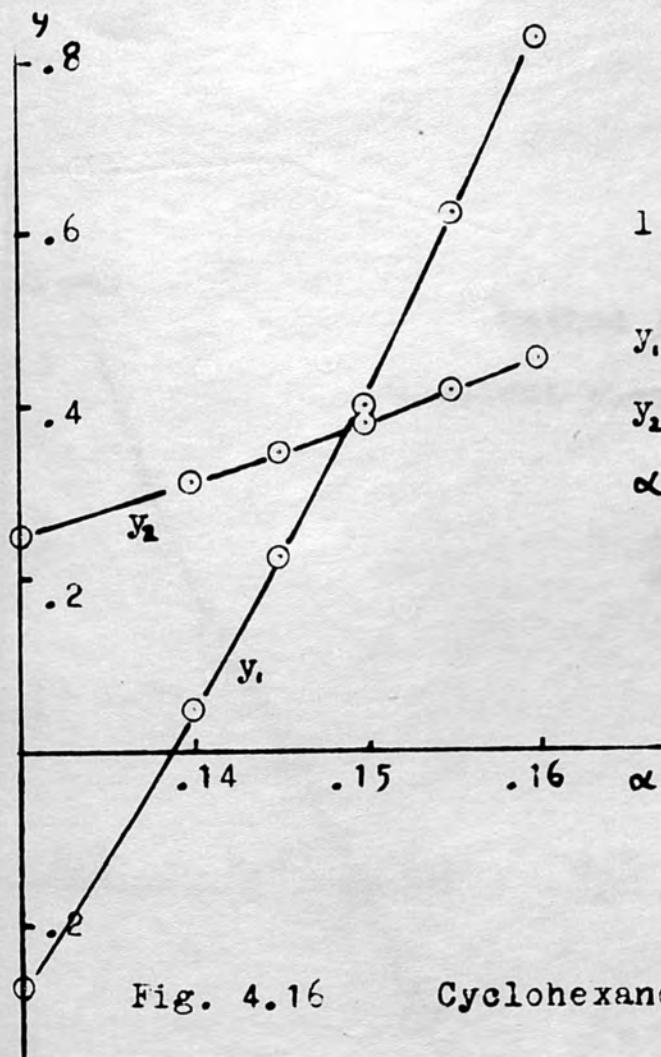


Fig. 4.16 Cyclohexanol.

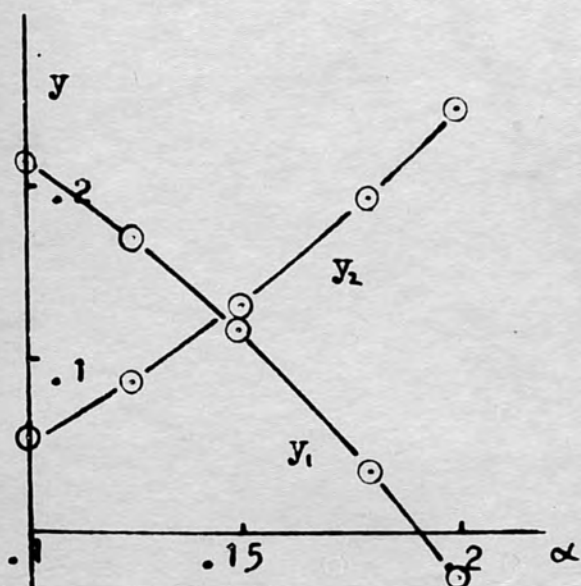


Fig. 4.18 Cyclohexanol.

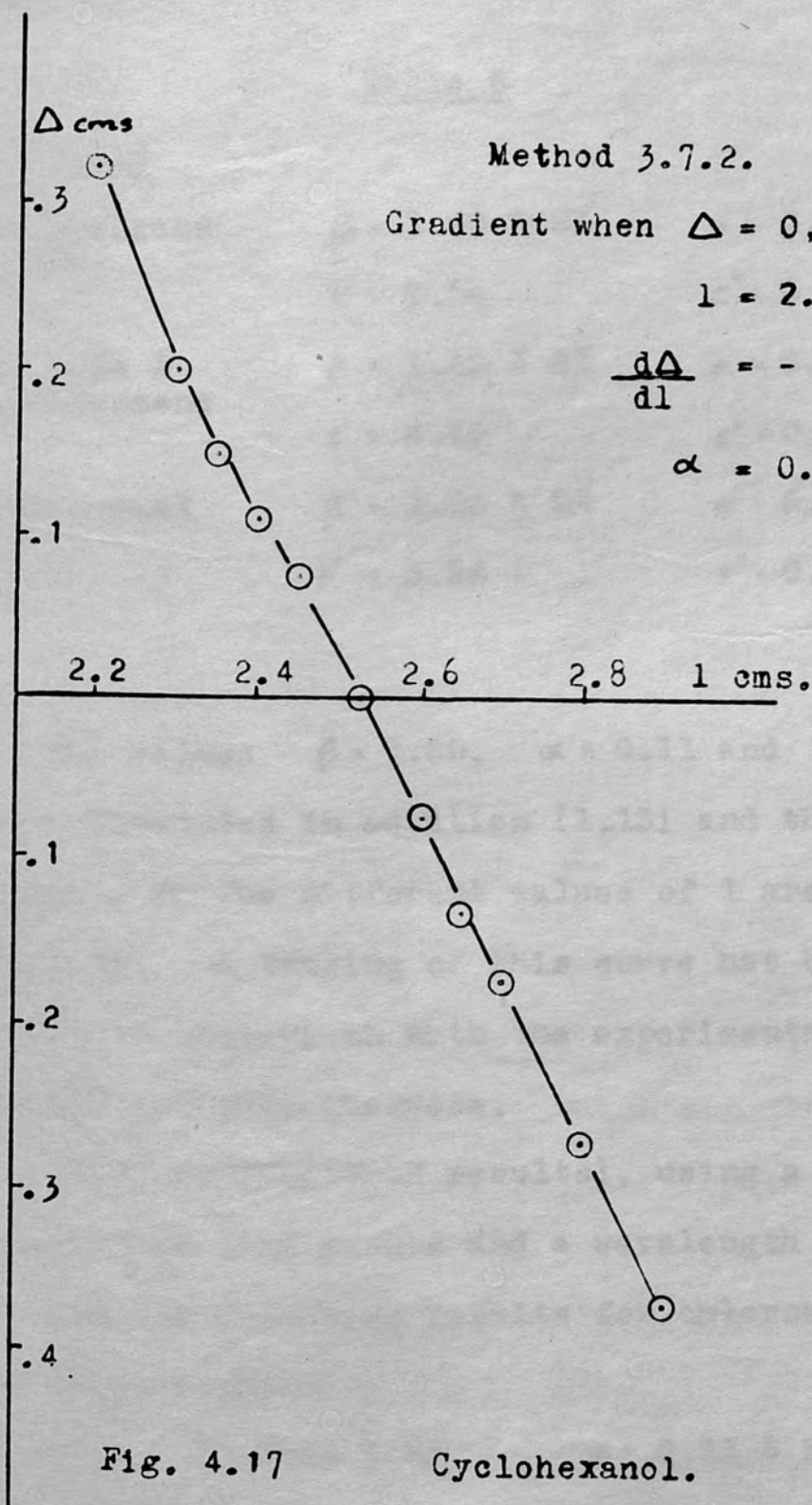


Table 6 gives the final values for α and β for the three liquids together with the calculated values of ϵ' and ϵ'' for comparison with other results.

Table 6

<u>Liquid</u>		
Chlorobenzene	$\beta = 1.60 \pm 2\%$	$\alpha = 0.115 \pm 2\%$
	$\epsilon' = 5.34$	$\epsilon'' = 0.771$
63.3 mole % chlorobenzene	$\beta = 1.45 \pm 2\%$	$\alpha = 0.080 \pm 2\%$
	$\epsilon' = 4.40$	$\epsilon'' = 0.486$
Cyclohexanol	$\beta = 1.23 \pm 2\%$	$\alpha = 0.15 \pm 2\%$
	$\epsilon' = 3.26$	$\epsilon'' = 0.778$

The values $\beta = 1.60$, $\alpha = 0.11$ and $\beta_0 = 0.69$ were substituted in equation (1.13) and the calculated values of Δ for different values of l are plotted in fig. 1.10. A tracing of this curve has been made to facilitate comparison with the experimental curve obtained for chlorobenzene.

Hill, (unpublished results), using a double probe transmission line method and a wavelength of 9.35 cms obtained the following results for chlorobenzene at room temperature:-

$$\beta = 1.56 \pm 2\% \qquad \alpha = 0.11 \pm 2\%$$

and for the 63.3 mole % chlorobenzene

$$\beta = 1.42 \pm 2\% \quad \alpha = 0.79 \pm 2\%$$

which, taking into account the slight difference in wavelength, agrees exactly with the present results.

²²
Branin and Smyth, using an accurate null method and a wavelength of 10 cms give the following results for chlorobenzene:-

<u>Temperature</u>	<u>ϵ'</u>	<u>ϵ''</u>
1°C	5.73	0.88
25	5.50	0.64
40	5.26	0.50
55	5.06	0.39

4.4 Experimental results for liquids with high values for both α and β .

4.4.1 Results for distilled water.

The variation of phase shift with liquid depth for distilled water at a room temperature varying between 17° and 19.3°C is plotted in fig. 4.19. The variation of galvanometer signal is shown in fig. 4.20.

Fig. 4.21 shows the experimental curve for distilled water at 37°C, obtained by the experimental arrangement of section 2.5.

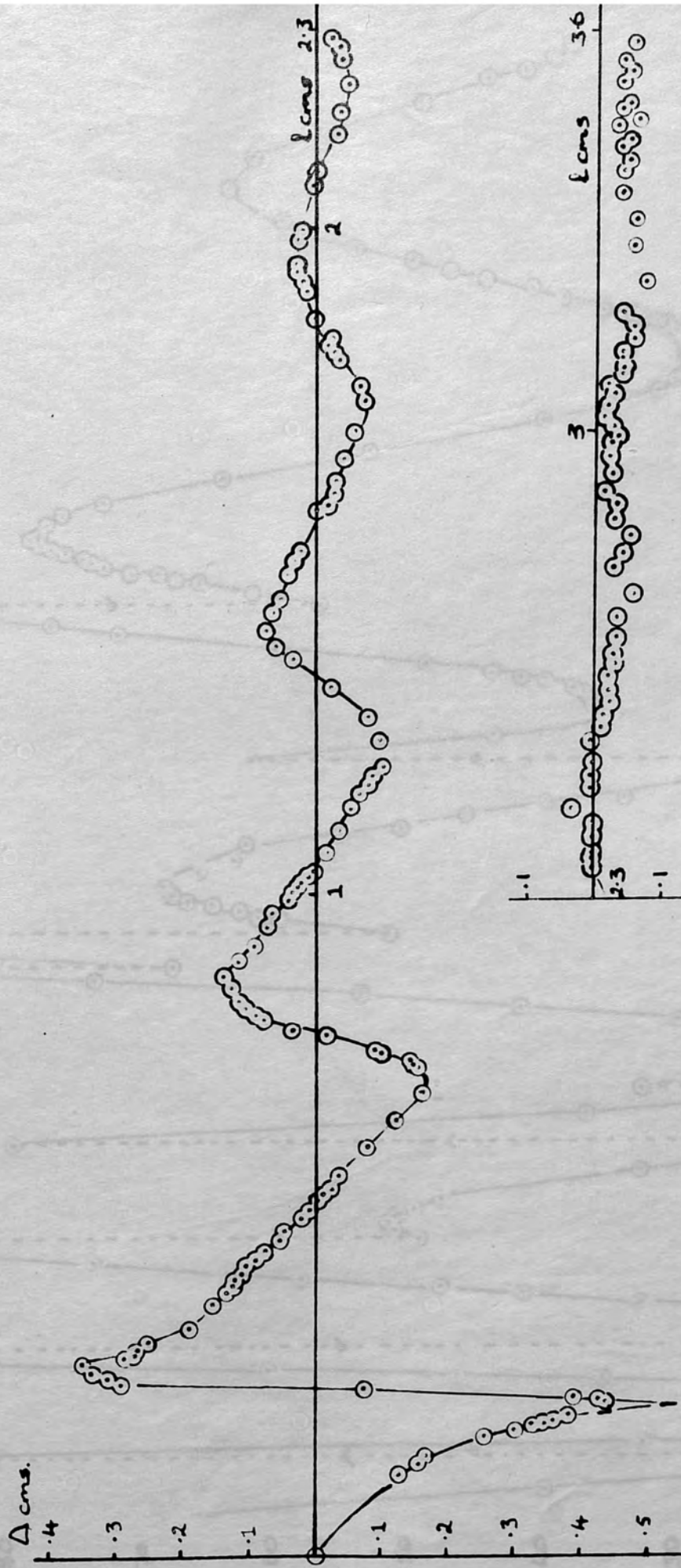


Fig. 4-19

Water 17 to 19°C 28.4.52.

Fig. 4-20 Water

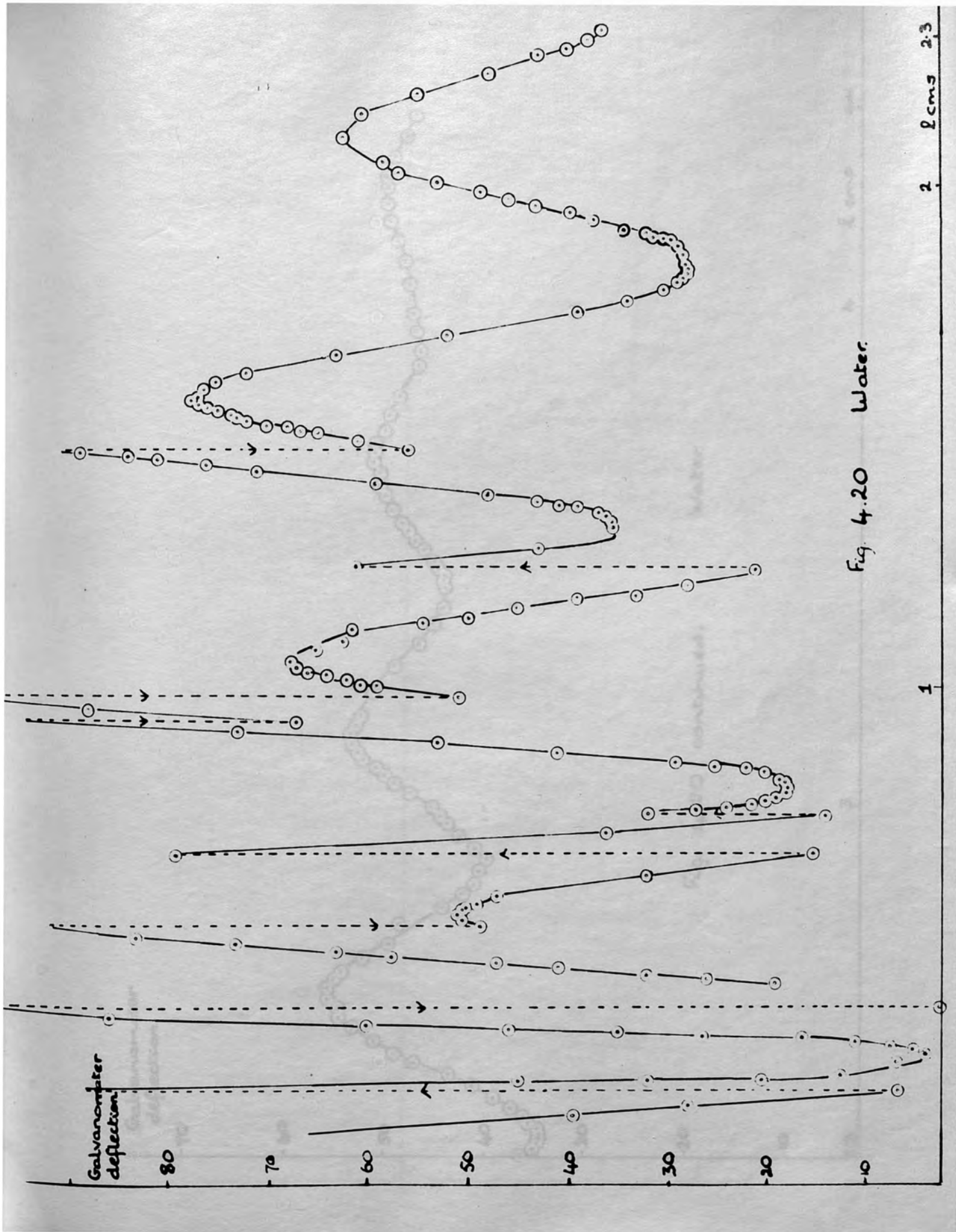


Fig. 4.20 Water.

2 2 cm 2.3

1

Galvanometer deflection

80

70

60

50

40

30

20

10

2 2 cm 2.3

Galvanometer deflection.

-70

-60

-50

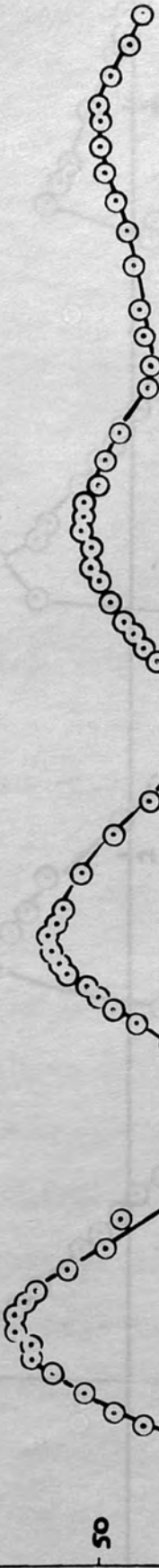
-40

-30

-20

-10

0



4.4

4 cm

4

3

Water.

Fig. 4.20 continued.

Water 37°C

Fig 4.21

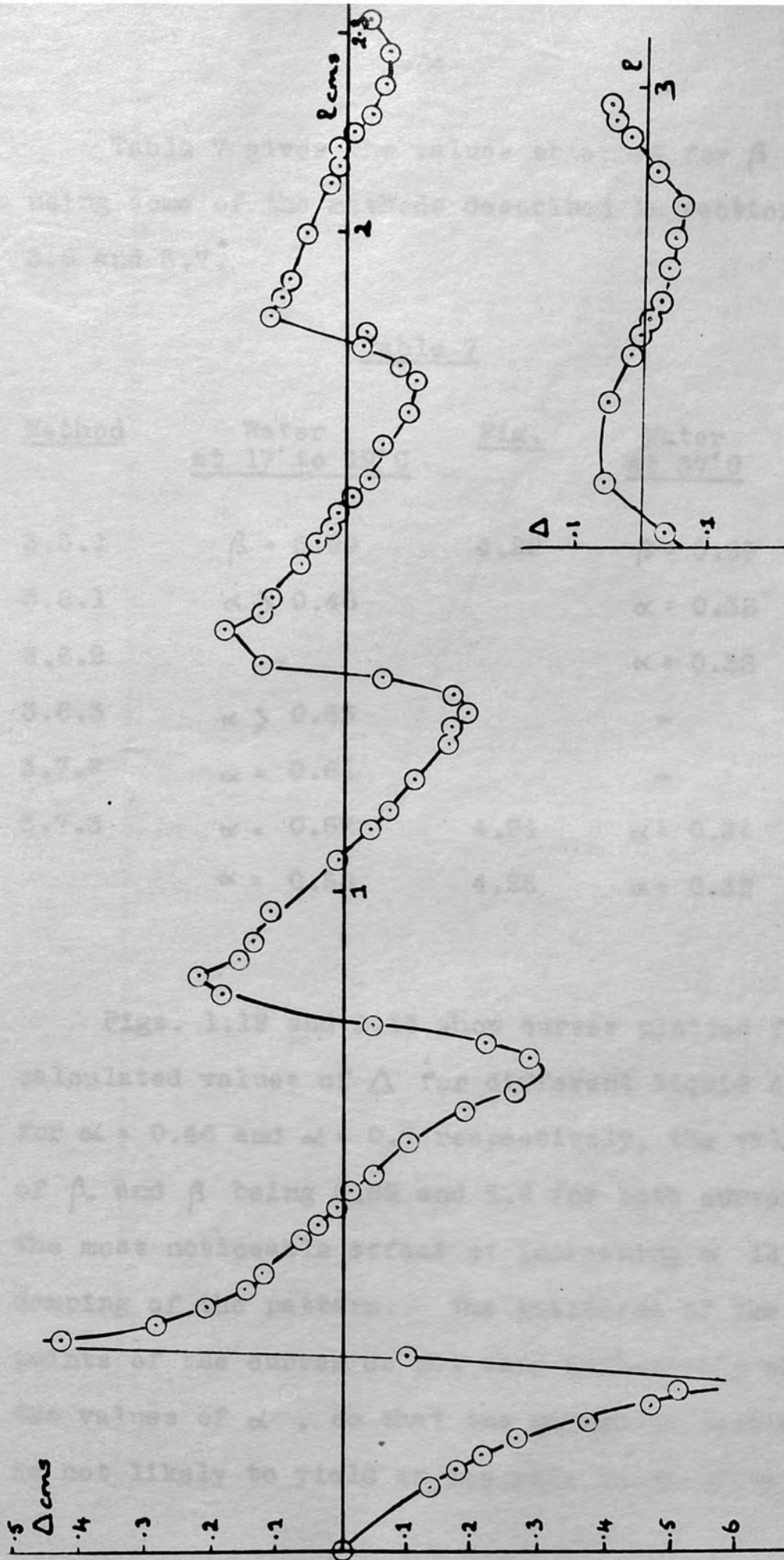


Fig. 4.21 Water 37°C 1.7.52

Table 7 gives the values obtained for β and α using some of the methods described in sections 3.5, 3.6 and 3.7.

Table 7

<u>Method</u>	<u>Water at 17° to 19° C</u>	<u>Fig.</u>	<u>Water at 37° C</u>	<u>Fig.</u>
3.5.1	$\beta = 5.99$	4.22	$\beta = 5.95$	4.23
3.6.1	$\alpha > 0.46$		$\alpha = 0.38$	
3.6.2	-		$\alpha = 0.38$	
3.6.3	$\alpha > 0.53$		-	
3.7.2	$\alpha = 0.61$		-	
3.7.3	$\alpha = 0.57$	4.24	$\alpha = 0.34$	4.26
	$\alpha = 0.56$	4.25	$\alpha = 0.39$	4.27

Figs. 1.12 and 1.13 show curves plotted from calculated values of Δ for different liquid depths for $\alpha = 0.46$ and $\alpha = 0.7$ respectively, the values of β_0 and β being 0.69 and 5.9 for both curves. The most noticeable effect of increasing α is in the damping of the pattern. The positions of the turning points of the curves do not vary appreciably with the two values of α , so that the method of section 3.7.1 is not likely to yield an accurate value of α . The

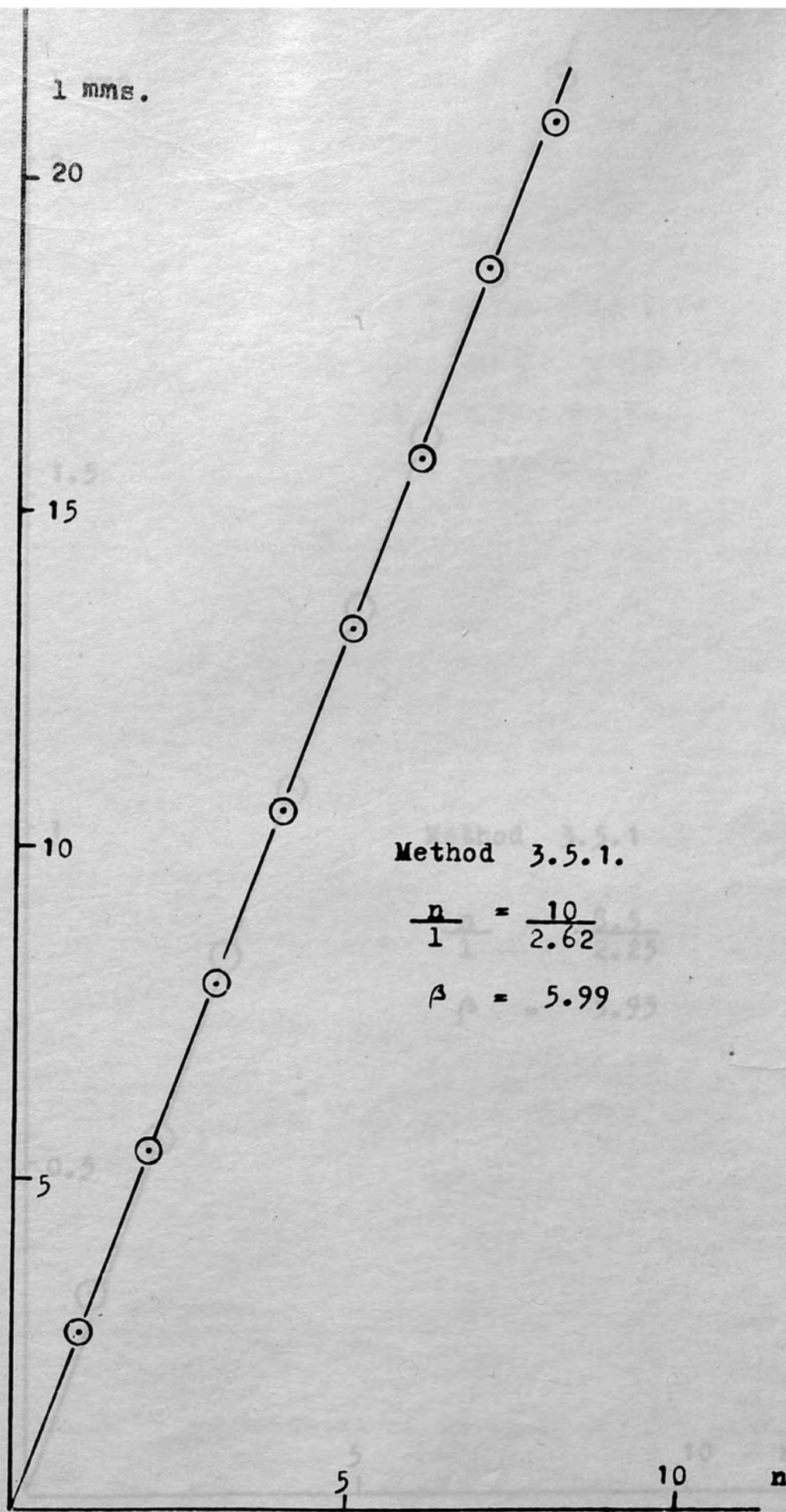


Fig. 4.22 Distilled water at room temperature.

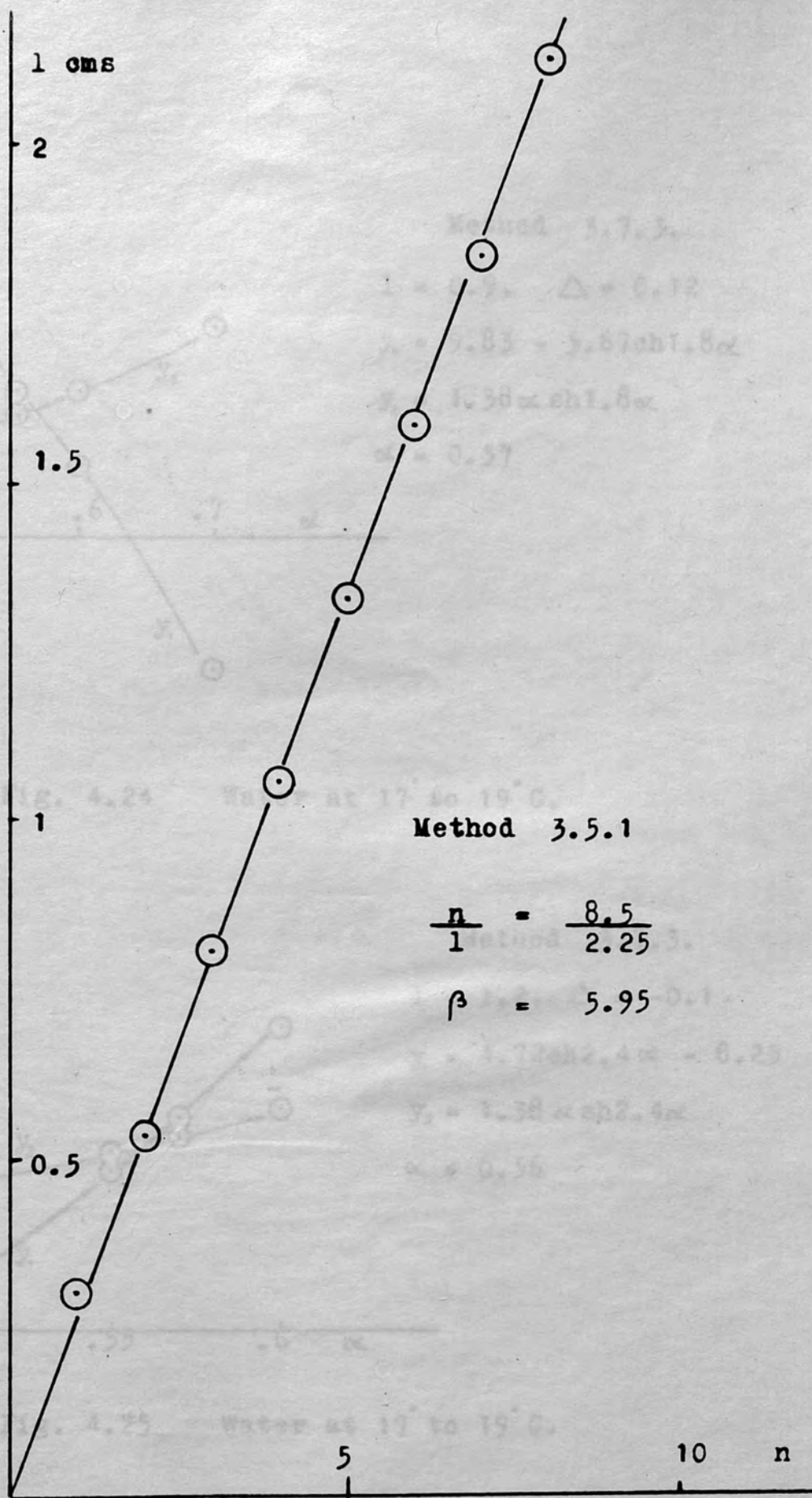
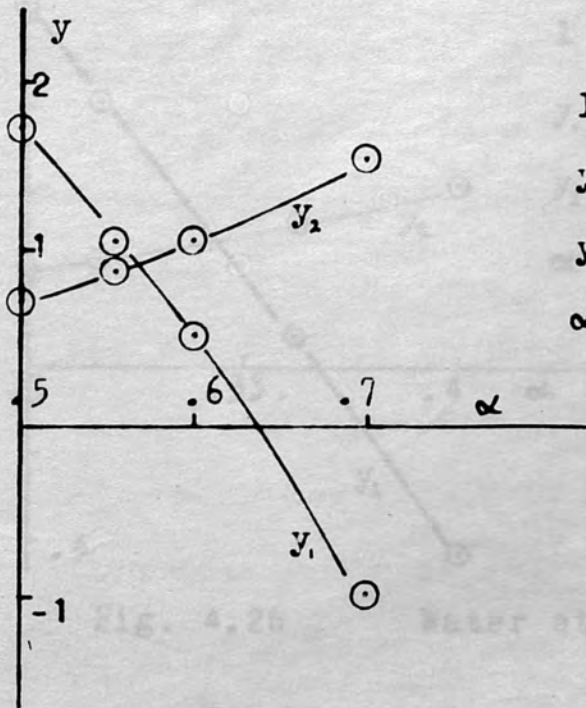


Fig. 4.23 Distilled water at 37°C



Method 3.7.3.

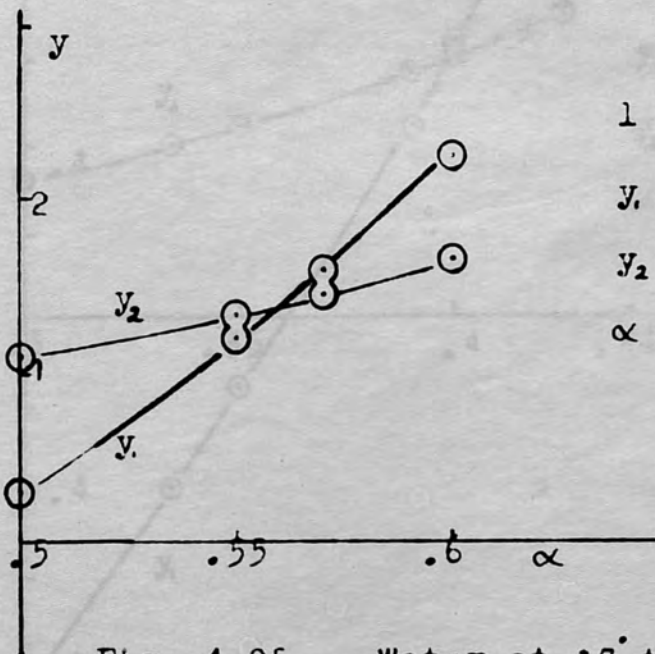
$$l = 0.9, \quad \Delta = 0.12$$

$$y_1 = 9.83 - 5.67 \operatorname{ch} 1.8\alpha$$

$$y_2 = 1.38 \alpha \operatorname{sh} 1.8\alpha$$

$$\alpha = 0.57$$

Fig. 4.24 Water at 17° to 19° C.



Method 3.7.3.

$$l = 1.2, \quad \Delta = -0.1$$

$$y_1 = 4.72 \operatorname{ch} 2.4\alpha - 8.25$$

$$y_2 = 1.38 \alpha \operatorname{sh} 2.4\alpha$$

$$\alpha = 0.56$$

Fig. 4.25 Water at 17° to 19° C.

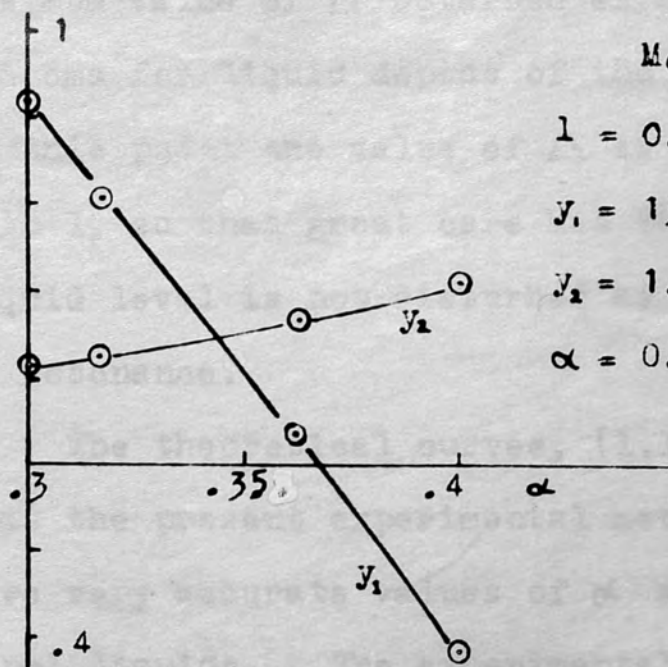


Fig. 4.26 Water at 37°C.

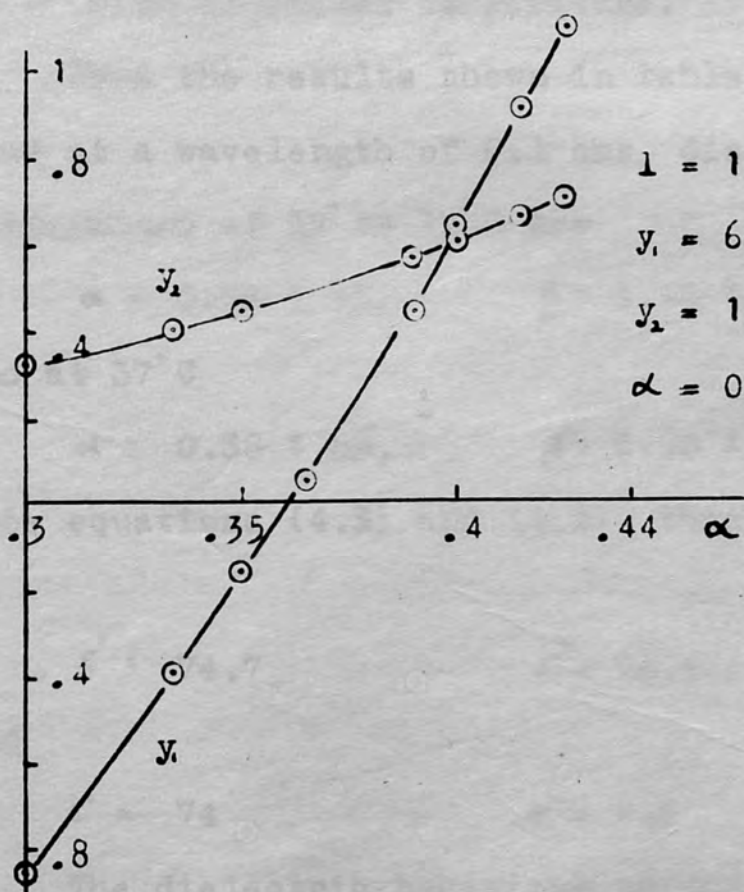


Fig. 4.27 Water at 37°C.

maximum value of Δ obtained experimentally is about 0.5 cms for liquid depths of the order of 0.2 cms. At this point the value of Δ is varying very rapidly with l , so that great care has to be taken that the liquid level is not disturbed as the line is adjusted to resonance.

The theoretical curves, (1.12) and (1.13), show that the present experimental method is unlikely to give very accurate values of α and β for the 'water-type' liquids. The experimental curves, (4.19) and (4.21), however do show immediately the marked decrease in α with increased temperature.

From the results shown in table 7 it is concluded that at a wavelength of 9.1 cms, distilled water at a temperature of 17° to 19° C has

$$\alpha = 0.57 \pm 5\%, \quad \beta = 5.99 \pm 3\%$$

and at 37° C

$$\alpha = 0.38 \pm 5\%, \quad \beta = 5.95 \pm 3\%$$

From equations (4.3) and (4.2), these values correspond to

$$\epsilon' = 74.7 \quad \epsilon'' = 14.4 \quad \text{at } 17^\circ - 19^\circ \text{ C}$$

and

$$\epsilon' = 74 \quad \epsilon'' = 9.5 \quad \text{at } 37^\circ \text{ C}$$

The dielectric behaviour of water at microwave frequencies has been widely investigated by many authors,

and, as was mentioned in the Introduction, the values obtained have not always been in agreement. The results obtained by Conner and Smyth²⁸ using a wavelength of 9.72 cms when investigating the variation of ϵ' and ϵ'' with temperature for water are plotted in fig. 4.28. They made measurements on the standing wave pattern set up in a coaxial line filled with a variable amount of water and calculated the wavelength in the water and the loss factor ϵ'' , using a method based on Drude's¹⁶ 'First method', from a graph showing the variation of detector signal with liquid depth.

In 1947 Collie, Hasted and Ritson¹¹ introduced a method of measuring the absorption coefficient by direct transmission through two waveguides, one just below and the other just above cut-off dimensions, and carried out an extensive investigation of the dielectric properties of water using this method in addition to a resonant cavity method. The absorption coefficient k and the real part of the refractive index measured by Collie et. al. is different from that defined in the Introduction, being related to the complex refractive index by the relationship

$$\bar{n} = n - jk$$

so that $\epsilon' - j\epsilon'' = (n - jk)^2$

and $\epsilon' = n^2 - k^2$

and $\epsilon'' = 2nk$

n and k are related to α and β by

$$\alpha = \frac{2\pi}{\lambda_0} k$$

$$\beta = \frac{2\pi}{\lambda_0} n$$

Fig. 4.29 shows their results for a wavelength of 10 cms expressed in terms of α and β . The accuracy is estimated as $\pm 1\%$. This curve shows the very rapid variation of α with temperature.

The rapid variation of α and β with wavelength is illustrated by the results obtained by Little²⁹ using a double probe method of measuring the standing wave pattern obtained when the depth of water above a short circuit in a waveguide is varied. These results for a temperature of 21° C are plotted in fig. 4.30 the estimated accuracy being $\pm 1\%$ at the longer and $\pm 2\%$ at the shorter wavelengths. Hill,³⁰ using a similar method with a coaxial line and a wavelength of 9.35 cms obtained the following results,

$$\alpha = 0.58 \pm 2\% \qquad \beta = 5.9 \pm 2\% \qquad \text{at } 17^\circ \text{C}$$

$$\alpha = 0.57 \pm 2\% \qquad \beta = 5.9 \pm 2\% \qquad \text{at } 19^\circ \text{C}$$

13

Cook recently carried out a series of measurements on water covering a wavelength range from 10 to 1.262 cms, and a temperature range from 0° to 60° C.

At 10 and 6.48 cms he used a coaxial line version of Drude's 'first method' and at 3.195 and 1.262 cms the Buchanan²¹ method. He checked the 10 cms results by using a cylindrical waveguide method similar to Collie et al. Fig. 4.31 shows the values of ϵ' and ϵ'' at 18° and 37°C extrapolated from his results and plotted on a logarithmic frequency scale. The values of ϵ' and ϵ'' at a wavelength of 9.1 cms are:-

$$\epsilon' = 77.2 \qquad \epsilon'' = 15 \qquad \text{at } 18^\circ\text{C}$$

and $\epsilon' = 73.8 \qquad \epsilon'' = 9.1 \qquad \text{at } 37^\circ\text{C}$

The present results are in fair agreement with these values. This is shown more readily by the Cole-Cole plots of fig. 4.32. The Cole-Cole semi-circles are drawn using $\epsilon_s = 80.82$ at 18°C, $\epsilon_s = 74.5$ at 37°C and $\epsilon_\infty = 5.0$, which data Cook found gave the best average fit to his experimental results. The results at the higher temperature are in better agreement with those of Cook than the ones at room temperature, as might be expected with the smaller value of α . The discrepancy at 18°C seems to be due to too small a value for β .

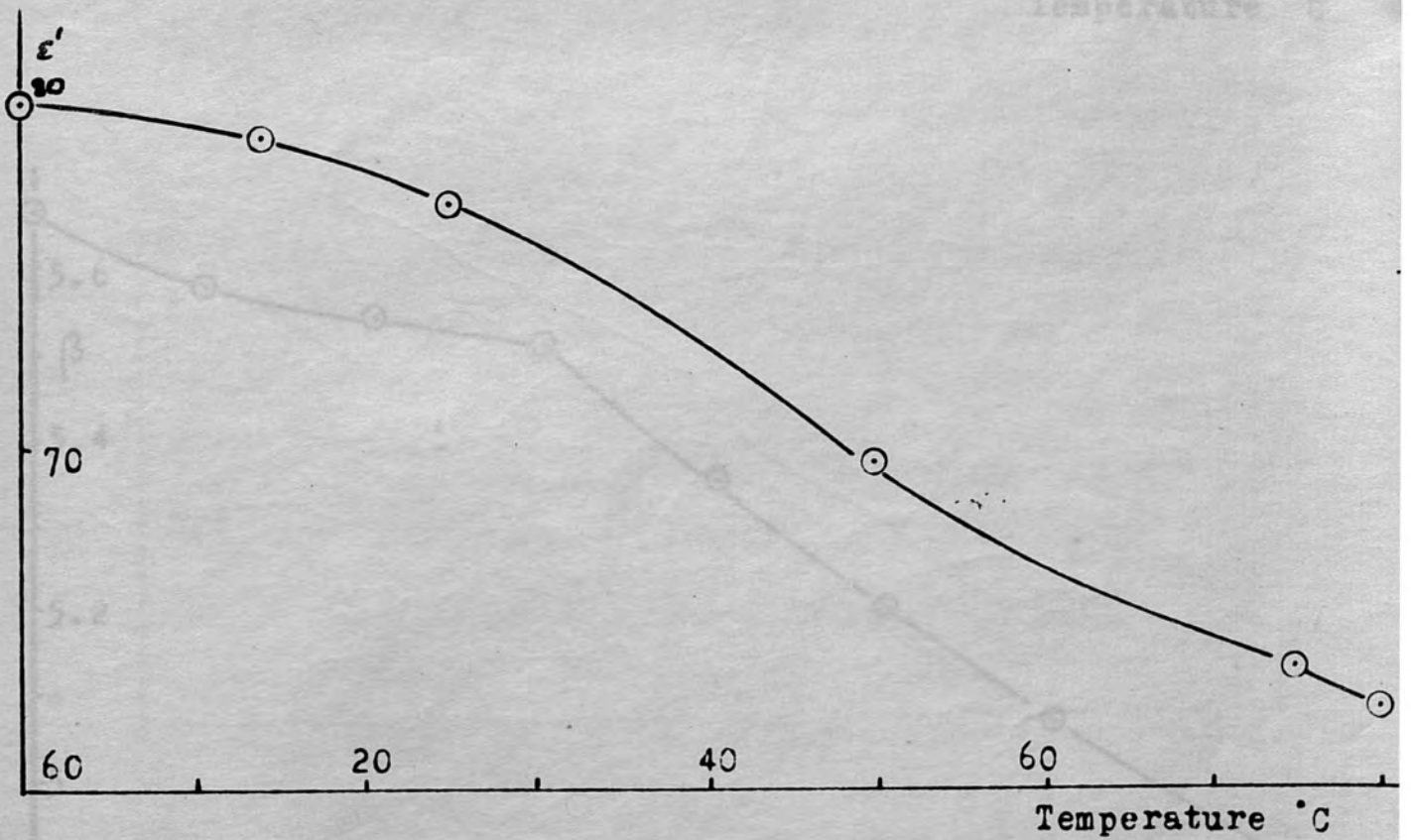
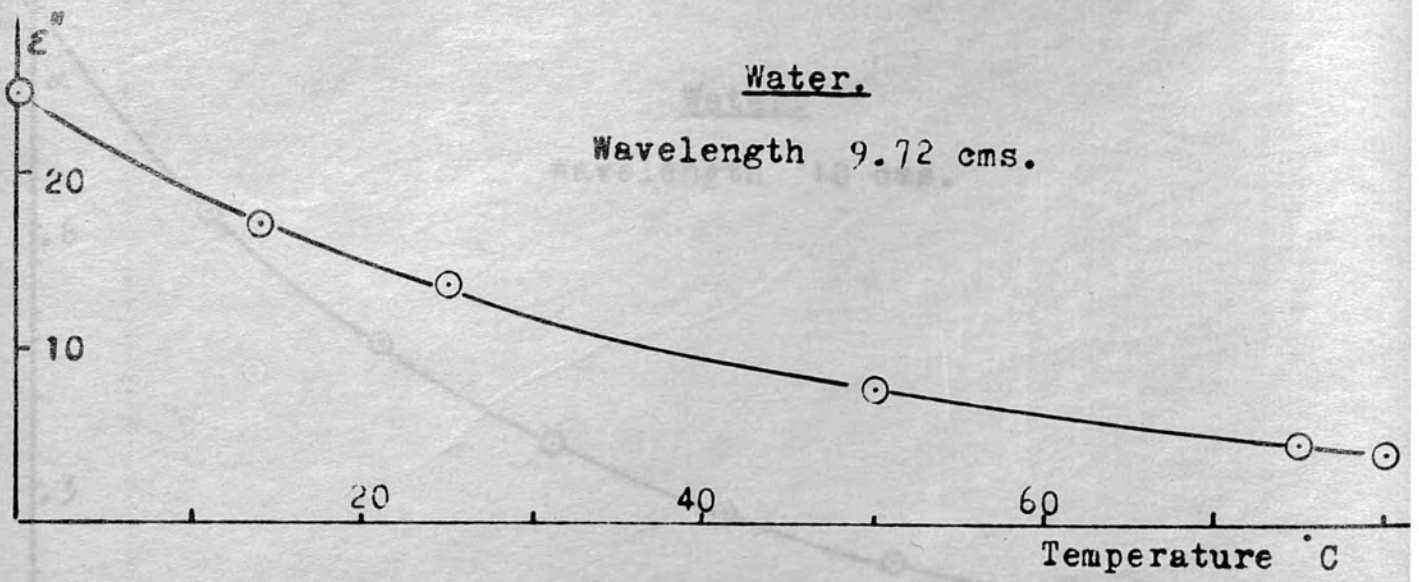


Fig. 4.28 Conner and Smyth's results.

Fig. 4.29 Collie, Hasted and Ritson's results.

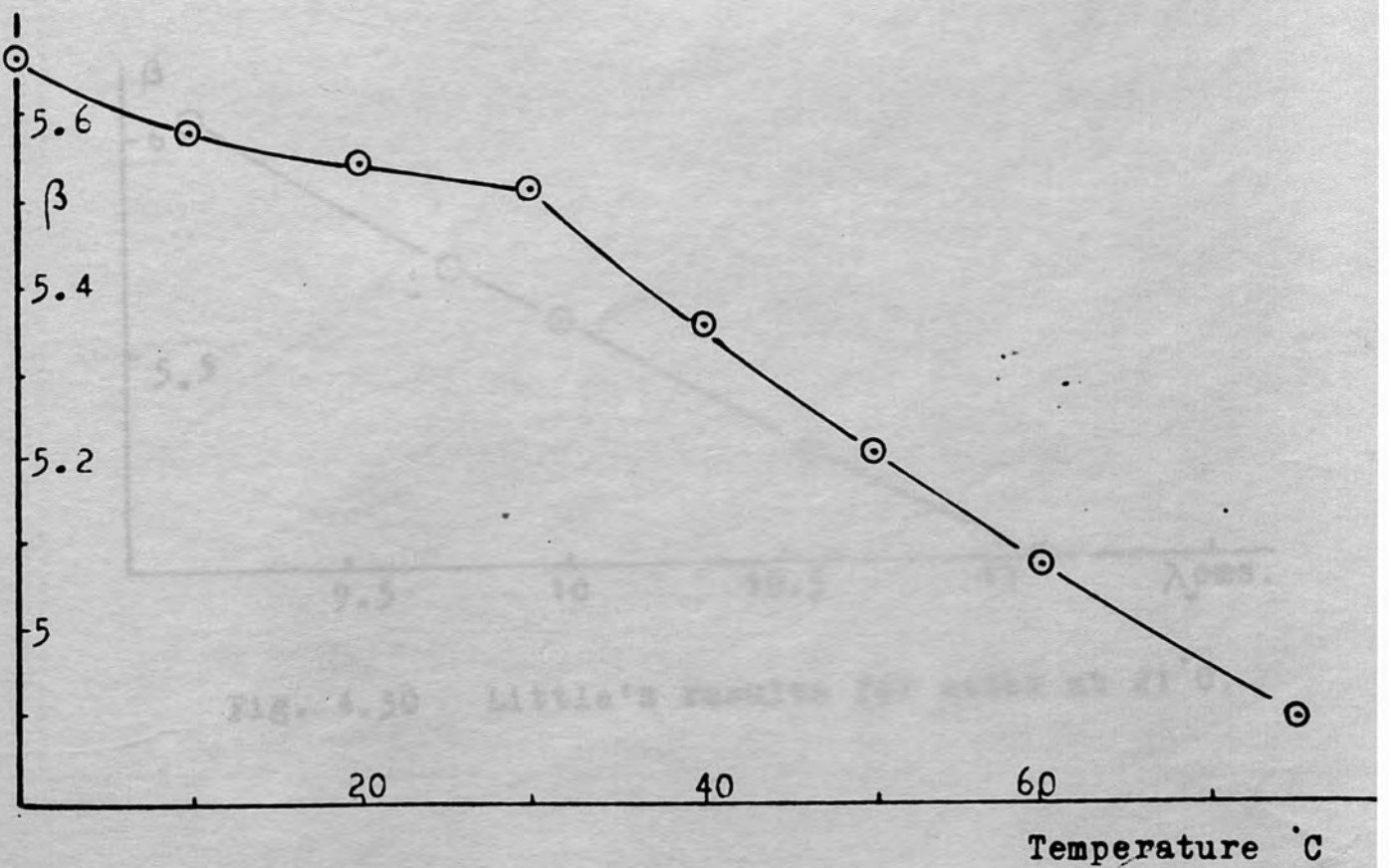
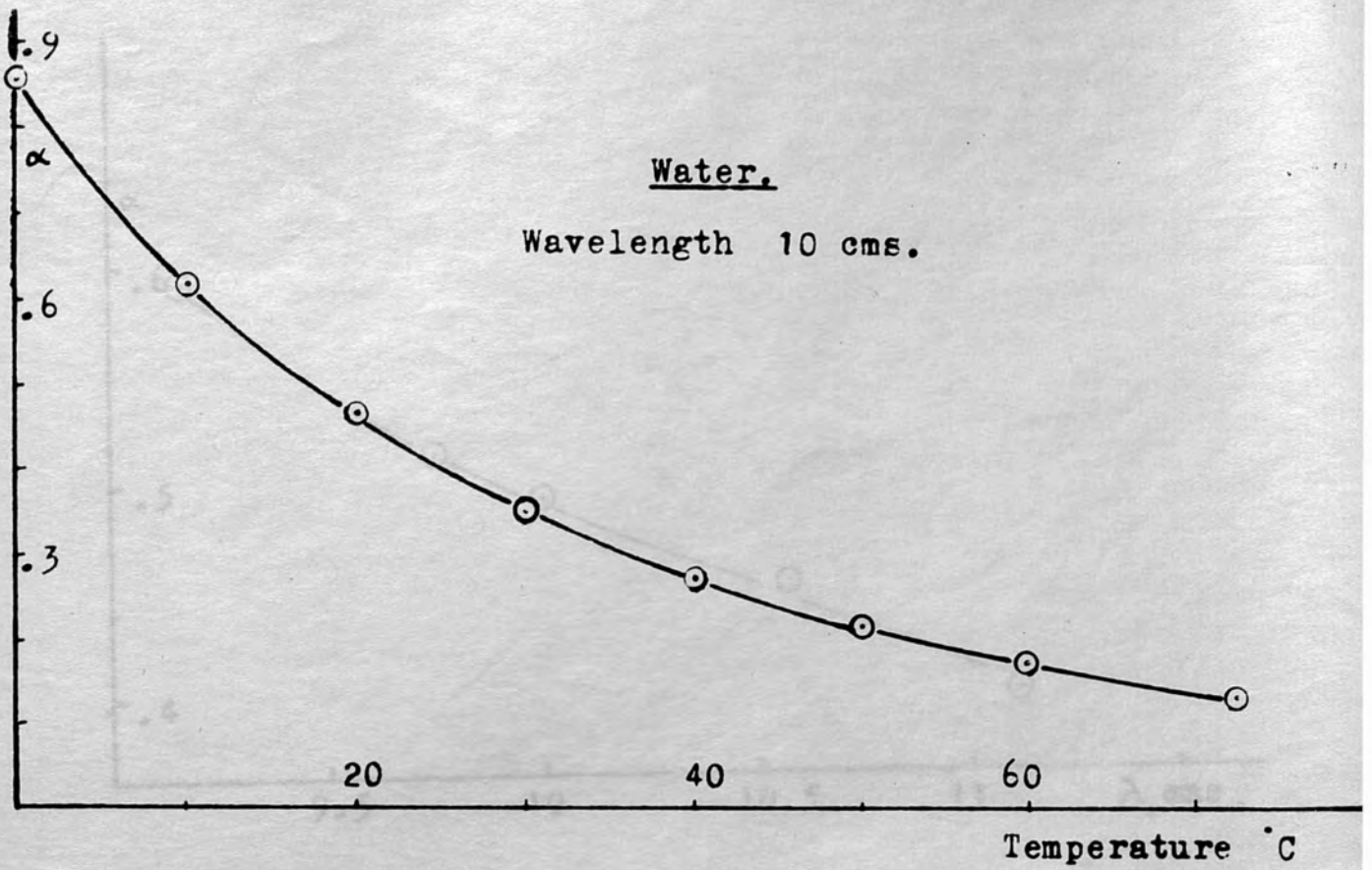


Fig. 4.29 Collie, Hasted and Ritson's results.

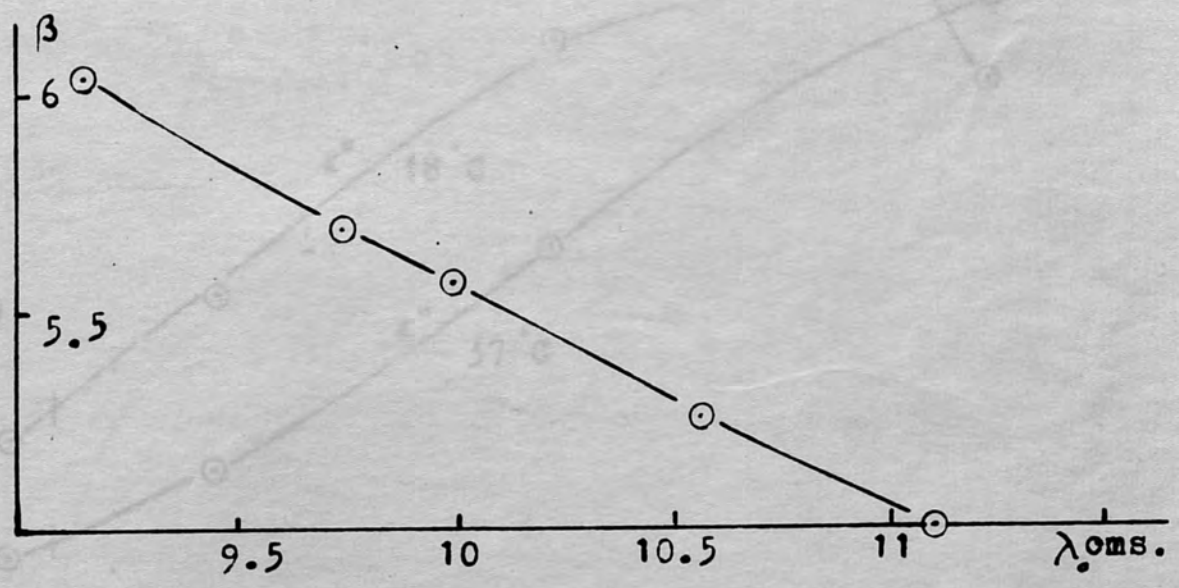
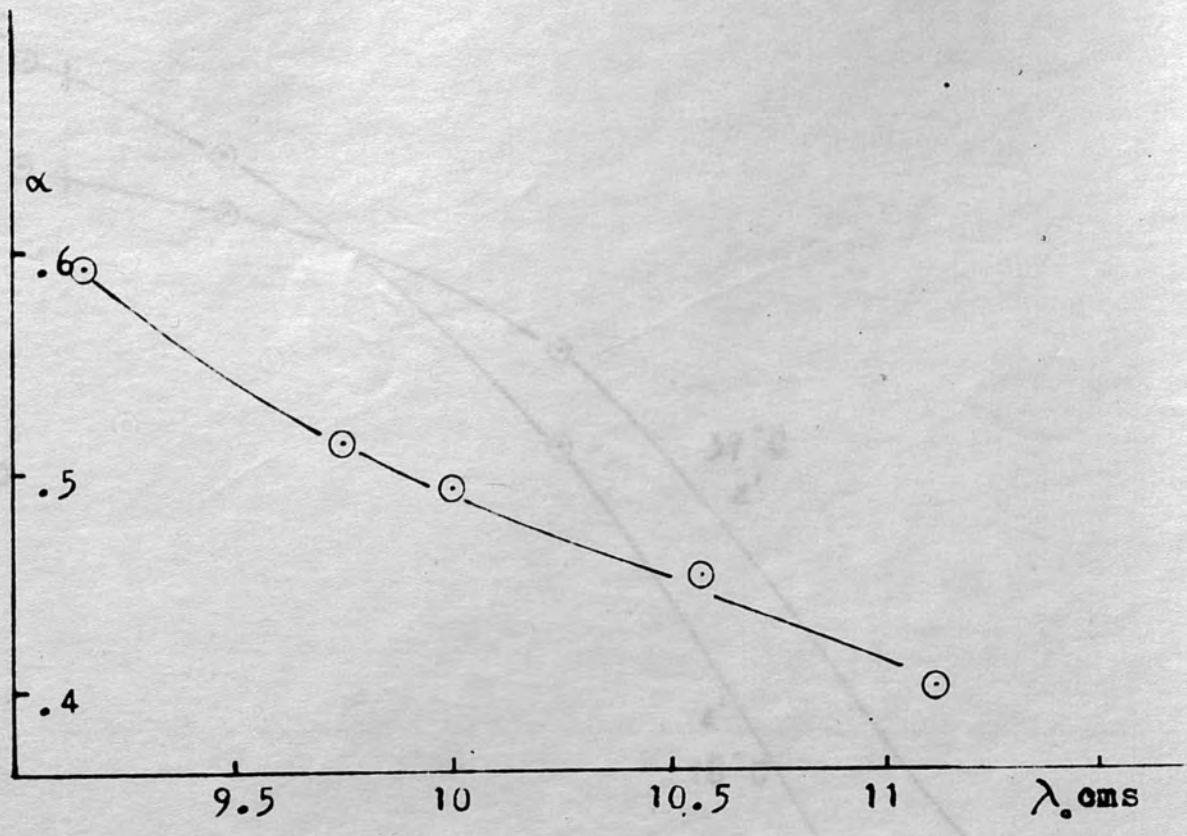


Fig. 4.30 Little's results for water at 21° C.

Fig. 4.31 Cook's results for water.

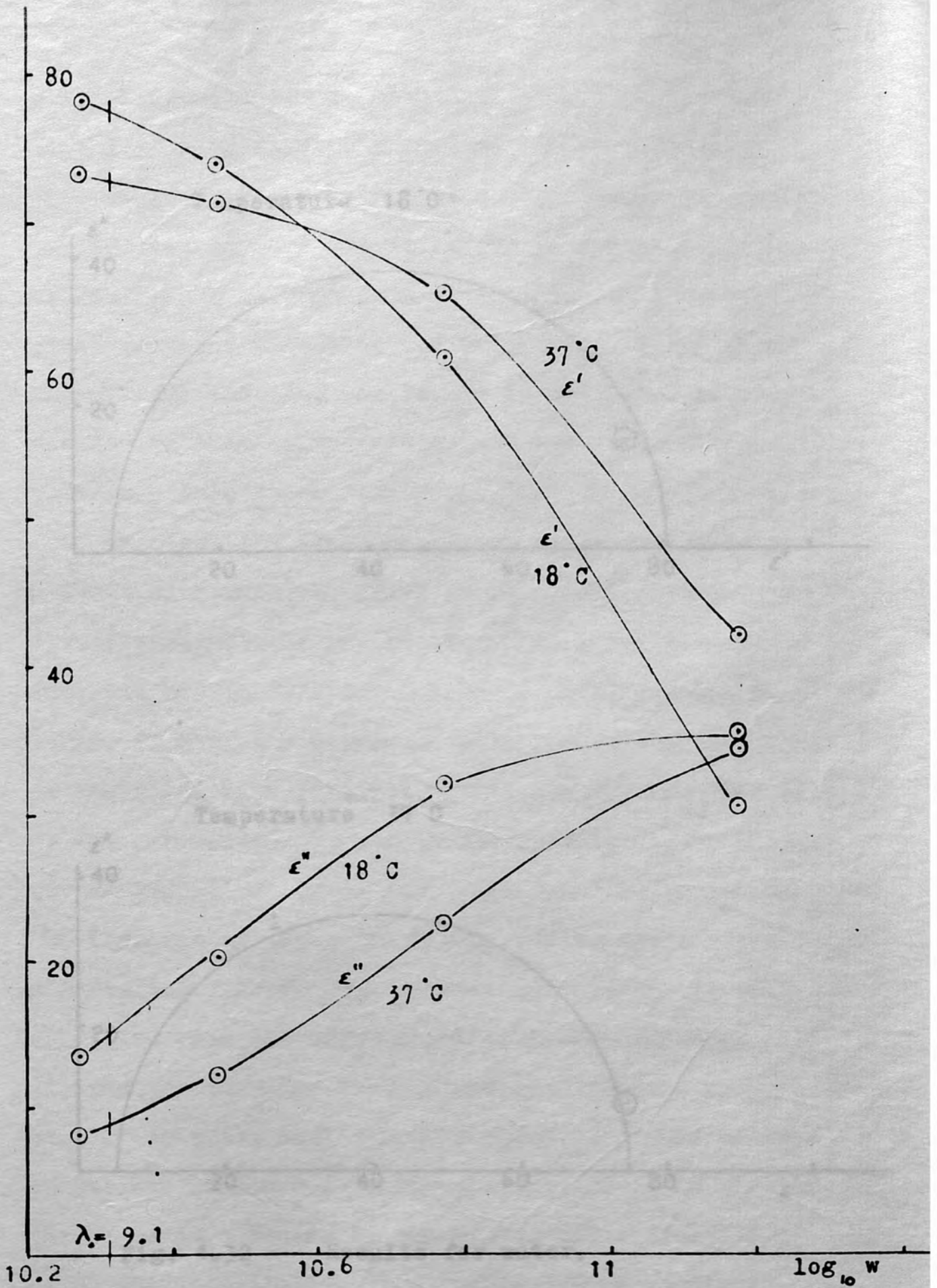


Fig. 4.31 Cook's results for water.

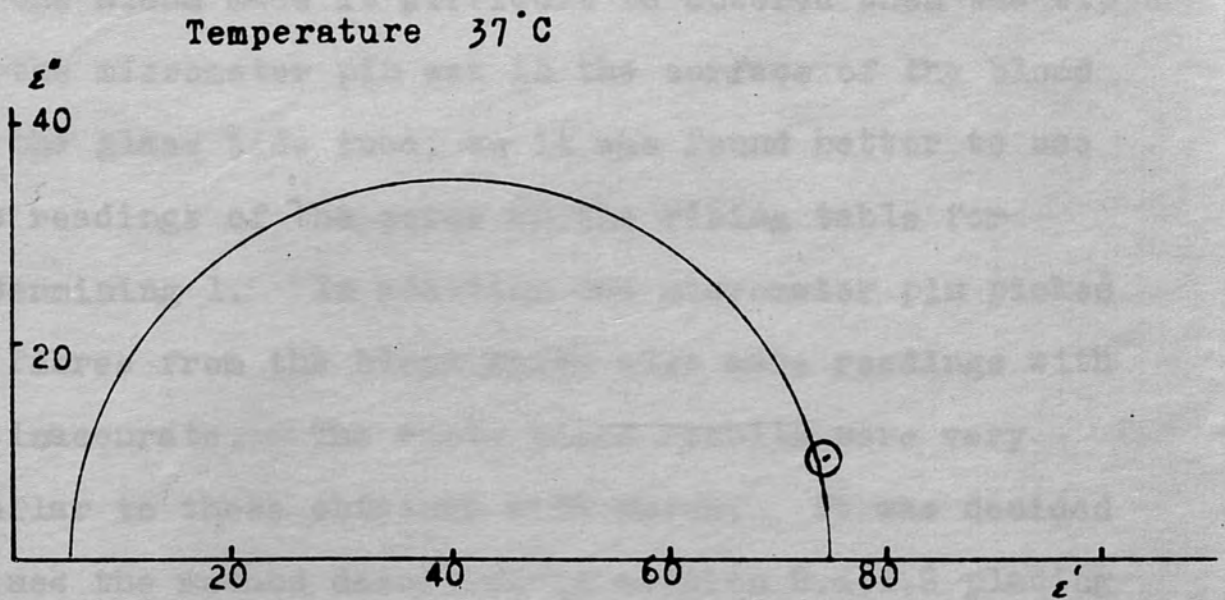
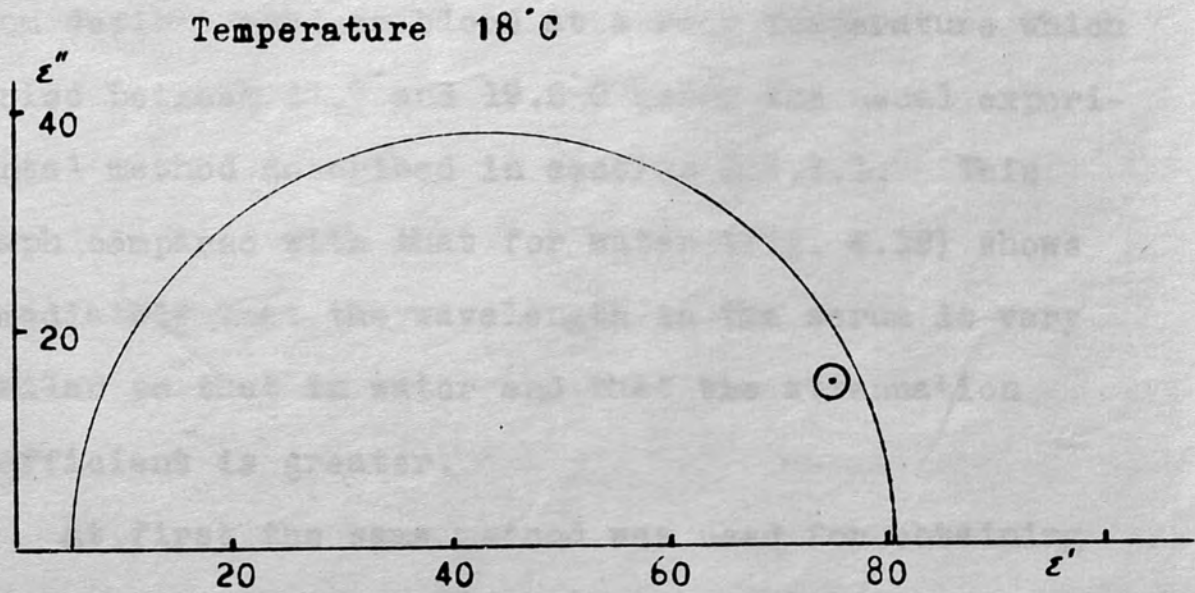


Fig. 4.32 Results for water.

4.4.2 Results for ox blood and serum.

Fig. 4.33 shows the results obtained using serum from defibrinated ox blood at a room temperature which varied between 17.7 and 19.6°C using the usual experimental method described in section 2.4.1.1. This graph compared with that for water (Fig. 4.19) shows immediately that the wavelength in the serum is very similar to that in water and that the attenuation coefficient is greater.

At first the same method was used for obtaining results with whole ox blood at room temperature. The higher viscosity of the blood meant that a longer interval had to be allowed after each alteration in l before finding the resonance position. The opaqueness of the blood made it difficult to observe when the tip of the micrometer pin was in the surface of the blood in the glass side tube, so it was found better to use the readings of the screw on the rising table for determining l . In addition the micrometer pin picked up fibres from the blood which also made readings with it inaccurate. The whole blood results were very similar to those obtained with serum. It was decided to use the method described in section 2.4.1.2 placing the blood in a beaker on the rising table directly below the transmission line. Successive readings

could then be taken much more rapidly. Fig. 4.34 shows the results obtained.

Ox serum was used again using the simplified experimental arrangement of section 2.4.1.2 to give a better comparison with whole blood. The results are plotted in fig. 4.35.

As the attenuation coefficient for water decreases so rapidly with temperature, it was thought that the values of α and β at the inner body temperature of 37°C would be of more value than those at room temperature. The thermostatic control arrangement described in section 2.5 was used. The results are plotted in figs. 4.36 and 4.37. Satisfactory results with whole ox blood at 37°C were not obtained, as a skin was found to form on the surface of the blood at this higher temperature which prevented the displaced blood from overflowing as l increased, which accounts for the larger positive values obtained owing to the inaccuracy in l . The general shape of the curve indicates a similar value of α to serum at this temperature.

Table 8 summarises the values of α and β calculated for serum and whole ox blood at the two temperatures. Figs. 4.38, 4.39 and 4.40 show the galvanometer reading plotted against liquid depth for ox serum and blood at room temperature, and serum at 37°C respectively.

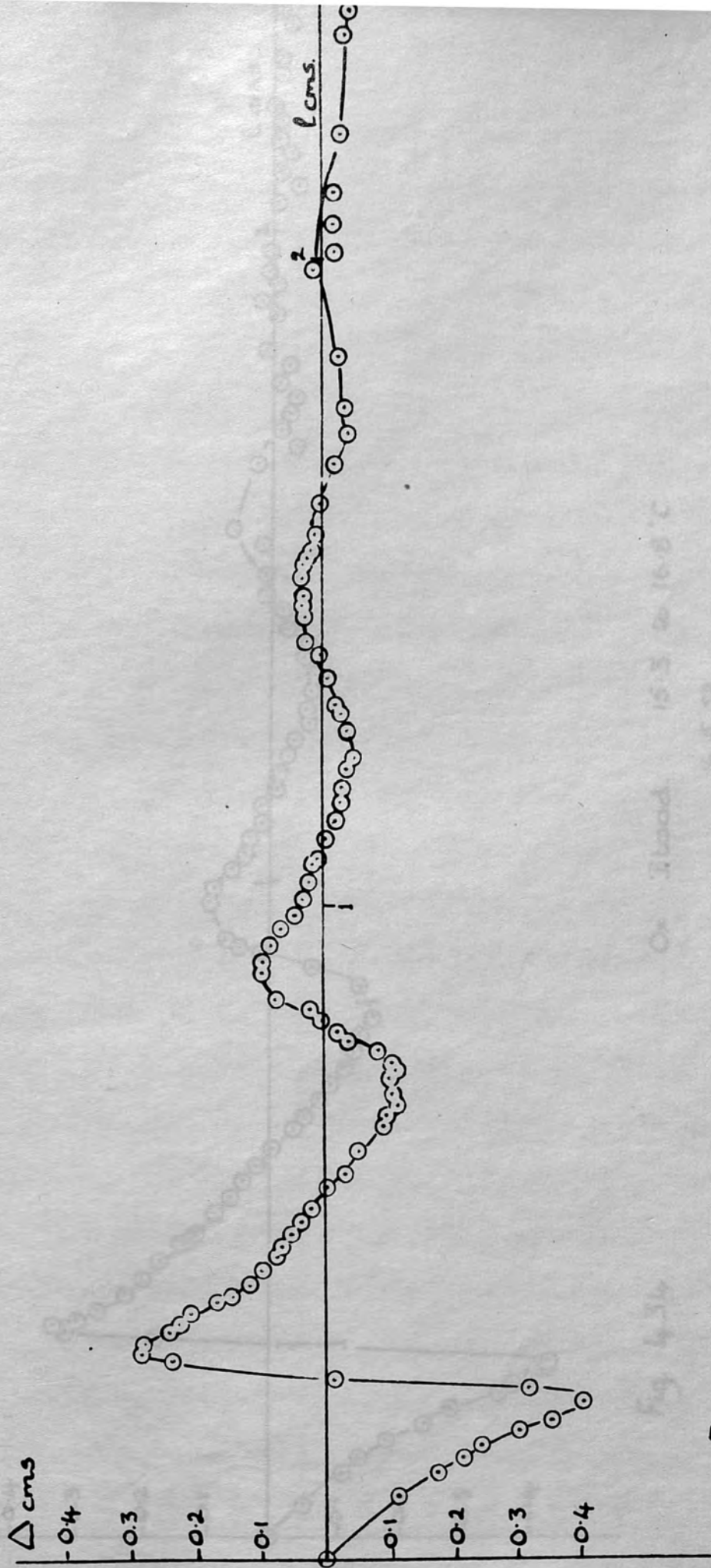


Fig. 4.33

Ox Serum 17.7 to 19.6°C

30.4.52.

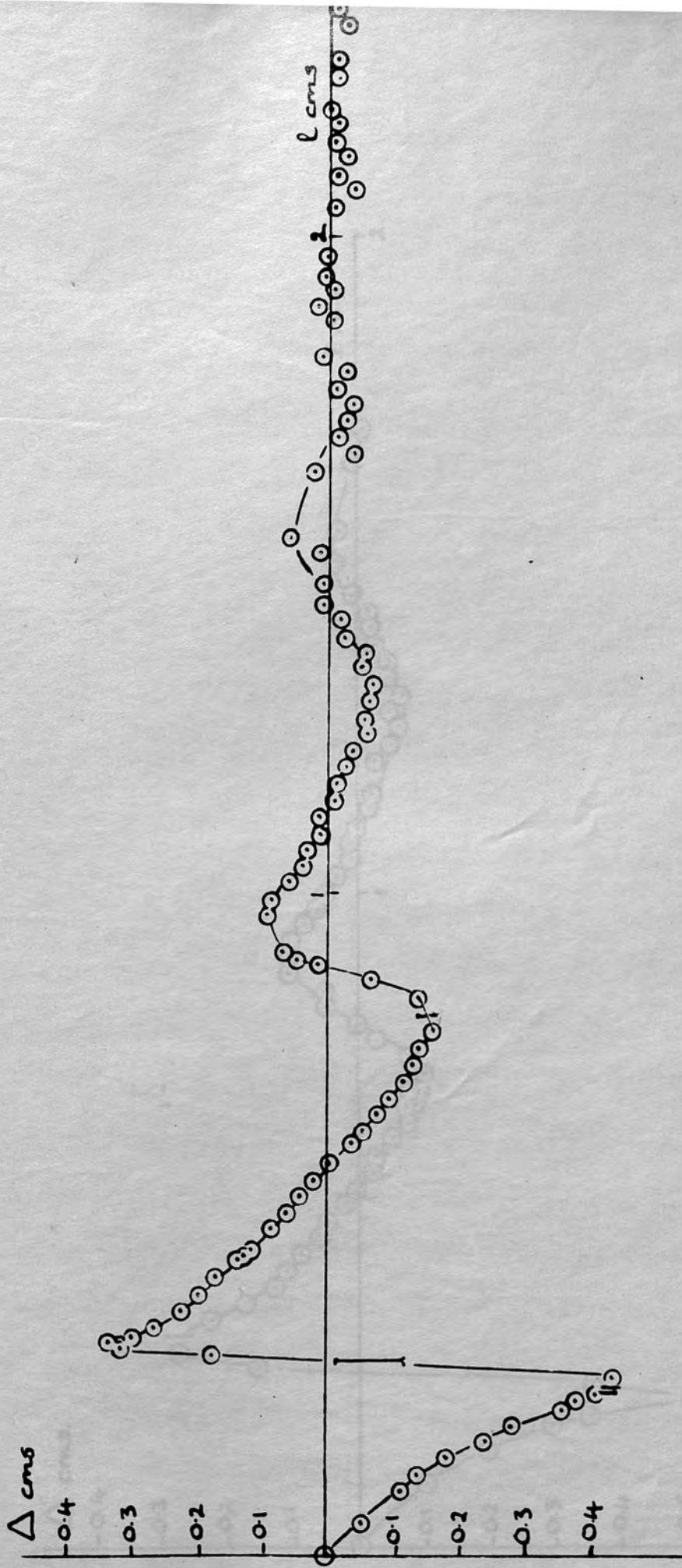
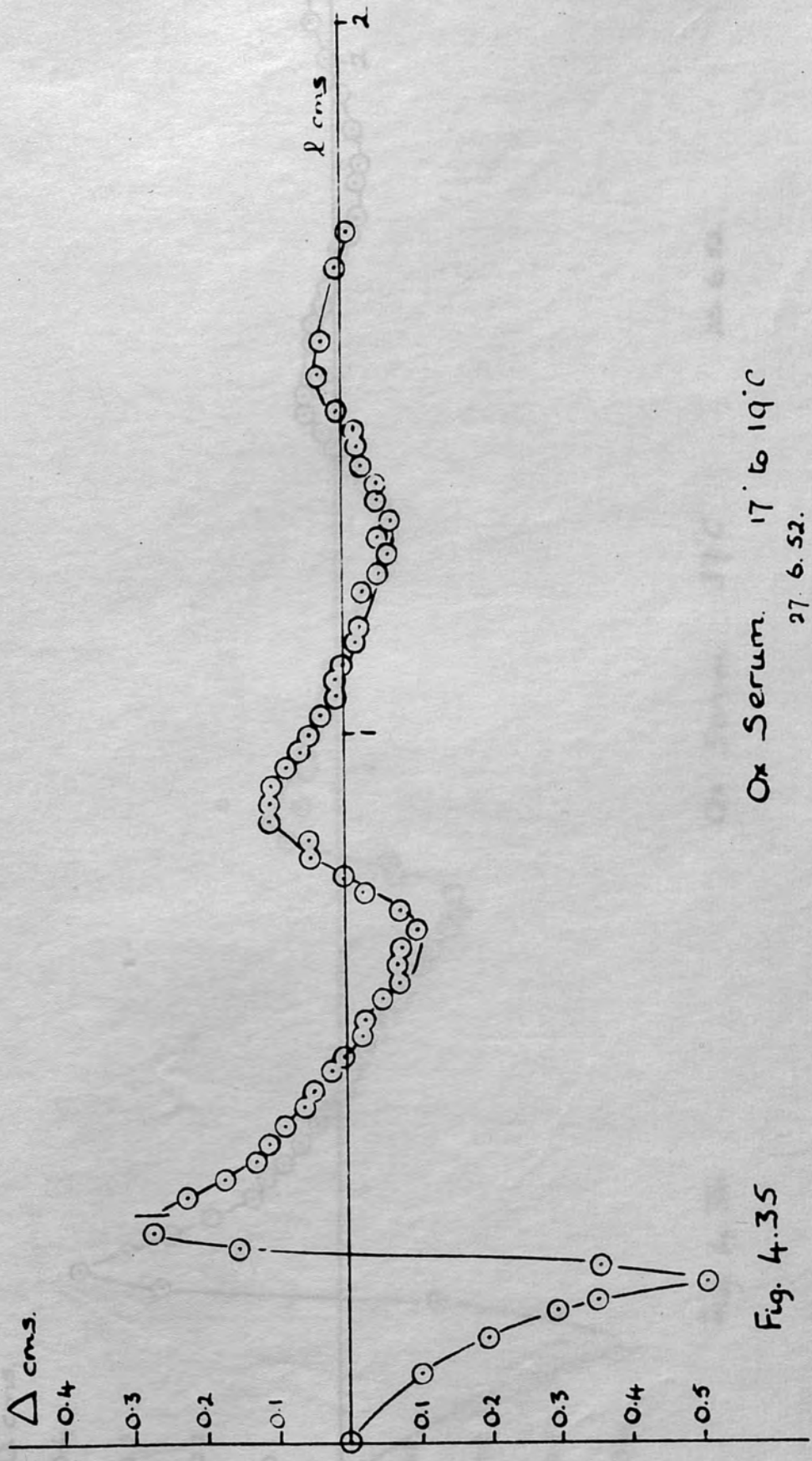


Fig. 4.34

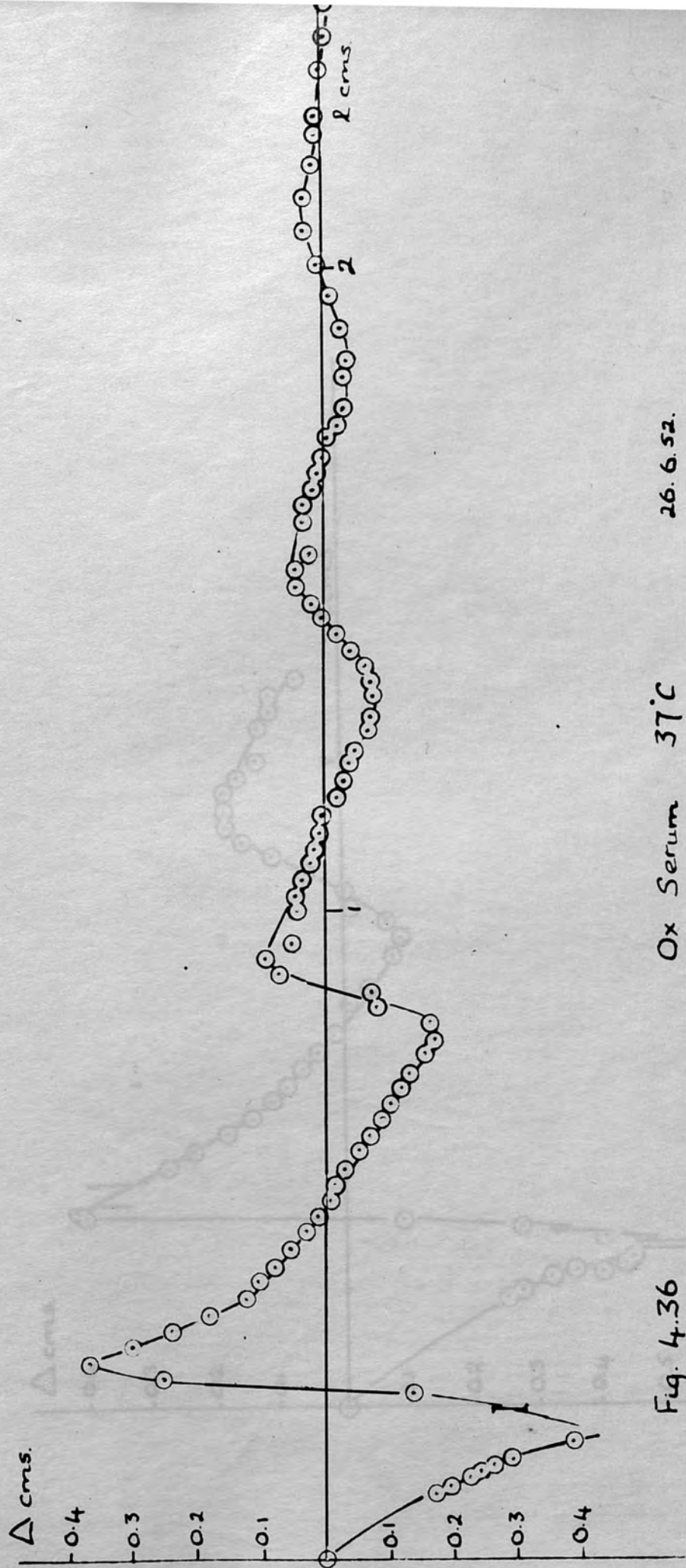
Ox Blood. 15.3 to 16.8 °C

14.5.52.



Ox Serum. 17 to 19°C
27. 6. 52.

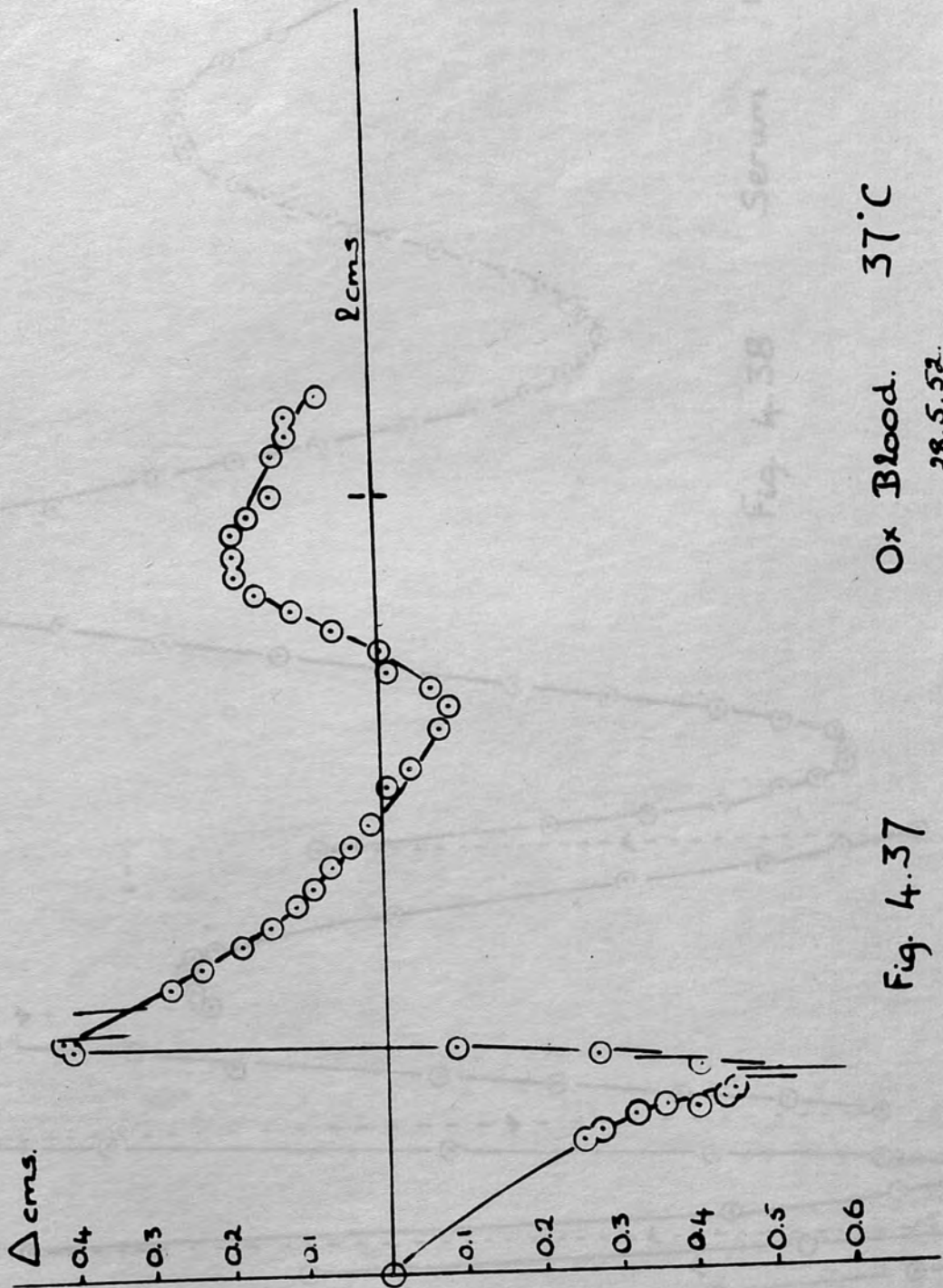
Fig. 4.35



26.6.52.

Ox Serum 37°C

Fig. 4.36



37°C

Ox Blood.

28.5.52.

Fig. 4.37

Serum 177 to 196°C.

Fig. 4.38

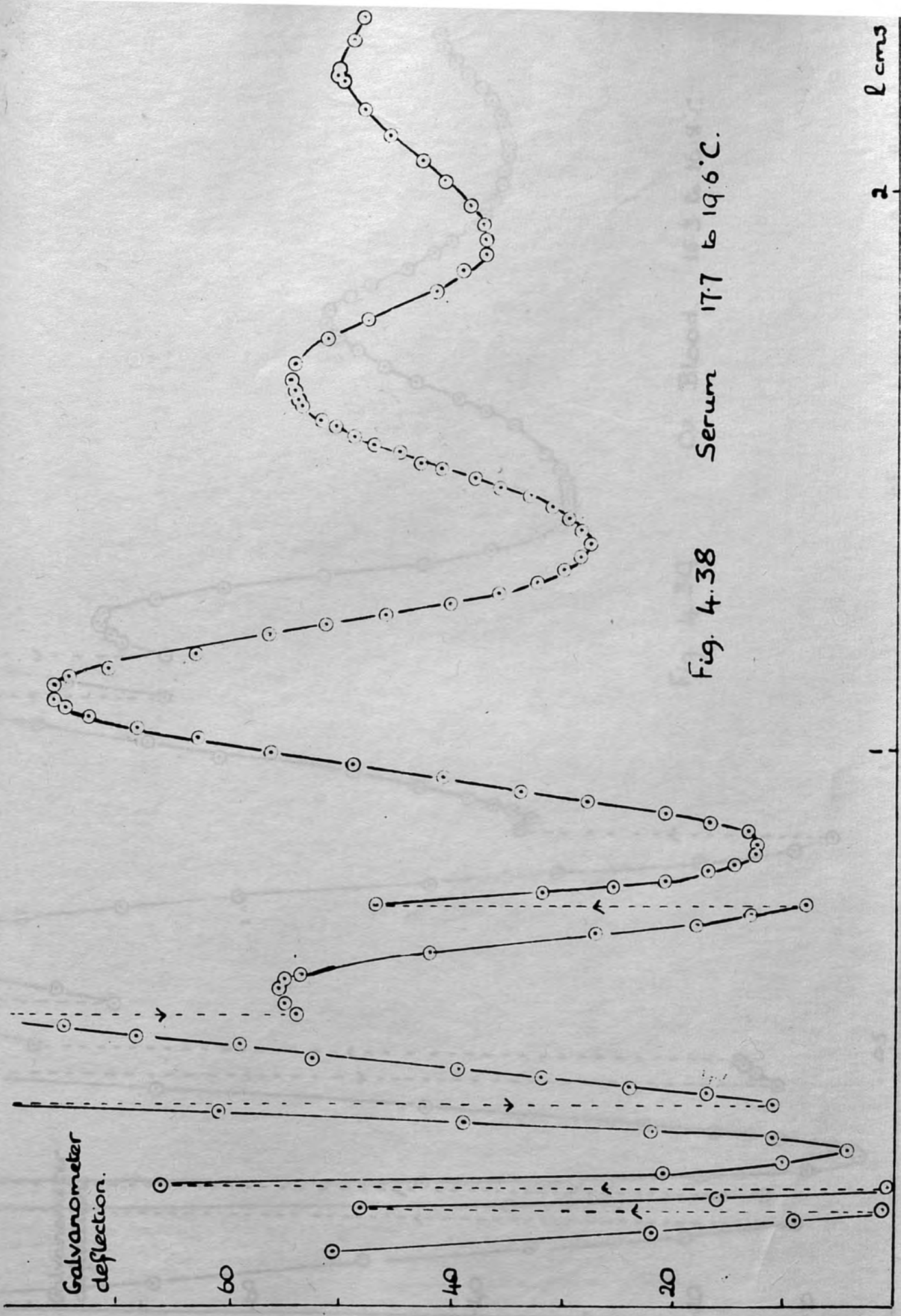


Fig. 4.38 Serum 17.7 to 19.6°C.

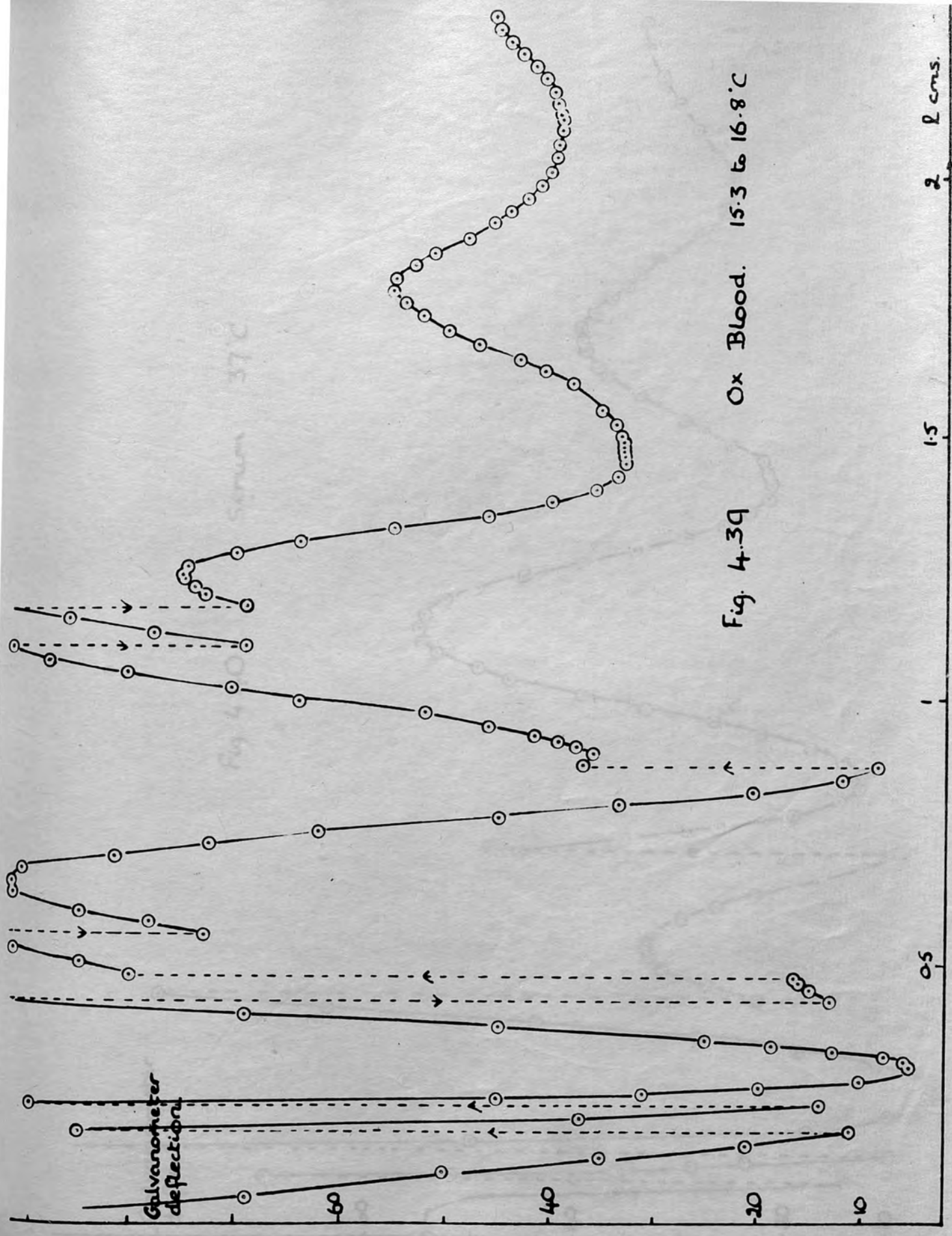


Fig. 4.39 Ox Blood. 15.3 to 16.8°C

Fig. 4.39 Ox Blood. 15.3 to 16.8°C

Galvanometer deflection.

Fig. 440 Serum 37°C.

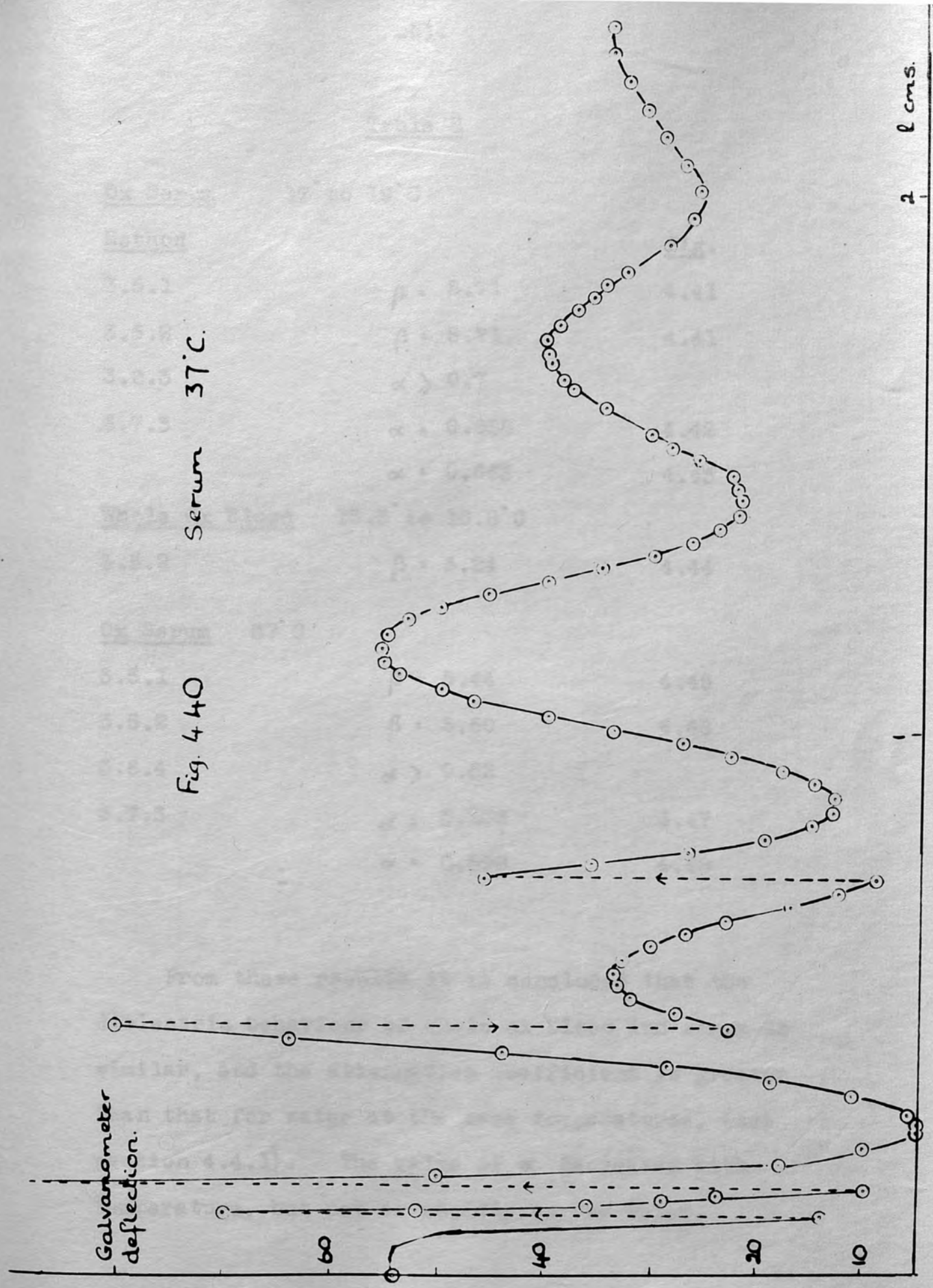


Table 8

<u>Ox Serum</u>	17° to 19° C		<u>Fig.</u>
<u>Method</u>			
3.5.1	$\beta = 5.71$		4.41
3.5.2	$\beta = 5.71$		4.41
3.6.3	$\alpha \gg 0.7$		
3.7.3	$\alpha = 0.688$		4.42
	$\alpha = 0.663$		4.43
<u>Whole Ox Blood</u>	15.3° to 16.8° C		
3.5.2	$\beta = 5.24$		4.44
<u>Ox Serum</u>	37° C		
3.5.1	$\beta = 5.44$		4.45
3.5.2	$\beta = 5.50$		4.46
3.6.4	$\alpha > 0.52$		
3.7.3	$\alpha = 0.556$		4.47
	$\alpha = 0.598$		4.48

From these results it is concluded that the dielectric behaviour of whole ox blood and serum is similar, and the attenuation coefficient is greater than that for water at the same temperatures, (see section 4.4.1). The value of α decreases with temperature, but not so rapidly as for water.

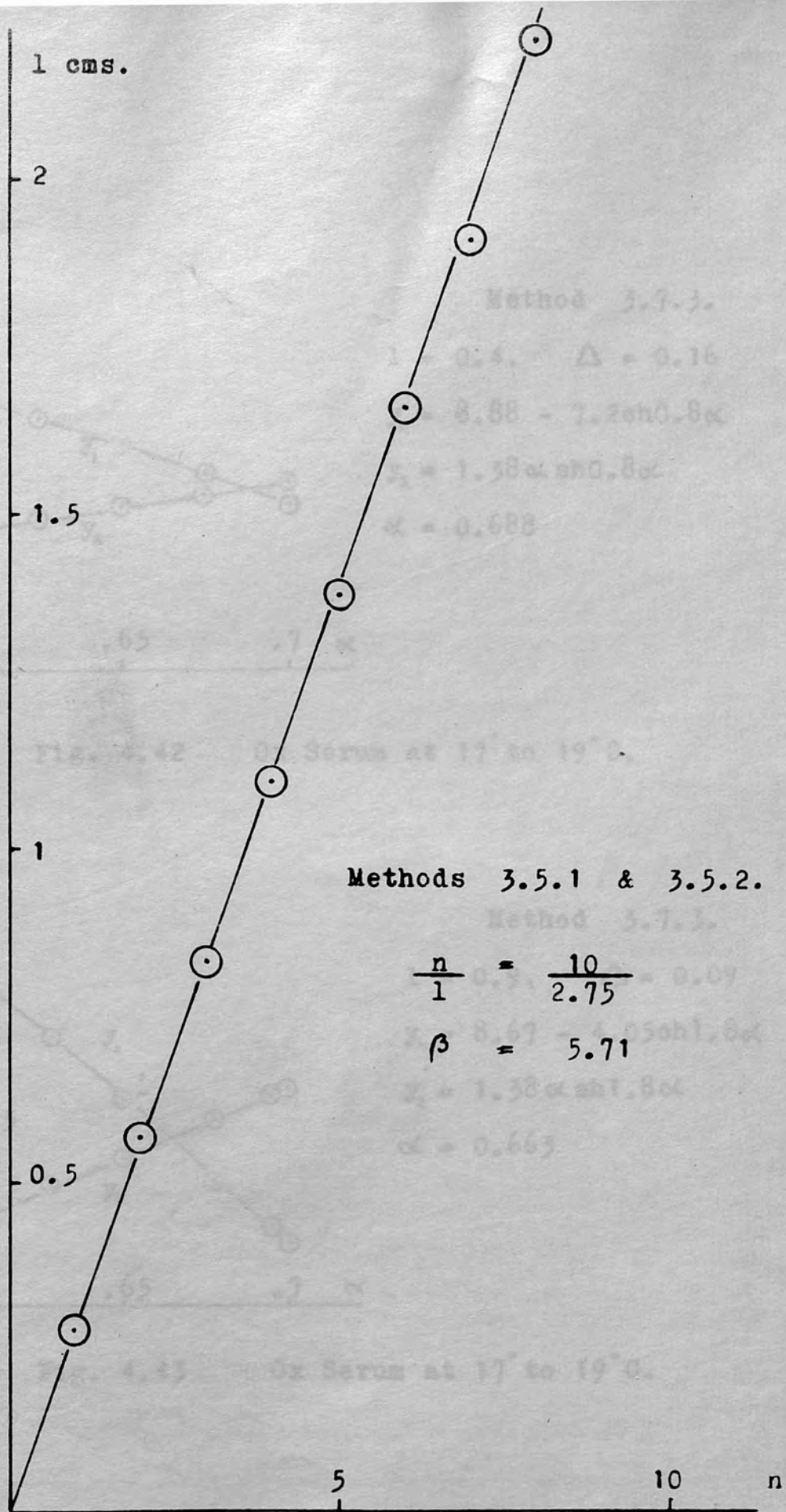
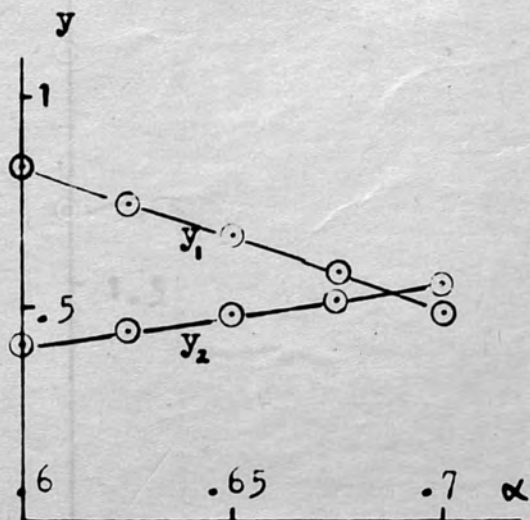


Fig. 4.41 Ox serum at room temperature.



Method 3.7.3.

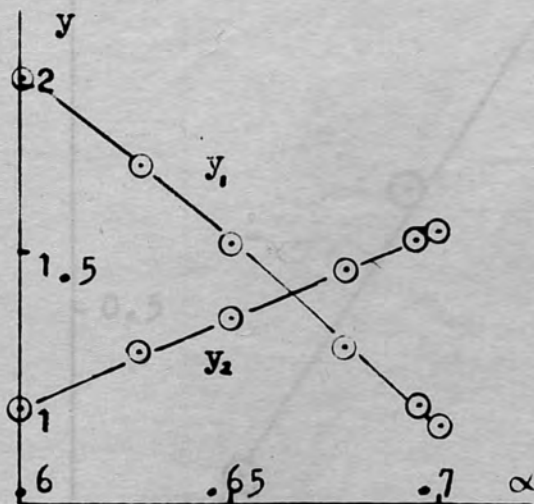
$$l = 0.4, \quad \Delta = 0.16$$

$$y_1 = 8.88 - 7.2 \operatorname{ch} 0.8\alpha$$

$$y_2 = 1.38\alpha \operatorname{sh} 0.8\alpha$$

$$\alpha = 0.688$$

Fig. 4.42 Ox Serum at 17° to 19° C.



Method 3.7.3.

$$l = 0.9, \quad \Delta = 0.09$$

$$y_1 = 8.67 - 4.05 \operatorname{ch} 1.8\alpha$$

$$y_2 = 1.38\alpha \operatorname{sh} 1.8\alpha$$

$$\alpha = 0.663$$

Fig. 4.43 Ox Serum at 17° to 19° C.

Fig. 4.44 Ox blood at room temperature.

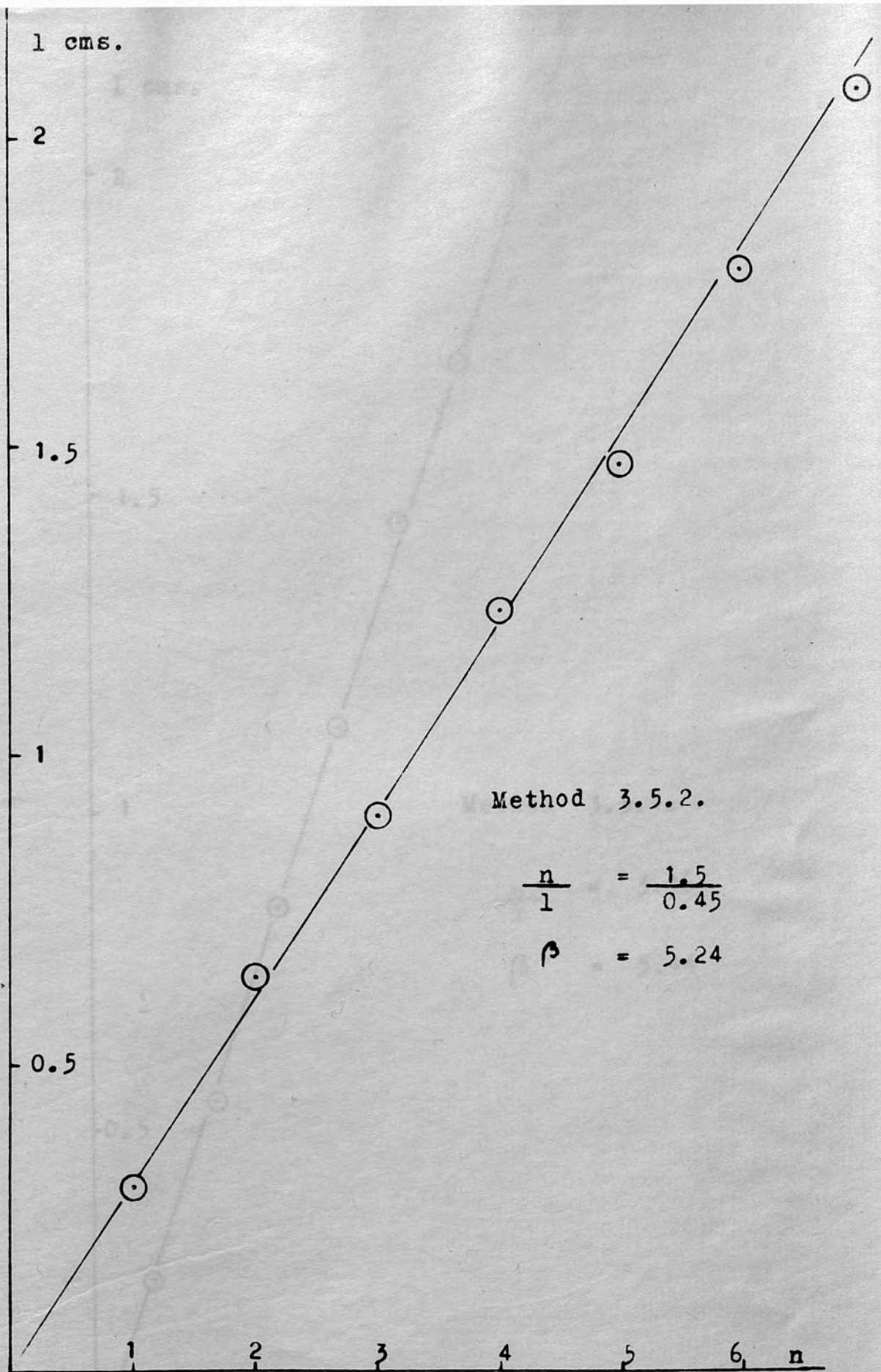


Fig. 4.44 Ox blood at room temperature.

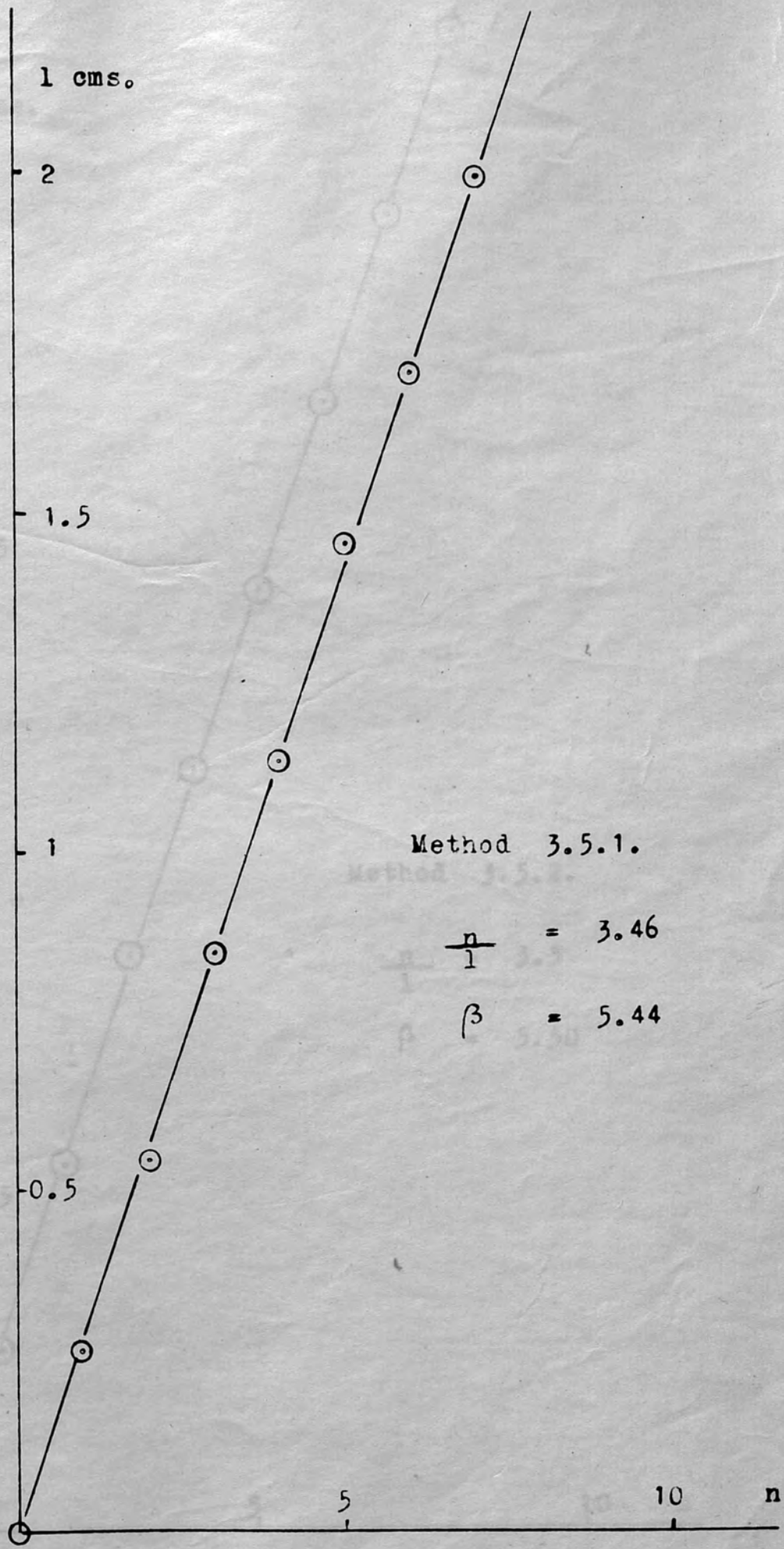


Fig. 4.45

Ox Serum at 37°C

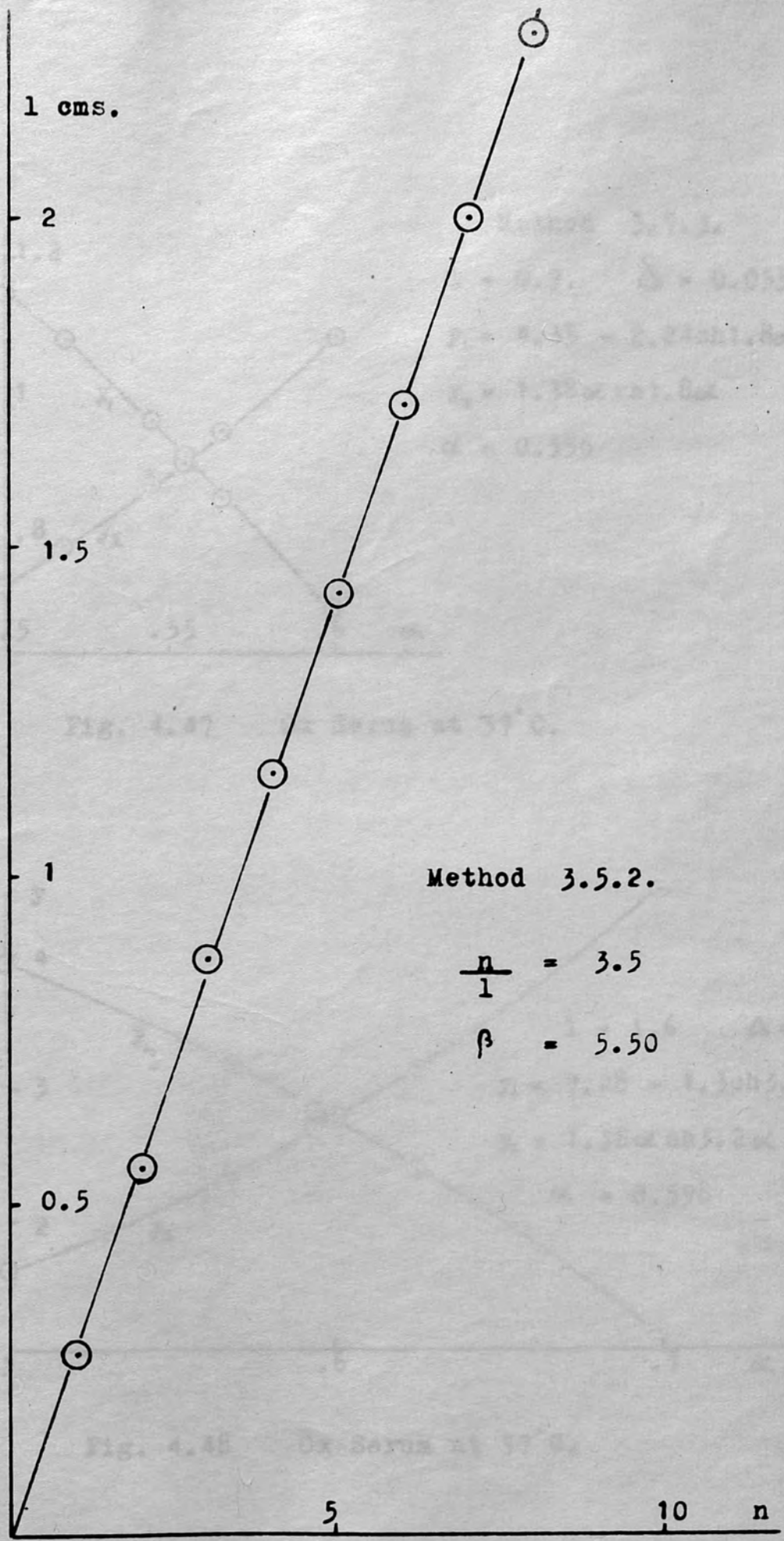
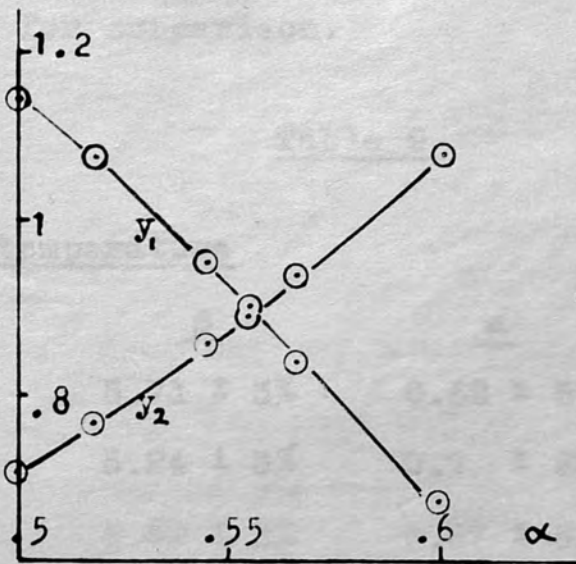


Fig. 4.46 Ox serum at 37°C



Method 3.7.3.

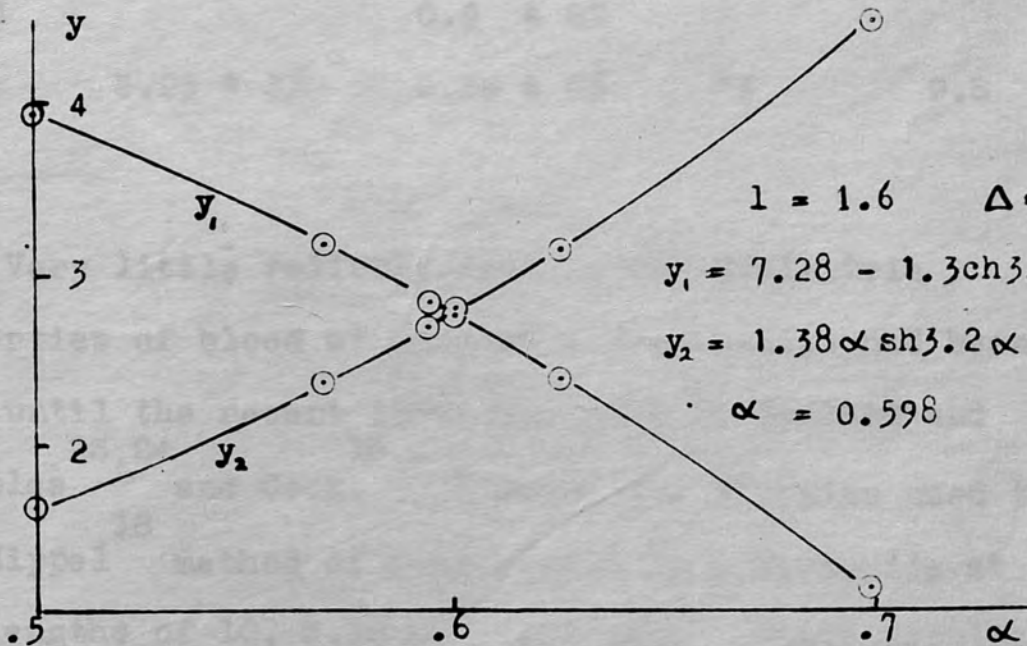
$$l = 0.9, \quad \Delta = 0.055$$

$$y_1 = 4.35 - 2.24 \operatorname{ch} 1.8\alpha$$

$$y_2 = 1.38 \alpha \operatorname{sh} 1.8\alpha$$

$$\alpha = 0.556$$

Fig. 4.47 Ox Serum at 37°C.



$$l = 1.6 \quad \Delta = -0.03$$

$$y_1 = 7.28 - 1.3 \operatorname{ch} 3.2\alpha$$

$$y_2 = 1.38 \alpha \operatorname{sh} 3.2\alpha$$

$$\alpha = 0.598$$

Fig. 4.48 Ox Serum at 37°C.

Table 9 sets out the concluded values of α , β , ϵ' and ϵ'' , together with those obtained for water for comparison.

Table 9

Room temperature

	β	α	ϵ'	ϵ''
Serum	5.71 \pm 3%	0.68 \pm 5%	67.2	16.3
Blood	5.24 \pm 3%	0.7 \pm 8%	56.6	15.3
Water	5.99 \pm 3%	0.57 \pm 5%	74.7	14.4

Inner body temperature 37°C

	β	α	ϵ'	ϵ''
Serum	5.44 \pm 3%	0.58 \pm 5%	61	13.2
Blood		0.6 \pm 8%		
Water	5.95 \pm 3%	0.38 \pm 5%	74	9.5

Very little reliable work on the dielectric properties of blood at microwave frequencies had been done until the recent investigations by England and Sharples^{23,24} and Cook.¹³ England and Sharples used the von Hippel¹⁸ method of measurement in a waveguide at wavelengths of 10, 3.18 and 1.27 cms. Their results for human blood at 10 cms were:-

<u>Specimen at 37° C</u>	<u>α</u>	<u>β</u>
Whole human blood	0.65 \pm 5%	4.6 \pm 2%
Blood serum	0.84 \pm 5%	5.3 \pm 2%
Water	0.3	5.4

Cook made a thorough investigation of whole human blood at four different wavelengths, 16.93, 10.03, 3.195 and 1.262 cms and four different temperatures, 15°, 25°, 35° and 45° C, using the same methods as he had used in his investigation of water. His results at 10.03 cms for whole human blood were:-

15° C	$\epsilon' = 59.9 \pm 2\%$	$\epsilon'' = 19.9 \pm 5\%$
35° C	$\epsilon' = 56.0 \pm 2\%$	$\epsilon'' = 15.9 \pm 5\%$

and for water at 10 cms

15° C	$\epsilon' = 78.6 \pm 1\%$	$\epsilon'' = 15.0 \pm 2\%$
35° C	$\epsilon' = 74.0 \pm 1\%$	$\epsilon'' = 8.7 \pm 2\%$

The present results show that the dielectric properties of ox blood are similar to those of human blood.

4.4.3 Results for NaCl solutions of varying concentrations.

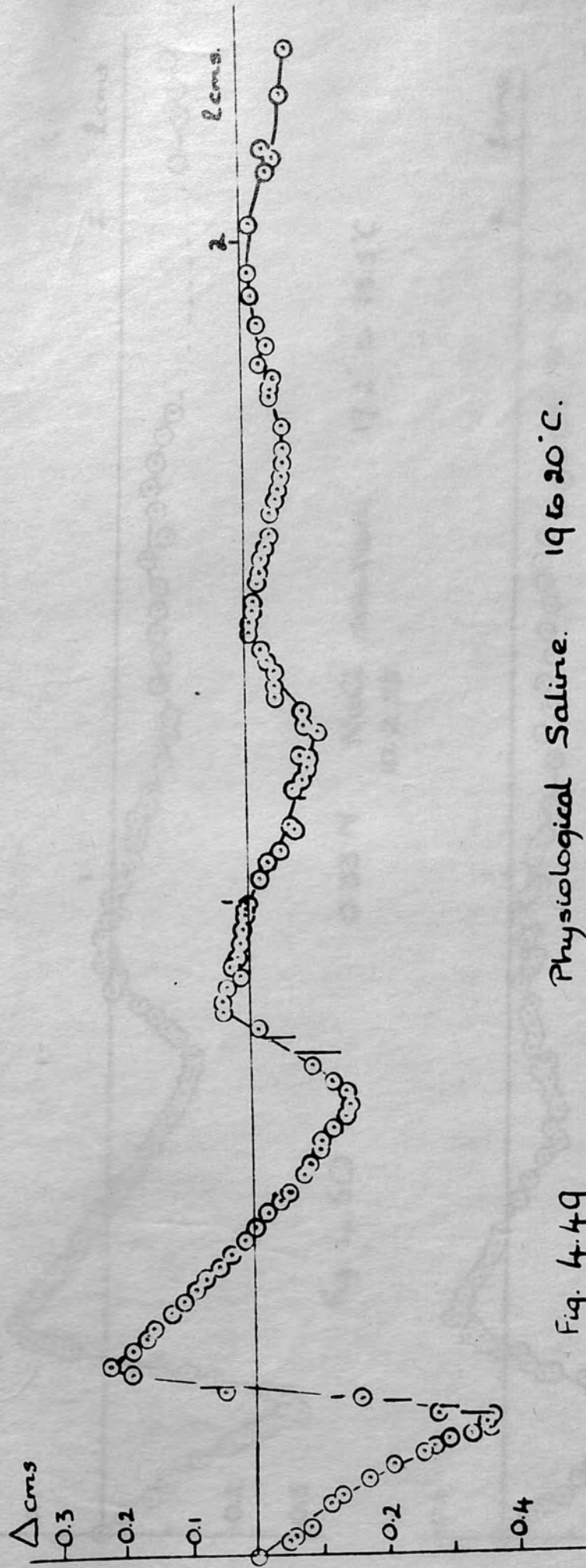
Figs. 4.49 to 4.60 show the results obtained using NaCl solutions of concentrations varying from 0.15N up to 2N in distilled water. Physiological saline, Ringer Tyrode solution, was used for the 0.15N solution. This consists of:-

NaCl	0.8	gr
KCl	0.02	
CaCl ₂	0.02	
NaHCO ₃	0.1	
NaH ₂ PO ₄	0.005	
MgCl ₂	0.01	
Glucose	0.1	

in 100 gr of water.

The variation of galvanometer signal with liquid depth is shown for each solution. Table 10 in the Appendix gives the experimental readings recorded when Physiological saline was used. They are typical of the results obtained for the 'water-type' liquids.

It is immediately seen from these graphs that α increases very rapidly with increased concentration. This is almost entirely due to the conductivity of the liquid. The total effective value ζ_c'' of the imaginary



Physiological Saline. 19 to 20°C.

18. 2. 53.

Fig. 4.49

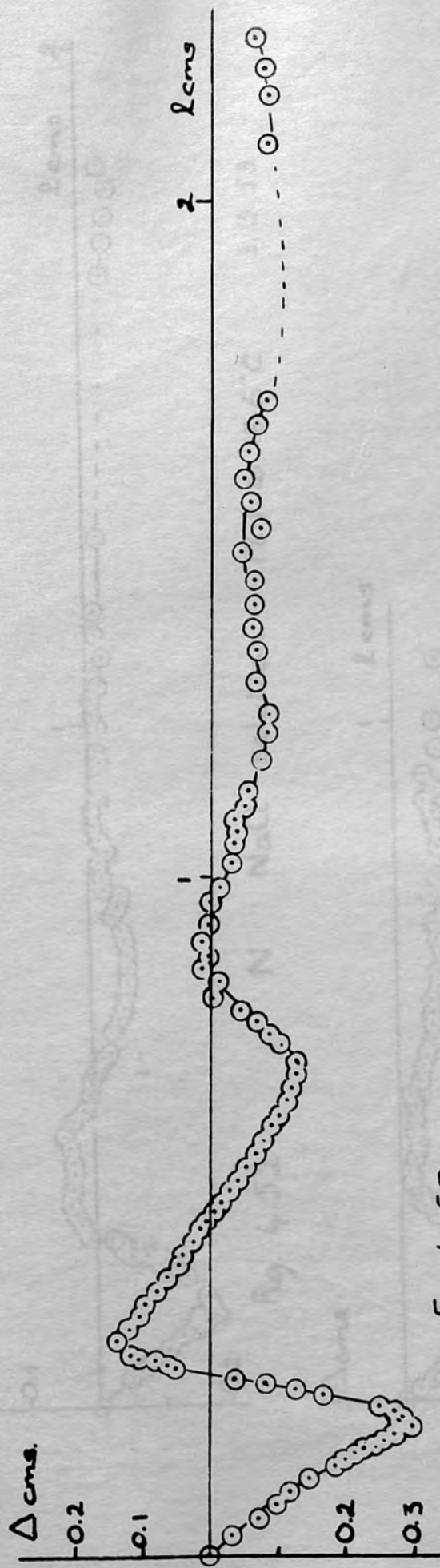


Fig. 4.50 0.33 N NaCl solution. 17.2° to 18.5°C
10.2.53.

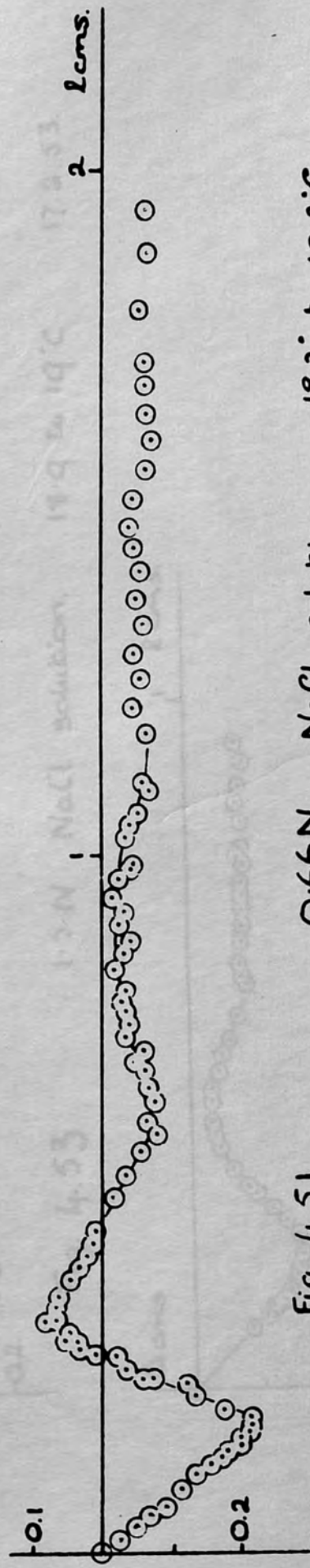


Fig. 4.51 0.66 N NaCl solution. 18.2° to 19.2°C
11.2.53.

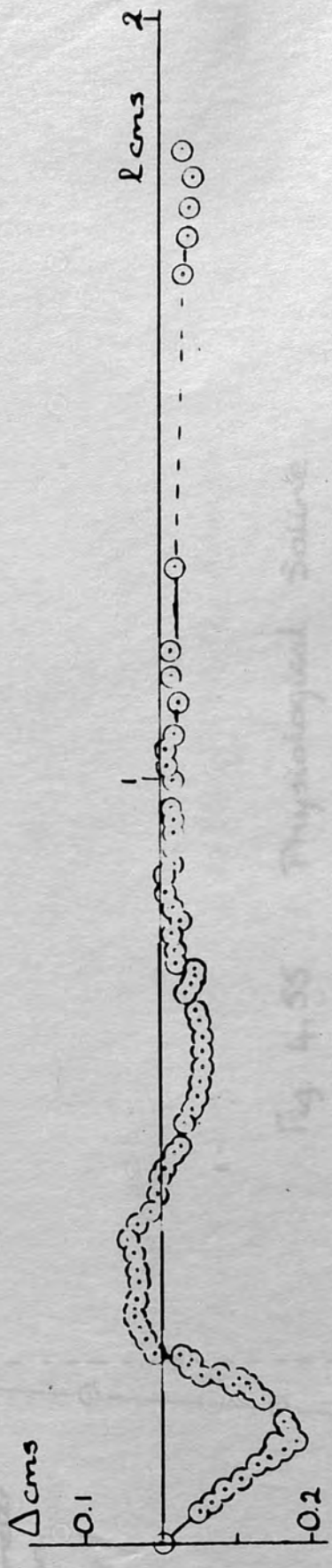


Fig. 4.52 N NaCl solution. 18.1 to 18.6°C 3.3.53.

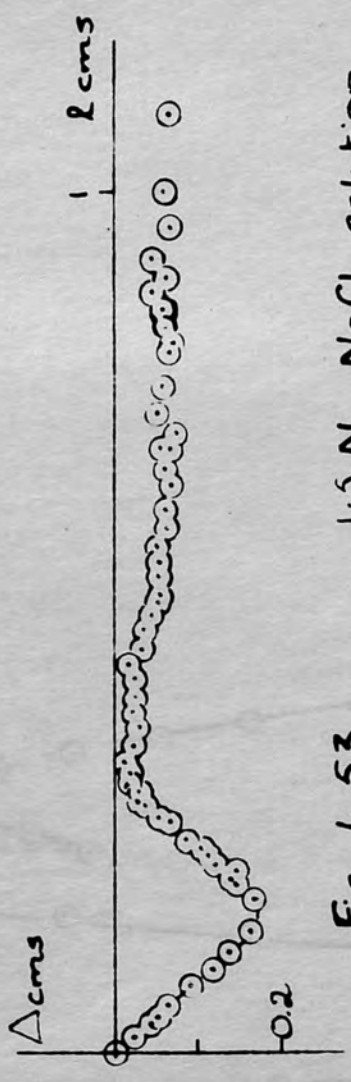


Fig. 4.53 1.5 N NaCl solution. 18.9 to 19°C 17.2.53.

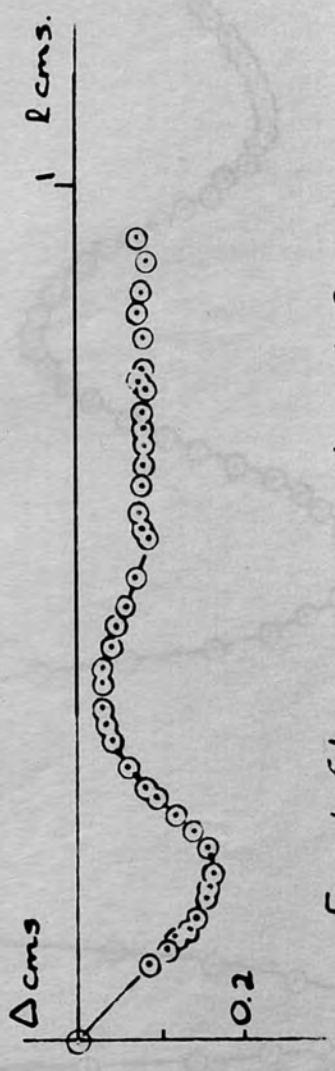


Fig. 4.54 2 N NaCl solution. 17.8 to 17°C 2.2.53.

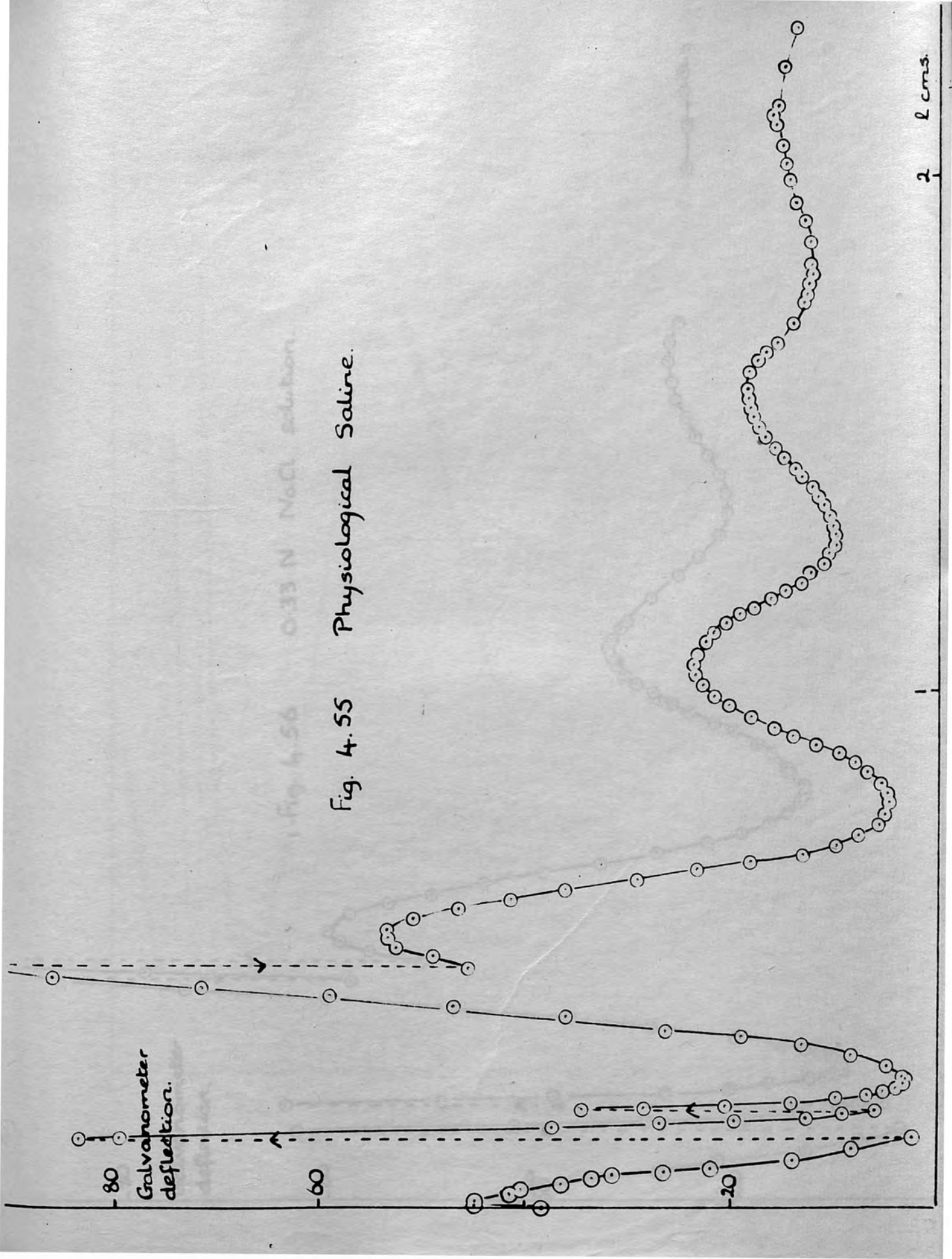


Fig. 4.56 0.33 N NaCl solution

Fig. 4.55 Physiological Saline.

Galvanometer deflection.

80

60

40

20

0

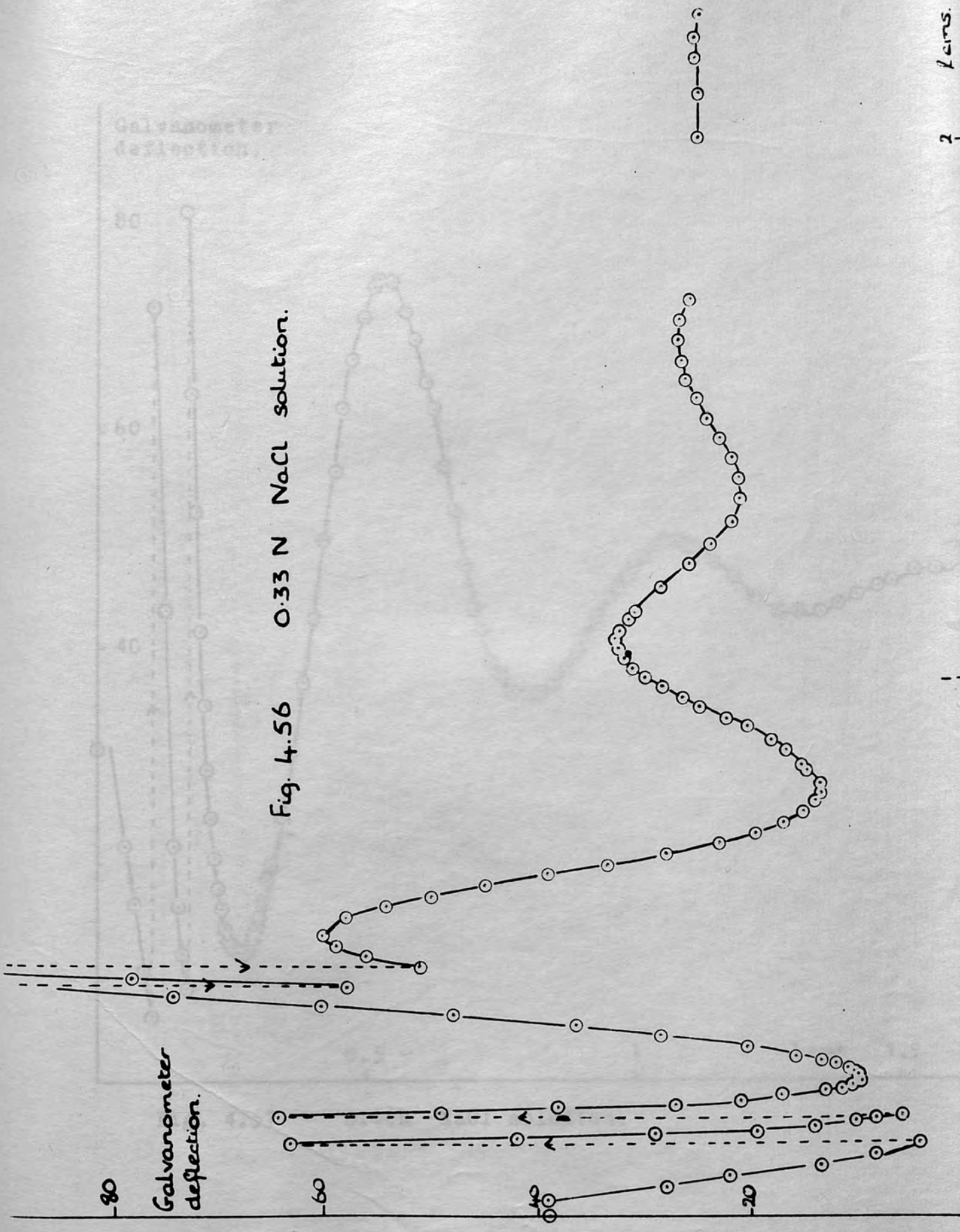
-20

-40

-60

Galvanometer deflection.

Fig. 4.56 0.33 N NaCl solution.



2 cm.

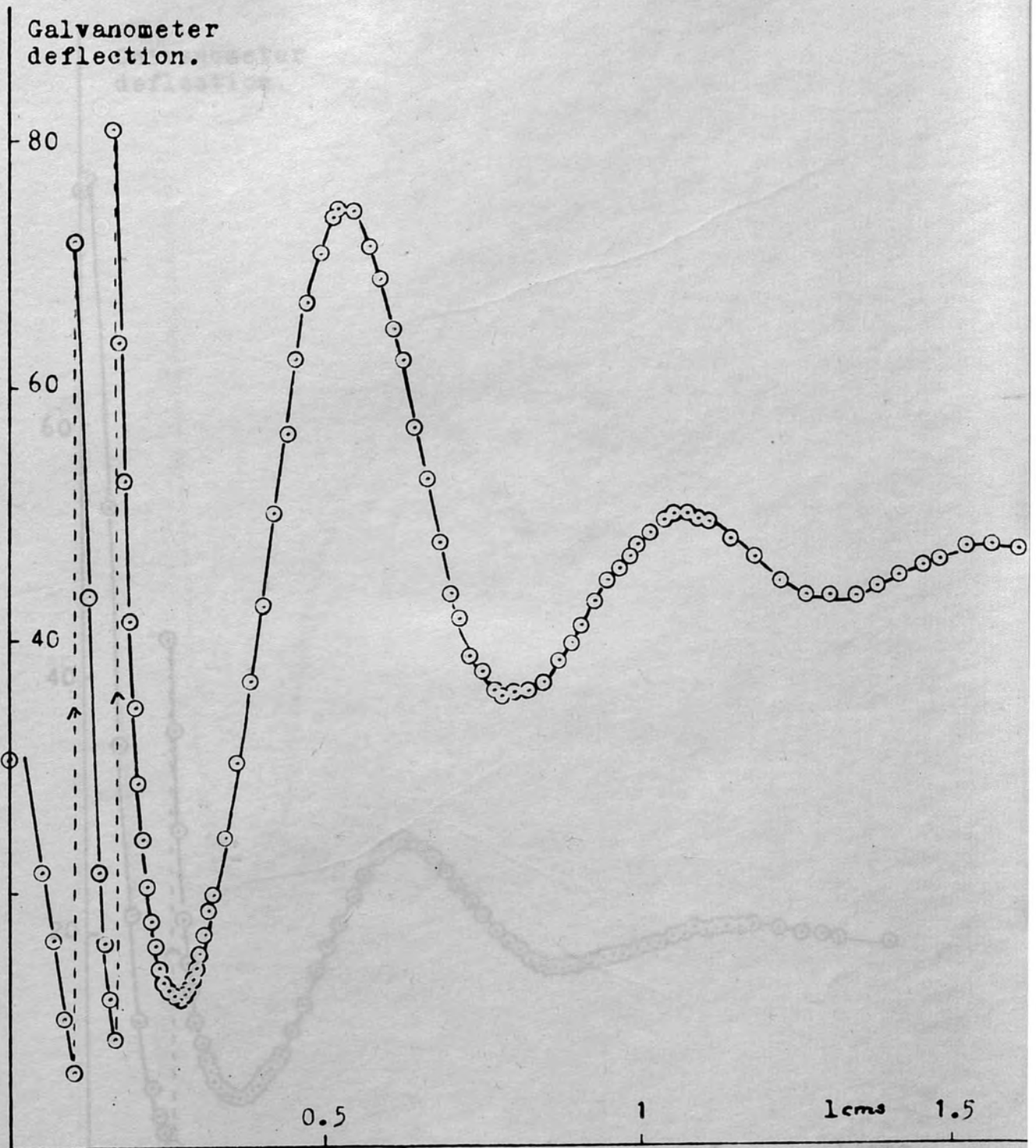


Fig. 4.57 0.66N NaCl solution.

Fig. 4.58 Normal NaCl solution.

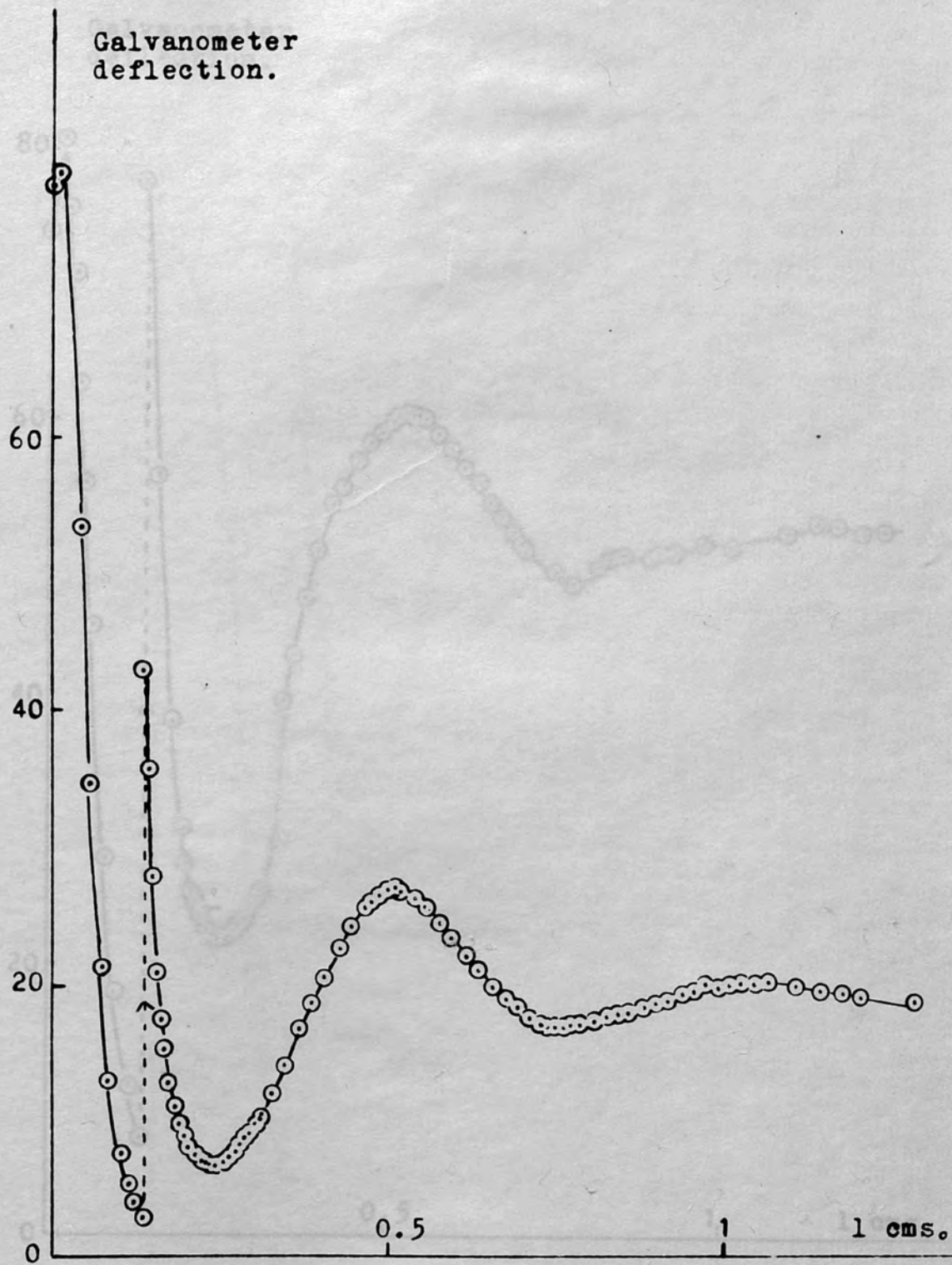


Fig. 4.58

Normal NaCl solution.

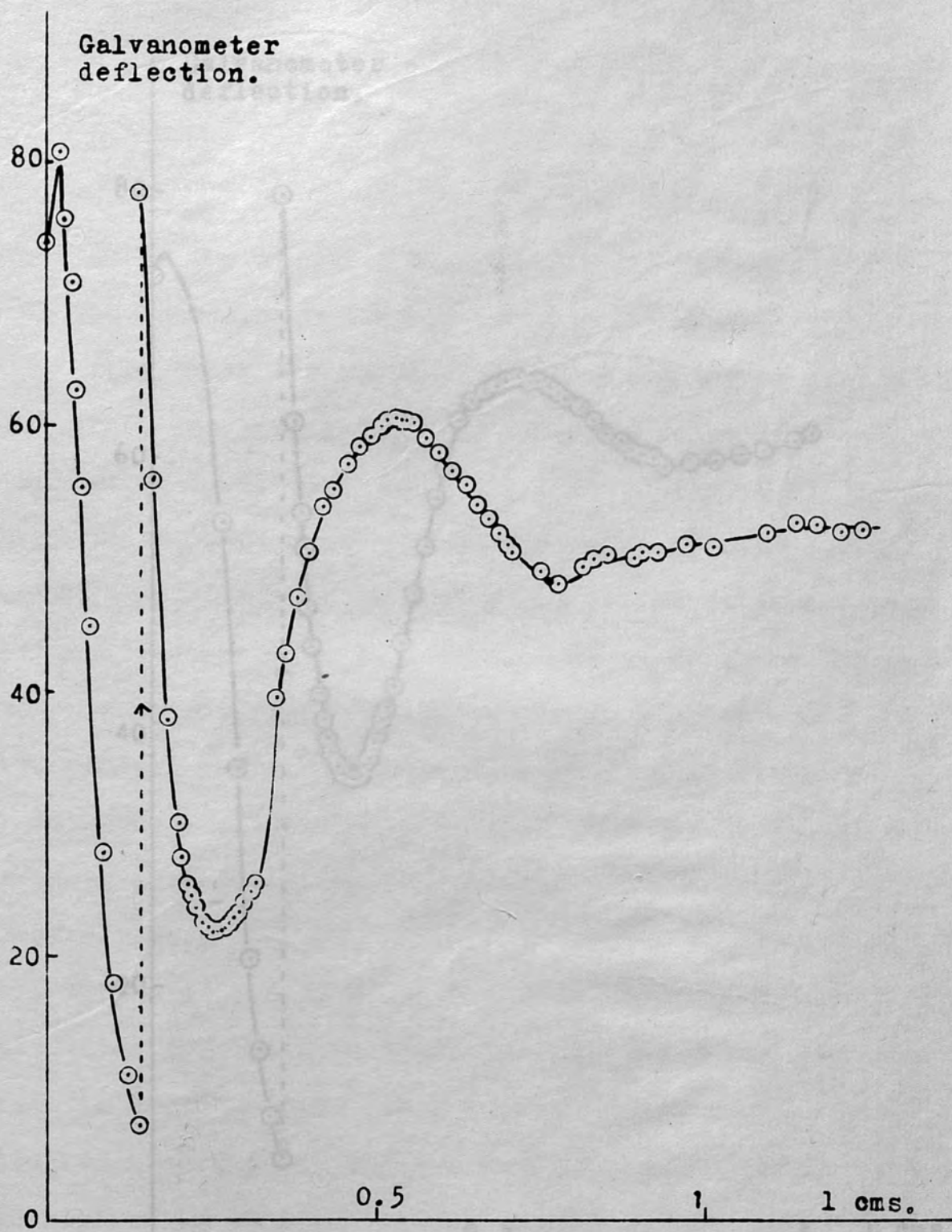


Fig. 4.59 1.5N NaCl solution.

Galvanometer deflection.

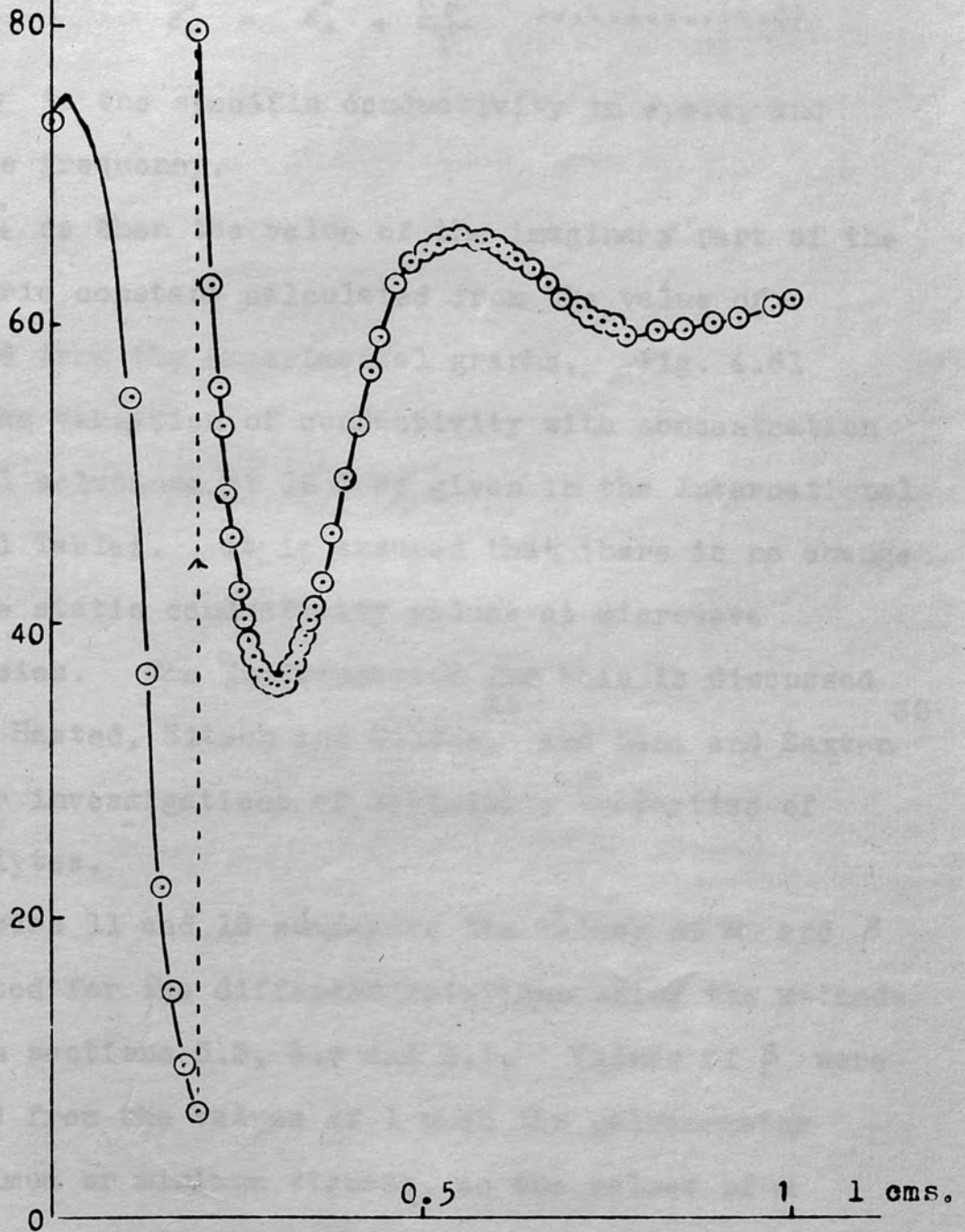


Fig. 4.60

2N NaCl solution.

part of the dielectric constant is made up of two terms, one being the contribution from dipole relaxation ϵ''_d , and the other from the ionic conductivity of the solution.

$$\epsilon''_t = \epsilon''_d + \frac{2\sigma}{f} \dots\dots\dots(4.6)$$

where σ is the specific conductivity in e.s.u. and f is the frequency.

ϵ''_t is then the value of the imaginary part of the dielectric constant calculated from the value of α obtained from the experimental graphs. Fig. 4.61 shows the variation of conductivity with concentration for NaCl solutions at 18°C as given in the International Critical Tables. It is assumed that there is no change in these static conductivity values at microwave frequencies. The justification for this is discussed by both Hasted, Ritson and Collie, and Lane and Saxton in their investigations of dielectric properties of electrolytes.

Tables 11 and 12 summarise the values of α and β calculated for the different solutions using the methods given in sections 3.5, 3.6 and 3.7. Values of β were obtained from the values of l when the galvanometer had maximum or minimum signals, as the values of α were too large for the method of section 3.5.1 to be

valid. Approximate values of α could be obtained, either by inspection of the experimental curves, or by one of the methods of section 3.6. If $\alpha \gg 1$, it is not permissible to neglect terms in α^2 when applying the methods of section 3.7; so that this approximate value of α was substituted for α^2 and the equation solved for α . The resulting value of α was then used for α^2 in subsequent calculations.

Table 11

Values of β calculated by the method of section 3.5.2 for NaCl solutions.

<u>Concentration</u>	<u>β</u>	<u>Fig.</u>
0.15 N	6.03	4.62
0.33N	5.75	4.63
0.66N	5.88	4.64
1 N	6.3	4.65
1.5N	6.28	4.66
2 N	5.72	4.67

Fig. 4.61. Dependence of β on concentration of NaCl solutions at 18°C.

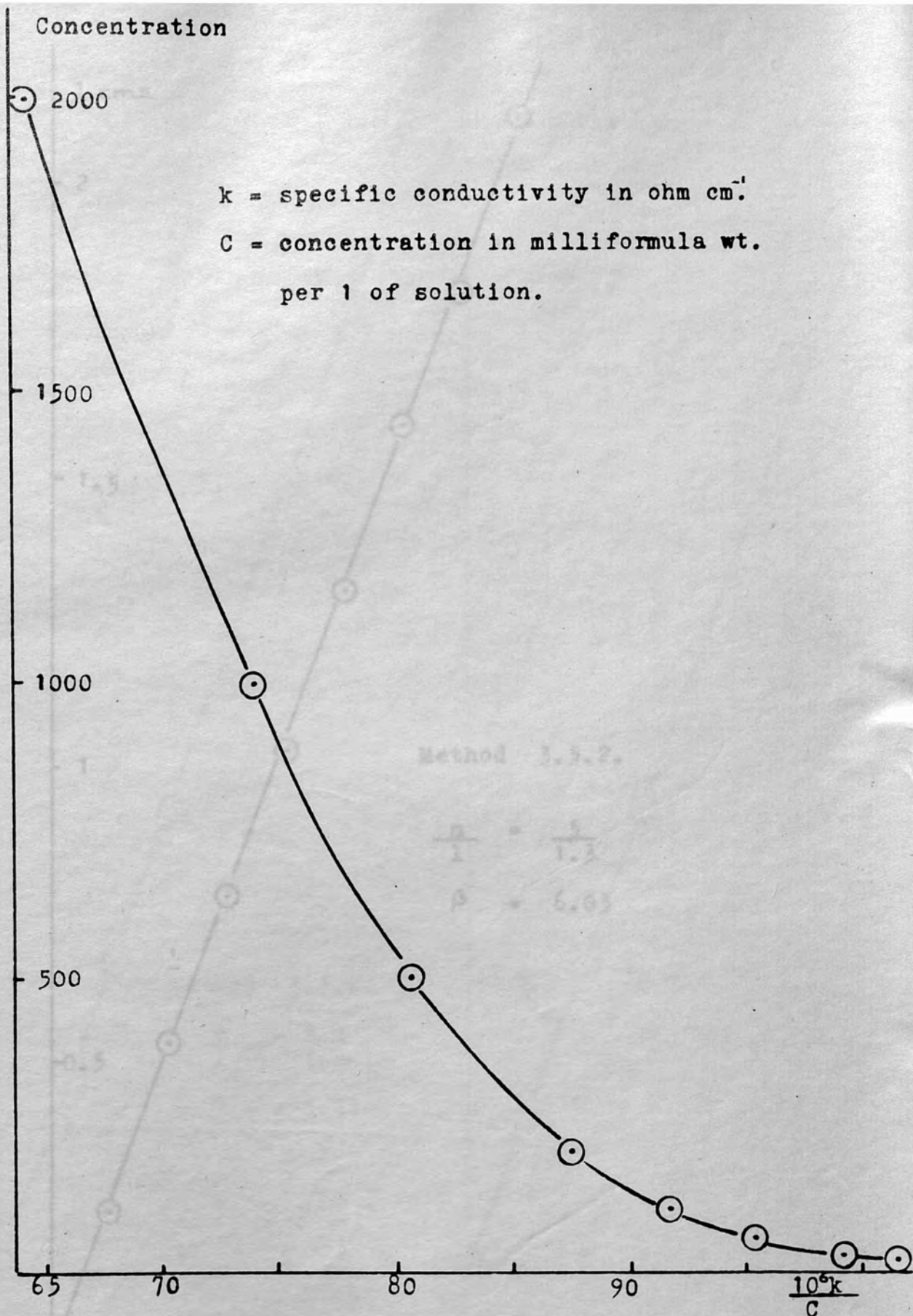


Fig. 4.61 Conductivity of NaCl solutions at 18°C

Fig. 4.62 Phys from I.C.T. line.

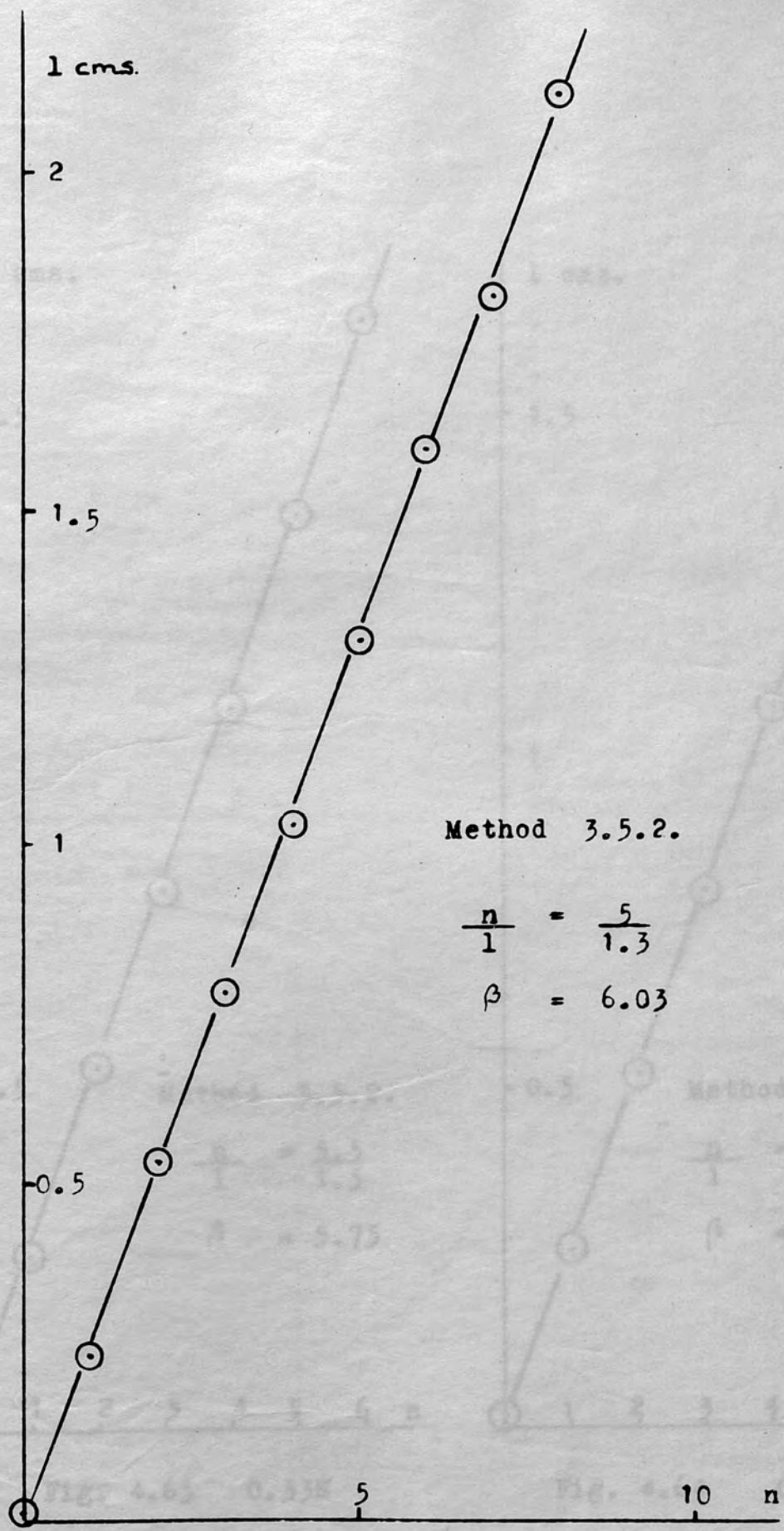


Fig. 4.62 Physiological saline.

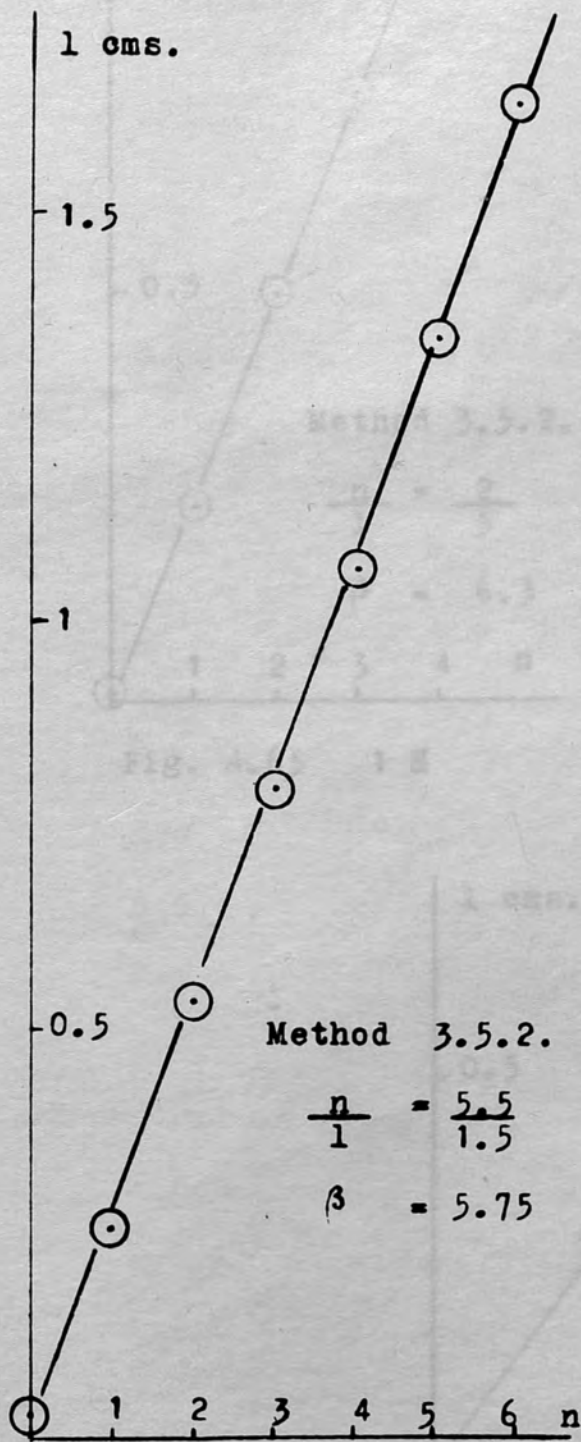


Fig. 4.63 0.33N

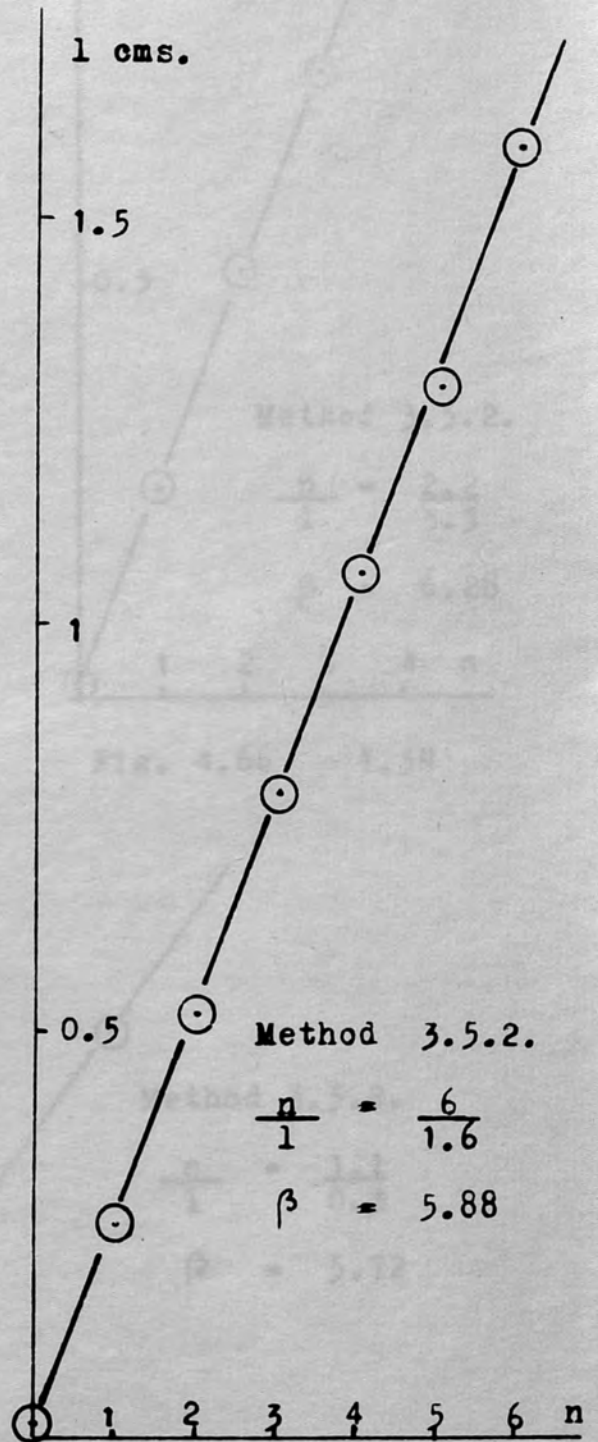


Fig. 4.64 0.66N

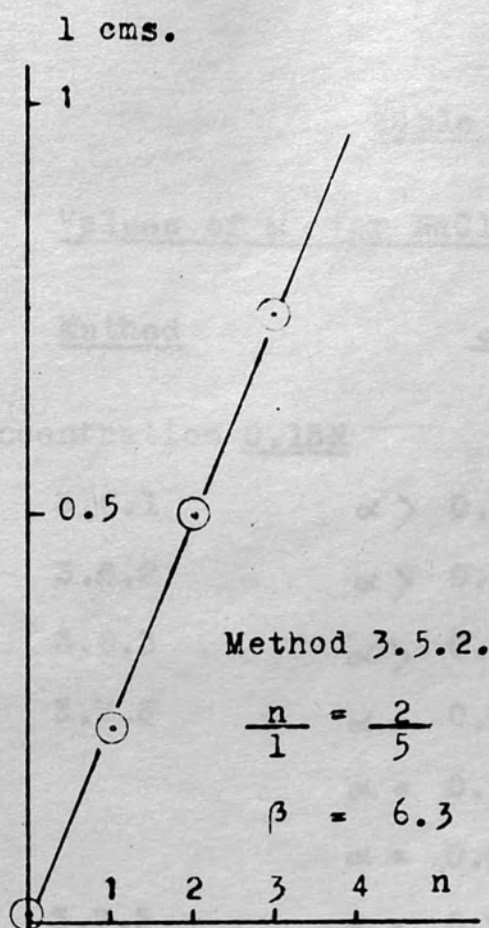


Fig. 4.65 1 N

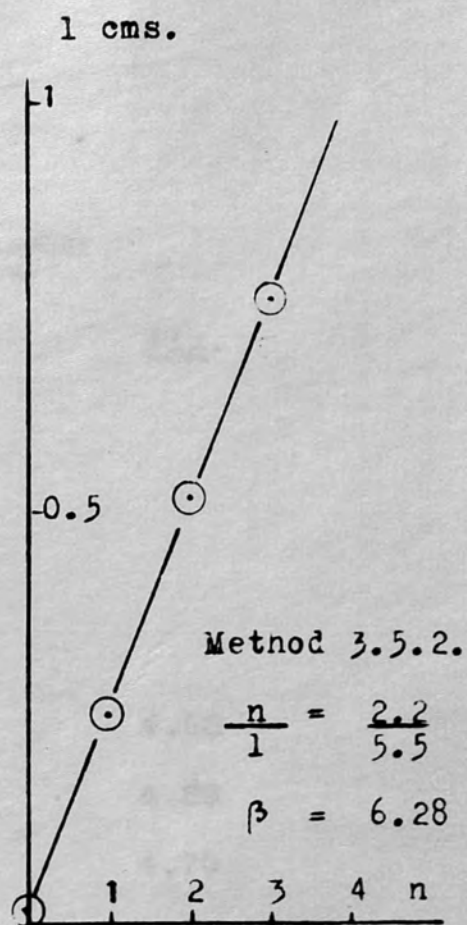


Fig. 4.66 1.5N

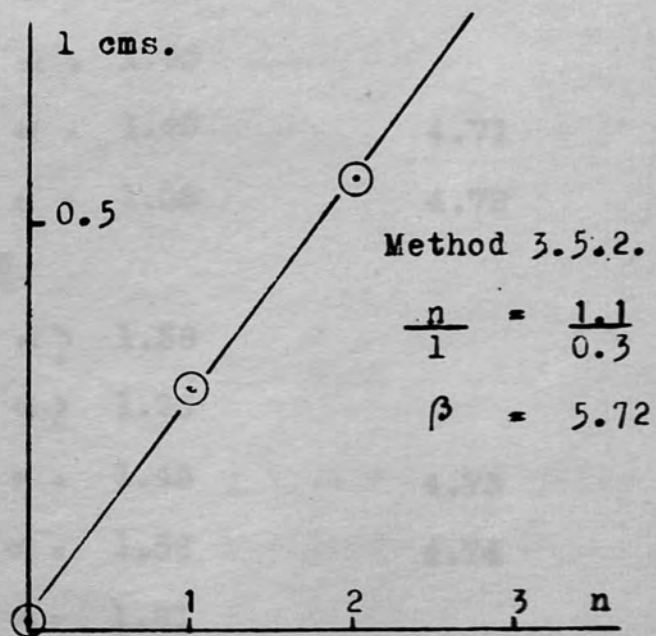
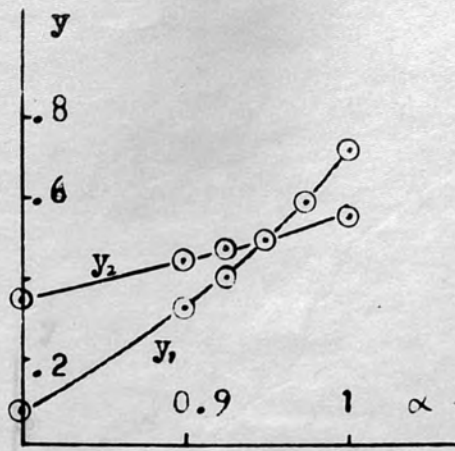


Fig. 4.67 2 N

Table 12

Values of α for NaCl solutions

<u>Method</u>	<u>α</u>	<u>Fig.</u>
Concentration <u>0.15N</u>		
3.6.1	$\alpha > 0.5$	
3.6.2	$\alpha > 0.5$	
3.6.3	$\alpha > 0.74$	
3.7.3	$\alpha = 0.95$	4.68
	$\alpha = 0.98$	4.69
	$\alpha = 0.895$	4.70
3.7.5	$\alpha = 0.91$	
Concentration <u>0.33N</u>		
3.6.3	$\alpha > 0.91$	
3.6.4	$\alpha > 1.05$	
3.7.3	$\alpha = 1.09$	4.71
	$\alpha = 1.08$	4.72
Concentration <u>0.66N</u>		
3.6.3	$\alpha > 1.38$	
3.6.4	$\alpha > 1.25$	
3.7.3	$\alpha = 1.43$	4.73
	$\alpha = 1.56$	4.74
3.7.4	$\alpha = 1.81$	



Method 3.7.3

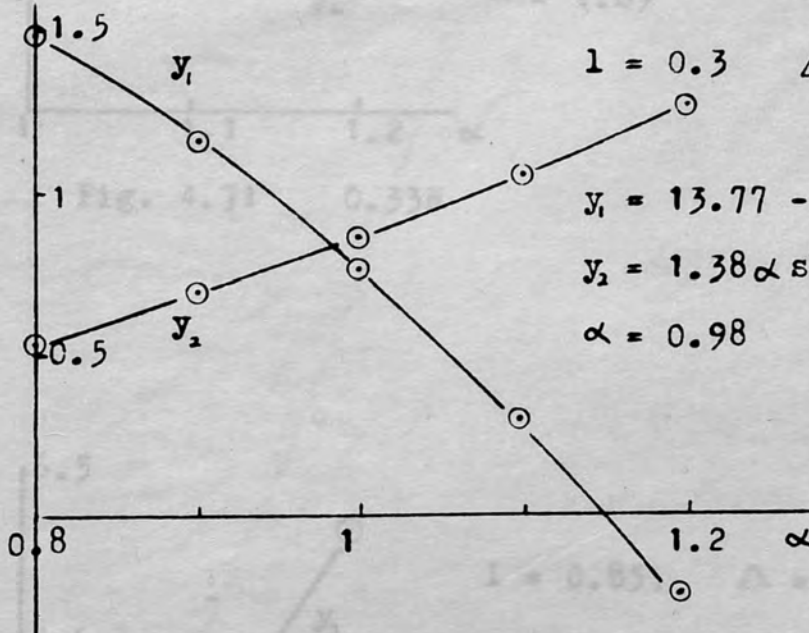
$$l = 0.2, \quad \Delta = 0.36$$

$$y_1 = 19.9 \operatorname{ch} 0.4\alpha - 20.82$$

$$y_2 = 1.38\alpha \operatorname{sh} 0.4\alpha$$

$$\alpha = 0.95$$

Fig. 4.68 0.15N



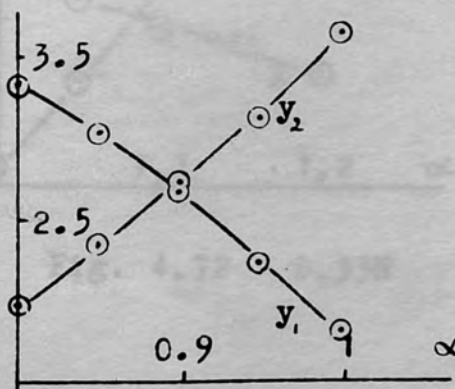
$$l = 0.3 \quad \Delta = 0.21$$

$$y_1 = 13.77 - 10.97 \operatorname{ch} 0.6\alpha$$

$$y_2 = 1.38\alpha \operatorname{sh} 0.6\alpha$$

$$\alpha = 0.98$$

Fig. 4.69 0.15N



$$l = 0.85 \quad \Delta = 0.04$$

$$y_1 = 7.59 - 2.04 \operatorname{ch} 1.7\alpha$$

$$y_2 = 1.38\alpha \operatorname{sh} 1.7\alpha$$

$$\alpha = 0.895$$

Fig. 4.70 0.15N

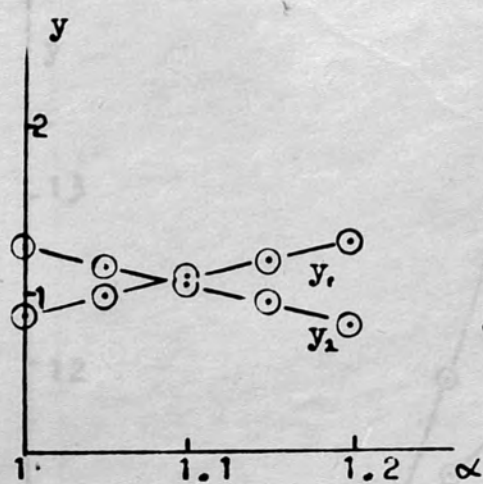


Fig. 4.71 0.33N

Method 3.7.3.

$$l = 0.3 \quad \Delta = 0.12$$

$$y_1 = 7.9 - 5.6 \operatorname{ch} 0.6\alpha$$

$$y_2 = 1.38\alpha \operatorname{sh} 0.6\alpha$$

$$\alpha = 1.09$$

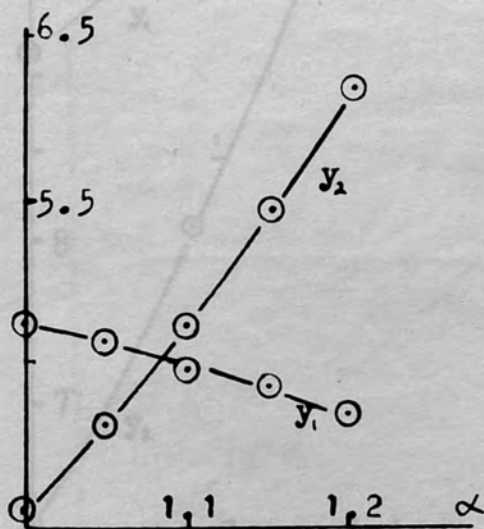


Fig. 4.72 0.33N

Method 3.7.3.

$$l = 0.85, \quad \Delta = -0.02$$

$$y_1 = 6.17 - 0.49 \operatorname{ch} 1.7\alpha$$

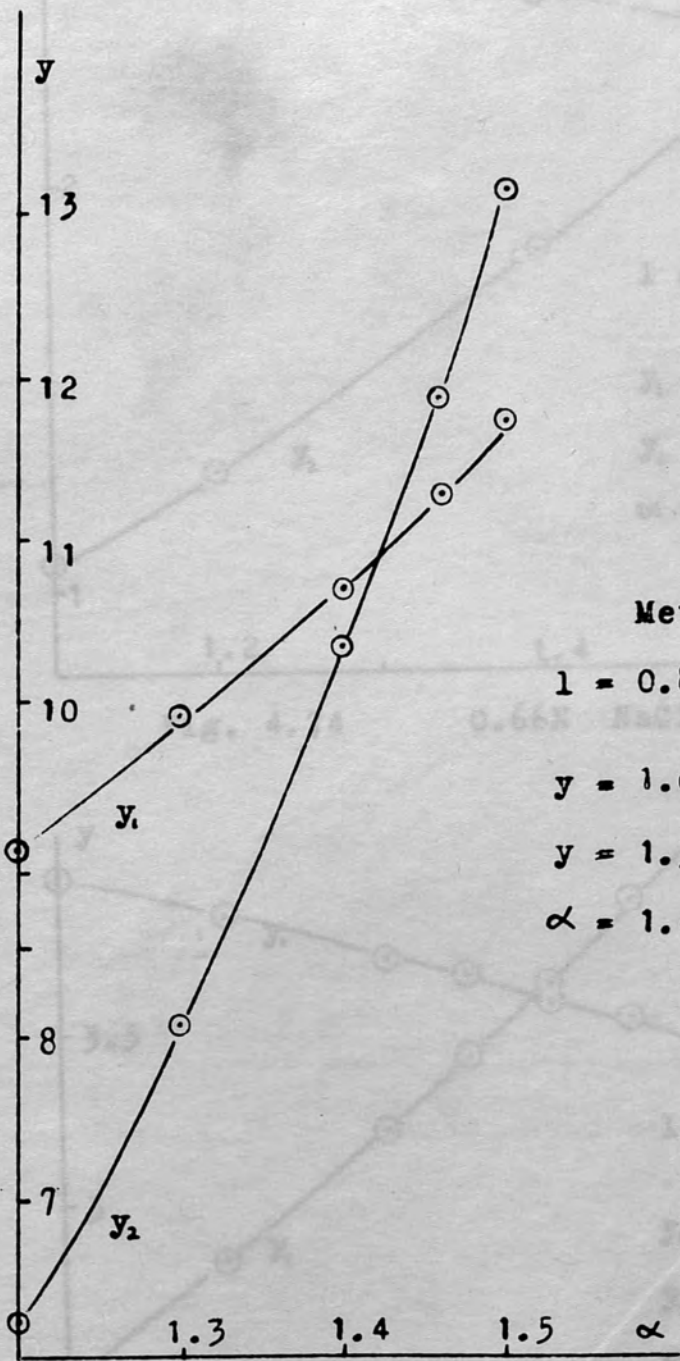
$$y_2 = 1.38\alpha \operatorname{sh} 1.7\alpha$$

$$l = 0.85, \quad \Delta = 0.01$$

$$y_1 = 6.17 - 0.49 \operatorname{ch} 1.7\alpha$$

$$y_2 = 1.38\alpha \operatorname{sh} 1.7\alpha$$

$$\alpha = 1.08$$



Method 2.7.3.
 $l = 0.3, \Delta = 0.025$
 $y = 4.35 - 1.37 \operatorname{sh} 0.6x$
 $x_1 = 1.38 = \operatorname{sh} 0.6x$
 $x = 1.38$

Method 3.7.3.
 $l = 0.85, \Delta = -0.02$
 $y = 1.04 \operatorname{ch} 1.7\alpha + 5.06$
 $y = 1.38 \alpha \operatorname{sh} 1.7\alpha$
 $\alpha = 1.43$

Fig. 4.73 0.66N

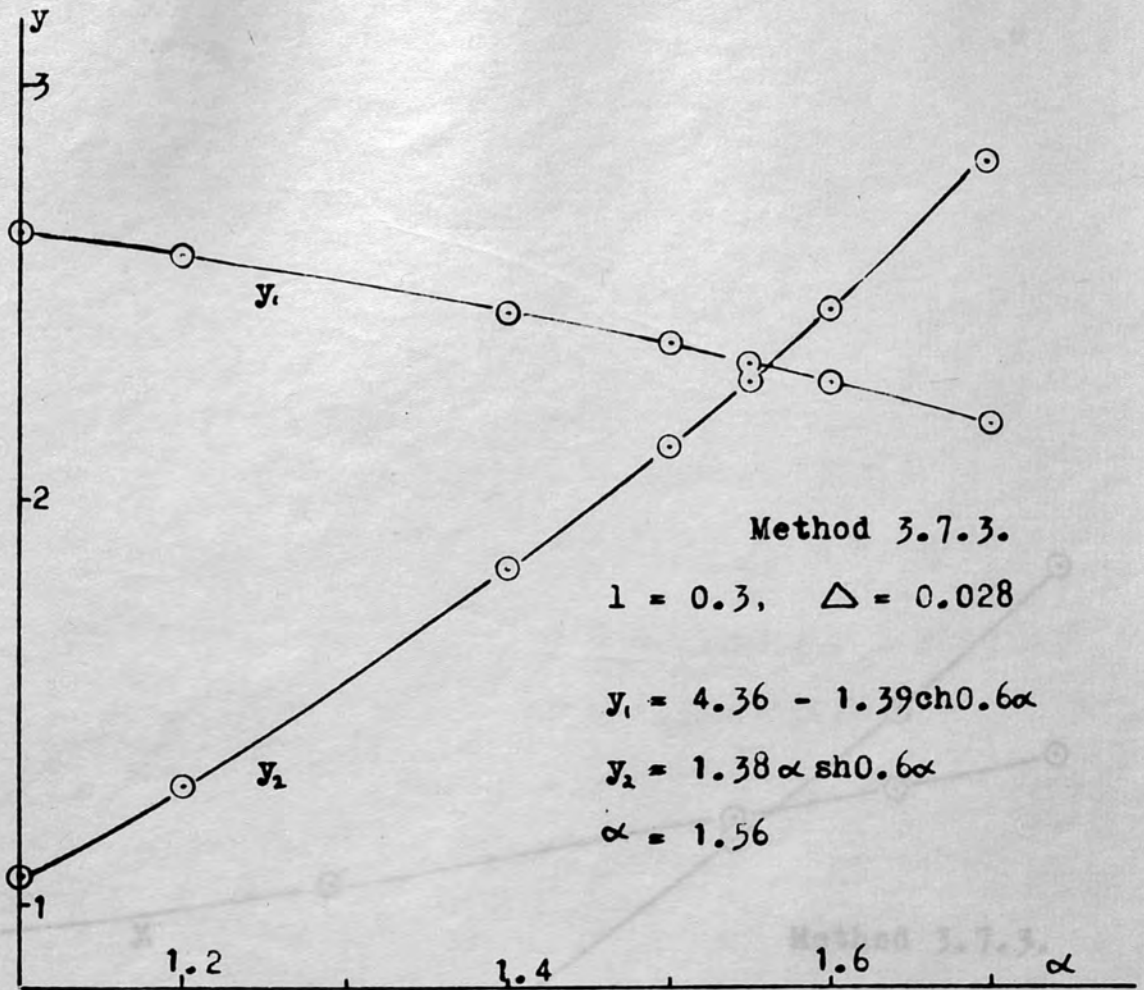


Fig. 4.74 0.66N NaCl solution.

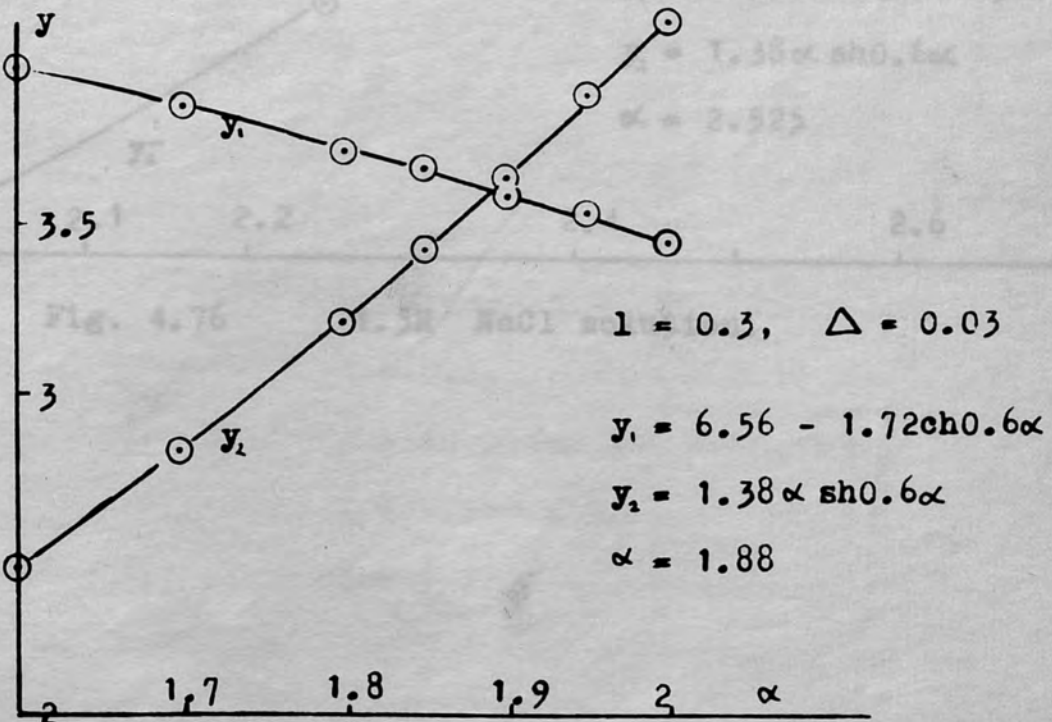


Fig. 4.75 Normal NaCl solution.

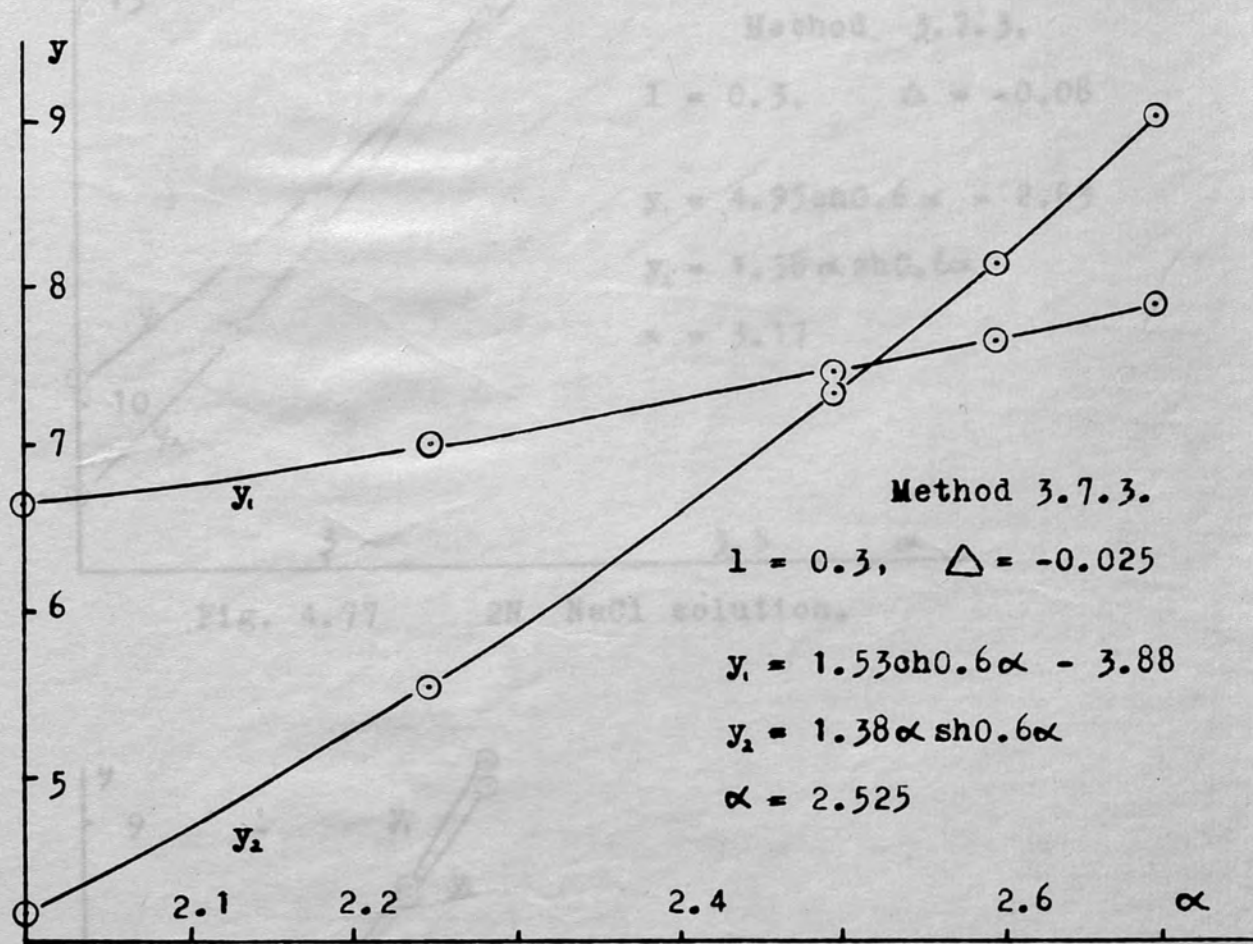


Fig. 4.76 1.5N NaCl solution.

Fig. 4.78 2N NaCl solution.

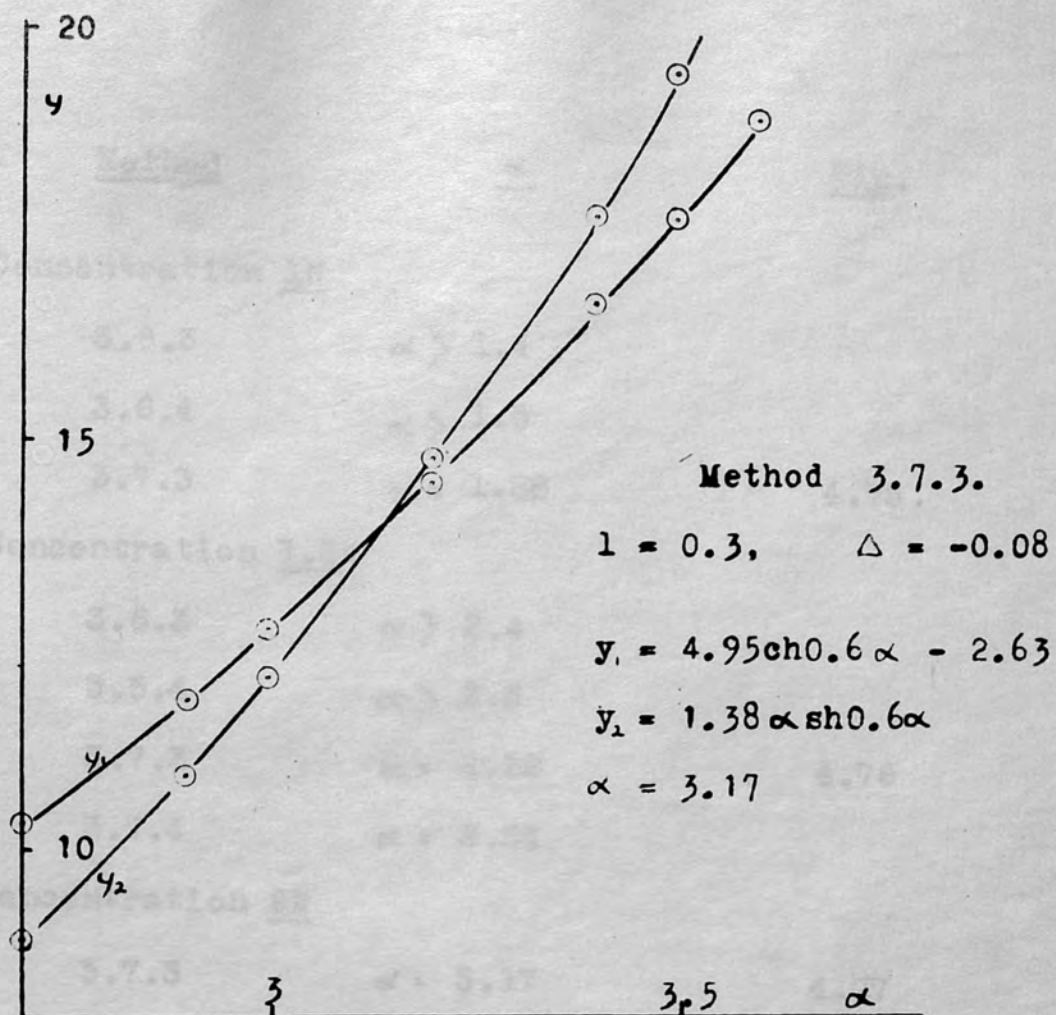


Fig. 4.77 2N NaCl solution.

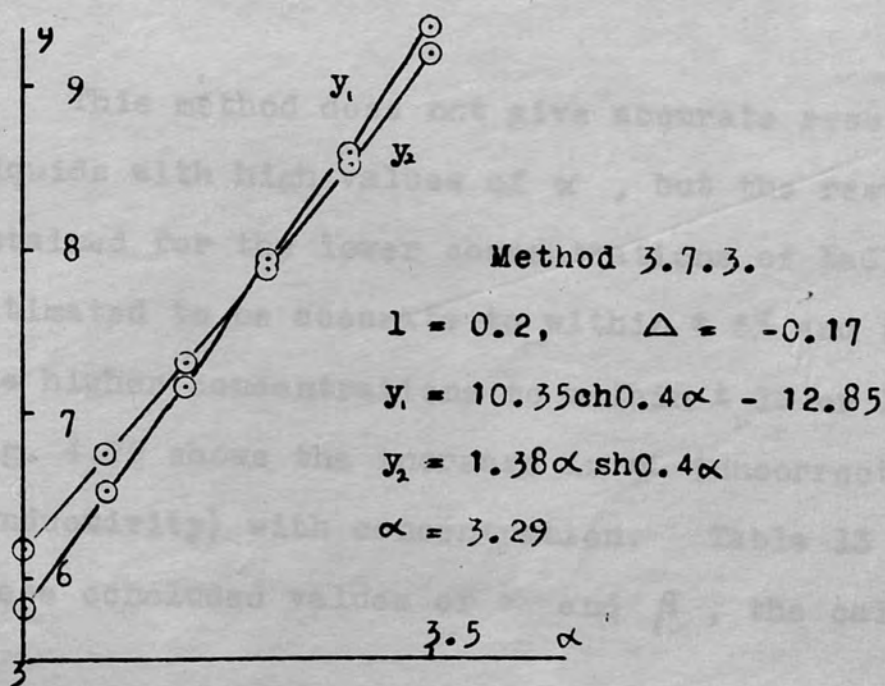


Fig. 4.78 2N NaCl solution.

<u>Method</u>	<u>α</u>	<u>Fig.</u>
Concentration <u>1N</u>		
3.6.3	$\alpha > 1.4$	
3.6.4	$\alpha > 1.5$	
3.7.3	$\alpha = 1.88$	4.75
Concentration <u>1.5N</u>		
3.6.3	$\alpha > 2.4$	
3.6.4	$\alpha > 2.3$	
3.7.3	$\alpha = 2.52$	4.76
3.7.4	$\alpha = 2.54$	
Concentration <u>2N</u>		
3.7.3	$\alpha = 3.17$	4.77
	$\alpha = 3.29$	4.78
3.7.4	$\alpha = 3.25$	

This method does not give accurate results for liquids with high values of α , but the results obtained for the lower concentrations of NaCl are estimated to be accurate to within $\pm 5\%$ and those for the higher concentrations to within ± 10 or 15% . Fig. 4.79 shows the increase in α (uncorrected for conductivity) with concentration. Table 13 gives these concluded values of α and β , the calculated

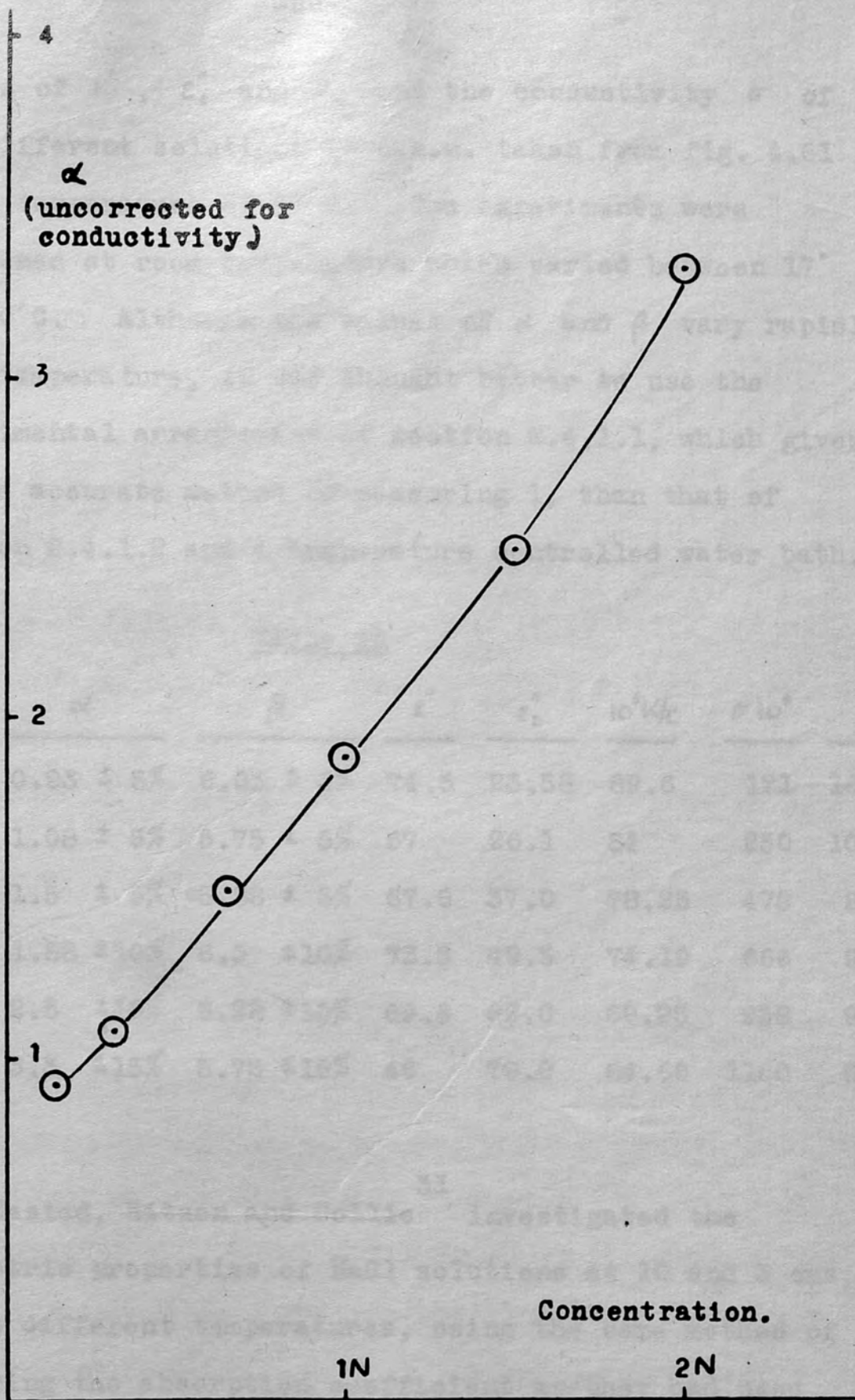


Fig. 4.79 Variation of α for NaCl solutions.

values of ϵ' , ϵ''_t and ϵ''_d and the conductivity σ of the different solutions in e.s.u. taken from fig. 4.61 for a temperature of 18°C. The experiments were performed at room temperature which varied between 17° and 20°C. Although the values of α and β vary rapidly with temperature, it was thought better to use the experimental arrangement of section 2.4.1.1, which gives a more accurate method of measuring ϵ' , than that of section 2.4.1.2 and a temperature controlled water bath.

Table 13

<u>N</u>	<u>α</u>	<u>β</u>	<u>ϵ'</u>	<u>ϵ''_t</u>	<u>$10^4 K/c$</u>	<u>$\sigma 10^9$</u>	<u>ϵ''_d</u>
0.15	0.93 ± 5%	6.03 ± 3%	74.5	23.58	89.6	121	16.27
0.33	1.08 ± 5%	5.75 ± 5%	67	26.1	84	250	10.95
0.66	1.5 ± 5%	5.88 ± 5%	67.8	37.0	78.25	475	8.2
1	1.88 ± 10%	6.3 ± 10%	73.5	49.5	74.19	666	9.5
1.5	2.5 ± 10%	6.28 ± 10%	69.6	66.0	69.25	938	9.2
2	3.3 ± 15%	5.72 ± 15%	46	79.0	64.66	1160	8.6

31

Hasted, Ritson and Collie investigated the dielectric properties of NaCl solutions at 10 and 3 cms, and at different temperatures, using the same method of measuring the absorption coefficient as they had used for water. Their results at 10 cms and 21°C are given

below.

Normalcy	Equivalent conductivity	ϵ' $\pm 3\%$	ϵ''_t $\pm 3\%$	ϵ''_d
0.5	85.6	72.8	38.28	12.6
1	78.7	67.4	60.3	13.1
1.5	73.0	61.5	78.4	12.7
2	68.6	56.2	95	11.8

33

More recently Haggis, Hasted and Buchanan have published results for a large number of different salts in solutions using the Buchanan²¹ null method at wavelengths of 1.264, 3.175 and 9.22 cms. Only one measurement on a NaCl solution at 9.22 cms was reported.

<u>Molarity</u>	<u>Conductivity</u>	<u>ϵ'</u>	<u>ϵ''_t</u>	<u>ϵ''_d</u>	<u>Temperature</u>
0.33	97	72.4	33.5	14.3	25°C

32

Saxton and Lane have also recently published results at wavelengths of 0.62, 1.24 and 3.2 cms of the dielectric properties of electrolytes including NaCl solutions using a wave guide technique similar to that of Collie et al. The method involved the observation of the attenuation in transmission through waveguides of differing cross-sectional dimensions containing the liquid. In highly absorbing liquids the

measurements of the absorption coefficient k are more accurate than those of n the real part of the refractive index, and only the variation of k with concentration is given. At the very much shorter wavelengths their results are not comparable with those obtained by the present method.

4.5 Experimental results for liquids with a high value of α and a low value of β .

4.5.1 Results for ethyl alcohol.

Table 1~~4~~ in the Appendix gives the experimental readings recorded when ethyl alcohol at a temperature of 18°C was used. These results are plotted in fig. 4.80. The tuning was very flat for liquid depths between 0.7 and 1.2 cms. Fig. 4.81 shows the variation of galvanometer signal with liquid depth. The value of β can be deduced by the method of section 3.5.2 and fig. 4.82 shows the values of l when the galvanometer readings have maxima or minima values plotted against n . Figs. 1.14 and 1.17 show the variation of Δ with l and the square of the modulus of the reflection coefficient $|K|^2$ with l calculated from equations (1.13) and (1.24) respectively for $\beta_0 = 0.69$, $\alpha = 0.7$ and $\beta = 1.86$.

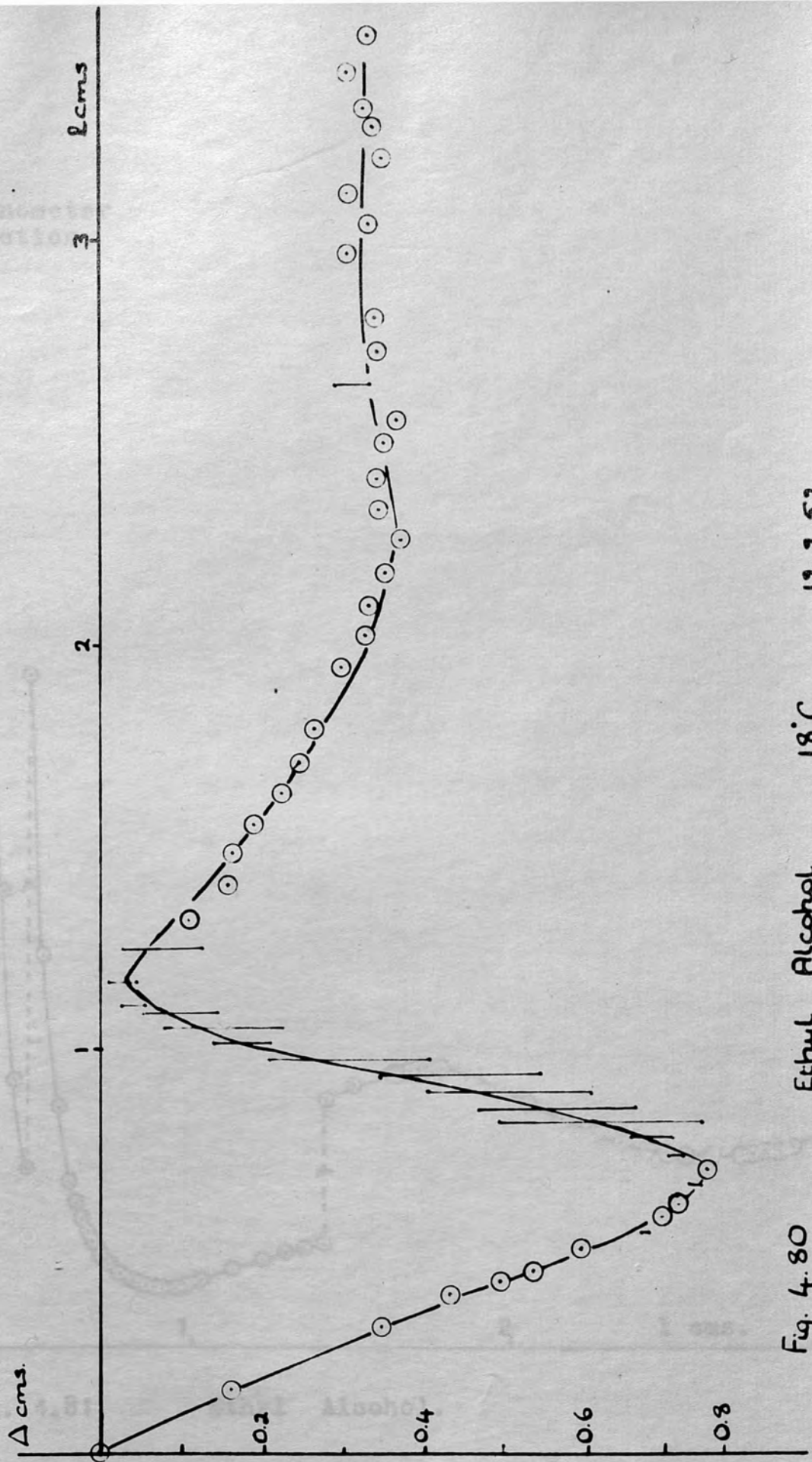


Fig. 4.80

Ethyl Alcohol

18°C

12.2.52.

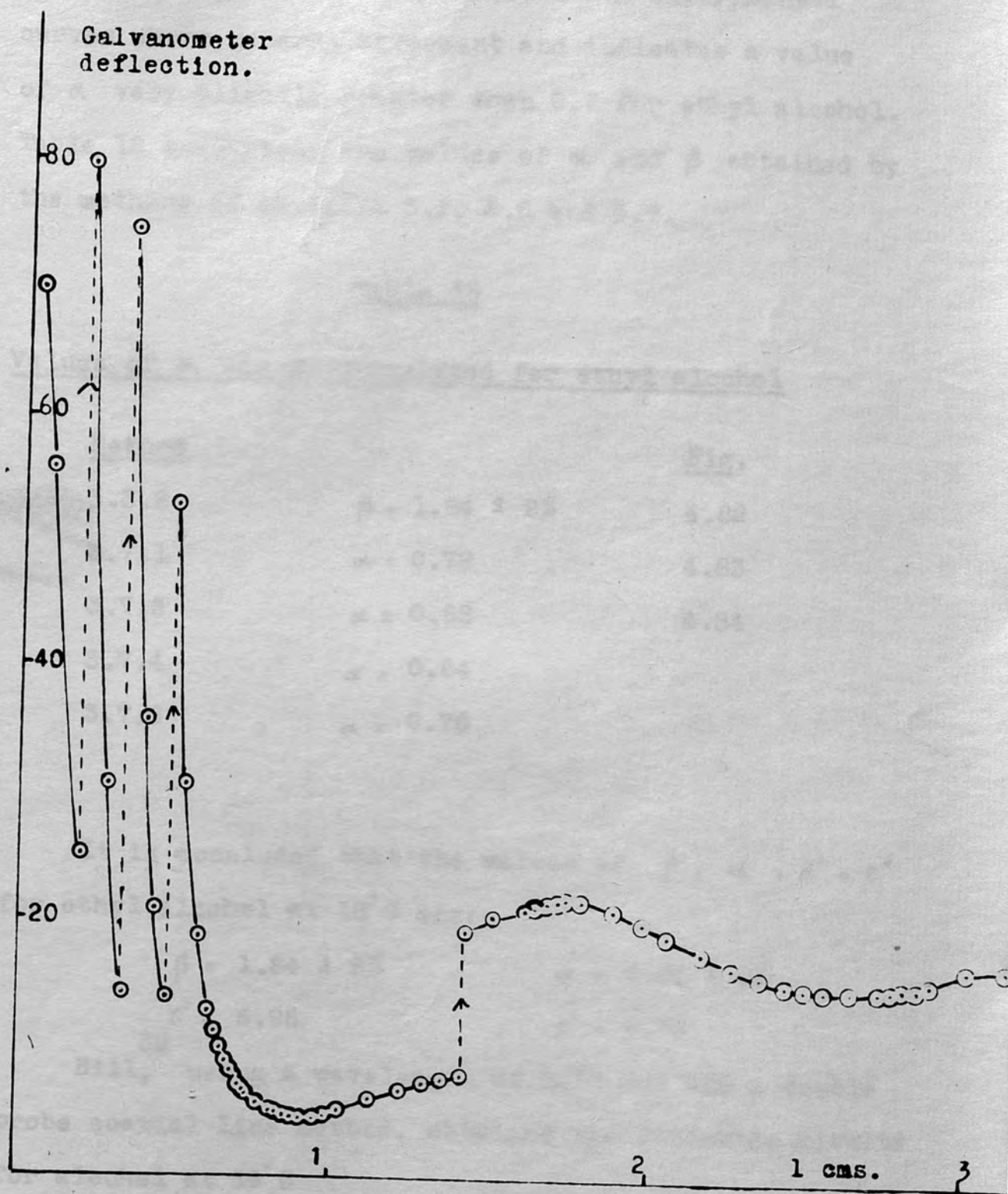


Fig. 4.81 Ethyl Alcohol.

Comparison between the theoretical and experimental curves shows general agreement and indicates a value of α very slightly greater than 0.7 for ethyl alcohol. Table 15 summarises the values of α and β obtained by the methods of sections 3.5, 3.6 and 3.7.

Table 15

Values of α and β calculated for ethyl alcohol

<u>Method</u>		<u>Fig.</u>
3.5.2	$\beta = 1.84 \pm 2\%$	4.82
3.7.1	$\alpha = 0.78$	4.83
3.7.3	$\alpha = 0.68$	4.84
3.7.4	$\alpha = 0.84$	
3.7.5	$\alpha = 0.70$	

It is concluded that the values of β , α , ϵ' & ϵ'' for ethyl alcohol at 18°C are:-

$$\beta = 1.84 \pm 2\%$$

$$\alpha = 0.74 \pm 8\%$$

$$\epsilon' = 5.95$$

$$\epsilon'' = 5.75$$

30

Hill, using a wavelength of 9.35 cms and a double probe coaxial line method, obtained the following results for alcohol at 19°C

$$\beta = 1.83 \pm 2\%$$

$$\alpha = 0.73 \pm 2\%$$

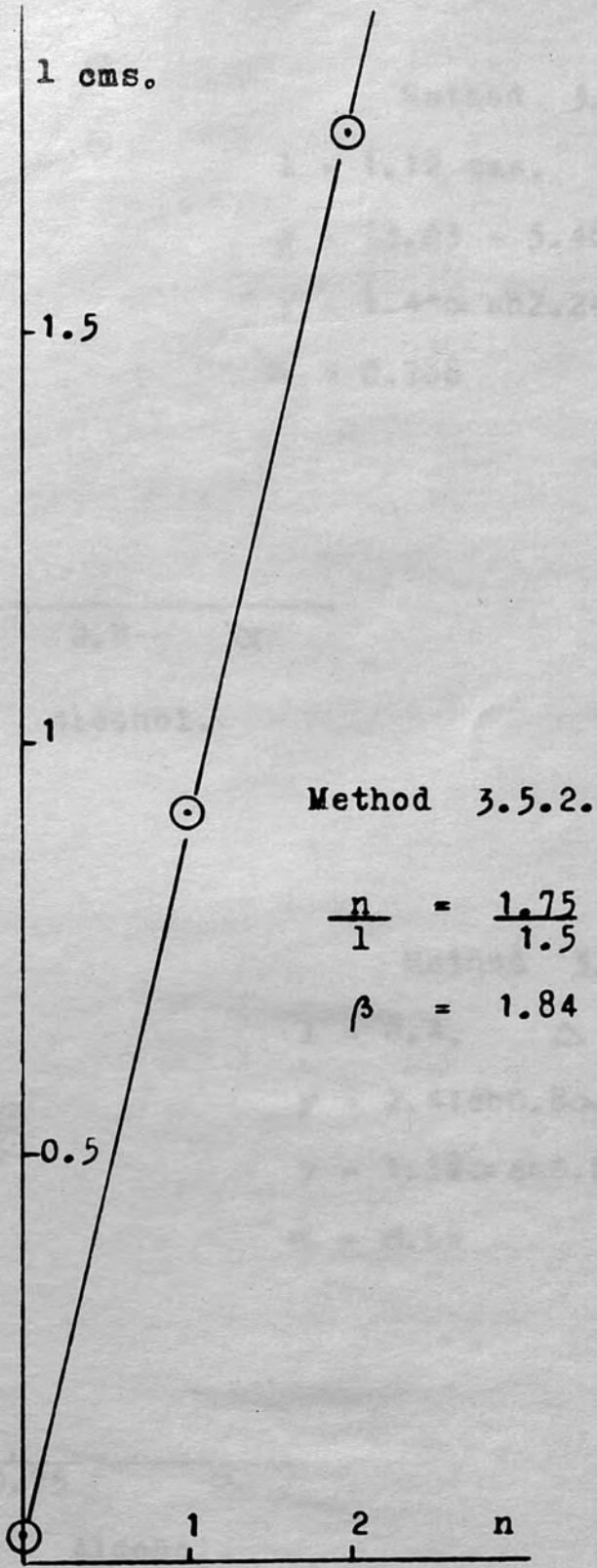
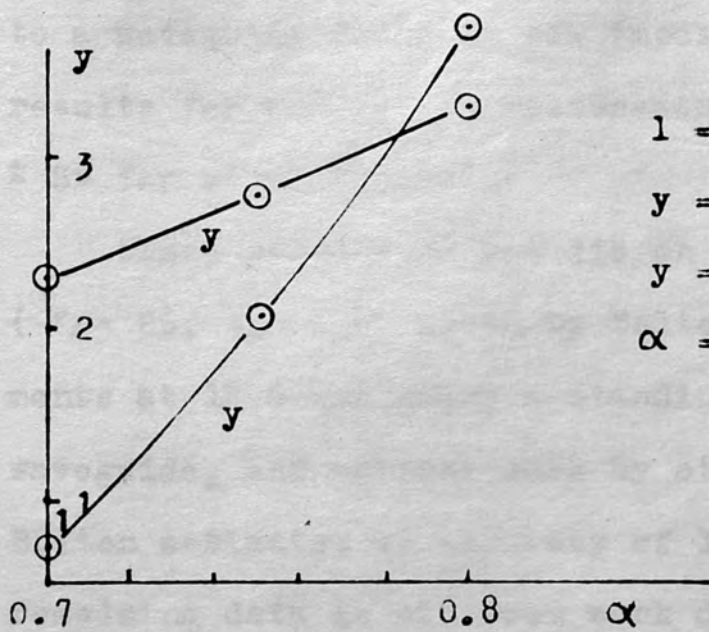


Fig. 4.82 Ethyl alcohol.



Method 3.7.1.

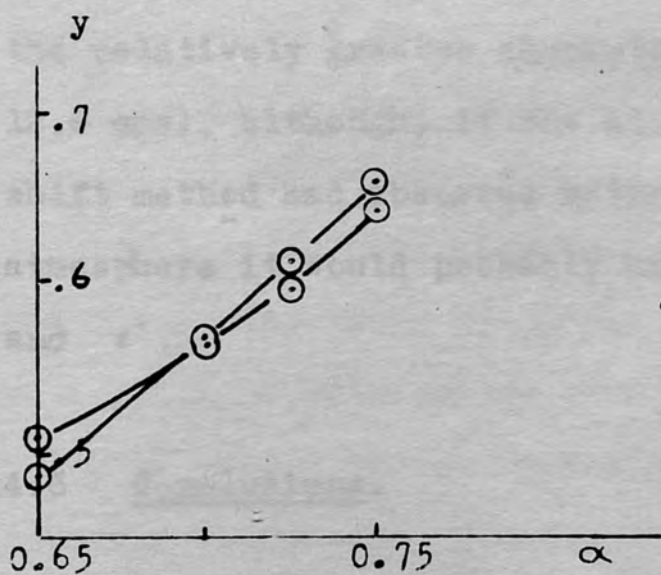
$$l = 1.12 \text{ cms.}$$

$$y = 13.03 - 5.48 \operatorname{ch} 2.24 \alpha$$

$$y = 1.44 \alpha \operatorname{sh} 2.24 \alpha$$

$$\alpha = 0.788$$

Fig. 4.83 Alcohol.



Method 3.7.3.

$$l = 0.4, \quad \Delta = -0.45$$

$$y = 2.41 \operatorname{ch} 0.8 \alpha - 2.23$$

$$y = 1.38 \alpha \operatorname{sh} 0.8 \alpha$$

$$\alpha = 0.68$$

Fig. 4.84 Alcohol.

Little²⁹ using the same method as Hill but applied to a waveguide found it was impossible to reproduce results for absorption measurements more closely than $\pm 5\%$ for ethyl alcohol.

These results do not lie on the Debye semi-circle ($\epsilon_s = 25$, $\epsilon_\infty = 1.9$) given by Bolton³⁷ from his measurements at 12.6 cms using a standing wave method in a waveguide, and earlier work by other authors. Although Bolton estimates an accuracy of 1% for his values, the remaining data is all from work done before 1940. The temperature at which the measurements were made is not stated. Bolton, however, used freshly dried and distilled ethyl alcohol, while no such precautions were taken with the present method. This might account for the relatively greater absorption ($\epsilon' = 5.5$, $\epsilon'' = 7.8$ at 12.6 cms), although, if the alcohol used in the phase shift method had absorbed water vapour from the atmosphere it would probably have increased both ϵ' and ϵ'' .

4.6 Conclusions.

In deducing values for α and β from the methods of sections 3.5, 3.6 and 3.7, it was found that the results obtained by some methods were more reliable

than those obtained by other methods. The method of section 3.7.2 for example, the value of the gradient to the experimental curve at $\tan \phi = 0$, does not give very reliable results owing to the difficulty of drawing the tangent to the curve. A slight variation in the value of $d\Delta/dl$ may easily give an insoluble quadratic equation or a value of $\cosh 2\alpha l < 1$. Again, the accuracy of the substitution method, 3.7.3, depends upon the position of the selected point, since $\tan \phi$ varies very rapidly when $\phi > 1.3$ or $\Delta > 0.9$. Substituted values of l and Δ if only very slightly out will give an insoluble equation for α . These points must be assessed in arriving at final values for α and β .

A method of dielectric measurement in the microwave region must yield values of α and β correct to at least $\pm 2\%$. This phase shift method, with the present apparatus only fulfills this requirement for liquids such as Chlorobenzene with low values of α . The higher the value of β the greater the accuracy obtainable. With Cyclohexanol, for example, the small value of β , 1.23 cms, means that the depth of liquid required before the pattern repeats is large, 5 cms, and owing to the method of measuring used at present, where the shift of the tuning cap is added to, or

subtracted from 1, any inaccuracy in 1, due to uncertainty as to when the liquid covers the short circuiting plate, increases with 1. Thus the larger value of β (5.9 cms^{-1}) for water compared with alcohol ($\beta = 1.86$) makes measurements with the 'water-type' liquids more reliable than those with the 'alcohol-type' liquids.

Chapter 5

CRITICISM OF THE METHOD

5.1 Introduction.

The apparatus and method were devised originally to test if the equation

$$\tan \phi = \frac{2\beta_0(\alpha \sinh 2\alpha l + \beta \sin 2\beta l)}{(\beta_0^2 - \alpha^2 - \beta^2) \cosh 2\alpha l - (\beta_0^2 + \alpha^2 + \beta^2) \cos 2\beta l}$$

which had been derived from theoretical considerations, did actually represent the behaviour of liquid dielectrics. The results (chapter 4) obtained for a wide variety of liquids confirmed this relationship. It was found in addition that the values of α and β derivable from the graph of the observed phase shift Δ against the liquid depth l compared well with those values obtained by other methods. This chapter discusses the use of this variation of phase shift with liquid depth for microwave absorption measurements in liquids.

5.2 A suggested modification to the apparatus and the experimental method.

For this phase shift method to be suitable for measurements of α and β a quicker experimental procedure is necessary. The present method is tedious and inaccuracies may be introduced by temperature variation and evaporation during the readings. A limitation on the accuracy obtainable with the present experimental arrangement is that the measurements of Δ and l are not independent. These difficulties could be overcome by the use of a movable short circuiting plunger in place of the fixed short circuit. Fig. 5.1 shows the suggested design.

In this new design the maximum length of the air filled portion of the line would be $3/4\lambda_0$ (6.825 cms for $\lambda_0 = 9.1$ cms) while the length of the liquid filled portion would depend upon the type of liquid it was required to use. Even for liquids with a low absorption a total length of transmission line of about 20 cms should be sufficient. The movement of the short circuiting plunger would be controlled by a micrometer on a rack and pinion. This micrometer would give the value of l . There would now be no need of a tuning cap, so that the input and output coupling loops would be

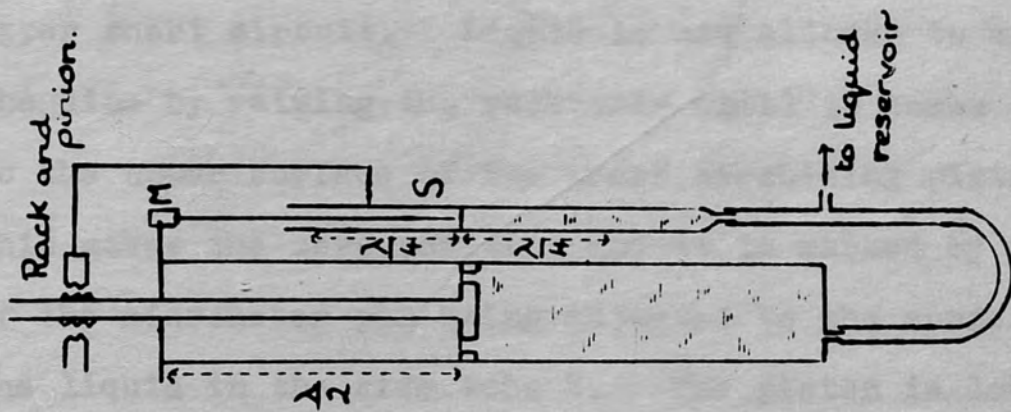


Fig. 5.1

Diagram illustrating the suggested modification to the apparatus.

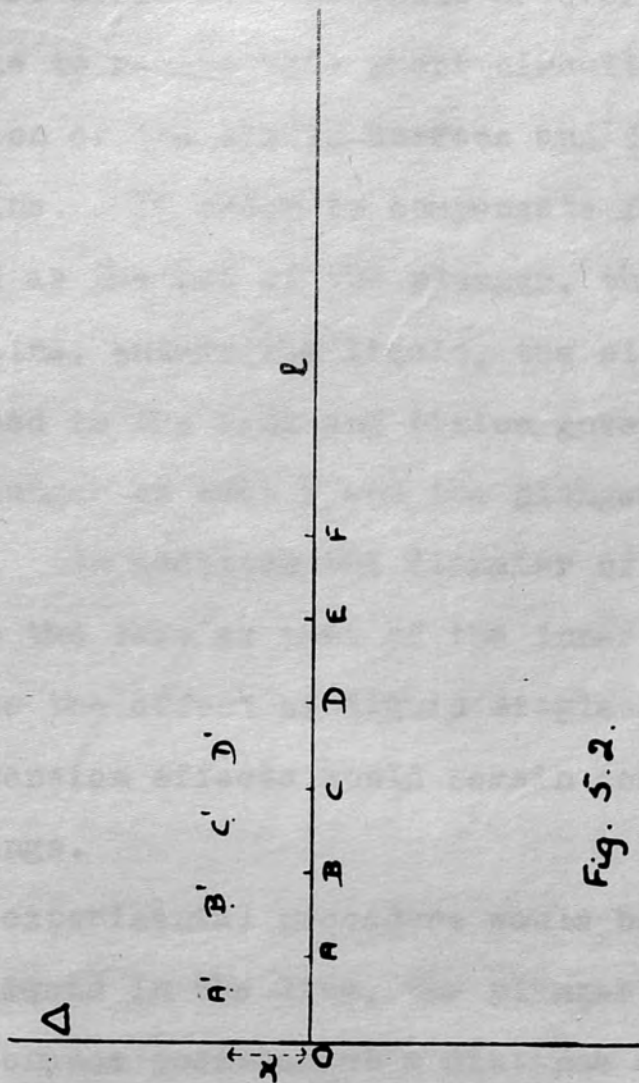


Fig. 5.2.

housed in the same way as before but attached to a fixed short circuit. It would however, be necessary to be able to remove this short circuiting cap for observation of the liquid surface and for the cleaning of the line. In order to compensate for the liquid displaced as the rod of the plunger, the inner of the coaxial line, enters the liquid, the side tube S would be attached to the rack and pinion governing the motion of the plunger so that S and the plunger would move together. In addition the diameter of the glass tube S must be the same as that of the inner. This would compensate the effect of liquid displacement. Any surface tension effects would remain constant throughout the readings.

The experimental procedure would be as follows. With no liquid in the line, the plunger is moved to the first resonance position at a distance of $\lambda_0/2$ from the upper short circuit. Liquid is now allowed to enter the line by raising the reservoir until it comes just up to the upper surface of the short circuiting piston. This gives the zero position and it is marked by means of the micrometer pin being adjusted to the surface of the liquid in the side tube S. The piston is lowered into the liquid until resonance is obtained and l is

read off from the plunger micrometer. The plunger is lowered further into the liquid, the value of l at each resonant position being recorded. These readings give the points A, B, C, ... in fig. 5.2, so that if the absorption is not too high β can be deduced. The plunger is then returned to its zero position and the depth of liquid in the line is altered, by raising or lowering the reservoir, by an amount x as measured by the micrometer pin in S. The new resonant positions are found, A', B', C', ... and marked on the graph. This process is repeated until sufficient points have been obtained to enable one of the methods of determining α to be used.

This method would enable limits between which α must lie to be quickly determined. For, after finding the positions where the phase shift is zero, the positions corresponding to $\Delta = \pm \lambda/8$, i.e. $\tan \phi = \pm \infty$, could then be plotted. The greatest value of l , for a given liquid, at which a phase angle of $\pi/2$ occurs and the least value of l when the phase angle is less than $\pi/2$ is found, and the limits between which α must lie can be calculated by the method of section 3.6.1.

This modification has not so far been adopted owing to the difficulty of producing a movable short

circuiting piston at these wavelengths. Cook, who used a simple short circuiting plunger at 10 and 6.48 cms in his measurements with water and blood, was consulted. He said that he had had no difficulties with this plunger for high loss liquids such as water, but that in his method, which was a coaxial version of Drude's 'first method', it had not been necessary to raise the plunger nearer to the liquid surface than about six centimeters. Although he had not tried making measurements with smaller liquid depths it seems likely that the plunger would not act as a complete short circuit as it approaches the surface. As the variation of $\tan \phi$ with l has reached a constant negative value for liquid depths greater than four or five centimeters for the 'water-type' liquids it does not seem that a simple plunger, making good contact with the walls of the outer conductor by means of a fringe of small phosphor bronze spring contacts, would be satisfactory for this phase shift method of measurement. It is felt that the difficulties in the design of a suitable movable piston which would act as a true short circuit in low loss liquids or very small depths of high loss liquids, would detract from the very simple apparatus required for this phase shift method of measurement.

Although this suggested modification enables the phase shift and liquid depth to be measured independently it does not overcome the difficulty of knowing the exact moment that the liquid enters the line, or covers the short circuiting piston. This means that the exact location of the origin of the Δ / l graph is in doubt. The silver or gold plating of the inner surface of the line, in addition to increasing the conductivity, should improve the at present irregular flow of liquid across the short circuit, and so minimise this source of error.

The maximum phase shift for liquids with a low absorption is $\pm \lambda_e/4$, which at the frequency investigated is ± 2.275 cms, while for the 'water' and 'alcohol-type' liquids it is $\pm \lambda_e/8$, i.e. ± 1.138 cms. Table 1 of section 1.5.4 shows that the measurement of Δ should be capable of greater accuracy at a longer wavelength.

The replacement of the galvanometer by a super-heterodyne receiver might enable measurements of the very slight variations of Δ to be made at sufficiently large liquid depths for the suggested modifications of the apparatus using a simple short circuiting plunger to be used.

It seems then that for equation (1.13) to give a method of dielectric absorption measurement yielding

values of α and β accurate to at least $\pm 2\%$, the liquids should have values of α in the range 0 to 0.5, and of β greater than 1.5, and that the modified apparatus must be used with a much more sensitive detector.

5.3 Comparison with other methods.

In chapter 10 of 'Technique of Microwave Measurements' Redheffer²⁰ summarises the many different methods used for microwave dielectric measurements. These methods may be divided into three general classes:

- (a) Transmission methods, (transmission line or free space).
- (b) Reflection methods, (transmission line or free space), including the short circuited line method.
- (c) Resonant cavity methods.

In many of these methods it is in general necessary to make use of two equations and to measure two distinct quantities, such as amplitude and phase angle, in order to calculate the two parameters, α and β , n and k , or $\tan \delta$ and σ , which give the real and imaginary parts of the dielectric constant.

In the method developed here only one quantity phase shift, is measured, and α and β are deduced from

the variation of phase shift with liquid depth. The advantages of the method are:-

- (1) The system is closed, so that there is no loss of radiation from slots, as with the travelling probe methods, and the position of the observer with respect to the line does not affect the readings.
- (2) The method is independent of any variation in the strength of the input signal; for the detector is only used to indicate when the line is resonant.
- (3) The method is independent of the crystal law for the same reason.
- (4) Only small quantities of the liquid under investigation are required. (In the present apparatus about 300 cc of the 'water-type' liquids were used, but, if necessary, this volume could be considerably reduced.
- (5) The same apparatus can be used to find α and β for all types of liquid dielectrics, although it is better for liquids with a low value of α and a large value of β .

- (6) The apparatus required is very simple.
- (7) There is no limitation ^{in principle} on the wavelength that may be used.

The disadvantages of the method are, that with the apparatus and experimental arrangement used at present:-

- (1) The experimental procedure is lengthy and the deduction of α and β tedious.
- (2) The accuracy is not greater than $\pm 2\%$ and often considerably less.

A number of methods, (Drude, Cooper, Knerr, Conner and Smyth, Abadie, Cook, Little, Ichikawa) are based on the variation in signal strength obtained at a fixed detector in a resonant line as the depth of liquid above a short circuit is varied. Values of α and β are obtained from the graph showing the variation in detector deflection against liquid depth. These methods are not independent of the detector law or, except where special precautions have been taken, of any input fluctuations. The difference between these methods and the phase shift method is that in the latter the line is adjusted to resonance between each incremental

variation of liquid depth. Although the variation of detector signal is not used for the determination of the parameters, (except for finding β for highly absorbing liquids) since no precautions have been taken to ensure a constant input or to investigate the crystal law, it is of interest to compare the curves obtained.

Abadie's method ²⁶ gives the most easily comparable curve. Fig. 5.3 shows his apparatus for liquids with normal absorption. His equation for the variation δ in signal strength at the detector is

$$\delta = C \left\{ \frac{1 + \frac{\tanh^2 \frac{2\pi kx}{\lambda} \cdot \tan^2 \frac{2\pi x}{\lambda}}{\tanh^2 \frac{2\pi kx}{\lambda} + \tan^2 \frac{2\pi x}{\lambda}}}{\dots} \right\} \dots\dots(5.1)$$

where $\delta \propto |I|^2$, $\lambda = \lambda_0/n$, $\sqrt{(z' - j\varepsilon'')} = n(1 - jk)$
 x = liquid depth and C = a constant.

Since $\frac{2\pi}{\lambda} = \beta$ and $k = \frac{\alpha}{\beta}$

this expression may be written

$$\delta = |I|^2 = \frac{C(1 + \tanh^2 \alpha x \cdot \tan^2 \beta x)}{\tanh^2 \alpha x + \tan^2 \beta x} \dots\dots(5.2)$$

$$= \frac{C(\text{ch}^2 \alpha x \cos^2 \beta x + \text{sh}^2 \alpha x \sin^2 \beta x)}{\text{sh}^2 \alpha x \cos^2 \beta x + \text{ch}^2 \alpha x \sin^2 \beta x}$$

$$= \frac{C(\cosh 2\alpha x + \cos 2\beta x)}{\cosh 2\alpha x - \cos 2\beta x} \dots\dots(5.2)$$

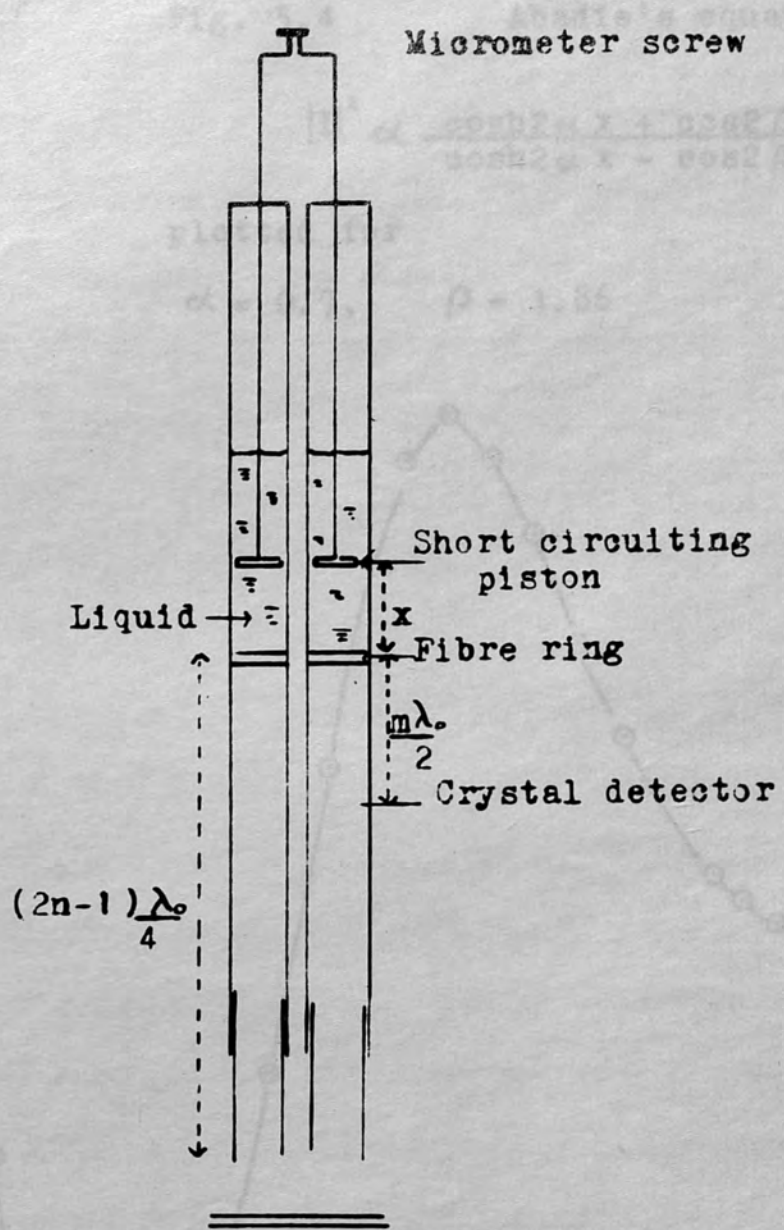
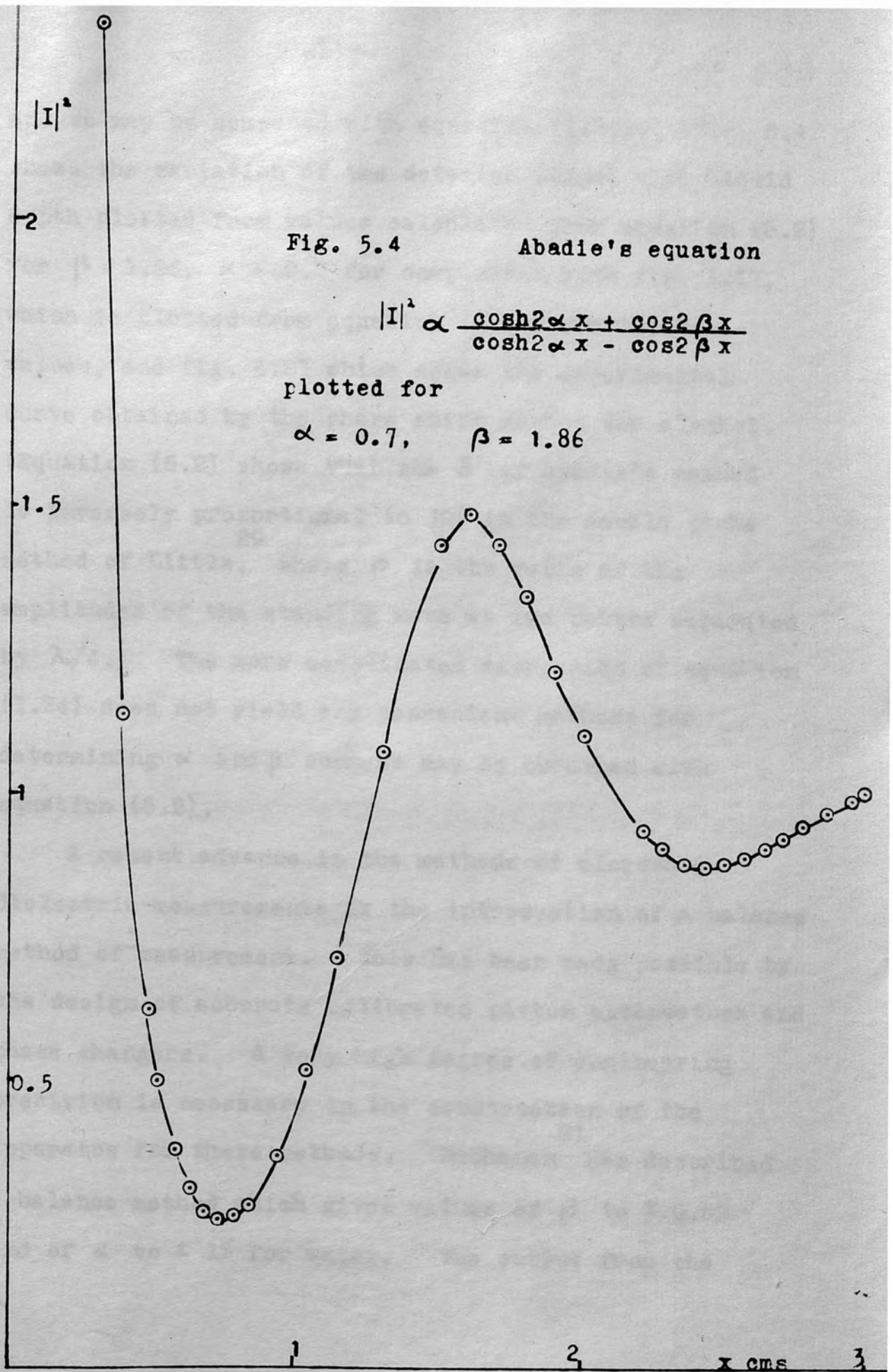


Fig. 5.3 Coaxial line used by Abadie for liquids with normal absorption.



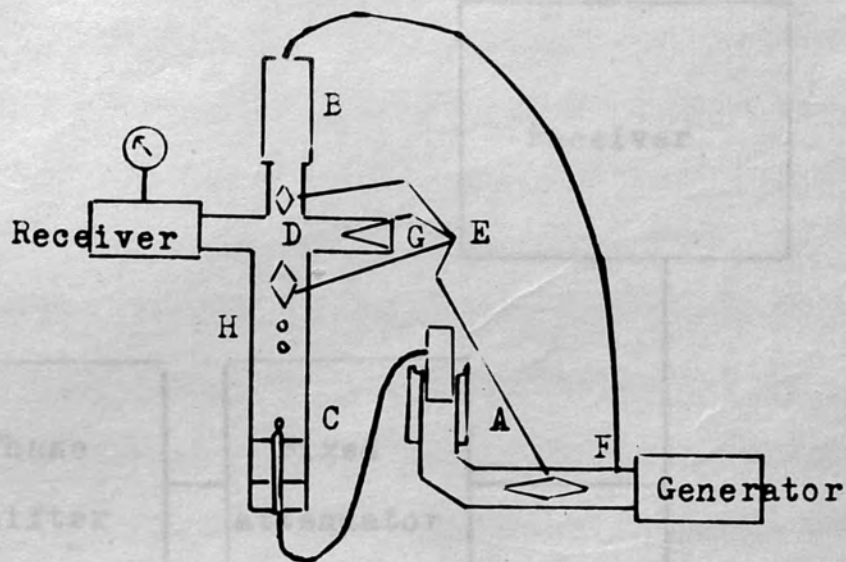
and so may be compared with equation (1.24). Fig. 5.4 shows the variation of the detector signal with liquid depth plotted from values calculated from equation (5.2) for $\beta = 1.86$, $\alpha = 0.7$ for comparison with fig. 1.17, which is plotted from equation (1.24) for the same values, and fig. 4.81 which shows the experimental curve obtained by the phase shift method for alcohol. (Equation (5.2) shows that the δ of Abadie's method is inversely proportional to $|\rho|^2$ in the double probe method of Little, where ρ is the ratio of the amplitudes of the standing wave at two points separated by $\lambda/4$.) The more complicated expression of equation (1.24) does not yield any convenient methods for determining α and β such as may be obtained with equation (5.2).

A recent advance in the methods of microwave dielectric measurements is the introduction of a balance method of measurement. This has been made possible by the design of accurate calibrated piston attenuators and phase changers. A very high degree of engineering precision is necessary in the construction of the apparatus for these methods. Buchanan has described a balance method which gives values of β to $\pm 0.5\%$ and of α to $\pm 1\%$ for water. The output from the

generator is divided, (fig. 5.5), part being transmitted through a water cell of variable length (this cell is similar to that used by Collie et al.) and a phase changer to the H arm of a hybrid tee, and the remaining part being fed through a cut-off attenuator to the E arm of the T-junction. The two outputs are combined vectorially in the hybrid T-junction and the resultant fed to a superheterodyne receiver. By manipulation of the cut-off attenuator and the phase changer the receiver output can be made zero for any liquid depth. The method can be extended so that α and β may be measured for low loss liquids and solids.

22

Branin and Smyth have described a somewhat similar null method applied to measurements either of the travelling waves set up in a dielectric filled slotted line terminated in a matched load, or the standing waves set up in a short circuited coaxial line. A block diagram of their apparatus is shown in fig. 5.6. They estimate an accuracy of $\pm 0.1\%$ for both the travelling and standing wave methods in medium and low loss dielectrics, the accuracy being somewhat less (no figure is stated) in high loss dielectrics. They give a minimum instrumental error of $\pm 0.2\%$ in ϵ' and $\pm 1.4\%$ in ϵ'' , whereas Buchanan



- A Water-cell
- B Cut-off attenuator
- C Phase-changer
- D Hybrid-tee
- E Fixed attenuators
- F Probe
- G Resistive load
- H Tuning stubs

Fig. 5.5 Diagram of Buchanan's apparatus.

Fig. 5.6 Block diagram of Brainin and Syath's Apparatus

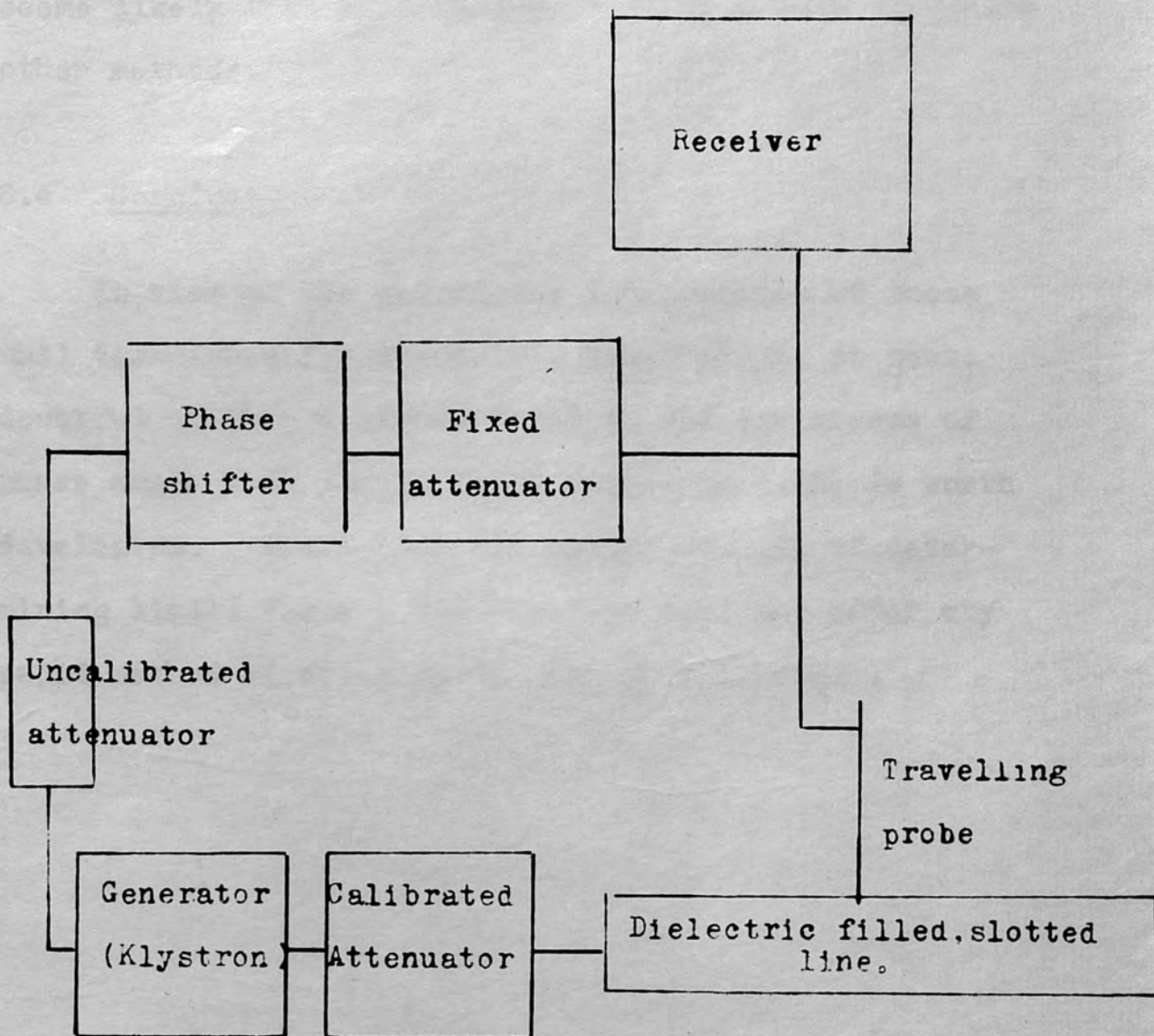


Fig. 5.6 Block diagram of Branin and Symth's apparatus.

estimates an accuracy of better than $\pm 1\%$ in both ϵ' and ϵ'' at the two wavelengths, 3.2 and 1.26 cms, so far investigated using high loss dielectrics. It seems likely that this balance technique will supercede other methods.

5.4 Conclusion.

In view of the successful introduction of these null techniques for dielectric measurement, it seems doubtful whether a method based on the variations of phase angle with liquid depth (equation 1.13) is worth developing. Apart from the method (3.6.1) of determining limits for α , the equation does not offer any rapid method of deducing α and β accurately.

APPENDIX

Typical Experimental Results

The three tables given in this Appendix show the results obtained with

- (a) a liquid with low absorption, (Table 2)
- (b) a 'water-type' liquid, (Table 10)
- (c) an 'alcohol-type' liquid, (Table 14).

Each is representative of the results obtained for other liquids of the same type.

In these tables:

Column A gives the screw setting on the rising table,
Column B the micrometer reading in inches when the stick
is in the surface of the liquid in S,

Column C the reading of the positions of the tuning cap
on resonance,

Column D the galvanometer deflection,

Column x the change in length of the line to obtain
resonance again after the addition of 1 cm
of liquid.

f indicates that the tuning was flat and the
figure given C is then an average one.

O.S. indicates that the galvanometer deflection
went off the scale.

C.I. indicates coupling between the input and output loops was increased.

C.D. indicates coupling between the input and output loops was decreased.

Table 2

Results for Chlorobenzene

Temperature $19^{\circ}\text{C} \pm 1^{\circ}\text{C}$

Date: 4th and 5th March 1952

A	B	l cms	C cms	x cms	Δ cms
	4.02	0	5.97	0	0
3	2.91	.282	5.98	.01	-.292
4	2.66	.345	6.00	.03	-.375
0	2.29	.44	6.03	.06	-.5
1	C.I. 2.01	.51	6.08	.11	-.62
2	1.80	.564	6.11	.14	-.704
3	1.49	.644	6.22	.25	-.894
3.5		.688	6.255	.285	-.973
4	C.I. 1.14	.733	6.34	.37	-1.103
4.5		.774	6.46	.49	-1.264
0	.80	.816	6.575	.605	-1.421
0.5		.853	6.69	.72	-1.573
1	.50	.89	6.80	.83	-1.72
	4.65 ^o		2.25*		
1.5		.915	2.34	.92	-1.835
2	4.44	.945	2.475	1.055	-2

^oThe micrometer had come to the end of its thread so the stick was shortened and the micrometer reset.

* This represents a shift of $\lambda/2$, $\frac{4.55}{2.295}$ cms, to an adjacent maximum.

Results for chlorobenzene continued

A	B	l cms	C cms	x cms	Δ cms
2.5		1.979	2.60	1.18	-2.159
3	4.145	1.018	2.80	1.38	-2.398 or +2.152 [†]
3.25		1.038	2.90	1.48	-2.518 or 2.032
3.5		1.059	2.975	1.555	-2.614 or 1.936
3.75		1.079	3.10	1.68	-2.759 or 1.791
4	3.83	1.1	3.19	1.77	-2.87 or 1.68
4.25		1.12	3.30	1.88	-3 or 1.55
4.5		1.14	3.35	1.93	-3.07 or 1.48
4.75		1.16	3.44	2.02	-3.18 or 1.37
0	3.51	1.18	3.50	2.08	-3.26 or 1.29
0.5		1.215	3.59	2.17	-3.385 or 1.165
1	3.23	1.25	3.675	2.255	-3.505 or 1.045
2	2.985	1.31	3.77	2.35	-3.66 or .89
3	2.69	1.385	3.875	2.455	-3.84 or .71
4	2.35	1.475	3.94	2.52	-3.995 or .555
0	2.015	1.56	3.99	2.57	-4.13 or .42
1	1.735	1.65	3.99	2.57	-4.22 or .33
2	1.50	1.69	4.01	2.59	-4.28 or .27
3	1.20	1.77	4.01	2.59	-4.36 or .19
4	.86	1.85	4.01	2.59	-4.44 or .11
0	.53	1.91	4.00	2.58	-4.49 or .06
0.5		1.97	4.00	2.58	-4.55 or 0
1	.25°	2	3.99	2.57	-4.57 or -.02
	4.47				
3	3.94	2.134	3.99	2.57	-4.704 or -.145
0	3.28	2.302	4.00	2.58	-4.882 or -.332
2	2.77	2.435	4.055	2.635	-5.07 or -.52
3	2.45	2.514	4.1	2.68	-5.194 or -.644
3.5		2.558	4.11	2.69	-5.248 or -.698
4	2.10	2.602	4.15	2.73	-5.332 or -.782
4.5		2.641	4.20	2.78	-5.421 or -.871
0	1.79	2.68	4.22f	2.8	-5.48 or -.93
0.5		2.712	4.28to	2.86to	-5.572 or -1.022to
			4.32	2.90	-5.612 or -1.062

[†] $\Delta = -2.398$ is a shift of more than $\lambda/4$, (2.275 cms) and it was decided in section (1.4) to confine the variations of Δ to between plus and minus $\lambda/4$ which corresponds to the phase angle ϕ varying between plus and minus π .

Results for chlorobenzene continued

A	B	l cms	C cms	x cms	Δ cms
1	1.54	2.745	4.25to 4.35	2.83to 2.93	-5.575 or -1.025to -5.675 or -1.125
1.5		2.775	4.35f	2.93	-5.705 or -1.155
2	1.30	2.805	4.35to 4.4	2.93to 2.98	-5.735 or -1.185to -5.785 or -1.235
2.25		2.825	4.38to 4.55	2.96to 3.13	-5.785 or -1.235to -5.955 or -1.405
2.5		2.845	4.45to 4.6	3.03to 3.18	-5.875 or -1.335to -6.025 or -1.475
2.75		2.866	4.55to 4.7	3.12to 3.28	-5.986 or -1.436to -6.146 or -1.596
3	.98	2.886	4.55to 4.8	3.12to 3.38	-6.0 ⁰ 6 or -1.456to -6.266 or -1.716
3.25		2.908	4.65to 4.85	3.23to 3.43	-6.138 or -1.588to -6.338 or -1.788
3.5		2.93	4.85to 5.1	3.43to 3.68	-6.36 or -1.81to -6.61 or -2.06
3.75		2.953	5.1to 5.4	3.68to 3.98	-6.633 or -2.083to -6.933 or 2.167
4	.64	2.975	5.3to 5.5	3.88to 4.08	-6.858 or 2.252to -7.055 or 2.045
4.5		3.01	5.7to 5.8	4.28to 4.38	-7.29 or 1.81to -7.39 or 1.71
0	.33° 4.62	3.05	6 to 6.2	.03to .23	-3.08 or 1.47to -3.28 or 1.27
0.5		3.084	1.6f	.18	-3.264 or 1.286
1	4.35	3.118	1.75	.33	-3.448 or 1.102
2	4.10	3.182	1.85f	.43	-3.612 or .938
3	3.78	3.254	1.95	.53	-3.784 or .766
4	3.43	3.36	2.02to 2.05	.6 to .63	-3.96 or .59 to -3.99 or .66
0	3.11	3.43	2.10	.68	-4.11 or .44
1	2.86	3.496	2.09	.67	-4.166 or .384
2	2.60	3.562	2.10	.68	-4.242 or .308
3	2.275	3.644	2.10	.68	-4.324 or .226
4	1.91	3.737	2.10	.68	-4.417 or .133
0	1.62	3.81	2.10	.68	-4.49 or .06
1	1.38	3.87	2.09	.67	-4.54 or .01
1.5		3.903			
2	1.12	3.937	2.08	.66	-4.597 or -.047
3	.80	4.02	2.06	.64	-4.66 or -.11
4	.455	4.11	2.04	.62	-4.73 or -.18

Results for chlorobenzene continued

A	B	l cms	C cms	x cms	Δ cms
0	.15° 4.385	4.21	2.05	.63	-4.84 or -.29
1	4.12	4.277	2.02	.60	-4.877 or -.327
2	3.88	4.338	2.04	.62	-4.958 or -.408
3	3.56	4.42	2.01	.59	-5.01 or -.46
3.5		4.461	2.04f	.62	-5.081 or -.531
4	3.23	4.502	2.03	.61	-5.112 or -.562
4.5		4.534	2.05	.63	-5.164 or -.614
0	2.97	4.566	2.0 to 2.05	.58 to .63	-5.146 or -.596to -5.196 or -.646
0.5		4.599	1.96to 2.04	.54 to .62	-5.139 or -.589to -5.219 or -.669
1	2.72	4.633	2.0f	.58	-5.213 or -.663
1.5		4.667	2.0 to 1.95	.58 to .53	-5.247 or -.697to -5.197 or -.647
2	2.45	4.701	1.95f	.53	-5.231 or -.681
2.5		4.74	1.93f	.51	-5.25 or -.70
3	2.13	4.78	2.0 to 1.75	.58 to .33	-5.36 or -.81 to -5.11 or -.56
3.5		4.826	1.95to 1.7	.53 to .28	-5.356 or -.806to -5.106 or -.556
4	1.77	4.873	1.8 to 1.3	.38 to -.12	-5.253 or -.703to -4.753 or -.203
4.5		4.909	5.55to 5.8	-.42 to -.17	-4.489 or .061to -4.732 or -.189
0	1.485	4.946	5.3 to 5.8	-.67 to -.17	-4.276 or .274to -4.776 or -.226
0.5		4.976	5.0 to 5.25	-.97 to -.72	-4.006 or .544to -4.256 or .294
1	1.235	5.006	5.0f	-.97	-4.036 or .514f
2	.96	5.08	5.0 to 4.85	-.97 to -1.12	-4.11 or .44 to -3.96 or .59
3	.635	5.157	4.85f	-1.12	-4.037 or .513f

5.3.52 A little liquid evaporated overnight, so the rising table was raised until the pin was again in the surface of the liquid.

4.5	.635		4.9		
0.5	.37° 4.46	5.23	4.85	-1.12	-4.11 or .44

Results for chlorobenzene continued

A	B	l cms	C cms	x cms	Δ cms
1.5	4.225	5.289	4.85	-1.12	-4.169 or .381
2.5	3.925	5.366	4.85	-1.12	-4.246 or .306
3.5	3.565	5.458	4.85	-1.12	-4.338 or .212
0.5	2.995	5.602	4.79	-1.18	-4.422 or .128
1.5	2.75	5.664	4.75 to 4.8	-1.22 to -1.17	-4.444 or .106to -4.494 or .056
2.5	2.45	5.743	4.75	-1.22	-4.523 or .027
3.5	2.10	5.829	4.725	-1.245	-4.584 or -.03
4.5	1.78	5.91	4.70	-1.27	-4.63 or -.08
0.5	1.51	5.978	4.67	-1.3	-4.678 or -.128
2.5	.96	6.12	4.63	-1.34	-4.78 or -.23
4.5	.335° 4.77	6.276	4.55	-1.42	-4.856 or -.306
1.5	4.26	6.405	4.50	-1.47	-4.935 or -.385
2.5	3.95	6.484	4.50	-1.47	-5.014 or -.464
3.5	3.60	6.573	4.3 to 4.4	-1.67 to -1.57	-4.903 or -.353to -5.003 or -.453
4.5	3.30	6.649	4.25 to 4.3	-1.72 to -1.67	-4.929 or -.379to -4.979 or -.329
0.5	3.055	6.711	4.05 to 4.25	-1.92 to -1.72	-4.971 or -.241to -4.991 or -.441
1.5	2.805	6.774	3.95 to 4.1	-2.02 to -1.87	-4.754 or -.204to -4.904 or -.354
2.5	2.465	6.862	3.6 to 3.8	-2.37 to -2.17	-4.492 or .058to -4.692 or -.142
3.5	2.14	6.943	3.45 to 3.55	-2.52 to -2.42	-4.423 or .127to -4.523 or .027
4		6.976	3.45 to 3.35	-2.52 to -2.62	-4.456 or .094to -4.356 or .194
4.5	1.88	7.01	3.35 to 3.3	-2.62 to -2.67	-4.39 or .16 to -4.34 .21
0		7.039	3.25	-2.72	-4.319 or .231
0.5	1.65	7.068	3.25	-2.72	-4.348 or .202
1.5	1.395	7.131	3.19	-2.78	-4.351 or .199
3.5	.71	7.306	3.04	-2.93	-4.376 or .174
4.5	.42	7.386	2.97	-3.0	-4.386 or .164
0.5	.18° 4.80	7.436	2.95	-3.02	-4.416 or .134
2.5	4.21	7.586	2.85	-3.12	-4.466 or .084
3.5	3.87	7.672	2.85	-3.12	-4.552 or -.002
4.5	3.59	7.743	2.78	-3.19	-4.553 or -.003
0.5	3.35	7.804	2.76	-3.21	-4.594 or -.044

Results for chlorobenzene continued

A	B	l cms	C cms	x cms	Δ cms
1		7.838	2.76	-3.21	-4.628 or -.078
1.5	3.08	7.873	2.75	-3.22	-4.653 or -.103
3.5	2.41	8.043	2.65	-3.32	-4.723 or -.173
4.5	2.12	8.116	2.61	-3.36	-4.756 or -.206
0.5	1.89	8.172	2.60 to	-3.37 to	-4.802 or -.252 to
			2.55	-3.42	-4.752 or -.202
1.5	1.62	8.242	2.55	-3.42	-4.822 or -.272
2.5	1.30	8.323	2.50	-3.47	-4.853 or -.303
3.5	.97	8.407	2.40	-3.57	-4.837 or -.287
4.5	.69	8.476	2.37	-3.6	-4.876 or -.326
0.5	.42	8.546	2.30	-3.67	-4.876 or -.326
1.5	.14°	8.616	2.15 to	-3.82 to	-4.796 or -.246 to
	4.98		2.25	-3.72	-4.896 or -.346
2.5	4.64	8.702	1.95 to	-4.02 to	-4.682 or -.132 to
			2.05	-3.92	-4.782 or -.232
3.5	4.35	8.776	1.80 to	-4.17 to	-4.606 or -.056 to
			1.75	-4.22	-4.556 or -.006
4.5	4.08	8.844	1.70 to	-4.27 to	-4.574 or -.024 to
			1.75	-4.22	-4.524 or .026
0		8.879			
0.5	3.81	8.914	1.60 to	-4.37 to	-4.544 or .006 to
			1.55	-4.42	-4.494 or .056
1.5	3.525	8.985	1.45 to	-4.52 to	-4.465 or .085 to
			1.55	-4.42	-4.565 or -.015
3.5	2.92	9.139	1.20 to	-4.77 to	-4.369 or .181 to
			1.3	-4.67	-4.469 or .081
4.5	2.645	9.209	5.8	-.17	9.039 or .061
0.5	2.31	9.292	5.7	-.27	9.022 or .078
2.5	1.76	9.434	5.6	-.37	9.064 or .036
3.5	1.49	9.501	5.5	-.47	9.031 or .059
4.5	1.18	9.582	5.5	-.47	9.112 or -.012
0.5	.93	9.646	5.45	-.52	9.126 or -.026
1.5	.61	9.726	5.40	-.57	9.156 or -.056
2.5	.33	9.796	5.35	-.62	9.176 or -.076
3.5	.02°	9.876	5.30	-.67	9.206 or -.106
	4.84				
0.5	4.27	10.021	5.25	-.72	9.301 or -.201
2.5	3.68	10.17	5.15	-.82	9.35 or -.25
0	2.985	10.346	4.95 to	-1.02 to	9.326 or -.226 to
			5.0	-.97	9.376 or -.276
1	2.73	10.411	4.9	-1.07	9.341 or -.241
3	2.125	10.562	4.7	-1.27	9.292 or -.192

Results for chlorobenzene continued

A	B	l cms	C cms	x cms	Δ cms
0	1.59	10.701	4.4	-1.57	9.131 or -.031
1	1.325	10.766	4.4	-1.57	9.196 or -.096
2		10.8	4.2	-1.77	9.03 or .07
2.5	.89	10.876	4.2 to	-1.77 to	9.106 or -.006to
			4.15	-1.82	9.056 or .044
3.5	.49°	10.982	4.05 to	-1.92 to	9.062 or .038to
	4.65		4.15	-1.82	9.162 or -.062
4.5	4.42	11.04	3.95	-2.02	9.02 or .08
0.5	4.125	11.115	3.9	-2.07	9.045 or .055
1.5	3.73	11.215	3.85	-2.12	9.095 or .005
2.5	3.47	11.282	3.78	-2.21	9.072 or .028
3.5	3.21	11.346	3.70	-2.27	9.076 or .024
4.5	2.87	11.435	3.67	-2.3	9.135 or -.035
0.5	2.65	11.489	3.625	-2.345	9.144 or -.044
1.5	2.24	11.594	3.55	-2.42	9.174 or -.074
2.5	1.99	11.657	3.45	-2.52	9.137 or -.037
3.5	1.71	11.727	3.42	-2.55	9.177 or -.077
4		11.767			
4.5	1.40	11.807	3.40	-2.57	9.237 or -.137
0.5	1.125	11.878	3.35	-2.62	9.258 or -.158
1.5	.76	11.970	3.27	-2.70	9.27 or -.17
2.5	.47	12.042	3.23	-2.74	9.302 or -.202

Table 10Results for Ringer Tyrode physiological saline, (0.15N)

Temperature 21.2' - 20°C

Date: 18th February 1953

A	B	l cms	C cms	Δ cms	D cms
3.5	4.66	0	6.01	0	39
3.6		0.008	6.01	-0.018	46
3.7		0.016	6.015	-0.021	46
3.8		0.024	6.02	-0.044	42
3.9		0.032	6.025	-0.057	41
4	4.50	0.041	6.03	-0.071	41
4.1		0.048	6.03	-0.077	37
4.2		0.055	6.03	-0.084	34
4.3		0.062	6.03	-0.091	32
4.4		0.069	6.03	-0.098	27
4.5	4.36	0.076	6.035	-0.111	23.5
4.75		0.092	6.045	-0.137	14.5
0	4.20	0.117	6.055	-0.172	8.5
.25		0.136	6.075	-0.211	4 CI 80
.5		0.154	6.10	-0.254	38
.6		0.162	6.11	-0.272	27.5
.7		0.169	6.12	-0.289	20
.8		0.176	6.12	-0.296	13
.9		0.184	6.15	-0.334	9.4
1	3.91	0.191	6.17	-0.361	6 CI 24
1.1		0.198	6.15	-0.348	21
1.2		0.205	6.15	-0.355	14.5
1.3		0.212	6.15	-0.362	10
1.4		0.219	6.10 to 6.06	-0.309 to -0.279	7
1.5		0.227	6.07f	-0.297	5.25
1.6		0.234	6.01 to 5.96	-0.244 to -0.194	4
1.7		0.241	5.88f	-0.121	3.5
1.8		0.248	5.825to 5.80	-0.073 to -0.048	3.3
1.9		0.255	5.70	0.045	3.5
2	3.63	0.262	5.70 to 5.65	0.038 to 0.088	3.6
2.25		0.280	5.53	0.190	4.9

Results for Ringer Tyrode physiological saline continued

A	B	l cms	C	Δ cms	D cms
2.5		0.298	5.49	0.213	8.5
2.75		0.315	5.495	0.190	13.4
3	3.35	0.333	5.5	0.167	19.5
3.25		0.343	5.5	0.157	27
3.5		0.374	5.5	0.129	36.5
3.75		0.391	5.5	0.109	47.5
4	3.045	0.41	5.5	0.09	59.5
4.25		0.430	5.5	0.071	72
4.5		0.449	5.5	0.051	86.5
4.75		0.468	5.495	0.037	OS CD 46
0	2.74	0.488	5.5	0.012	49.5
0.25		0.506	5.5	-0.006	53
0.5		0.525	5.5	-0.025	54
0.75		0.543	5.5	-0.043	54
1	2.45	0.561	5.494	-0.056	51.5
1.25		0.58	5.5	-0.08	47
1.5		0.599	5.49	-0.089	42
1.75		0.618	5.49	-0.108	36.5
2	2.155	0.637	5.47	-0.107	29.5
2.25		0.654	5.47	-0.124	23.8
2.5		0.672	5.47	-0.142	18.4
2.75		0.689	5.465	-0.154	13.4
3	1.875	0.706	5.44	-0.146	10.1
3.25		0.726	5.40	-0.126	7.7
3.5		0.747	5.35	-0.097	5.9
3.75		0.767	5.34 to	-0.157 to	5.2
			5.30	-0.057	
4	1.56	0.787	5.28 to	-0.067 to	4.7
			5.24	-0.027	
4.25		0.807	5.21	-0.017	5
4.5		0.828	5.13	0.043	5.6
4.75		0.848	5.11	0.042	6.8
0	1.24	0.868	5.10	0.032	8
.25		0.884	5.10	0.016	9.7
.5		0.900	5.07	0.03	12
.75		0.916	5.065	0.019	14.2
1	0.985	0.932	5.055	0.013	16.1
1.25		0.953	5.04	0.007	18.5
1.5		0.974	5.02	0.006	20.5
1.75		0.995	5.00	0.005	22
2	0.66	1.016	4.99	-0.008	23.3
2.25		1.037	4.98	-0.017	24
2.5		1.059	4.98	-0.039	24.25

Results for Ringer Tyrode physiological saline continued

A	B	l cms	C	Δ cms	D cms
2.75		1.080	4.975	-0.055	23.8
3	0.32	1.101	4.97	-0.071	23
3.25		1.118	4.945	-0.063	20.4
3.5		1.135	4.95	-0.085	19
3.75		1.152	4.94 to	-0.092 to	17.6
			4.92	-0.072	
4	0.6-	1.169	4.90	-0.069	16.2
	4.60				
4.25		1.185	4.90	-0.085	14.6
4.5		1.201	4.895	-0.096	13
4.75		1.217	4.88	-0.097	11.5
0	4.35	1.233	4.85	-0.083	10.5
.25		1.251	4.86	-0.111	9.2
.5		1.270	4.82	-0.09	8.7
.75		1.289	4.80	-0.089	8.2
1	4.055	1.308	4.74	-0.048	8.2
1.25		1.326	4.72	-0.046	8.3
1.5		1.345	4.70	-0.045	8.6
1.75		1.363	4.67	-0.033	9.2
2	3.76	1.382	4.64	-0.022	9.7
2.25		1.401	4.60	-0.001	10.4
2.5		1.420	4.59	-0.010	11.4
2.75		1.439	4.58	-0.019	12.1
3	3.46	1.459	4.56	-0.019	13.1
3.25		1.478	4.545	-0.023	14
3.5		1.498	4.53	-0.028	15
3.75		1.518	4.51	-0.028	15.6
4	3.145	1.538	4.50	-0.038	16.2
4.25		1.556	4.49	-0.046	16.5
4.5		1.573	4.475	-0.049	16.7
4.75		1.591	4.45	-0.041	16.8
0	2.8675	1.609	4.44	-0.049	16.3
.25		1.627	4.43	-0.057	16.1
.5		1.646	4.42	-0.066	15.5
.75		1.664	4.40	-0.064	14.8
1	2.58	1.682	4.39	-0.072	13.8
1.5		1.721	4.34	-0.061	12.2
2	2.265	1.760	4.285	-0.045	11.2
2.25		1.780	4.27	-0.050	10.9
2.5		1.800	4.255	-0.055	10.65
2.75		1.819	4.21	-0.029	10.15
3	1.96	1.839	4.20	-0.039	10.4
3.5		1.879	4.15	-0.029	10.5
4	1.65	1.918	4.10	-0.018	11

Results for Ringer Tyrode physiological saline continued

A	B	l cms	C	Δ cms	D cms
4.5		1.955	4.06	-0.015	12
0	1.36	1.991	4.01	-0.002	12.4
.5		2.029	3.99	-0.019	12.8
1		2.067	3.95	-0.017	13.4
1.5		2.105	3.94	-0.045	14
1.75		2.124	3.93	-0.054	14.2
2	0.765	2.143	3.90	-0.043	13.7
3	0.47	2.22	3.85	-0.07	13
4	0.17-	2.295	3.78	-0.075	12
	4.23				
4.5		2.332	3.75	-0.082	11.6
4.75		2.351	3.70	-0.051	11.5
0		2.369	3.67	-0.039	11.4
.25		2.388	3.68	-0.068	11.5

Table 14Results for Ethyl Alcohol

Temperature 18°C

Date: 12th February 1952

A [*]	l cms	C	x cms	Δ cms
0	0	5.87	0	0
2	.156	5.875	0.005	-0.161
4	.312	5.90	0.03	-0.342
0	.390	5.91	0.04	-0.43
0.5	.429	5.93	0.06	-0.489
1	.468	5.94	0.07	-0.538
1.5	.507	5.96	0.09	-0.597
2	.546	5.99 to 6.0	0.12 to 0.13	-0.666 to -0.676
2.5	.585	5.98	0.11	-0.695
3	.624	5.975	0.095	-0.719
3.5	.663	5.95 to 5.94	0.08 to 0.07	-0.743 to -0.733
4	.702	5.92	0.05	-0.752
4.5	.741	5.85 to 5.83	0.02 to 0.04	-0.721 to -0.701
0	.780	5.80 to 5.75	0.07 to 0.12	-0.71 to -0.66
0.5	.819	5.80 to 5.65	0.07 to 0.22	-0.749 to -0.599
1	.858	5.7 to 5.5	0.17 to 0.37	-0.688 to -0.488
1.5	.897	5.6 to 5.4	0.27 to 0.47	-0.627 to -0.427
2	.936	5.5 to 5.3	0.37 to 0.57	-0.566 to -0.366
2.5	.975	5.3 to 5.1	0.57 to 0.77	-0.405 to -0.205
3	1.014	5.1 to 5.0	0.77 to 0.87	-0.244 to -0.144
3.5	1.053	5.05 to 4.90	0.82 to 0.97	-0.233 to -0.083
4	1.092	4.92 to 4.89	0.95 to 0.98	-0.142 to -0.112

* One division of the screw on the rising table corresponds to a change of 0.078 cm in the liquid level.

Results for Ethyl Alcohol continued

A	l cms	C	x cms	Δ cms
0	1.17	4.76 to	1.11 to	-0.06 to
		4.73	1.14	-0.03
1	1.248	4.75 to	1.12 to	-0.128 to
		4.65	1.22	-0.028
2	1.326	4.66	1.21	-0.116
3	1.404	4.625	1.245	-0.159
4	1.482	4.55	1.32	-0.162
0	1.56	4.50	1.37	-0.19
1	1.638	4.46	1.41	-0.228
2	1.716	4.40	1.47	-0.246
3	1.794	4.34	1.53	-0.264
4	1.872	4.32	1.55	-0.322
0	1.95	4.22	1.65	-0.3
1	2.028	4.17	1.7	-0.328
2	2.106	4.10	1.77	-0.336
3	2.184	4.04	1.83	-0.354
4	2.262	3.98	1.89	-0.372
0	2.34	3.87	2.0	-0.34
1	2.418	3.79	2.08	-0.338
2	2.496	3.72	2.15	-0.346
3	2.574	3.66	2.21	-0.364
4	2.652	3.55 to	2.32 to	-0.332 to
		3.50	2.37	-0.282
0	2.73	3.48	2.39	-0.34
1	2.808	3.40	2.47	-0.338
2	2.886	3.34	2.53	-0.356
3	2.964	3.21	2.66	-0.304
4	3.042	3.16	2.71	-0.332
0	3.12	3.05	2.82	-0.3
1	3.198	3.02	2.85	-0.348
2	3.276	2.93	2.94	-0.336
3	3.354	2.84	3.03	-0.324
4	3.432	2.75	3.12	-0.312
0	3.51	2.70	3.17	-0.34
1	3.588	2.67	3.20	-0.388
2	3.66	2.56	3.31	-0.356
3	3.744	2.51	3.36	-0.384
4	3.822	2.37	3.50	-0.322
0	3.9	2.31	3.56	-0.34
1	3.978	2.24	3.63	-0.348
2	4.056	2.18	3.69	-0.366
4	4.212	2.04	3.83	-0.382

Results for Ethyl Alcohol continued

A	l cms	C	x cms	Δ cms
1	4.368	1.90	3.97	-0.398
3	4.524	1.70	4.17	-0.354
0	4.68	1.55	4.32	-0.36
2	4.836	1.40	4.47	-0.366
4	4.992	1.25	4.62	-0.372
1	5.148	1.10	4.77	-0.378

References

- 1 Cole, K.S. and Cole, R.H., J. Chem. Phys.
9, 341, (1941)
- 2 Debye, P., 'Polar Molecules' (New York.,
The Chemical Catalog. Co. Inc. 1929)
- 3 Onsager, L., J. Amer. Chem. Soc., 58, 1486, (1936)
- 4 Perrin, F., J. Phys. Radium, (7), 5, 497, (1934)
- 5 Oncley, J.L., Chem. Revs., 30, 433, (1942)
- 6 Kirkwood, J.G., J. Chem. Phys. 4, 592, (1936)
- 7 Trans. Faraday Soc., 'Discussion on Dielectrics'
42A, (1946)
- 8 Frohlich, H., 'Theory of Dielectrics', (Oxford 1949)
- 9 Böttcher, C.J.F., 'Theory of Electric Polarisation'
(Elsevier Publishing Co. 1952)
- 10 Lane, J.A. and Saxton, J.A., Proc. Royal Soc. A,
213, 400, (1952)
Saxton, J.A., Proc. Royal Soc. A, 213, 473, (1952)
- 11 Collie, C.H., Ritson, D.M. and Hasted, J.B.,
Proc. Phys. Soc., 60, 145, (1948)
- 12 'The Principles of Microwave Circuits' edited by
C.G. Montgomery, p. 380, Fig. 11.7, (McGraw-
Hill, 1948)
- 13 Cook, H.F., Brit. J. App. Phys. 3, 249, (1952)

- 14 Baz, G. *Physik. Z.*, 40, 394, (1939)
- 15 Kebbel, W., *Hoch: tech. u Elek akus* 53, 81 (1939)
- 16 Drude, P., *Wied. Ann* 55, 633 (1895); 61, 466 (1897)
- 17 Knerr, H.W., *Phys. Rev.*, 52, 1054, (1937)
- 18 Roberts, S., and von Hippel, A., *J. App. Phys.*,
17, 610, (1946)
- 19 Horner, F., Taylor, Dunsmuir, R., Lamb, J.,
Willis Jackson, *J.I.E.E.*, 93, Pt.III, 33 (1946)
- 20 Redheffer, R.M., 'Technique of Microwave Measurements',
Chapter 10 (McGraw-Hill, 1947)
- 21 Buchanan, T.J., *J.I.E.E.*, 99, Pt.III, 61, (1952)
- 22 Branin, F.H., and Smyth, C.P., *J. Chem. Phys.*,
20, 1121, (1952)
- 23 England, T.S., and Sharples, N.A., *Nature*, 163,
487, (1949)
- 24 England, T.S., *Nature*, 166, 480, (1950)
- 25 Jackson, W., 'High Frequency Transmission Lines'
(Methuen Monograph 1945)
- 26 Abadie, P., *Trans. Faraday Soc.*, 42A, 143, (1946)
- 28 Conner, W.P. and Smyth, C.P., *J. Amer. Chem. Soc.*,
65, 382, (1943)
- 29 Little, V.I., *Proc. Phys. Soc.*, 66, 175, (1953)
- 30 Hill, N., Thesis, University of London, (1953)
- 31 Hasted, J.B., Ritson, D.M. and Collie, C.H.,
J. Chem. Phys. 16, 1, (1948)

- 32 Lane, J.A., and Saxton, J.A., Proc. Roy. Soc. A,
214, 531 (1952)
- 33 Haggis, G.H., Hasted, J.B., and Buchanan, T.J.
J. Chem. Phys., 20. 1452 (1952)
- 34 Cooper, R., J.I.E.E., 93, Pt.III, 69, (1946)
- 36 Jackson, W. Trans. Faraday Soc., 42A, 91, (1946)
- 37 Bolton, H.C., Proc. Phys. Soc., 61, 294, (1948)
- 38 Ichikawa, T., Yamamura, H. and Negita, H.,
J. Sci. Hiroshima Univ., A 15, 73, (1951)